DOTTORATO IN SCIENZE CHIMICHE
E FARMACEUTICHE E INNOVAZIONE INDUSTRIALE

XXXVII ciclo

UNIVERSITÀ DI PAVIA

Coordinatore: Chiar.mo Prof. Giorgio Colombo

New Uncharged Precursors for Photoredox-mediated Radical Generation

Tutore
Chiar.mo Prof. Maurizio Fagnoni
Co-tutore
Chiar.mo Prof. Stefano Protti

Tesi di Dottorato di
Adrián Luguera Ruiz

2021/2024

UNIVERSITÀ DEGLI STUDI DI PAVIA

DOTTORATO IN SCIENZE CHIMICHE E FARMACEUTICHE E INNOVAZIONE INDUSTRIALE

XXXVII Ciclo

Coordinatore: Chiar.mo Prof. Giorgio Colombo

New Uncharged Precursors for Photoredox-mediated Radical Generation

Tesi di Dottorato di
Adrián Luguera Ruiz

AA 2021/2024

Tutore
Chiar.mo Prof. Maurizio Fagnoni

Co-tutore
Chiar.mo Prof. Stefano Protti

Table of contents

Acknowledgements

This thesis has been made possible thanks to the funding received from the European Union's Horizon 2020 research and innovation programme under the Marie Skłodowska-Curie PhotoReAct Innovative Training Network grant agreement No 956324. Additional support from the Ministero dell'Università e della Ricerca (MUR) and the University of Pavia through the program "Dipartimenti di Eccellenza 2023–2027" was received during the development of this thesis.

Today, 3 years later, it is time to say goodbye to one of the most important and rewarding experience I have had in my life despite the bad moments and feeling so lonely. This couldn't be possible without Maurizio and Stefano. They trusted me to join this adventure giving me the opportunity to join the MSCA-PhotoReAct-ITN and PhotoGreen Lab. I wanted to thank you first for the opportunity and for introducing me into Photochemistry, a completely new world for me at that moment, and part of the chemist I am today. I really appreciate the time discussing about chemistry with Maurizio and learning from you and your Photochemistry classes. Thank you for your availability when I have needed your help. I cannot forget to mention Davide too, chemist, IT technician, maintenance service… For sure you are doing a huge contribution to the group. I hope I was not so disturbing as I have in mind. I wish I could work closer. You all were always there helping me, open to talk about chemistry and available even if you do not have time enough. I want to specially thank Stefano, as you were the first person I met when I arrived that super-hot summer. I wanted to thank you for the time we spent together in the lab and having some aperitivo or gelato after work. For the good and not so good days and for your help every time I have needed you. I wish you all the best, not only in your career but in your life too. You deserve it.

I cannot forget all the people I met in the lab during those 3 years. Je, Fra, Robi, Camilla, Daniele, nonna Maria (we missed you a bunch at gelato time, thank you for being so kind with us). Chiara! What a lot of good moments. We had so much fun! I hope to see you soon but not dressed as a sumo fighter. I am 100% sure you will have an amazing career. Luchino and Sere! Thank you for the dinners, beers, wines and the time together. I am waiting for you in Spain to make some more memories together! Ari!! I hope everything will be good with your PhD. Thanks for being so sweet and take care of us and for the half of the gatino fotoreattivo. Vale!! Thanks for the moments working and laughing together. You are almost at the end, and I know that you will do an amazing job. I wish you all the best. Federico, I cannot forget you. You have taught me more than you think, and I need to thank you for that. Just try to be more self-confident. You can do everything you want, just believe in you as we have done. I am probably missing someone. Please, forgive me.

My partner in Lab, Lori. We were alone almost till the end. Thank you for your warm welcome when I arrived, since the first day. For being my translator at the beginning. We have spent a lot of time in the lab together having a lot of nice moments. Even if we were in different countries, we continued to manage to send us stupid things (as we are still doing) … I am sure you will have an amazing career. You deserve it. You are a great chemist!

Ele… What can I say to you? You were like my little sorellina. Probably I cannot find the proper words, but since the first day you were there helping me without asking for anything. You are a great student, a stubborn one, but the best colleague in the lab and the best friend outside I could ask for. My pizza and gelato mate! I am not going to wish you the best, because I know you deserve even more. I miss you, my friend! Hope to see you soon! Ti voglio bene amica!

A big thank to all the people I could meet during these 3 years thanks to the Marie Curie meetings, you all guys are amazing. Special mention to Stefano and Matteo. I will not forget the time working together at UvA. Thank you for that!

Barb!! Thank you very much for being so kind and sweet. Thank you or helping me, for being my best team mate ever: Fit Fatty but Happy!! It will not be the same to go to the box and to not have fun with you, to workout with you… To go to the theater and say … lets go home! This is not for us… I can write thousands of moments and memories. Thank you for being my friend! I love you so much! Thanks to the Skydome family too, specially to Dani.

Y… llegó el momento de agradecer a toda la gente que durante estos tres años me habéis acompañado desde la distancia. Gracias a mis amigos de siempre. Los de toda la vida. Esos que, aunque nos veamos poco, siempre podemos contar los unos con los otros. Espacial mención a Gus, que, durante estos tres años, a pesar de la distancia, hemos sabido estar ahí el uno para el otro en los momentos de alegría y en los de tristeza. Te quiero hermano.

Gracias a todos los que habéis contribuido al químico que soy hoy. Gracias Aurelio, Carlos, Mario, Amaiur, Jaime, María Jesús, Marta… y a todos los que me quedan por el camino.

Gracias a los compis de Janssen: Santi, Lourdes y Javi. Un capítulo de esta tesis no podría estar escrito si no fuera por vuestra ayuda y paciencia. Ha sido un placer trabajar con vosotros y aprender de vosotros. Me he divertido mucho durante esos 4 meses. Ojalá nos veamos en el futuro. Un abrazo a todos.

A mis chicos del Pluri: Álvaro, Víctor y Silvia. Pasan los años, pero es bueno seguir en contacto y ver que vamos saliendo adelante y alcanzando metas. Gracias Víctor y Silvia, porque he experimentado muchas de las situaciones en las que quizá os puse en su momento cuando era estudiante. Espero no haberos dado mucha guerra. Gracias infinitas por todo lo que me enseñasteis. ¡Nos vemos pronto para celebrarlo!

Gracias a mi familia: a mi abuela, a mis tíos, a mis primas y primos, los de siempre y los nuevos. Dicen que la familia no se elige, pero… tampoco nos obligan a mantenerla. Espero que sigamos juntos muchos años más. A mi Kira, Toni y a mi pequeño Rocky (no te olvidamos). Os quiero.

Gracias a mis padres por apoyarme siempre en todas mis locuras, en todas mis decisiones y en todo lo que hago. Siempre habéis creído en mí y en mis objetivos, aunque suponga estar lejos y vernos poco. No os lo digo a menudo, pero os quiero mucho. Todo lo que soy hoy es gracias a vosotros y a vuestro esfuerzo. ¡GRACIAS!

Y tú abuela, mi ángel de la guarda. Siempre conmigo a donde vaya. Me has cuidado siempre sin importar lo que pase y me sigues ayudando incluso sin estar. No te lo dije en su momento, pero gracias por todo lo que has hecho, lo que haces y lo que harás por mí. ¡Te quiero!

Nieves: podría escribir una tesis entera hablando de ti. Gracias por estos 12 años de amor, por estos años de risas, de llantos, de momentos buenos y malos. Gracias por estar en lo bueno y más en lo malo. Gracias por estos años de madrugones, de aviones, de pocas llamadas, de poco tiempo para hablar… Gracias por aguantarme en estos últimos meses de estrés y nervios. Gracias por ser mi apoyo cuando más lo necesito, mi mujer, mi compañera y mi amiga. Gracias por ir conmigo de la mano mientras conseguimos y cumplimos objetivos. Gracias por ser tú. Gracias por ser casa. Eres la mejor compañera de vida que podría haber imaginado encontrar. ¡Nos vemos en el altar! Te amo.

“Only when we are brave enough to explore the darkness,
we will discover the infinite power of light.”

A mi abuela Leo

Chapter 1

The Chemistry of Excited States: Photochemistry

1.1 Introduction.

Light induced reactions have been taking place since the creation and evolution of our world itself. Daily different photochemical reactions are occurring in absence of human intervention and without being notice, i.e. photosynthesis in plants, the perception of colors by human eyes, color changes in materials exposed to sunlight, etc. In fact, thousands of years ago, in the ancient world wise men studied how to properly use the power of sunlight.[1]

During the 18th and 19th centuries scientists left their observation on photochemical processes. First reported photoisomerization was described by Trommsdorff. He was able to explain that the elemental analysis of Santonin before and after light irradiation did not show any change in the composition of Santonin, while a white powder became yellow before bursting after irradiation under a certain wavelength, demonstrating the wavelength dependence of the photochemical reactions.[2] Those pioneering studies and those performed by Sestini and Cannizzaro (20 years later) were the first stone to impel Italian photochemistry. However, it was not possible to elucidate and properly describe the formation of photosantonic acid and the reaction intermediates until the early 1960s (Scheme 1.1).[3]

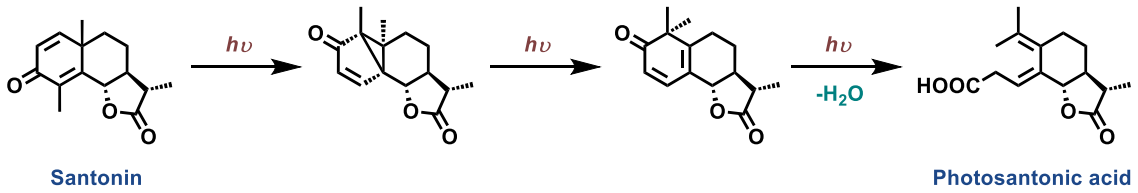

Scheme 1.1. Photoreaction of Santonin and elucidated intermediates.

In the end of the 19th and beginning of 20th century, photochemistry raised as a significant branch of chemistry. The next decades are recognized as the "gold age" of photochemistry. Ciamician and Silber studied the chemical consequence of light irradiation in diverse transformations like photoreduction of carbonyl groups or intramolecular cycloadditions among others, introducing for the first-time the concept of photochemical reaction. They studied the photo-reduction of benzoquinone into hydroquinone and acetaldehyde in alcoholic solution after sunlight exposure. Silber found the transformation of nitrobenzene in aniline, acetaldehyde and surprisingly methylquinoline in an ethanol solution.[1,4] Moreover,

Paternó, Chieffi and Büchi observed the cycloaddition of carbonyl derivatives onto olefins, a 2+2 photocycloaddition, for the formation of oxetanes (Paternó-Büchi reaction, Scheme 1.2).[5]

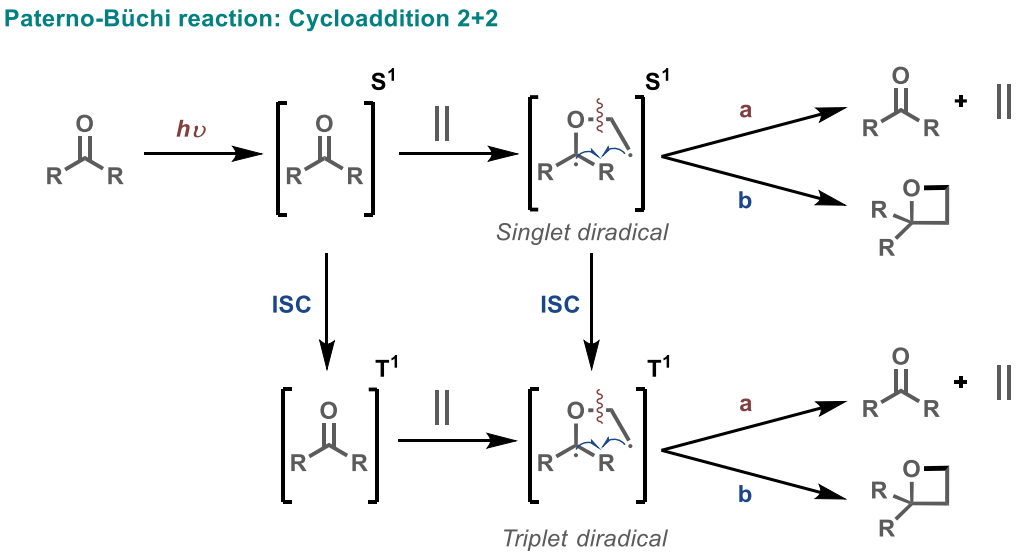

Scheme 1.2. Paterno-Büchi cycloaddition. Reaction mechanism.

In the mid-1930s Norrish studied the chemistry of carbonyl group (aldehydes and ketones) by explaining two different processes currently known as Norrish Type I and II reaction (Scheme 1.3).[6] The first one is based on the photolysis (homolysis of C-C bond). Those radicals can follow different paths. Both radicals can be recombined to form the starting materials. Via α-H or β-H hydrogen abstraction it can lead to the corresponding ketene or the formation of the aldehyde. In addition, via CO extrusion and further recombination of both radicals a new C-C bond can be formed. Norrish Type II is described as an intramolecular γ-hydrogen abstraction. Ita can be followed by the Cβ-Cγ bond fragmentation obtaining an olefin and enol or it can react via intramolecular recombination forming 1,2-polysubstituted cyclobutanols (Norrish-Yang reaction).

Therefore, physical studies, directly related to photochemistry, were developed by Planck leading to the concept of "quanta" or "quantum" of energy.[7] Einstein made his contribution to the filed by explaining that light irradiation and subsequent absorption of a "quanta" of light by a metal lead to the emission of one electron. This theory is known as "photoelectric effect" as precursor of the first law of photochemistry.[8] Perrin proposed the existence of a "metastable" triplet state lower

in energy than the excited state itself, later recognized by Lewis and Kasha. Jablonsky correlated phosphorescent phenomena with this triplet state that is involved in many photochemical processes, then corroborated by Lewis and Calvin. These findings promoted new studies on triplet energy transfer (EnT) events.[9]

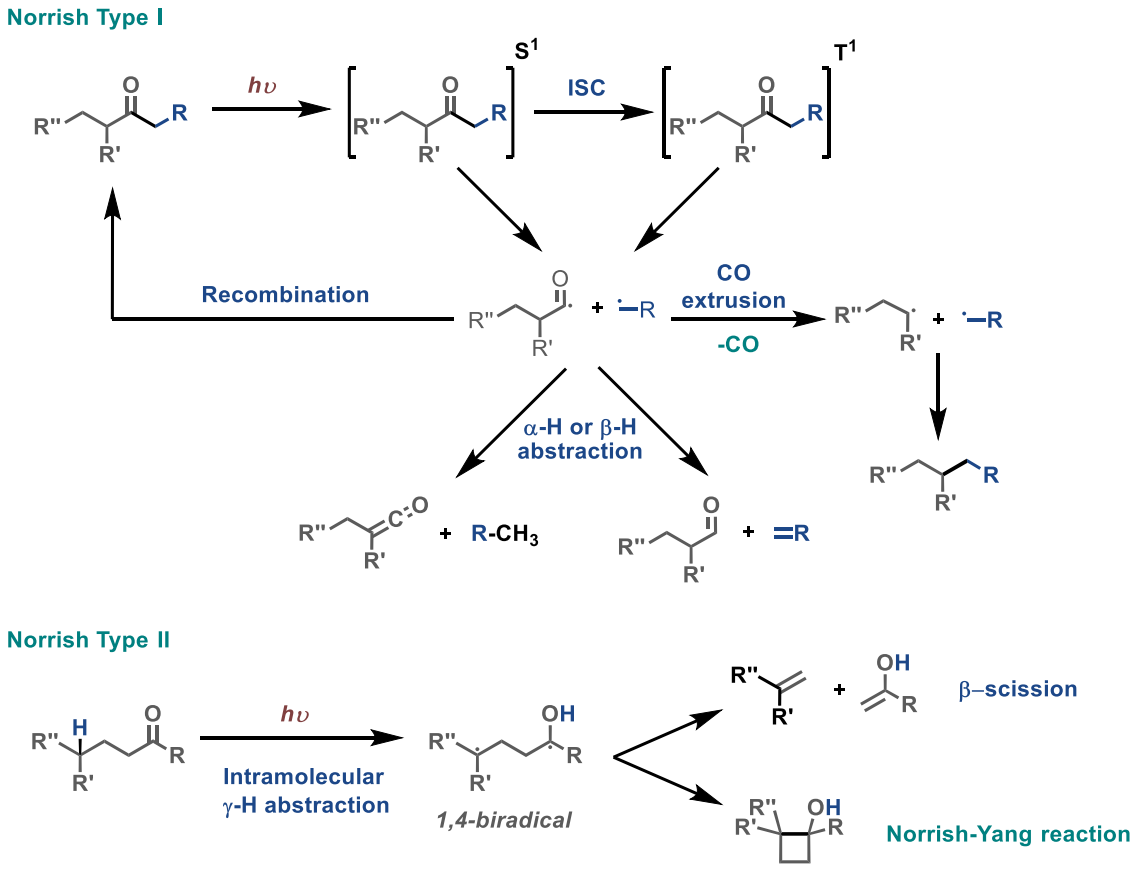

Scheme 1.3. Norrish Type I and Type II photoreaction and possible paths of reaction intermediates.

In the 20th century photochemistry experimented a loose of interest in this field and it is not until the end of the 20th and beginning of the 21st century when the "renascence" of photochemistry took place, being even more important in the last decades. The main reason is that the new chemical transformations can be explored when chemists make use of the chemistry of the excited state, as from this chemical species can react in unconventional from inconceivable paths from the point of view of traditional ground state organic chemistry. During this new trend in photochemistry, chemists found the manner to exploit the ability of absorbing species to harness light energy to speed up chemical reactions by the merge of photochemistry and catalysis.

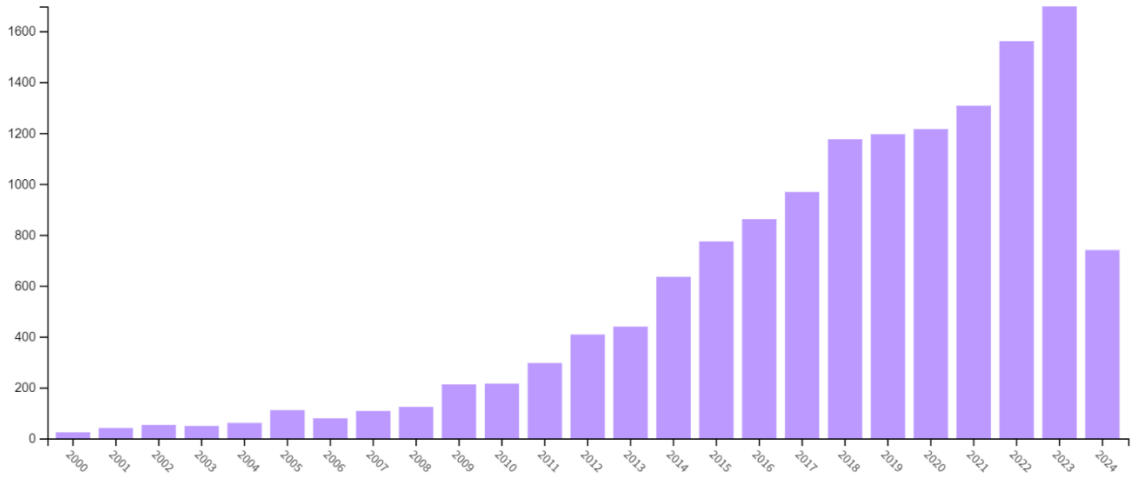

Figure 1.1. Plot of number of publications per year concerning "photocatalysis". Source: "Web of Science".

Photocatalysis provoked interest and found application in a large variety of study fields (Figure 1.1). Regarding Organic Chemistry, photocatalysis encompasses different well-known manifolds that are still being studied, where Energy Transfer (EnT), Electron Transfer (ET), Hydrogen Atom Transfer (HAT), Halogen Atom Transfer (XAT) are the principal-studied mechanisms. The wide versatility of the photochemical processes mentioned above expanded the synthetic toolbox for synthetic organic chemistry accessing non-conventional products, via excited state chemistry, in a more sustainable, easier and smoother manner. Photocatalysis is being applied in combination to new chemical technologies (flow, high throughput experimentation (HTE), automation, etc.) in relevant industries (pharmaceutical, agrochemical, etc.) showing its power and convenience as synthetic organic tools.

1.2 Photochemistry fundamentals.

IUPAC defined photochemistry as *"the branch of chemistry concerned with the chemical effects of light"*.[10] Therefore, a photochemical process (reaction or rearrangement) requires the absorption of electromagnetic radiation of the appropriate wavelength.[11] The absorbing molecule promotes one electron from its ground state (**S_0**) to an excited state. From the singlet or triple excited state (**S_n** or **T_n**), higher in energy (**E**). it subsequently undergoes a chemical transformation into a more stable product or a reaction intermediate that further reacts with other

species. Otherwise, the excited state can be photophysically deactivated without any chemical change.

Visible light (400 nm – 800 nm) and near UV (200 nm - 400 nm) is the range of the electromagnetic spectrum where photons have an E that promotes transitions of the electrons between molecular orbitals (valence electrons). Lower wavelengths correspond to more energetic radiation.

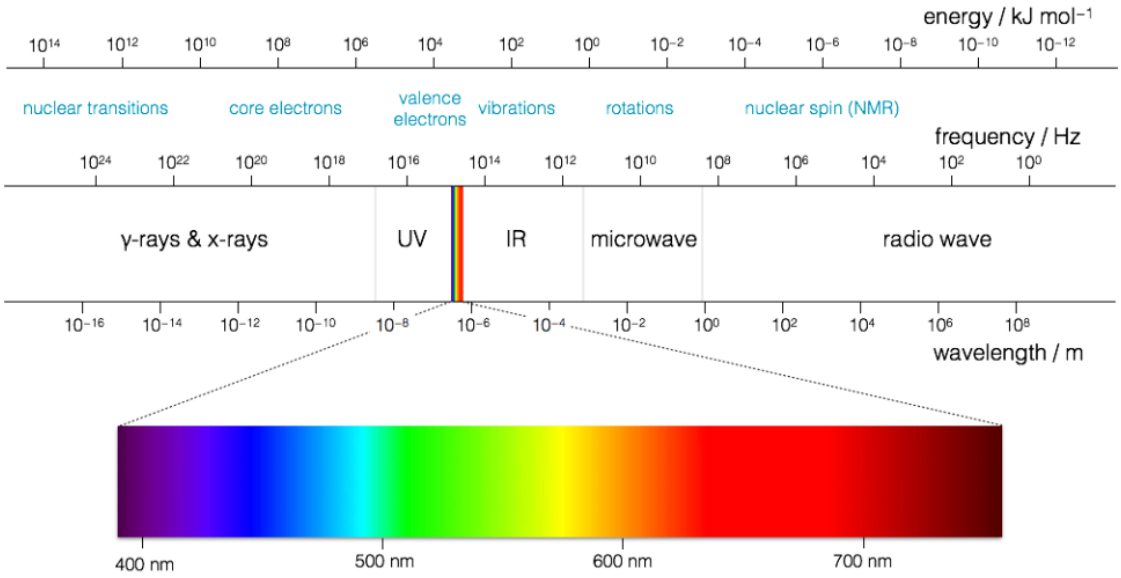

Figure 1.2. Electromagnetic spectrum of light.

The first law of photochemistry or Grotthuss-Draper law claimed that a compound must absorb light to promote a photochemical transformation: ***"Only absorbed photons can cause a chemical change"***. The second law or Stark-Einstein law also know as **"quantum equivalence law"**: ***"Each absorbed quantum of radiation causes one equivalent of a chemical reaction".***[12]

$$E = h\nu = h\ c/\lambda\ \ [\mathrm{J \cdot photon^{-1}}] \quad \text{where} \quad \begin{array}{l} h\text{: Planck's constant } (6.6256 \times 10^{-34}\ \mathrm{J \cdot S \cdot photon^{-1}}) \\ \nu\text{: frequency of radiation } [\mathrm{s^{-1}}] \\ c\text{: speed of light } (2.9979 \times 10^{-8}\ \mathrm{m \cdot s^{-1}}) \\ \lambda\text{: wavelength of radiation [m]} \end{array} \qquad (1.1)$$

The interaction of a molecule with a photon results on its absorption by the molecule promoting the electronic transition of one electron to an excited state. The probability of being absorbed (absorbance, **A**) by the molecule depends on and the molar extinction coefficient ($\boldsymbol{\varepsilon_\lambda}$) constant at a specific irradiation wavelength

(wavelength dependent), the concentration of the sample (**C**) and the "path length" (**l**) as described in Beer-Lambert Law.

$$log\frac{I_0}{I} = A = \boldsymbol{\varepsilon_\lambda}\, lC \quad \text{where}$$

$\boldsymbol{\varepsilon_\lambda}$*: molar absorption coefficient* [L · mol^{-1} · cm^{-1}]
C: molar concentration of absorbing species [M]
l: "path length" traversed by light [cm]
I_0/I*:* initial intensity/ experimental intensity (1.2)

This law applies only if there are not interaction between absorbing species, in homogeneous non-emissive diluted solutions.[13]

Molecules exist on the lowest energy state (ground state, S_0) where the electrons are occupying the lowest energetic molecular orbitals: HOMO orbital, the highest occupied molecular orbital and the empty LUMO orbital, lowest unoccupied molecular orbital. In the occupied molecular orbitals only two electrons can be contained characterized by antiparallel spins obeying "Pauli's exclusion principle", so the minimum energy that a molecule needs to absorb (photon) to be excited is the corresponding energy between the HOMO and LUMO orbitals.[14] The transition starts from the ground state (HOMO) to the excited state (LUMO*) which has a different energy, structure and lifetime. In molecules the HOMO-LUMO transition is not the unique available transition and other transitions are probable to occur.

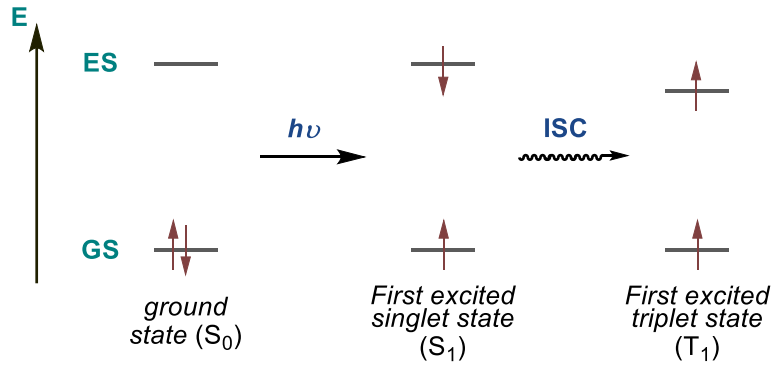

Figure 1.3. Spin configuration of ground and excited states. (ES: excited state, GS: ground state).

In accordance with Hund's Law of maximum multiplicity the lowest energetic state is the one that is fully occupied by paired electrons. Spin multiplicity (**S**) is the sum of the spins in the molecular orbitals, easily calculated as 2S + 1. When **S = 0** (2S + 1 = 1), the state is named as ***singlet***, characterized by paired spins and shorter lifetimes (10^{-12}-10^{-6} s). When **S = 1** (2S + 1 = 3), the state is named ***triplet***,

characterized by unpaired parallel spins and a longer lifetime (10^{-7}-10s). Triplet states are lower in energy than the homologous singlet state as the electrons are organized to minimize coulombic interactions between the charges (Pauli's exclusion principle). Two electrons in the same region, destabilizes the singlet state being more energetic than the triplet state.[15] The electronic structure of free radicals is described by the presence of 1 unpaired electron when **S = ½** (2S + 1 = 2), called ***doublet***.

The most important requirement for an electronic transition to be permitted is to not have a change on the spin multiplicity ($\Delta S = 0$), in other words, no "flipping" electrons spin during the transition. This means that a transitions $\mathbf{S_0 \rightarrow S_1}$, while $\mathbf{S_0 \rightarrow T_1}$ is a spin-forbidden transition (Wigner's rule). Although flipping of electron spin is forbidden it can occur when Intersystem Crossing (ISC) processes take place. One electron can transit from a singlet state to occupy a triplet state ($\mathbf{S_1 \rightarrow T_1}$).[16] The probability of this non-radiative transition (ISC) is proportional to the intensity of the "spin-orbit coupling" and inversely to the energy of the transition $\mathbf{S_1 \rightarrow T_1}$. It is stronger when heavier atoms are present in the molecule (Cl, Br, S, etc.).

Delocalized π and non-bonding electrons are easy to excite, and they are basically present in all organic molecules. In photochemistry there are two different types of electronic transitions:

- $\boldsymbol{\pi \rightarrow \pi^*}$: between a bonding **π** orbital and antibonding **π*** orbital. The corresponding transitions are named as: $\mathbf{S_0 \rightarrow S_1}$, $\mathbf{^1(\pi,\pi^*)}$ and $\mathbf{S_0 \rightarrow T_1}$, $\mathbf{^3(\pi,\pi^*)}$. Due to the orbital overlapping these transitions are more prone to be produced.
- $\mathbf{n \rightarrow \pi^*}$: between a non-bonding **n** orbital and antibonding **π*** orbital. Non-bonding orbitals are present in heteroatoms (N, O) containing non-bonding electrons. The corresponding transitions are named as: $\mathbf{S_0 \rightarrow S_1}$, $\mathbf{^1(n,\pi^*)}$ and $\mathbf{S_0 \rightarrow T_1}$, $\mathbf{^3(n,\pi^*)}$. Due to the poo orbital overlapping these transitions are less probable to occur. However, the low energy difference between the corresponding $\mathbf{S_1}$ $\mathbf{^1(n,\pi^*)}$ and $\mathbf{T_1}$ $\mathbf{^3(n,\pi^*)}$ excited states and the change of orientation of the plane of symmetry during $\mathbf{n \rightarrow \pi^*}$ increases the effect of spin-orbit coupling promoting the singlet-triplet ISC.[17]

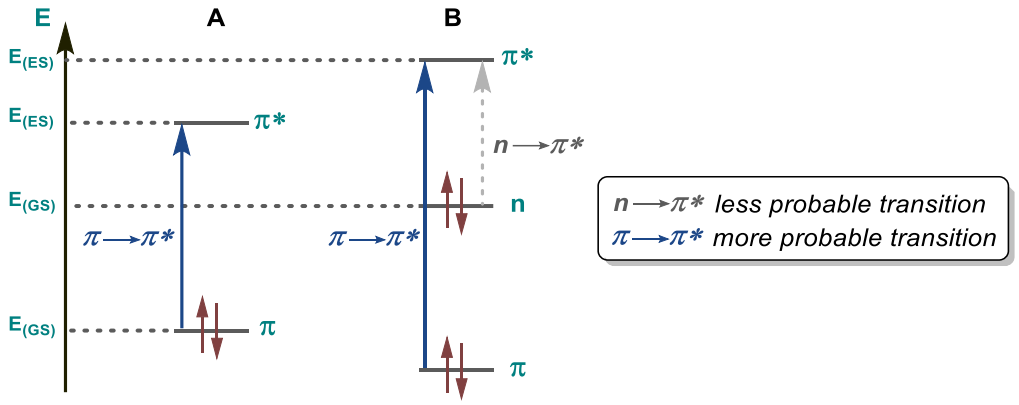

Figure 1.4. Electronic transitions in A) π / π* in ethylene bond. B) Molecular orbitals in C=O group.

When a molecule absorbs energy, it is excited to an excited state. The absorbed energy must be dissipated by photochemical transformations or photophysical processes. A ***photochemical reaction*** is a deactivation process of an excited state. While molecules absorb and accumulate energy by promoting electronic transitions, the reactivity of the excited state is different from one molecule to another. When this energy makes thermodynamically favorable the conversion of the molecule into products a photochemical process is taking place, even on the formation of products that are not accessible by thermal synthetic strategies (rearrangements, isomerization, bond fragmentation, radical formation, etc.). Additionally, ***photophysical deactivation processes*** can occur by two different mechanisms:

- Radiative deactivation: when the emission takes place between states of the same multiplicity (**S_1 → S_0**) the process is named fluorescence. In this case the frequency of the emissive process (**0 → 0'**) is the energy difference between the two states. When emission is between states with different multiplicity (**T_1 → S_0**) it is known as phosphorescence.
- Non-radiative deactivation: the molecule loses vibrational energy through ***vibrational relaxation*** to arrive to the most stable excited state (vibrational level 0', lower in energy) caused by collisions with other molecules. Normally, the electronic transition goes from **S_0** to a higher Sn excited state higher in energy than **S_1**. In accordance with Kasha's rule, the radiative and photochemical processes are taking place from the lowest energetic excited state (**S_1**), thus by ***internal conversion*** (IC) processes energy is dissipated from a higher **S_n** till reach the more stable excited state **S_1** thanks to the overlap of the vibrational levels

between those states (10^{-13}-10^{-12s}). The intersystem crossing (ISC) is an IC between excited states with different multiplicity: **S_1 → T_1** (10^{-11}-10^{-6} s) or **T_1→S_0** (10^{-7}-10 s). As **T_1 → S_0** is slower than **S_1 → S_0** the lifetime of triplet state (T_1) is longer than the singlet state (S_1). This means that an important number of photochemical reactions are taking place from the lowest T_1.

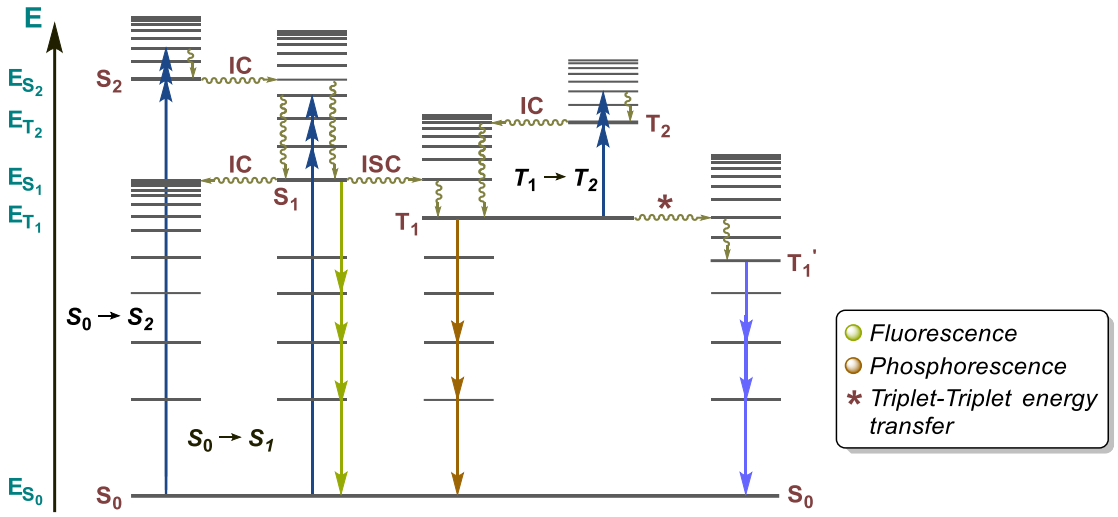

Figure 1.5. Jablonsky diagram. Description of possible electronic transitions and radiative and non-radiative deactivation paths.

1.3 Photocatalysis.

IUPAC defined the term **photocatalysis** as *"change in the rate of a chemical reaction or its initiation under the action of ultraviolet, visible or infrared radiation in the presence of a substance—the **photocatalyst**—that absorbs light and is involved in the chemical transformation of the reaction partners".*[18] It is considered a photo-induced process where the photocatalyst absorbs photons promoting one electron from ground state to the excited state, the subsequent thermodynamic conversion of the substrate produce chemical modifications in the reactant obtaining the corresponding product.

$$A + \text{Photocatalyst (PC)} \xrightarrow{h\upsilon} A + \mathbf{PC^*} \longrightarrow B \qquad (1.3)$$

The photocatalyst is an organic molecule or a metal-based species that can act in the same phase as the reactants (homogeneous) or in a different phase (heterogeneous). The main advantages of photocatalysis reside in the use of photons (energy source)

to promote the reaction. Photons are a greener trace-less agents and a more sustainable energy source without evolving into undesired subproducts. There are several activation manifolds have been described within the years.

A. **Energy transfer (EnT):** during this photophysical deactivation process a molecule in excited state (donor, **D**) transfer the energy to another molecule (acceptor, **A**). The donor returns to its ground state while the acceptor receives the energy, being promoted to an excited state. This process is called ***photosensitization***, where **D** is a ***sensitizer*** while **A** is a ***quencher*** or ***photoinhibitor***. This process can follow three different paths. The first one is by ***dipole-dipole*** interaction. The excited donor interacts with the acceptor (quencher) that deactivates the donor returning to the ground state while the acceptor is taking the energy by being excited: **Förster resonance energy transfer**.[12] The second manifold is **Dexter energy transfer**: there is a concerted net electron exchange (double substitution of electrons) produced by the overlap of the electronic clouds of the donor, in excited state, and the acceptor, in ground state.[19] The last one is the **Triplet-Triplet annihilation**: due to the forbidden transition $\mathbf{T_1 \rightarrow S_0}$, triplet states have a long lifetime. There is a deactivation mode in which two triplet excited states can interact with the subsequent net electron exchange forming a ground state species and a singlet excited state.

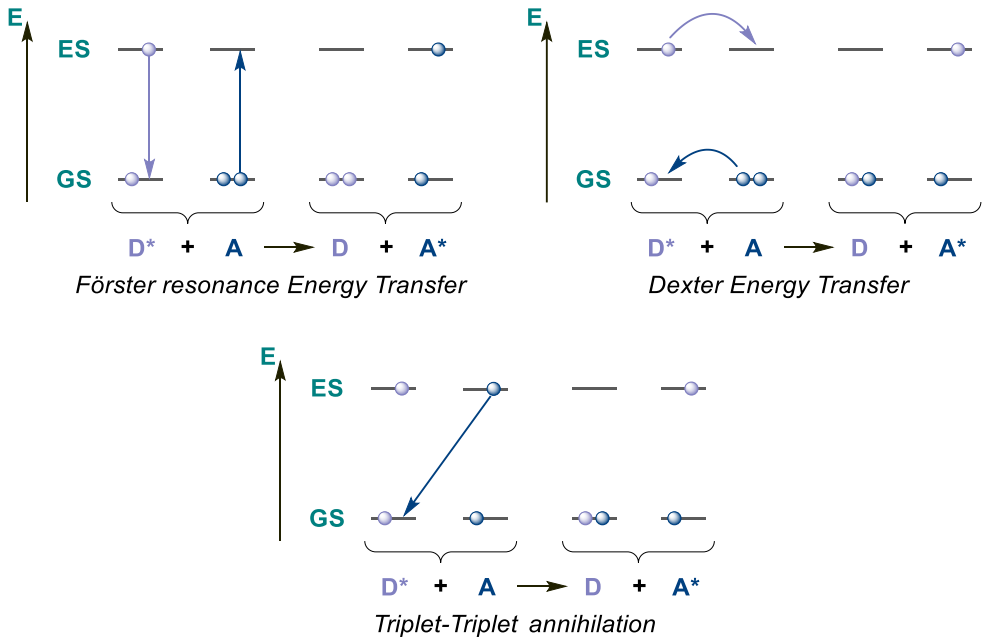

Figure 1.6. Different paths for Energy transfer processes.

B. Hydrogen Atom Transfer (HAT): is characterized by the C-H bond dissociation energy as driving force of the process.

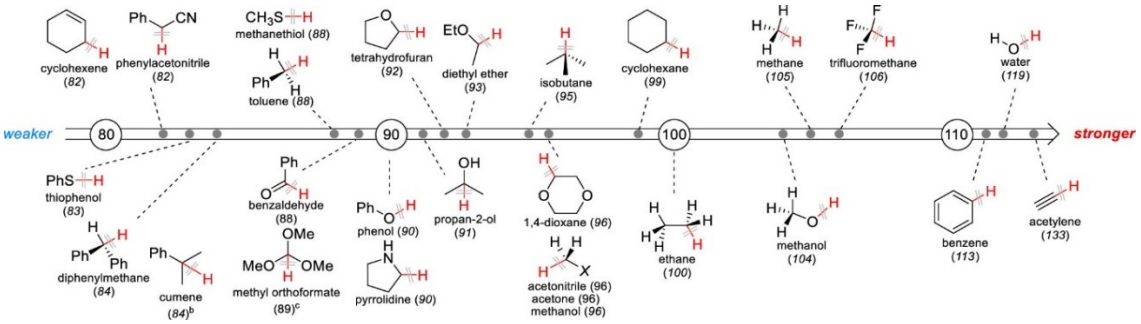

Figure 1.7. Experimental C-H and heteroatom-H bond dissociation energy (kcal mol^{-1}). Reprinted with permission under Creative Common License (CC-BY 4.0) from Capaldo, 2022.

The PC, usually aromatic ketones as benzoquinone or polyoxometalates as tetrabutylammonium decatungstate (TBAD), can homolitically cleave the C-H bond by abstracting H· releasing the corresponding C-centered radical. This is possible due to the existence of an abstractor X-O· moiety in the PC* that allows the hydrogen abstraction. When the PC can abstract a hydrogen from the molecule this process is described as a direct HAT even (*d*-HAT). However, when the PC* generates, via single electron transfer events, a species that can act as hydrogen abstractor (X·), an indirect HAT process is taking place. Highly reactive species, due to its radical-like character and unstability are known to promote HAT processes: alkoxyl radical (RO·), aminoxyl radical (R_2N-O·), amidyl radical (ArCON·-R), thiyl radical (RS·), halogen atom (X·), C-centered radical (C·), dioxirane, amine radical cation ($R_3N^{·+}$) and metal-oxo species.[20]

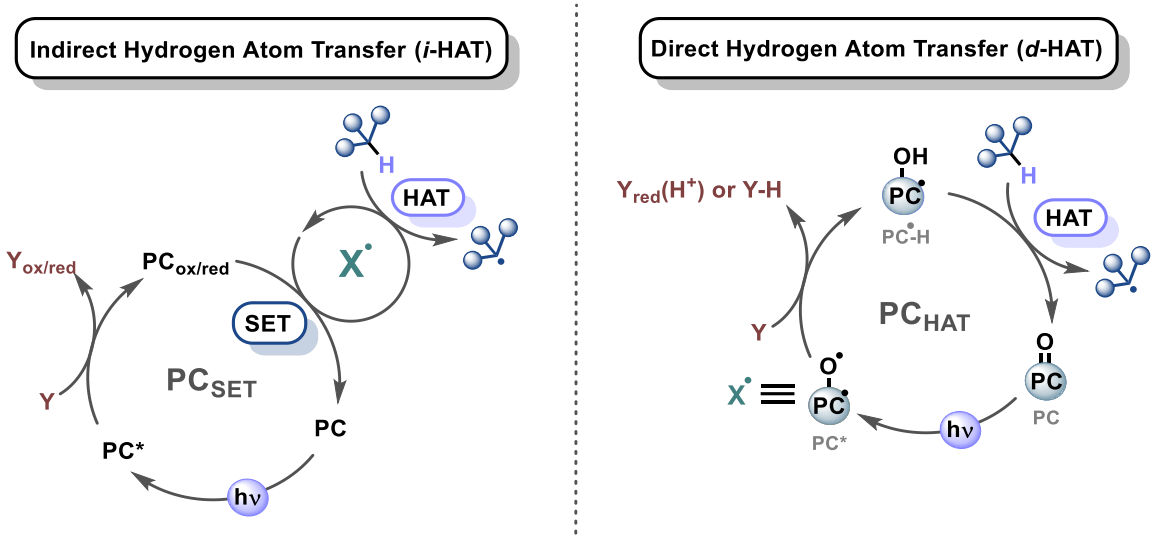

Scheme1.4. Manifolds on HAT processes.

C. Halogen Atom Transfer (XAT): an organic halide reacts with a halogen atom abstractor promoting the homolytic C-X bond fragmentation with the subsequent C-centered radical formation. Commonly, tin, silicon and C-centered radicals can be used as halogen abstractor agents previously generated via photocatalyzed processes. Even in this case, the XAT event is driven by the dissociation bond energy of the C-X bond. Most common halogen abstractors are based on organosilicon compounds and amines, that are previously oxidized forming the corresponding radical that acts as halogen atom abstractor.[21]

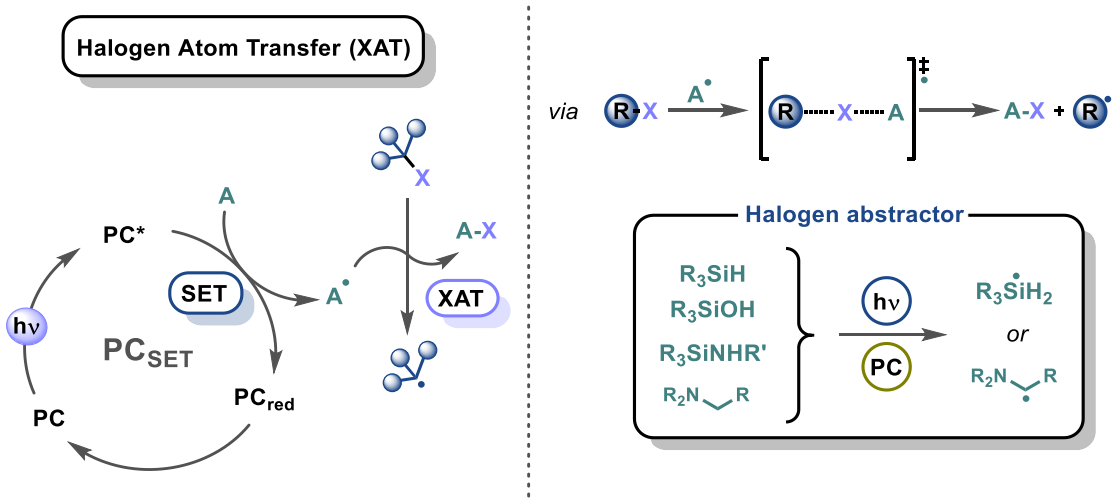

Scheme1.5. Halogen atom transfer (XAT).

D. Photo-induced Electron Transfer (PET): single electron transfer (SET) events are characterized by the transference of one electron from one species to another forming radical charged species. The renaissance of photochemistry paved the irruption of ***photoredox catalysis*** as an interesting organic synthetic tool. The PC (organometallic or organic molecule) is excited by absorbing light irradiation. The PC*can act as a strong reductant or oxidant. If it acts as an oxidant the reaction mechanism follows a ***reductive quenching cycle***, while if it acts as a reductant, it follows an ***oxidative quenching pathway***. The PC* interacts with another molecule (electron donor (D) or electron acceptor (A)) oxidizing or reducing the substrate forming the corresponding radical cation(**R-X**$^{\cdot+}$) or radical anion(**R-X**$^{\cdot-}$) that upon further fragmentation can generate a radical specie (**R**$^{\cdot}$). A second SET between the radical cation or radical anion specie derived from the PC (**PC**$^{\cdot+}$, **PC**$^{\cdot-}$) and a reaction intermediate or an external reductant (D) or oxidant (A) enable the PC turnover.[22]

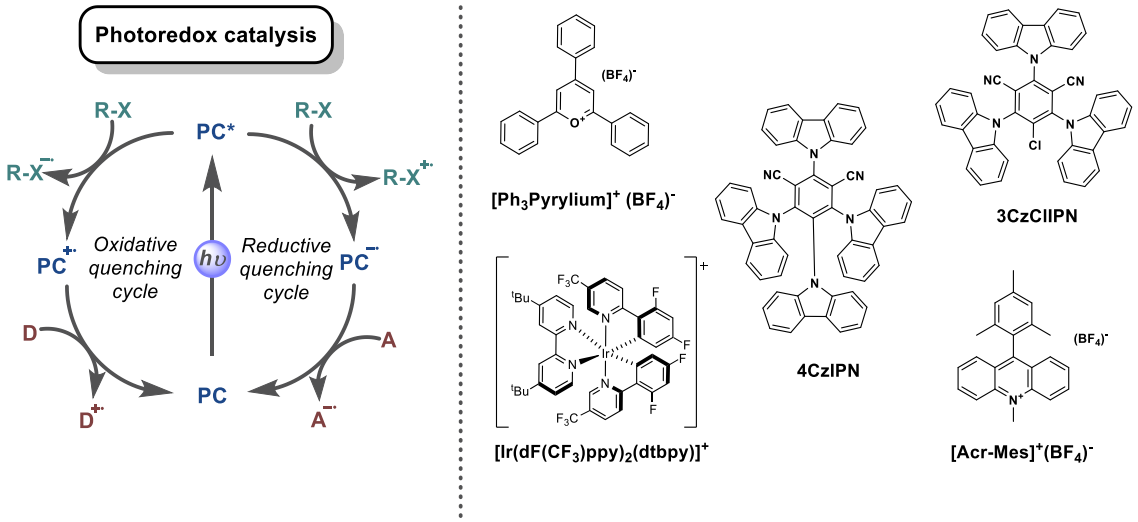

Scheme1.6. Pathways in photoredox catalysis and common photocatalysts.

The PC plays a key role in this process. It must absorb light irradiation in the visible region, it must have a lifetime long enough to interact with the substrates and to be characterized by reversible photophysical and reversible electrochemical properties to avoid degradation. In addition, the oxidation potentials of the PC should match the oxidation potentials of the substrates.[23]

Photoredox catalysis have gained importance in sustainable and green chemistry enabling to obtain unconventional synthetic targets by employing smoother

reaction conditions. The possibility of using a wide variety of different starting materials (carboxylic acids, alcohols, aldehydes, etc.) makes this protocol an emerging synthetic tool in organic chemistry and medicinal chemistry due to the formation of $C(sp^3)$-$C(sp^3)$ bonds through the generation of C-centered radicals (alkyl radicals), currently a hot topic in synthetic organic chemistry.

Photocatalysis has been adopted even by important industries for the synthesis of small molecules such as in Pharmaceutical and Agrochemical industry.[24] The possibility to modify bioactive compounds and drug-like molecules via Late-Stage Functionalization (LSF) or to be able to access new chemical spaces, rapidly and more efficiently, through photochemical processes, make these new synthetic methodologies an attractive synthetic tool.[25]

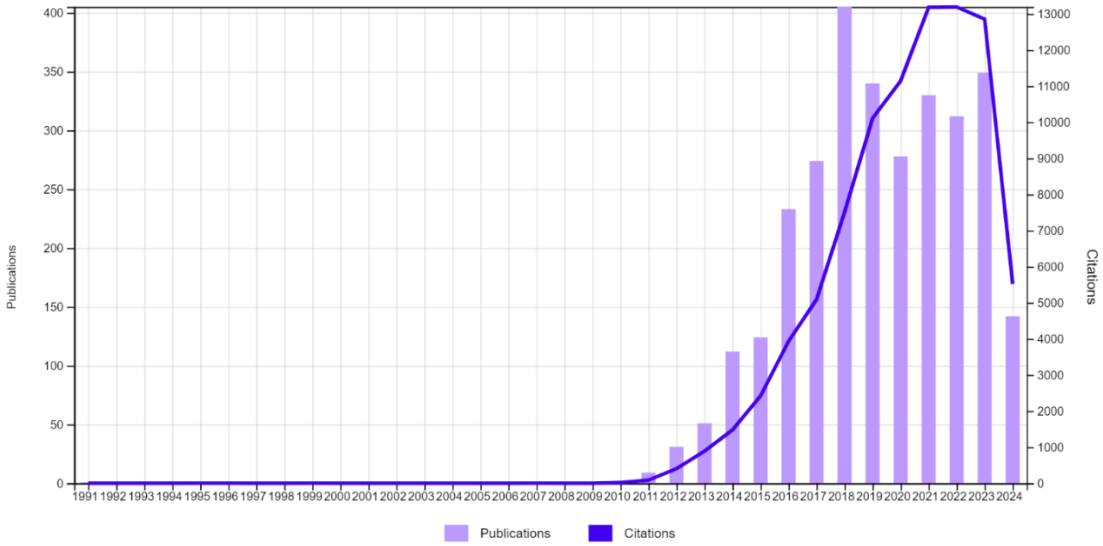

Figure 1.8. Plot of number of publications and citations per year concerning "photoredox chatalysis". Source: "Web of Science".

1.4 Radical Precursors in Photoredox Processes.

Alkyl radicals or C-centered radicals are nucleophilic open-shell species extensively used in synthetic organic chemistry for the formation of C-heteroatom, $C(sp)$-$C(sp^3)$, $C(sp^2)$-$C(sp^3)$ and $C(sp^3)$-$C(sp^3)$ bonds.[26]

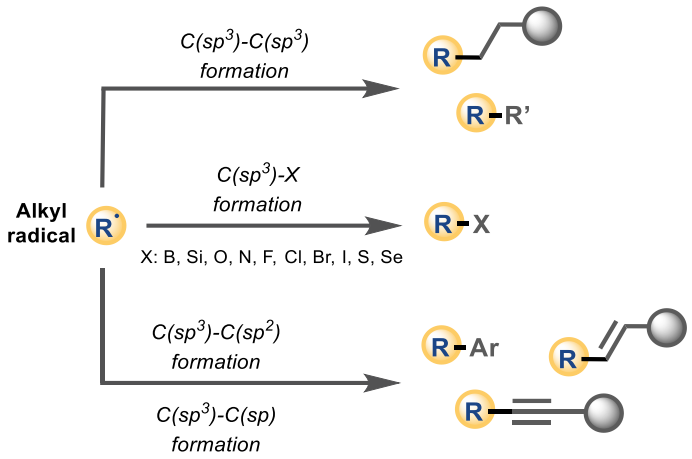

Scheme 1.7. Possible bonds formed by C-centered radicals.

Historically, in the mid-20th century, Bu_3SnH was reported for the generation of alkyl radicals via halogen abstraction, generating the corresponding C-centered radical from alkyl halides.[27] The generated radical is added onto an electron-poor olefin, alkylating it and further being protonated by hydrogen abstraction from Bu_3SnH, promoting a chain reaction well known as Giese reaction (Scheme 1.7).[28] The driving force of the process is based on the bond energy dissociation of the different bonds thar are broken and formed. Those new bonds formed, after recombination, are stronger than those existing before bond fragmentation. [29] The main drawback of this process resides on the use of stoichiometric amounts of organotin compounds and the generation of highly toxic organotin coproducts.[30] Several studies were performed to substitute tin as reagent like the employment of metal oxidants and reductants, as well as the use of different radical precursors.[29c] When Barton esters were reported as radical precursors it supposed a valuable impulse on the replacement of tin derivatives as radical generator. The derivatization of a carboxylic acid into a redox-active moiety, also known as electroauxiliary group, allowed the transformation of a stronger O-H bond (440 kJ/mol) into a more labile O-N bond (118 kJ/mol). Due to the colored aspect of Barton esters, it is possible for them to absorb light irradiation, with a subsequent fragmentation of the labile O-N bond when irradiated at 320 nm, therefore, harmful irradiation. [29c]

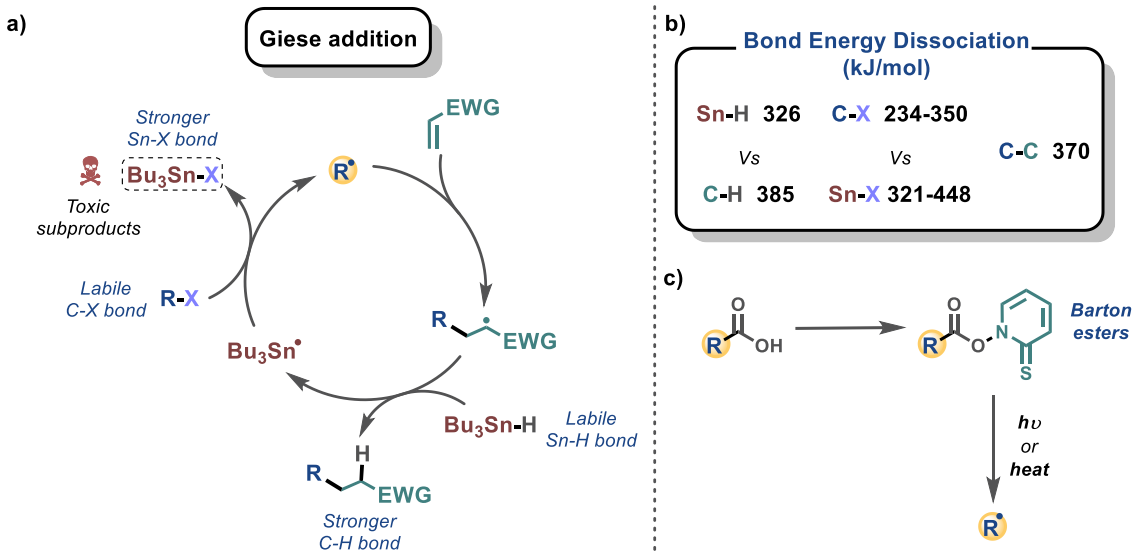

Scheme 1.8. a) Giese addition promoted by organotin derivatives. b) Bond energy dissociation of different bonds. c) Barton ester as alternative reagent for alkyl radical generation under thermal and/or photochemical conditions.

Photocatalytic approaches permit the generation of stabilized (α-oxy, α-amino, benzylic, allylic) and unstabilized alkyl radical species giving access to unconventional transformations in a more sustainable process by using photons as traceless reagents, using and generating less toxic compounds under milder conditions. While HAT or XAT gained more importance in synthetic chemistry, photoredox catalyzed processes remained less utilized as common functional groups (radical precursors) commonly have prohibitive oxidation pontentials (E_{ox}, E_{red}). It means that derivatization of functional groups needs to be done in order to access more oxidizable or reducible compounds. This derivatization is known as electroauxiliary group (EA), which confers a redox-active behaviour to the molecule.[31] The EA moiety is prone to be oxidized or reduced by the action of a photocatalyst via photoredox catalysis (SET event).

Once the original functional group is converted into an EA group (functional group interconversion, FGI) it can interact with a photocatalyst in its excited state. The radical precursor can be oxidized or reduced via a SET event by the PC* following a reducing quenching pathway or oxidizing quenching pathway respectively forming the corresponding radical ions and electrofugal subproducts (EA^+, EA^-). The unstable intermediate radical ion, upon further fragmentation, releases the alkyl

radical (Scheme 1.9). Anionic species are prone to be oxidized, i.e. alkyl carboxylates, while cationic species are prone to be reduced.

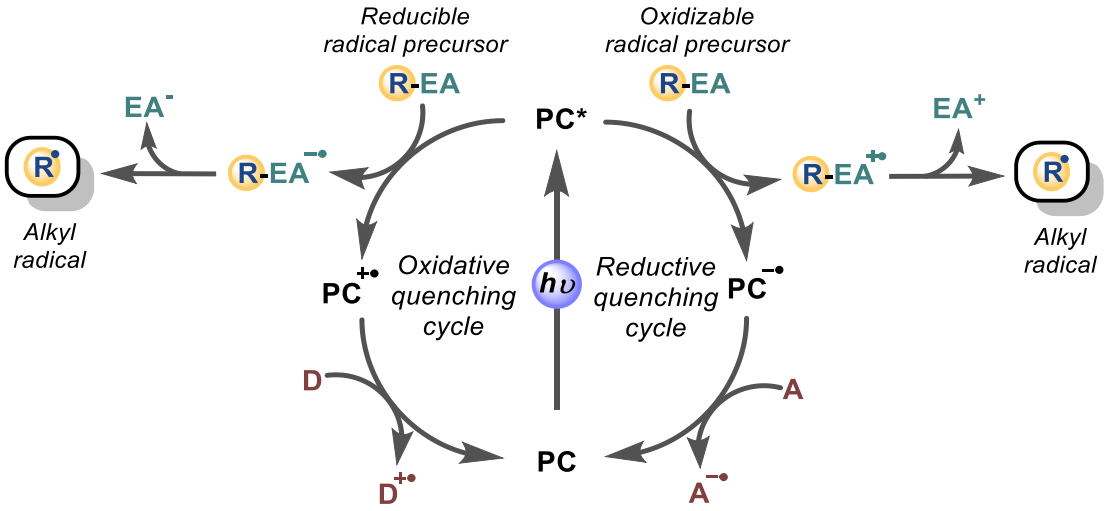

Scheme 1.9. Electroauxiliary groups (EA) as radical precursors on the photoredox-mediated alkyl radical generation.

Several radical precursors have been developed within the renaissance of photochemistry and photoredox catalysis. The generation of alkyl radicals can be achieved via C-heteroatom or C-C bond cleavage and the corresponding radical precursors can be divided in those oxidizable and those reducible (Figure 1.9). [32,33]

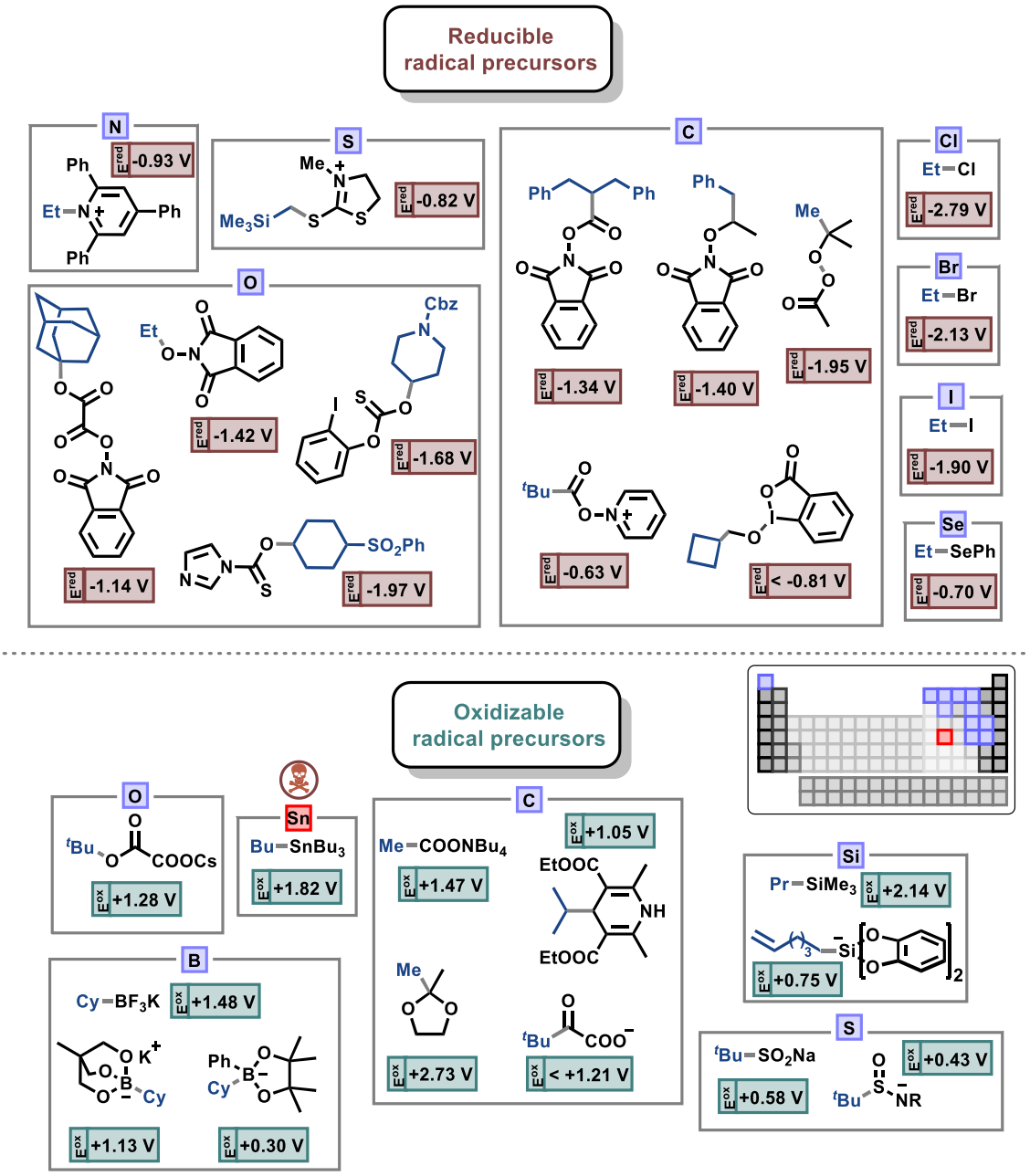

Figure 1.9. Oxidizable and reducible radical precursors for photoredox-mediated alkyl radical generation.

Carefully studying the reported radical precursors in Figure 1.9, it is worthy to mention that there is a big variety of uncharged reducible radical precursors. On the contrary, oxidizable uncharged radical precursors are underdeveloped. Due to solubility concerns, salts and charged radical precursors are limited to be employed when polar solvents are used, limiting factor on the application of this synthetic methodology. However, the development of oxidizable uncharged radical precursors via photoredox processes is certainly a niche to be covered. Due to this

fact, we think there is a niche for the development of new uncharged radical precursors to have access to more general C(sp^3)-C(sp^3) bond formation.

The main objective of this PhD dissertation is to discover new families of uncharged radical precursors. Chapters 2, 4 and 5 described the development of different uncharged radical precursors for the generation of alkyl radicals in a more effective, sustainable and efficient manner. We have demonstrated the applicability of those precursors on Late-Stage Functionalization (LSF) and in flow systems to synthesize building blocks or drug-like molecules. The automated synthesis of building blocks and drug-like molecules by using methodologies described in Chapter 5, is described in Chapter 6 during a secondment in Johnson & Johnson. In Chapter 3 it is reported a photoredox process for C1 homologation and synthesis of β-arylethylamines by using uncharged radical precursors demonstrating its potential in medicinal chemistry by the photo-induced functionalization of polypeptides in solid-state.

1.5 References.

1) Roth, H. D. The Beginnings of Organic Photochemistry. *Angew. Chem. Int. Ed. Engl.,* **1989**, *28*, 1193-1207.
2) Trommsdorff, H. Ueber Santonin. *Ann. Chem. Pharm. If*. **1834**, *11*, 190–207.
3) (a) Van Tamelen, E. E., Levin, S. H., Brenner, G., Wolinsky, J., Aldrich, P. The structure of photosantonic acid. *J. Am. Chem. Soc.* **1958**, *80*, 501 -502 (b) Chapman, O. L. and Englert, L. F. A Mechanistically Significant Intermediate in the Lumisantonin to Photosantonic Acid Conversion. *J. Am. Chem. Soc.* **1963**, *85*, 3028–3029. (c) Fisch, M. H. and Richards, G. H. The Mechanism of the Photoconversion of Santonin*. J. Am. Chem. Soc.* **1963**, *85*, 3029–3030.
4) Ciamician, G. The Photocehmistry of the Future. *Science*. **1912**, *36*, 385–394
5) (a) Büchi, G., Inman, C. G. and Lipinsky, E. S. Light-catalyzed Organic Reactions. I. The Reaction of Carbonyl Compounds with 2-Methyl-2-butene in the Presence of Ultraviolet Light. *J. Am. Chem. Soc.* **1954**, *76*, 4327 (b) Fréneau, M. and Hoffmann, N. The Paternò-Büchi reaction—Mechanisms and application to organic synthesis. *J. Photochem. Photobiol.* **2017**, *33*, 83-108.
6) Norrish, R. G. W. and Bamford, C. H. Photodecomposition of Aldehydes and Ketones. *Nature.* **1936**, *138*, 1016.

7) Planck, M. On the Law of Distribution of Energy in the Normal Spectrum. *Ann. Physik.* **1901**, *4*, 553.
8) Einstein, A. Concerning a Heuristic Point of View Toward the Emission and Transformation of Light. *Ann. Physik.* **1905**, *17*, 132-148.
9) Hammond, G. S. and Turro, N. J. Organic Photochemistry: The study of photochemical reactions provides new information on the excited states of molecules. *Science*. **1963**, *142*, 1541-1553.
10) Verhoeven, J. W. "Glossary of terms used in photochemistry (IUPAC Recommendations 1996)". *PAC*. **1996**, *68*, 2223-2286.
11) Braun, A.M., Maurette, M.-T. and Oliveros, E. *Photochemical technology*. **1991**. Jhon Wiley & Sons Ltd, West Sussex, England.
12) Scaiano, J.C. *Photochemistry essentials*. American Chemical Society, **2022**, DOI: 10.1021/acsinfocus.7e5031
13) Swinehart, D. F. The Beer-Lambert Law. *J. Chem. Educ.* **1962**, *39*, 333.
14) Dewar, M.J.S., Dougherty, R.C. *The PMO Theory of Organic Chemistry*. **1975**. Prentice-Hall, Englewood Cliffs, NJ.
15) Turro, N.J. *Modern Molecular Photochemistry*, **1978**. Benjamin/Cummings, Menlo Park, Calif.
16) McGlinn, S.P., Azumi, T. and Kinoshita, N. *Molecular spectroscopy of triplet state*. **1969**. Prentice-Hall, Englewood Cliffs, NJ.
17) Lefebvre-Brion, H. and Field, R. W. *The Spectra and Dynamics of Diatomic Molecules*, Edt: Lefebvre-Brion, H. and Field, R. W. **2004**. Academic Press.
18) Braslavsky, S. E. *"Glossary of terms used in photochemistry, 3rd edition* (IUPAC Recommendations 2006)" *Pure Appl. Chem*. **2007**, *79*, 293-465.
19) Dexter, D.L. A Theory of Sensitized Luminescence in Solids *J. Chem. Phys.* **1953**, *21*, 836-850.
20) Capaldo, L., Ravelli, D. and Fagnoni, M. Direct Photocatalyzed Hydrogen Atom Transfer (HAT) for Aliphatic C–H Bonds Elaboration. *Chem. Rev.* **2022**, *122*, 1875–1924.
21) Juliá, F., Constantin, T. and Leonori, D. Applications of Halogen-Atom Transfer (XAT) for the Generation of Carbon Radicals in Synthetic Photochemistry and Photocatalysis. *Chem. Rev*. **2022**, *122*, 2292–2352.

22) Prier, C. K., Rankic, D. A. and MacMillan, D. W. C. Visible Light Photoredox Catalysis with Transition Metal Complexes: Applications in Organic Synthesis. *Chem. Rev*. **2013**, *113*, 5322–5363.

23) Hassaan, M.A., El-Nemr, M.A., Elkatory, M.R. Ragab, S., Niculescu, V.-C. and El Nemr, A. Principles of Photocatalysts and Their Different Applications: A Review. *Top Curr. Chem.* **2023**, *381*, 31.

24) (a) Pijper, B., Abdiaj, I., Leonori, D. and Alcázar. J. Development of an Automated Platform for C(sp3)-C(sp3) Bond Formation via XAT Chemistry. *ChemCatChem*. **2023**, *15*, e202201289. (b) Pijper, B., Martín, R., Huertas-Alonso, A. J., Linares, M. L., López, E., Llaveria, J., Díaz-Ortiz, Á., Dixon, D. J., De la Hoz, A. and Alcázar, J. Fully Automated Flow Protocol for $C(sp^3)–C(sp^3)$ Bond Formation from Tertiary Amides and Alkyl Halides. *Org. Lett*. **2024**, *26*, 2724–2728.

25) (a) Lovering, F. Escape from Flatland 2: complexity and promiscuity. *Med. Chem. Commun.* **2013**, *3*, 515–519. (b) Meyers, J., Carter, M., Mok, N. Y. and Brown, N. On the origins of three-dimensionality in drug-like molecules. *Future Med. Chem*. **2016**, *8*, 1753–1767. (c) Wei, W., Cherukupalli, S., Jing, L., Liu, X. and Zhan, P. Fsp3: A new parameter for drug-likeness. *Drug Discov. Today*. **2020**, *10*, 1839-1845.

26) (a) Sadhna Shah, Braja Gopal Das, Vinod Kumar Singh. Recent advancement in copper-catalyzed asymmetric reactions of alkynes, *Tetrahedron Lett.* **2021**, *93*, 132238. (b) Dinh, L.P., Starbuck, H.F., Hamby, T.B. LaLama, M. J., He, C. Q., Kalyani, D. and Sevov, C. S. Persistent organonickel complexes as general platforms for Csp2–Csp3 coupling reactions. *Nat. Chem*. **2024**. DOI: 10.1038/s41557-024-01528-7. (c) Crespi, S. and Fagnoni, M. Generation of Alkyl Radicals: From the Tyranny of Tin to the Photon Democracy. *Chem. Rev.* **2020**, *120*, 9790–9833.

27) Kuivila, H. G. and Menapace, L. W. Reduction of Alkyl Halides by Organotin Hydrides. *J. Org. Chem*. **1963**, *28*, 2165–216.

28) (a) Giese, B. Formation of C-C Bonds by Addition of Free Radicals to Alkenes. *Angew. Chem., Int. Ed. Engl.* **1983**, *22*, 753–764. (b) Giese, B., González-Gómez, J. A. and Witzel, T. The Scope of Radical C-C Coupling by the "Tin Method". *Angew. Chem., Int. Ed. Engl*. **1984**, *23*, 69–70. (c) Giese, B., and Dupuis, J. Diastereoselective Syntheses of Glycopyranosides. *Angew. Chem. Int. Ed. Engl.*

1983, *22*, 622–623. (d) Giese, B. Syntheses with Radicals-C-C Bond Formation via Organotin and Organomercury Compounds. *Angew. Chem. Int. Ed. Engl.* **1985**, *24*, 553–565.

29) (a) Galli, C., and Pau, T. The Dehalogenation Reaction of Organic Halides by Tributyltin Radical: The Energy of Activation vs. the BDE of the C-X Bond. *Tetrahedron Lett.* **1998**, *54*, 2893–2904. (b) Luo, Y.-R. *Comprehensive Handbook of Chemical Bond Energies.* **2007**. CRC Press: Boca Raton. (c) Allonas, X., Dietlin, C., Fouassier, J.-P., Casiraghi, A., Visconti, M., Norcini, M., Bassi, G. Barton Esters as New Radical Photoinitiators for Flat Panel Display Applications. *J. Photopolym. Sci. Technol*. **2008**, *21*, 505–509.

30) Davies, A. G. *Organotin Chemistry, Second, Completely Revised and Updated ed.* **2004**. John Wiley & Sons, Ltd.

31) Yoshida, J., Shimizu, A. and Hayashi, R. Electrogenerated Cationic Reactive Intermediates: The Pool Method and Further Advances. *Chem. Rev*. **2018**, *118*, 4702–4730.

32) (a) Klauck, F. J. R., James, M. J., Glorius, F. Deaminative Strategy for the Visible-Light-Mediated Generation of Alkyl Radicals. *Angew. Chem. Int. Ed*. **2017**, *56*, 12336–12339. (b) Zhang, P., Le, C. C., MacMillan, D. W. C. Silyl Radical Activation of Alkyl Halides in Metallaphotoredox Catalysis: A Unique Pathway for Cross-Electrophile Coupling. *J. Am. Chem. Soc.* **2016**, *138*, 8084–8087. (c) Roth, H., Romero, N., Nicewicz, D. Experimental and Calculated Electrochemical Potentials of Common Organic Molecules for Applications to Single-Electron Redox Chemistry. *Synlett.* **2016**, *27*, 714–723. (d) Cossy, J., Ranaivosata, J.-L., Bellosta, V. Formation of Radicals by Irradiation of Alkyl Halides in the Presence of Triethylamine. *Tetrahedron Lett.* **1994**, *35*, 8161–8162. (e) Isse, A. A., Lin, C. Y., Coote, M. L., Gennaro, A. Estimation of Standard Reduction Potentials of Halogen Atoms and Alkyl Halides. *J.Phys. Chem. B.* **2011**, *115*, 678–684. (f) Lambert, F. L., Ingall, G. B. Voltammetry of Organic Halogen Compounds. IV. The Reduction of Organic Chlorides at the Vitreous (Glassy) Carbon Electrode. *Tetrahedron Lett.* **1974**, *15*, 3231–3234. (g) Lambert, F. L., Kobayashi, K. Polarography of Organic Halogen Compounds. I. Steric Hindrance and the Half-Wave Potential in Alicyclic and Aliphatic Halides 1,2. *J. Am. Chem. Soc.* **1960**, *82*, 5324–5328. (h) Vasudevan, D. Direct and Indirect Electrochemical Reduction of

Organic Halides in Aprotic Media. *Russ. J. Electrochem*. **2005**, *41*, 310−314. (i) Nawrat, C. C., Jamison, C. R., Slutskyy, Y., MacMillan, D. W.C., Overman, L. E. Oxalates as Activating Groups for Alcohols in Visible Light Photoredox Catalysis: Formation of Quaternary Centers by Redox-Neutral Fragment Coupling. *J. Am. Chem. Soc.* **2015**, *137*, 11270−11273. (j) Han, J. Bin, Guo, A., Tang, X. Y. Alkylation of Allyl/Alkenyl Sulfones by Deoxygenation of Alkoxyl Radicals. *Chem. Eur. J.* **2019**, *25*, 2989−2994. (k) Capaldo, L., Ravelli, D. Alkoxy Radicals Generation: Facile Photocatalytic Reduction of N -Alkoxyazinium or Azolium Salts. *Chem. Commun*. **2019**, *55*, 3029−3032. (l) Lackner, G. L., Quasdorf, K. W., Overman, L. E. Direct Construction of Quaternary Carbons from Tertiary Alcohols via Photoredox-Catalyzed Fragmentation of Tert-Alkyl N-Phthalimidoyl Oxalates. *J. Am. Chem. Soc.* **2013**, *135*, 15342−15345. (m) Chenneberg, L., Baralle, A., Daniel, M., Fensterbank, L., Goddard, J. P., Ollivier, C. Visible Light Photocatalytic Reduction of O-Thiocarbamates: Development of a Tin-Free Barton-McCombie Deoxygenation Reaction. *Adv. Synth. Catal.* **2014**, *356*, 2756−2762. (n) DiRocco, D. A., Dykstra, K., Krska, S., Vachal, P., Conway, D. V., Tudge, M. Late-Stage Functionalization of Biologically Active Heterocycles through Photoredox Catalysis. *Angew. Chem. Int. Ed.* **2014**, *53*, 4802−4806. (o) Wu, J., Bär, R. M., Guo, L., Noble, A., Aggarwal, V. K. Photoinduced Deoxygenative Borylations of Aliphatic Alcohols. *Angew. Chem, Int. Ed.* **2019**, *58*, 18830−18834. (p) Vara, B. A., Patel, N. R., Molander, G. A. O-Benzyl Xanthate Esters under Ni/Photoredox Dual Catalysis: Selective Radical Generation and Csp3−Csp2 Cross-Coupling. *ACS Catal*. **2017**, *7*, 3955−3959. (q) Lackner, G. L., Quasdorf, K. W., Pratsch, G., Overman, L. E. Fragment Coupling and the Construction of Quaternary Carbons Using Tertiary Radicals Generated from Tert-Alkyl N-Phthalimidoyl Oxalates by Visible-Light Photocatalysis. *J. Org. Chem*. **2015**, *80*, 6012−6024. (r) Syroeshkin, M. A., Krylov, I. B., Hughes, A. M., Alabugin, I. V., Nasybullina, D. V., Sharipov, M. Y., Gultyai, V. P., Terent'ev, A. O. Electrochemical Behavior of N-Oxyphthalimides: Cascades Initiating Self-Sustaining Catalytic Reductive N-O Bond Cleavage. *J. Phys. Org. Chem*. **2017**, *30*, No. e3744. (s) Yasu, Y., Koike, T., Akita, M. Visible Light-Induced Selective Generation of Radicals from Organoborates by Photoredox Catalysis. *Adv. Synth. Catal.* **2012**, *354*, 3414−3420. (t) Lima, F., Sharma, U. K., Grunenberg, L., Saha, D., Johannsen, S.,

Sedelmeier, J., Van der Eycken, E. V., Ley, S. V. A Lewis Base Catalysis Approach for the Photoredox Activation of Boronic Acids and Esters. *Angew. Chem. Int. Ed.* **2017**, *56*, 15136–15140. (u) Li, G. X., Morales-Rivera, C. A., Wang, Y., Gao, F., He, G., Liu, P., Chen, G. Photoredox-Mediated Minisci C-H Alkylation of NHeteroarenes Using Boronic Acids and Hypervalent Iodine. *Chem. Sci.* **2016**, *7*, 6407–6412. (v) Shu, C., Noble, A., Aggarwal, V. K. Photoredox-Catalyzed Cyclobutane Synthesis by a Deboronative Radical Addition–Polar Cyclization Cascade. *Angew. Chem. Int. Ed*. **2019**, *58*, 3870–3874. (w) Xue, F., Wang, F., Liu, J., Di, J., Liao, Q., Lu, H., Zhu, M., He, L., He, H., Zhang, D., et al. A Desulfurative Strategy for the Generation of Alkyl Radicals Enabled by Visible-Light Photoredox Catalysis. *Angew. Chem., Int. Ed.* **2018**, *57*, 6667–6671. (x) Knauber, T., Chandrasekaran, R., Tucker, J. W., Chen, J. M., Reese, M., Rankic, D. A., Sach, N., Helal, C. Ru/Ni Dual Catalytic Desulfinative Photoredox Csp2-Csp3 Cross-Coupling of Alkyl Sulfinate Salts and Aryl Halides. *Org. Lett.* **2017**, *19*, 6566–6569. (y) Xu, N., Zhang, Y., Chen, W., Li, P., Wang, L. Photoinduced N-Methylation and N-Sulfonylation of Azobenzenes with DMSO Under Mild Reaction Conditions. *Adv. Synth. Catal.* **2018**, *360*, 1199–1208. (z) Zemtsov, A. A., Ashirbaev, S. S., Levin, V. V., Kokorekin, V. A., Korlyukov, A. A., Dilman, A. D. Photoredox Reaction of 2-Mercaptothiazolinium Salts with Silyl Enol Ethers. *J. Org. Chem*. **2019**, *84*, 15745–15753.

33) (a) Pandey, G., Rao, K. S. S. P., Sekhar, B. B. V. S. Photosensitized One-Electron Reductive Cleavage of a Carbon–Selenium Bond: A Novel Chemoselective Deselenenylation and Phenylselenenyl Group Transfer Radical Chain Reaction. *J. Chem. Soc., Chem. Commun*. **1993**, *21*, 1636–1638. (b) Pandey, G., Sesha Poleswara Rao, K. S., Nageshwar Rao, K. V. Photosensitized Electron Transfer Promoted Reductive Activation of Carbon-Selenium Bonds to Generate Carbon-Centered Radicals: Application for Unimolecular Group Transfer Radical Reactions. *J. Org. Chem.* **1996**, *61*, 6799–6804. (c) Lucas, M. A., Schiesser, C. H. (Aryltelluro)Formates as Precursors of Alkyl Radicals: Thermolysis and Photolysis of Primary and Secondary Alkyl (Aryltelluro)Formates. *J. Org. Chem.* **1996**, *61*, 5754–5761. (d) Yamago, S. Development of Organotellurium-Mediated and Organostibine-Mediated Living Radical Polymerization Reactions. *J. Polym. Sci*., Part A: Polym. Chem. **2006**, *44*, 1–12. (e) Togo, H., Aoki,

M., Kuramochi, T., Yokoyama, M. Radical Decarboxylative Alkylation onto Heteroaromatic Bases with Trivalent Iodine Compounds. *J. Chem. Soc., Perkin Trans.* **1993**, *20*, 2417. (f) Wirth, T. *Hypervalent Iodine Chemistry.* **2003**, 224. Ed: Wirth, T. Topics in Current Chemistry, Springer: Berlin. (g) Gutierrez-Bonet, Á., Tellis, J. C., Matsui, J. K., Vara, B. A., Molander, G. A. 1,4-Dihydropyridines as Alkyl Radical Precursors: Introducing the Aldehyde Feedstock to Nickel/Photoredox Dual Catalysis. *ACS Catal.* **2016**, *6*, 8004−8008. (h) Nakajima, K., Nojima, S., Sakata, K., Nishibayashi, Y. Visible-Light-Mediated Aromatic Substitution Reactions of Cyanoarenes with 4-Alkyl-1,4-dihydropyridines through Double Carbon−Carbon Bond Cleavage. *ChemCatChem*. **2016**, *8*, 1028−1032. (i) Okada, K., Okamoto, K., Oda, M. A New and Practical Method of Decarboxylation: Photosensitized Decarboxylation of NAcyloxyphthalimides via Electron-Transfer Mechanism. *J. Am. Chem. Soc.* **1988**, *110*, 8736−8738. (j) Mella, M., Fasani, E., Albini, A. Electron Transfer Photoinduced Cleavage of Acetals. A Mild Preparation of Alkyl Radicals. *J. Org. Chem.* **1992**, *57*, 3051−3057. (k) Sun, A. C., McClain, E. J., Beatty, J. W., Stephenson, C. R. J. Visible Light-Mediated Decarboxylative Alkylation of Pharmaceutically Relevant Heterocycles. *Org. Lett*. **2018**, *20*, 3487−3490. (l) Benson, S. W. Kinetics of Pyrolysis of Alkyl Hydroperoxides and Their O−O Bond Dissociation Energies. *J. Chem. Phys*. **1964**, *40*, 1007−1013. (m) Liu, J., Liu, Q., Yi, H., Qin, C., Bai, R., Qi, X., Lan, Y., Lei, A. Visible-Light-Mediated Decarboxylation/Oxidative Amidation of α-Keto Acids with Amines under Mild Reaction Conditions Using O2. *Angew. Chem. Int. Ed.* **2014**, *53*, 502−506. (n) Chen, J.-Q., Chang, R., Wei, Y.-L., Mo, J.-N., Wang, Z.-Y., Xu, P.-F. Direct Decarboxylative−Decarbonylative Alkylation of α-Oxo Acids with Electrophilic Olefins via Visible-Light Photoredox Catalysis*. J. Org. Chem*. **2018**, *83*, 253−259. (o) Okada, K., Okamoto, K., Morita, N., Okubo, K., Oda, M. Photosensitized Decarboxylative Michael Addition through N-(Acyloxy)Phthalimides via an Electron-Transfer Mechanism. *J. Am. Chem. Soc.* **1991**, *113*, 9401−9402. (p) Zhang, J., Li, Y., Xu, R., Chen, Y. Donor−Acceptor Complex Enables Alkoxyl Radical Generation for Metal-Free C(sp3)−C(sp3) Cleavage and Allylation/Alkenylation. *Angew. Chem. Int. Ed.* **2017**, *56*, 12619−12623. (q) Beatty, J. W., Douglas, J. J., Cole, K. P., Stephenson, C. R. J. A Scalable and Operationally Simple Radical Trifluoromethylation. *Nat. Commun.*

2015, *6,* 7919. (r) Yang, J.-D., Li, M., Xue, X.-S. Computational I(III)-X BDEs for Benziodoxol(on)e-Based Hypervalent Iodine Reagents: Implications for Their Functional Group Transfer Abilities. *Chin. J. Chem.* **2019**, *37*, 359−363. (s) Hu, X., Li, G.-X., He, G., Chen, G. Minisci C−H Alkylation of N-Heteroarenes with Aliphatic Alcohols via β-Scission of Alkoxy Radical Intermediates. *Org. Chem. Front*. **2019**, *6*, 3205−3209.

Chapter 2

Silyl Ethers as Radical Precursors via Organophotocatalyzed C-Si Bond Fragmentation

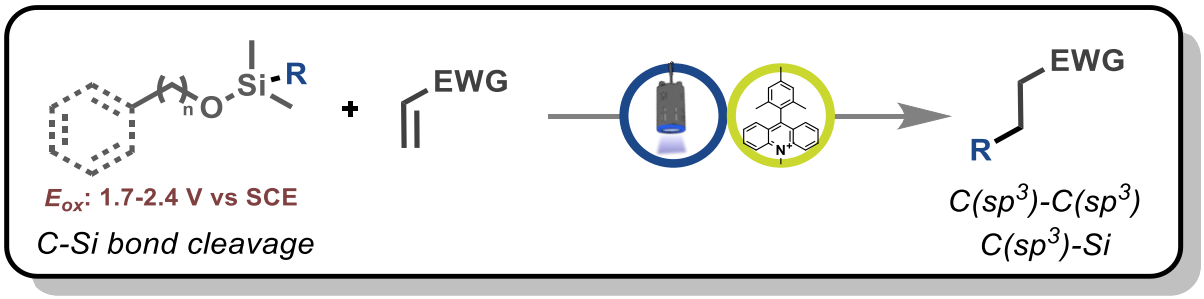

This chapter is based on:

Luguera Ruiz, A., Benazzi, V., Tucci, F., Rizzo, F., Merli, D., Protti, S. and Fagnoni, M. Silyl Ethers as Radical Precursors via Organophotocatalyzed C-Si Bond Fragmentation. *Adv. Synth. Catal.* **2024**, *366*, 1-8.

2.1 Introduction.

Photochemical carbon-centered radical generation is currently a hot topic since it allows the forging of C-X bonds in a sustainable manner compared with traditional methodologies, typically employing stoichiometric amounts of reductants or oxidants, toxic species, and harsh conditions.[1] Organosilicon compounds found application in the (photo)generation of reactive intermediates[2] even due to their lower toxicity in comparison to organostannanes.[1g,3] In this context, photogenerated silyl radicals are key-intermediates in XAT reactions,[4] benzoyldiisopropylchlorosilanes were purposely designed as photocleavable protecting group for alcohols[5] and silanols were used to generate alkyl radicals via β-scission of a LMCT complex by using Ce^{III} salts.[6] However, one of the main advantages in having a silicon atom in organic derivatives is the profound effect exerted on their electrochemical behaviour when they contain π-systems and/or heteroatoms.[7] Thus, in compounds bearing heteroatoms such as oxygen, nitrogen, and sulfur, the presence of a silyl group markedly makes them easier to be oxidized. This is apparent from the E_{ox} values of ethers (**2.I**) and (protected) amines (**2.II**) in comparison with the corresponding α-silyl ethers (**2.Ia**) or (protected) α-silylamines (**2.IIa**, see Figure 2.1a).[7] This has important implications in photoredox catalysis since easily oxidizable silanes were used for the release of carbon radicals. Indeed, the silyl moiety functions as a redox auxiliary group and is able to promote the formation of the corresponding radical cation that in turn fragments releasing the radical of interest.[8] Typical cases are the release of α-oxy radicals (from α-silyl ethers **2.Ia**[9]), α-amino radicals (from α-silylamines **2.III**[10]), allyl radicals (from allyl silanes **2.IV**[11]), benzyl radicals (from benzyl silanes **2.V**[12]) and acyl radicals (from acyl silanes **2.VI**,[13] Figure 1b). On the contrary, the reactivity of unfunctionalized tetraalkylsilanes **2.VII** towards monoelectronic oxidation is very low, since the oxidation potential of such compounds is > 2.5 V thus requiring harsh conditions.[7c,14]

Nevertheless, it was described in the early 90s detailing the photochemical alkylation of pyrylium salts[15] and of aromatic nitriles (e.g. 1,2,4,5 tetracyanobenzene, TCB)[16] via photoinduced electron transfer with tetralkylsilanes. In this case, the high reduction potential in the excited state of these aromatics

allowed for the oxidation of R_4Si and the radical released from the resulting radical cation is then able to couple with the aromatic radical anion. Despite this was an interesting case of aromatic carbon-carbon ipso-substitution reaction,[17] the only fate of the radical is the functionalization of the absorbing species. A recent and elegant strategy for the generation of alkyl radicals involves hypervalent bis-catecholato silicates **2.VIII** (E_{ox} < 1 V vs SCE[1c,1] Figure 2.1b) including Martin silicates **2.IX** (E_{ox} ca. 1.5 V vs SCE[19]). However, the preparation of these charged silicon derivatives is not so trivial.

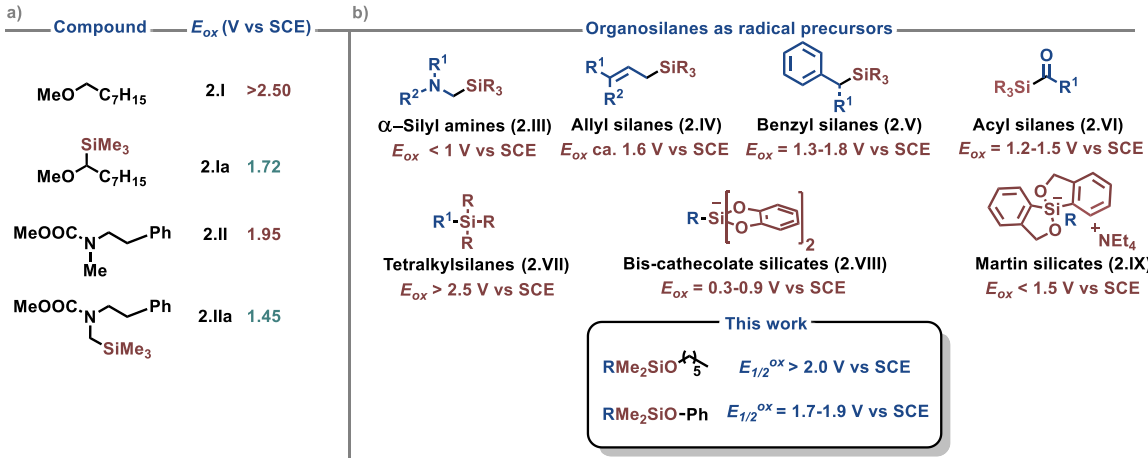

Figure 2.1. a) Comparison of the oxidation potential of organic compounds with those incorporating a trialkylsilyl groups. b) Silicon based derivatives used in photoredox catalysis and in this work.

On the other hand, despite alcohols are very difficult to oxidize (e.g. E_{ox} EtOH > 3.5 V vs SCE[20], Figure 1b) their conversion into silyl ethers was found to be beneficial (the E_{ox} $EtOSiMe_3$ was reported to be lower with respect to the corresponding alcohol; > 2.5 V vs SCE[21]). The oxidative capability of the silyl ether depends on the alcohol chain and not on the different substitutions in the silyl group (as an example the E_{ox} Et_3Si-H and Bu_3Si-H are 2.15 V vs SCE[22] and ca. 2.5 V vs SCE[23], respectively).

In the frame of finding new neutral radical precursors,[24] we deemed them worthwhile to investigate a more accessible class of silyl derivatives namely silyl ethers in the role of alkyl radical precursors.

Whereas the (direct) photochemistry of such compounds has received only few attentions,[25-27] sparse examples were reported on the photocatalyzed generation of alkyl radicals from silyl ethers by using cyanoarenes as photooxidants. Thus, 320

nm irradiation of TCB, in the presence of *tert*-butyldimethyl(octyloxy)silane led to the release of a *tert*-butyl radical **2.I** that coupled with the generated radical anion of the cyanoarene to afford tert-butylated tricyano benzene **2.II** as the exclusive product.[28] However, when an electron-poor olefin was present in the mixture, Giese-type reaction takes place, generating the radical adduct **2.III.** Functionalization of cyanoarene radical anion competes with the SET step, obtaining a mixture of ipsosubstituted derivative **2.IV** and **2.V** in 58% yield (path a) and the hydroalkylated product **2.VI** in 84% yield (path b).[29]

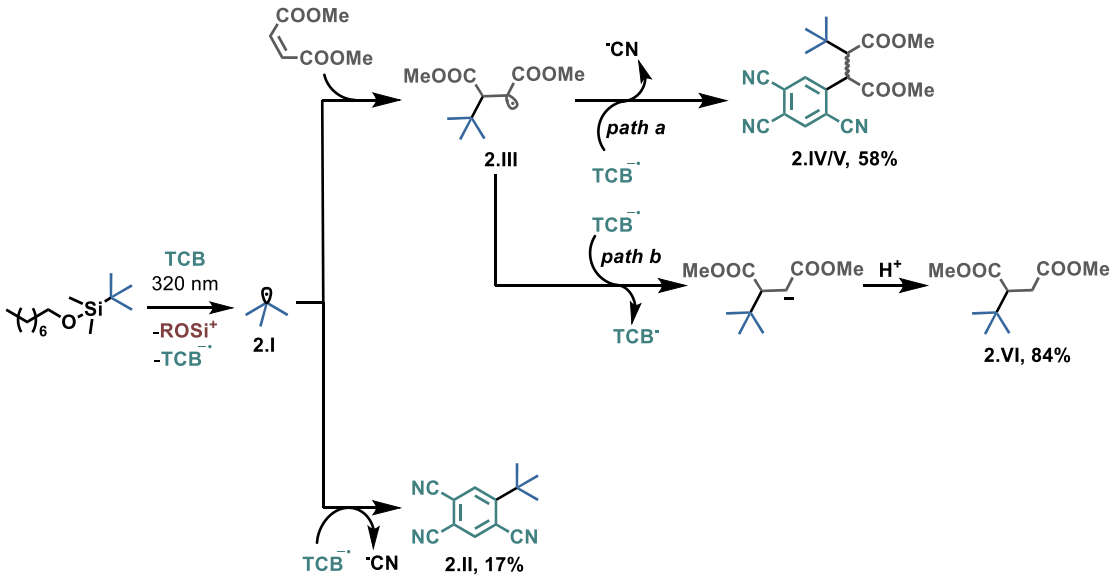

Scheme 2.1. Precedents on the use of silyl ethers as alkyl radical precursor under light irradiation.

In view of these premises, we thus reconsidered the potentialities of silyl ethers as C and Si radical precursors under photoredox catalyzed conditions, by taking advantage on the oxidizability of the Si-O bond in trialkylalkoxysilanes.

2.2 Results and discussions.

Two different families of silyl ethers were synthesized, namely phenyl silyl ethers **2.1a-g** and alkyl silyl ethers **2.1h-o** (Scheme 2.2). These compounds were easily prepared in excellent to quantitative yields starting from phenols or alcohols by treatment with the corresponding trialkyl silyl chloride in the presence of DBU.

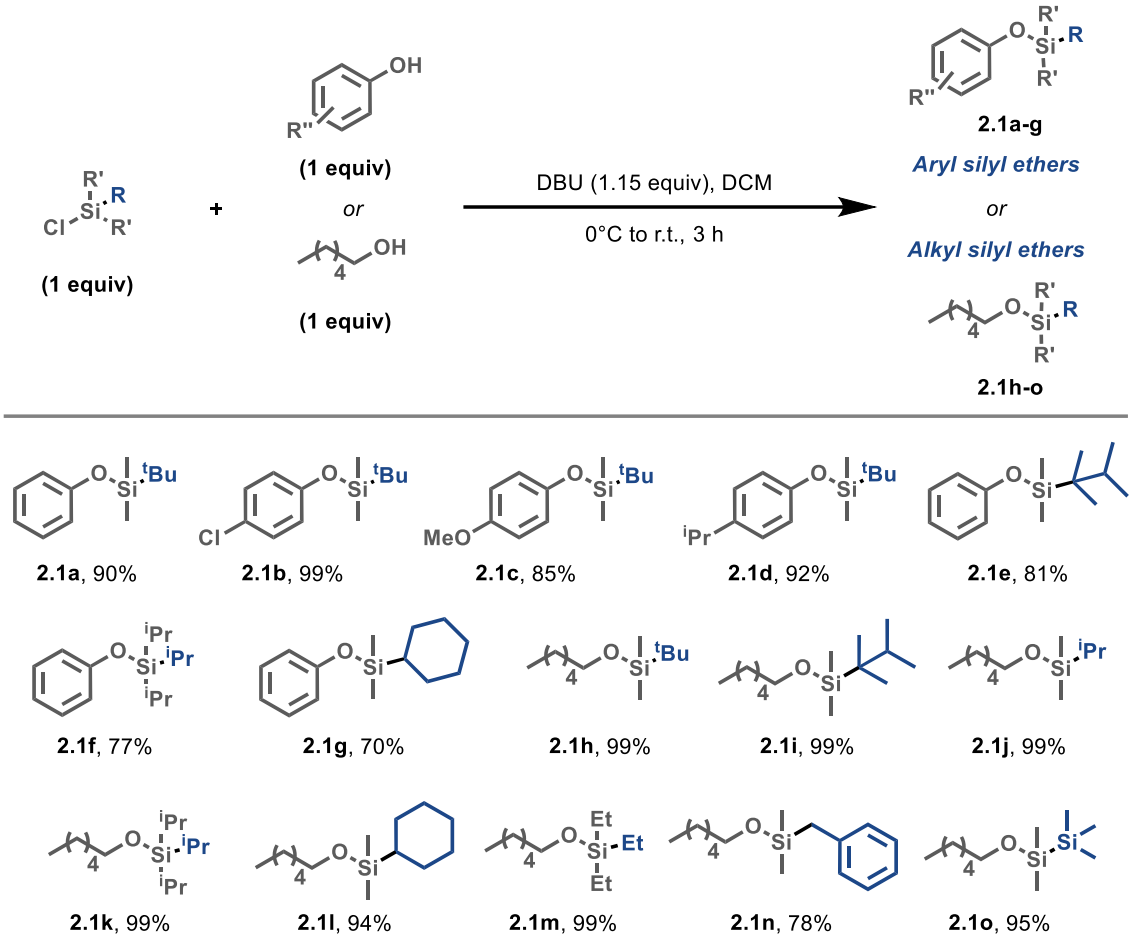

Scheme 2.2. Synthesis of silyl ethers tested in the present work.

We thus measured the oxidation potential of the synthesized silyl ethers (Table 2.1) to have indication on the choice of the photocatalyst to be used. The corresponding cyclic voltammetry of compounds **2.1e**, **2.1i**, **2.1o** and **biphenyl** (**BP**) are shown in Figures 2.1-2.2. As apparent from Table 2.1, compounds **2.1a-g**, derived from phenols, are markedly easier to be oxidized with respect to that formed from alcohols **2.1h-o**. The aromatic silyl ethers have an E_{ox} of about 1.7-1.9 V vs SCE whereas the aliphatic ones have E_{ox} values up to 2.4 V vs SCE except the case of disilane **2.1o** (E_{ox} = 1.55 V vs SCE).

Table 2.1. Oxidation potential of the silyl ethers tested in the present work.

Silyl ether	$E_{1/2}^{ox}$ ($R^{\cdot+}$/R) (V vs SCE)	Silyl ether	$E_{1/2}^{ox}$ ($R^{\cdot+}$/R) (V vs SCE)
2.1a	+ 1.84	2.1h	+ 2.03
2.1b	+ 1.70	2.1i	+ 2.27
2.1c	+ 1.68	2.1j	+ 2.32
2.1d	+ 1.68	2.1k	+ 2.44
2.1e	+ 1.94	2.1l	+ 1.95
2.1f	+ 1.69	2.1m	+ 2.45
2.1g	+ 1.82	2.1n	+ 2.05
BP	+ 1.95	2.1o	+ 1.55

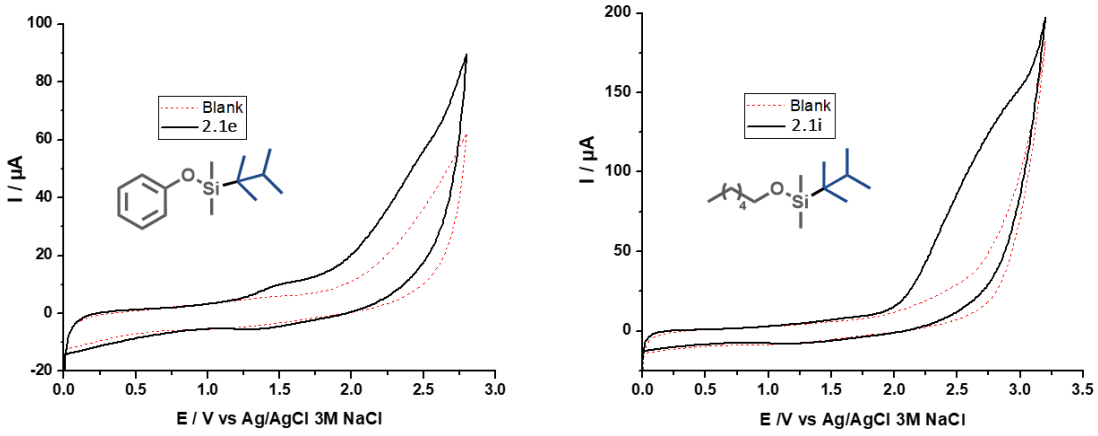

Figure 2.1. Cyclic voltammetry carried out on compound **2.1e** and **2.i**.

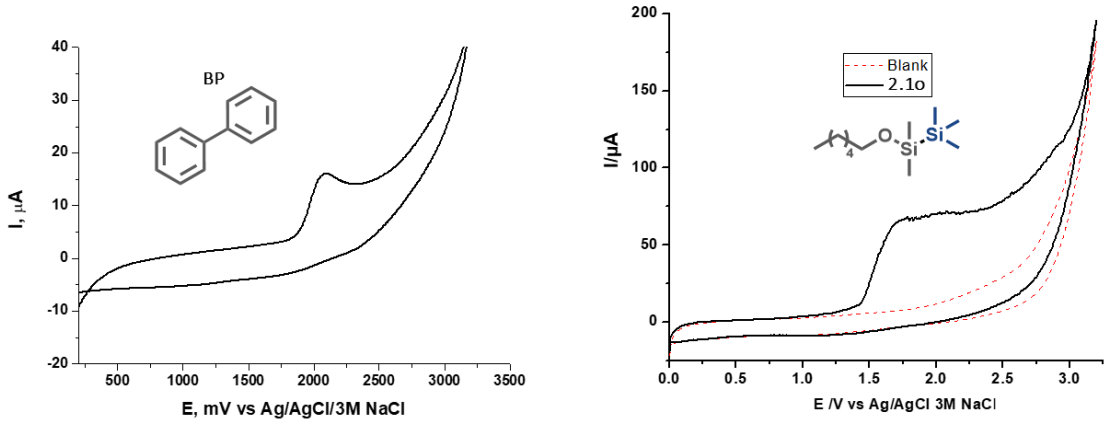

Figure 2.2. Cyclic voltammetry carried out on **BP** and compound **2.1o**.

To confirm our hypothesis, we focused on the *tert*-butylation of phenyl vinyl sulfone by **2.1a** to form compound **2.3** as the model reaction. We embarked on a deep optimization process by screening different solvents and solvent mixtures, different photocatalysts (including photoorganocatalysts Acr^+-Mes and NMQ^+ salts) under different conditions (Table 2.2).

The best conditions involved the use of Fukuzumi's catalyst, (9-mesityl-10-methylacridinium tetrafluoroborate, 10 mol%) having an E_{red} ($*PC^n/PC^{n-1}$) = +2.06 V vs SCE.[30] As previously observed in the oxidation of silanes,[12b] a lithium salt ($LiClO_4$, 0.2 equiv.) and biphenyl (BP, 0.5 equiv.) as additives were beneficial for the reaction. Upon irradiation of the solution containing phenyl vinyl sulfone **2.2a** (1 equiv.), in acetonitrile, at 405 nm (Evoluchem lamp, 18 W) for 24 h gave product **2.3** in 94% yield (Table 2.2, entry 1).

The additives have a key role on the performance of the reaction because their absence caused a yield drop (entry 6). Decreasing the amount of the acridinium salt to 5 mol % (entry 18) or of the silyl ether to 1 equiv. (entry 15) had a deleterious effect on the reaction yield. Addition of a protic solvent (water) to the reaction mixture was likewise detrimental to the reaction course (entries 4, 5). When the photocatalyst was replaced by other strong oxidizing PC such as NMQ^+ (E_{red} ($*PC^n/PC^{n-1}$) = +2.7 V vs SCE)[31] and pyrylium salt (E_{red} ($*PC^n/PC^{n-1}$) = +2.3 V vs SCE)[32] the product was not formed (entries 9-12).

Table 2.2. Optimization results for the synthesis of **2.3.**

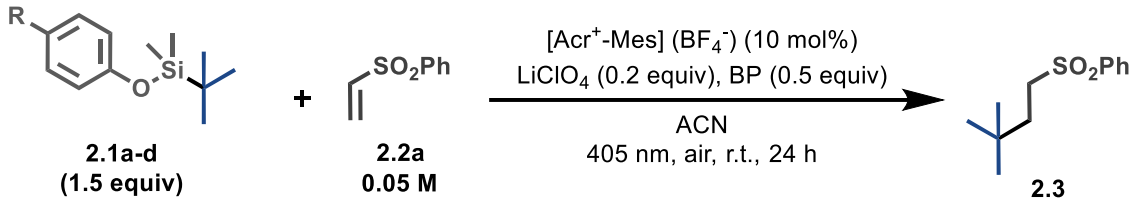

Entry	Deviations from the standard conditions	2.3 (% Yield)
1	**2.1a**	**94**
2	**2.1a**, MeOH as solvent, No additives	-
3	**2.1a**, MeOH as solvent, N_2, No additives, 72 h	-
4	**2.1a**, ACN/H_2O (9:1), N_2, No additives	-
5	**2.1a**, ACN/H_2O (9:1), No additives	-
6	**2.1a**, No additives, 72 h	61
7	**2.1a**, only BP (0.5 equiv.) as additive	59
8	**2.1a**, only $LiClO_4$ (0.2 equiv.) as additive	84
9	**2.1a**, $NMQ^+ I^-$ (10 mol%), N_2, No additives	-
10	**2.1a**, $NMQ^+ I^-$ (10 mol%), $LiClO_4$ only (0.2 equiv.) as additive	-
11	**2.1a**, $NMQ^+ I^-$ (10 mol%), No additives	-
12	**2.1a**, $NMQ^+ I^-$ (10 mol%), BP (0.5 equiv.)	-
13	**2.1a**, $[Ph_3Py]^+ (BF_4^-)$ (10 mol%), No additives	-
14	**2.1a**, $[Ph_3Py]^+ (BF_4^-)$ (10 mol%), N_2, No additives	-
15	**2.1a** (1.0 equiv.)	63
16	**2.1a** (1.3 equiv.)	87
17	**2.1b** (1.5 equiv.)	71
18	**2.1a** (1.5 equiv.), [Acr+-Mes] (BF_4^-) (5 mol%)	67
19	**2.1c** (1.5 equiv.)	-
20	**2.1d** (1.5 equiv.)	-
21	**2.1a** (1.5 equiv), No light	-
22	**2.1a** (1.5 equiv.), No PC	-
23	TEMPO (1.0 equiv)	-
24	**2.1h** (1.5 equiv.)	64

NMQ^+I^- has been prepared as described in literature.[52]

We next evaluated the effect of the substituents on the aromatic ring of the *tert*-butyl silyl ethers on the reaction outcome. Interesting is the fact that the substitution led to a better oxidizability of the silyl ethers (compare the E_{ox} of **2.1a** with **2.1b-d**, Table 2.1). Only in the case of chloroderivative **2.1b** product **2.3** was obtained to some extent (entry 17). No alkylation took place when the silyl ethers contained an electron-donating group such as in compounds **2.1c** or **2.1d** that are not significantly consumed in the reaction (entries 19, 20). The experiments performed in the absence of light (entry 21) and of the PC (entry 22) suggested a light-induced photocatalyzed process. Moreover, product **2.3** was likewise obtained (albeit in a lower yield, 64%) starting from aliphatic silyl ether **2.1h**. Sulfone **2.3** was likewise prepared in almost quantitative yield under flow conditions allowing to double the concentration of the olefin to 0.1 M and shortening the irradiation time from 24 h to 2 h (Table 2.3). The flow set-up used is shown in the experimental section Figure ES2.2).

Table 2.3. Optimization results for the synthesis of **2.3.**

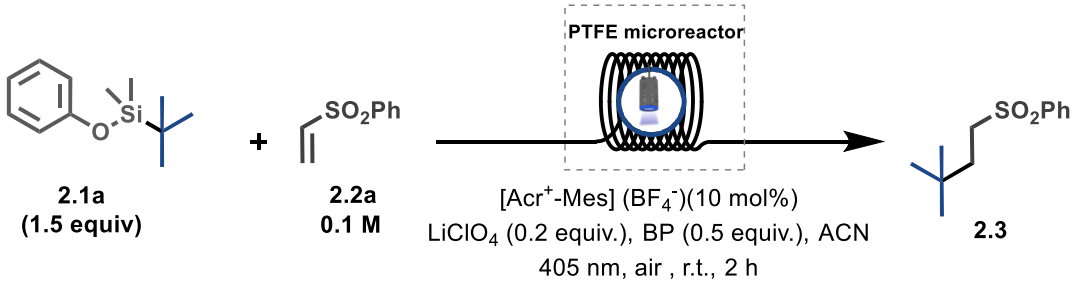

Entry	Deviations from the standard conditions	2.3 (% Yield)
1	**fr: 0.8 mL min^{-1}**	**99**
2	1 h, fr: 1.6 mL min^{-1}	80
3	**2.1a** (1.15 equiv.), 1 h, fr: 1.6 mL min^{-1}	64
4	**2.1a** (1.3 equiv.), 1 h, fr: 1.6 mL min^{-1}	72
5	[Acr^{+}-Mes] (BF$_4^{-}$) (5 mol%), fr: 0.8 mL min^{-1}	37

With these results in hand the scope was extended by combining electron-poor olefins **2.2a-f** and different silyl ethers, as depicted in Scheme 2.3. At first, both aromatic and aliphatic silyl ethers successfully generated different tertiary radicals (*ter*t-butyl and thexyl groups) and compounds **2.3-2.10** were obtained in moderate to excellent yields.

Secondary carbon-based radicals such as ^{i}Pr and cC$_6$H$_{11}$ were then obtained but only from aliphatic silyl ethers (compound **2.1f** is not consumed upon irradiation). This fact gave us the opportunity to compare the performance of silyl ether **2.1j** with the triisopropyl silyl ether **2.1k**.

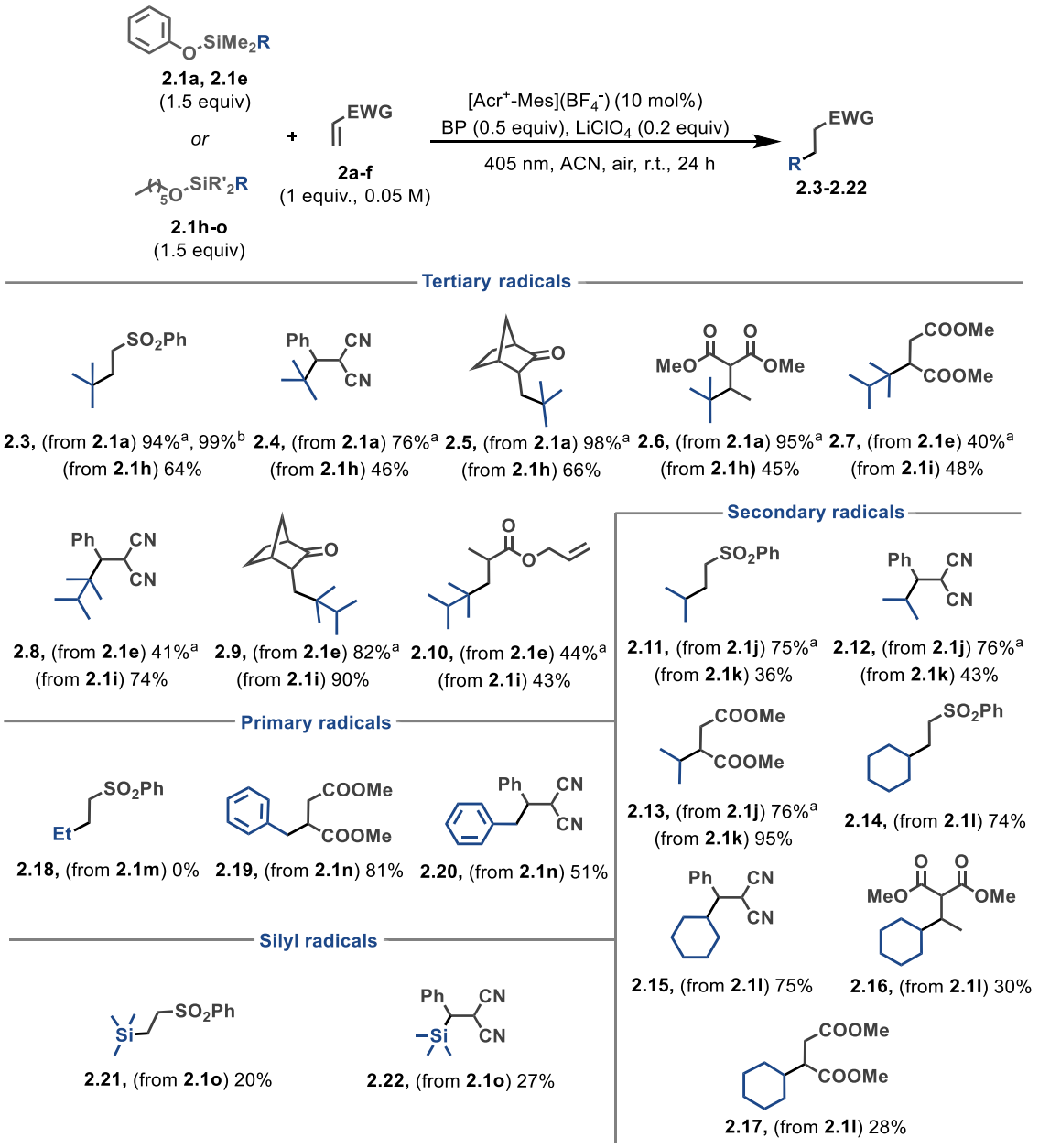

Scheme 2.3. Scope on the alkylation of Michael acceptors. Conditions: **2.1a, 2.1e, 2.1h-o** (0.075 M, 1.5 equiv., 0.375 mmol), **2.2a-j** (0.25 mmol), [Acr^{+}-Mes] (BF$_4^{-}$) (10 mol%), DCE (5 mL), air, under 18 W LED irradiation (405 nm) at r.t. for 24 h. Isolated yields. [a] GC-yield using undecane as standard. [b] Reaction performed under flow conditions: **2.2a** (0.1 M), 2 h.

The release of the secondary radical (via Si-^{i}Pr bond fragmentation) was exclusive even from **2.1j** where no competitive liberation of the Me radical occurred. As a

matter of fact, there is not a strict correlation between the formation yield of **2.11-2.13** (> 75% in the favorable cases) and the silyl ether used. The trapping of the cyclohexyl radical generated from **2.1l** was largely affected by the Michael acceptors employed (see the variable overall yields in the formation of compounds **2.14-2.17**).

No alkylation product **2.18** was detected when testing silyl ether **2.1m** as possible ethyl radical precursor in the reaction with **2.2a** (**2.1m** not consumed in the reaction). Nevertheless, primary benzyl radicals were photogenerated and used for the forging of a C-C bond in benzylated derivatives **2.19-2.20**. Gratifyingly, silicon centered radicals were generated as well via a Si-Si bond fragmentation in the photocatalyzed oxidation of **2.1o** to give silanes **2.21** and **2.22** in a modest yield.

Stern–Volmer quenching data on the photocatalyst employed[33] have been collected to have insights on the reaction mechanism. As a matter of fact, the photocatalyst emission was quenched both in the presence of aromatic silyl ether **2.1a** (Figure 2.3), and **BP** (Figure 2.4) but not with aliphatic derivative **2.1h** (Figure 2.5).

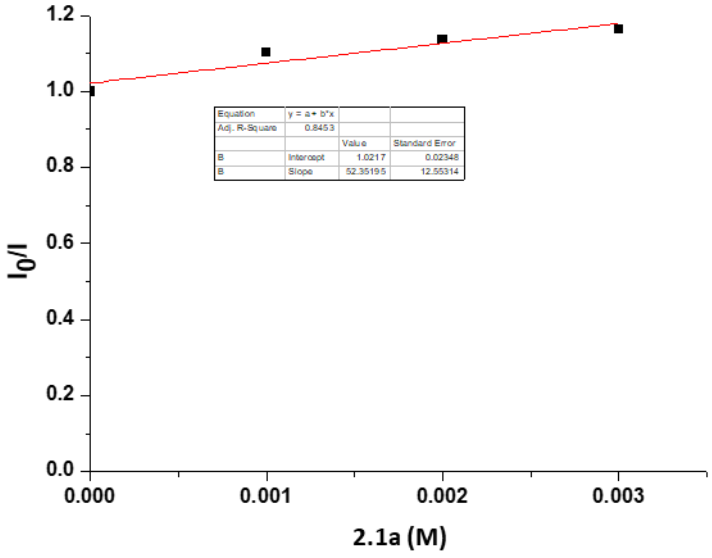

Figure 2.3. $[Acr\text{-}Mes]^{+}(BF_4)^{-}$ Stern-Volmer quenching experiment in the presence of **2.1a** (ext. $k = 8\times10^{9}$).

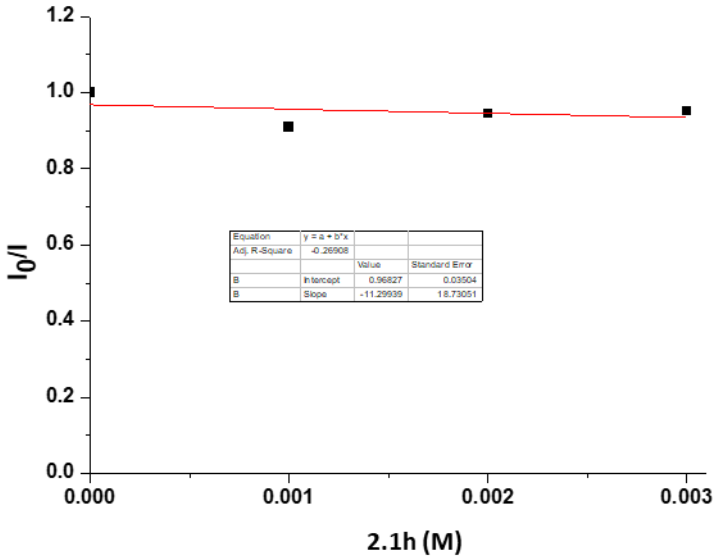

Figure 2.4. $[Acr\text{-}Mes]^{+}(BF_4)^{-}$ Stern-Volmer quenching experiment in the presence of **2.1h** (No interaction observed).

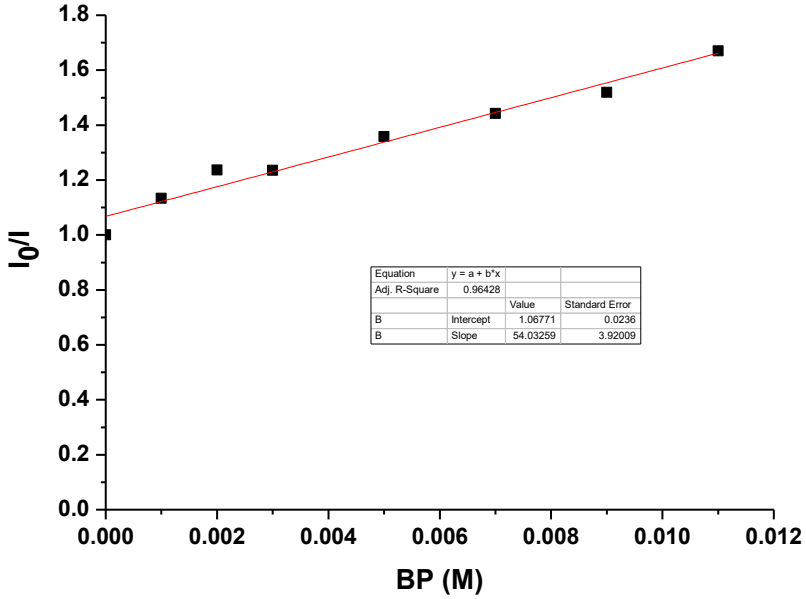

Figure 2.5. $[Acr\text{-}Mes]^{+}(BF_4)^{-}$ Stern-Volmer quenching experiment in the presence of **BP** (ext. $k = 9\times10^{9}$).

The effect of **BP** is apparent in the synthesis of ketone **2.9**. The absence of **BP** caused a dramatical decrease on the yield (40% by GC analysis) when starting from **2.1e**, but no reaction occurred when using the corresponding aliphatic derivative **2.1i.** No transformation of **2.1i** was observed after irradiation. Based on the results obtained we propose the mechanism summarized in Scheme 2.4. The photocatalyst absorbs the visible light radiation supplied and upon excitation interacted, in a first SET

event, with **BP** to release the corresponding radical cation **BP**$^{\bullet+}$. The latter species then is quenched by the silyl ether **2.1** (path a) allowing the regeneration of **BP** with the concomitant formation of the radical cation **2.1**$^{\bullet+}$.

Biphenyl has been previously used as secondary donor to ameliorate the performance of a SET reaction between the PC and the electron donor.[34,35] The oxidant capability of the **BP**$^{\bullet+}$ has been measured by CV technique ($E_{1/2}^{ox}$ BP = + 1.95 V vs SCE, Table 2.1, Figure 2.2) in accordance with the literature.[36] This value is not so different from that of the excited PC. This means that the oxidation of silyl ethers **2.1a-g** by **BP**$^{\bullet+}$ is always thermodynamically favoured, contrary to aliphatic silyl ethers **2.1h-o** (except for **2.1o**) where E_{ox} > 2.0 V vs SCE. Nevertheless, the difference on the E_{ox} of aliphatic silyl ethers and the oxidant capability of the **BP**$^{\bullet+}$ is, however small, and the SET may likewise take place. **BP** has the role to separate the reacting species formed following the initial SET between the **PC** and **2.1**. The quenching operated by **BP** on the excited PC (see Figure 2.5) avoids the unproductive back electron transfer between **PC**$^{\bullet-}$ and the silyl ether **2.1**$^{\bullet+}$. The direct SET between **PC*** and **2.1** (at least for aromatic derivatives, path *b*) is taking place during the process. As a matter of fact, aliphatic silyl ethers (contrary to BP) poorly quenched the excited acridinium salt confirming again the requirement of the secondary donor. This fact could be explained by the different lifetime of the oxidizing species viz. ca. 6 ns for the excited acridinium salt[30] and ca. 10 μs (in acetonitrile) for the biphenyl.[37] In addition, the use of $LiClO_4$ is crucial to improve the overall yield (see entries 6, 8, Table 2.2) since it is known to enhance the conductivity of the reaction media and to stabilize the charged species formed.[34] In analogy to tetraalkylsilanes, the radical cation **2.1**$^{\bullet+}$, upon fragmentation, releases a carbon or a silicon centered radical **2.VII**. The radical cation fragmentation leads in each case to the release of the more stable radical (e.g. tertiary, secondary, benzyl) and there is no competition of the methyl radical liberation in solution. Surprisingly, secondary radicals were generated only when using aliphatic but not aromatic silyl ethers. This fact could be justified by the higher stability of the radical cation intermediate in the latter case hampering the Si-C bond fragmentation when a less stable radical is released. The fate of the radical cation contrasts with that observed in the monoelectronic

electrochemical oxidation of trialkylsiloxybenzenes in protic media known to give quinones by a desilylation rather than a radical release.[38]

The photogenerated carbon or silicon-based radicals were engaged in a Giese reaction with Michael acceptors to afford radical adducts **2.VIII**·. The subsequent SET event with the reduced form of the photocatalyst turned over the catalytic cycle on one hand and formed the corresponding carbanion **2.VIII**⁻ on the other hand, that upon protonation (proton came from traces of water present in the solvent) yields the alkylated products **2.3-2.22**.

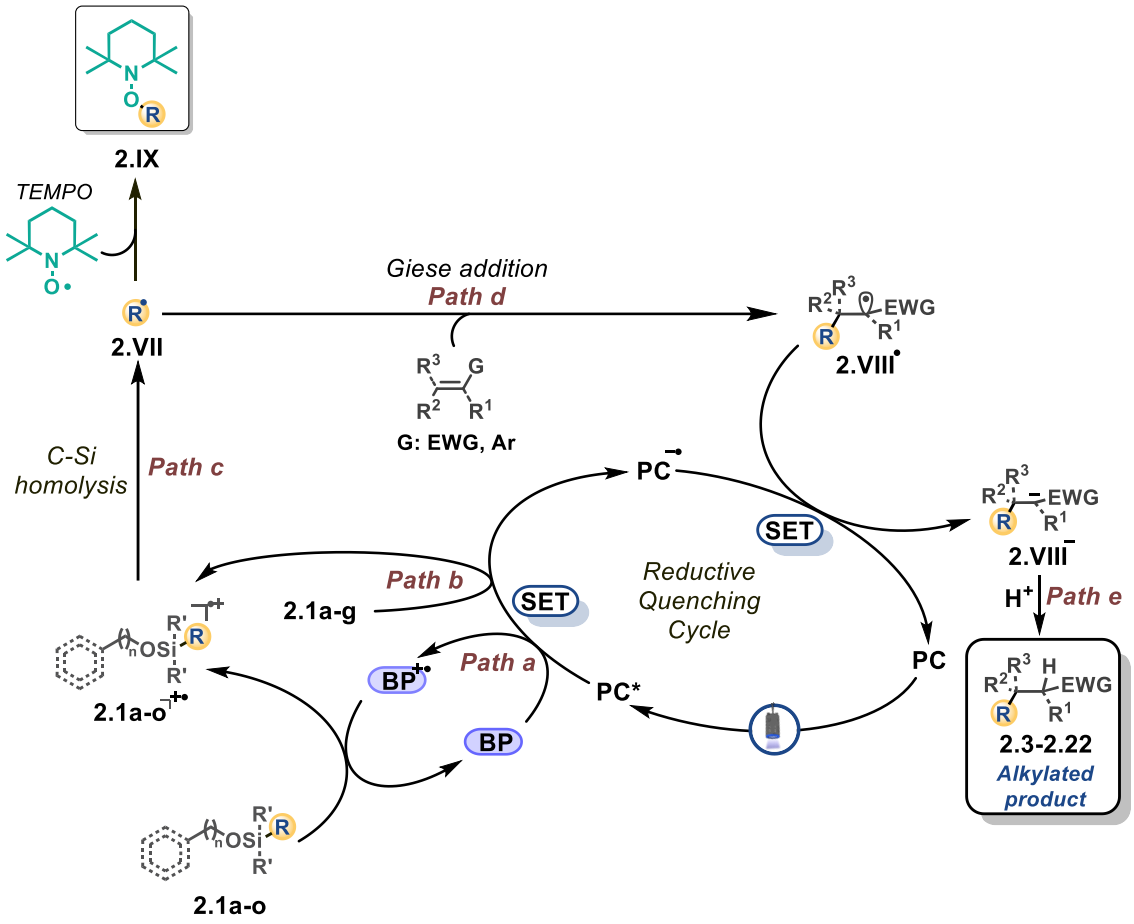

Scheme 2.4. Proposed mechanism.

2.3 Mechanistic studies.

2.3.1 Radical trapping experiments.

Two different experiments were performed by using TEMPO as radical scavenger:

Experiment A: **2.1a** was used as radical precursor. No product formation was observed when TEMPO (1 equiv.) was added to the reaction mixture. At the end of the reaction,

both remaining starting material (**2.2a**) and traces of the silyl ether **2.1a** were detected by GC analysis.

Experiment B: **2.1h** was used as radical precursor. No product formation was observed when TEMPO (1 equiv.) was added to the reaction mixture. At the end of the reaction, both remaining starting material (**2.2a**) and traces of the silyl ether **2.1a** were detected by GC analysis.

2.4 Conclusions.

The strategy reported herein represents an attractive approach for the generation of carbon-based and silicon-based radicals under free-metal visible light conditions. The uncharged radical precursors are easy to synthesize in excellent to quantitative yields and in a high purity by using cheap and commercially available starting materials. Besides, silyl ethers are bench stable compounds that can be stored with no precautions. The protocol developed has been applied on the functionalization of small molecules under batch or flow conditions and the thus formed derivative can serve as building blocks for further synthetic applications. This method allowed to forge mainly C(sp^3)-C(sp^3) bonds, currently a hot topic in synthetic chemistry, and extremely demanded in drug development processes by increasing the Fsp^3 (number of sp^3 hybridized carbons/total carbon count) thus enhancing the probabilities to obtain a bioactive compound.[39] The reaction described could have interesting implications in the degradation of thermally stable volatile methyl siloxanes (toxic and environmental persistent derivatives) where the cleavage of the inert Si–C bonds is mandatory for their complete degradation.[40]

2.5 Experimental section.

^1H and ^{13}C NMR spectra were recorded on a 300 e 75 MHz spectrometer, respectively. The attributions were based on ^1H and ^{13}C NMR experiments, chemical shifts are reported in ppm downfield from TMS (δ ppm), multiplicity (s = singlet, bs = broad singlet, d = doublet, t = triplet, q = quadruplet, quint = quintuplet, sext = sextuplet, sept = septuplet, m = multiplet), coupling constant (Hz) and integration.

GC analyses were performed using a HP SERIES 5890 II equipped with a fire ion detector (FID, temperature 350 °C). Analytes were separated using a Restek Rtx-5MS (30 m×0.25 mm×0.25 μm) capillary column with nitrogen as a carrier gas at 1 mL min^{-1}. The injector temperature was 250 °C. The GC oven temperature was held at 80 °C for 2 min, increased to 250 °C by a temperature ramp of 10 °C min^{-1}, and held for 10 min.

GC/MS analyses were carried out on a Thermo Scientific DSQII single quadrupole GC/MS system (TraceDSQII mass spectrometer, Trace GC Ultra gas chromatograph, TriPlus autosampler - ThermoFisher Scientific, Waltham, MA, USA). Chromatography was performed on a Rxi-5Sil MS capillary column (30 m length×0.25 mm ID×0.25 μm film thickness, Restek, Milan, Italy) with Helium (>99.99 %) as carrier gas at a constant flow rate of 1.0 mL min-1. An injection volume of 1 μL was employed. The injector temperature was set at 250 °C and it was operated in split mode, with a split flow of 10 mL min^{-1}. The oven temperature was programmed from 80 °C (isothermal for 2 min) to 220 °C at the rate of 10 °C min^{-1}, then from 220 °C to 300 °C (isothermal for 5 min) at the rate of 4 °C min^{-1}. Mass transfer line temperature was set at 260 °C. Total GC running time was 41 min. All mass spectra were acquired with an electron ionization system (EI, Electron Impact mode) with ionization energy of 70 eV and source temperature of 250°C, with spectral acquisition in Full Scan mode, positive polarity, over a mass range of 35–650 Da with a scan rate of 940 amu s^{-1}. The chromatogram acquisition, detection of mass spectral peaks and their waveform processing were performed using Xcalibur MS Software Version 2.1 (Thermo Scientific Inc.). Assignment of chemical structures to chromatographic peaks was based on the comparison with the databases for GC-MS NIST Mass Spectral Library (NIST 08) and Wiley Registry of Mass Spectral Data (8th Edition).

HRMS data were acquired using a X500B QTOF System (SCIEX, Framingham, MA 01701 USA) available at the CGS of the University of Pavia, equipped with the Twin Sprayer ESI probe and coupled to an ExionLC™ system (SCIEX). The SCIEX OS software 2.1.6 was used as operating platform. For MS detection the following parameters were applied: Curtain gas 30 psi, Ion source gas 1 45 psi, Ion source gas

2 55 psi, Temperature 450°C, Polarity negative, Ion spray voltage -4500 V, TOF mass range 50-1600 Da, declustering potential -60 V and collision energy -10 V.

Cyclic Voltammetry was carried out by means of a Amel model 4330 module equipped with a 20 mL standard three-electrode cell with a glassy carbon (0.49 cm^2 geometrical area) working electrode, a platinum wire as auxiliary electrode and an Ag/AgCl, 3 M NaCl reference electrode, all obtained from BASi Electrochemistry. Acetonitrile containing 0.1 M lithium perchlorate were used as solvent and supporting electrolyte, scanning the potential in the range from 0 mV to + 2500 mV, with a 5 mM compound concentration and a scan speed of 50 mV s^{-1}.

2.5.1 Chart of starting materials.

The starting materials were commercially available and used as received.

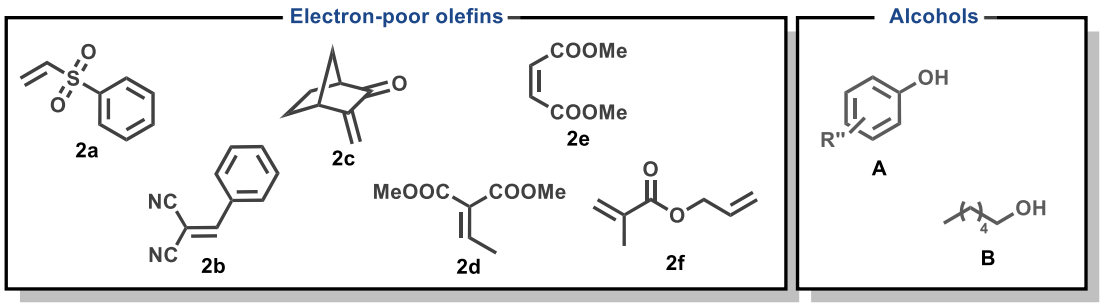

2.5.2 General procedures.

2.5.2.1 General procedure 2.1. Synthesis of synthesis of aryl silyl ethers.

Aryl silyl ethers **2.1a-g** have been synthesized according to reported procedures.[41] The corresponding silyl chloride (1 equiv.) was added dropwise to a stirred solution of phenol (1 equiv.) and DBU (1.15 equiv.) in DCM (1 M) previously cooled in an ice bath at 0 °C. The mixture was stirred for 3 h from 0 ºC to room temperature. The solution was then concentrated in vacuo and purified by flash column chromatography (eluant: cyclohexane containing 1% $_{v/v}$ Et_3N) to afford the corresponding silyl ethers **2.1a-g**.

2.5.2.2 General procedure 2.2. Synthesis of aliphatic silyl ethers.

Aliphatic silyl ethers **2.1h-o** have been synthesized according to a reported procedure.[41] The corresponding silyl chloride (1 equiv.) was added dropwise to a

stirred solution of hexanol (1 equiv.) and DBU (1.15 equiv.) in DCM (1 M) previously cooled in an ice bath at 0 °C. The mixture was stirred for 3 h from 0 °C to room temperature. The solution was then concentrated in vacuo yielding the corresponding silyl ether **2.1h-o,** without further purification.

2.5.2.3 General procedure 2.3. Giese addition in batch.

A solution of the chosen silyl ether (**2.1a-g** or **2.1h-o**, 1.5 equiv. 0.075 M), an electron-poor olefin (**2a-f**, 1 equiv., 0.05 M), [Acr$^+$-Mes] (BF_4^-) (10 mol %), lithium perchlorate (0.2 equiv.) and biphenyl (0.5 equiv.) in MeCN (0.05 M) was prepared in a Pyrex glass vessel and irradiated for 24 h at 405 nm (18 W Evoluchem lamp). By using **2.1a-g**, the yield was determined by GC, adding a C_{11} standard solution and injecting the mixture on the GC. By using **2.1h-o**, the crude mixture was concentrated in vacuo and the residue was purified by flash column chromatography (SiO_2) yielding the desired products.

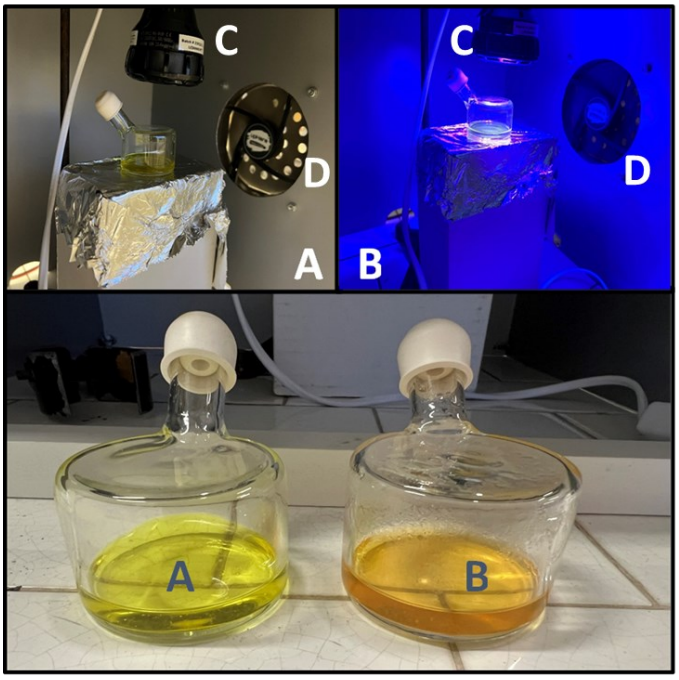

Figure ES2.1. (A) Reaction mixture before irradiation. (B) Reaction after irradiation. (C) Lamp (Evoluchem 405 nm, 18 W). (D) Fan to avoid overheating.

2.5.2.4 General procedure for the preparation of compound 2.3 under flow conditions.

A solution of silyl ether **2.1a** (78.1 mg, 0.375 mmol, 1.5 equiv.), **2.2a** (40.05 mg, 0.25 mmol, 1 equiv.) and [Acr$^+$-Mes](BF_4^-) (10 mg, 0.03 mmol, 10 mol %) in MeCN (2.5

mL) was charged into a coiled tubing reservoir (PTFE, 1 mm internal diameter, see Figure S7). Then, the reaction mixture was flown through a coiled reactor (PTFE, 1 mm internal diameter, 1.7 mL) by using a syringe pump while irradiated for 2 h with a 405 nm lamp (EvoluChem, 18W). Fan cooling was applied to maintain the reaction at room temperature. The resulting solution was collected and concentrated in vacuo. The residue was purified by flash column chromatography (SiO_2, DCM/MeOH 100/0 to 95:5) to yield compound **2.3** (yellowish oil, 56.0 mg, 99%). Space time yield (STY) = 184 mmol L^{-1} h^{-1}. Specific productivity: SP = 0.026 mmol W^{-1} h^{-1}.

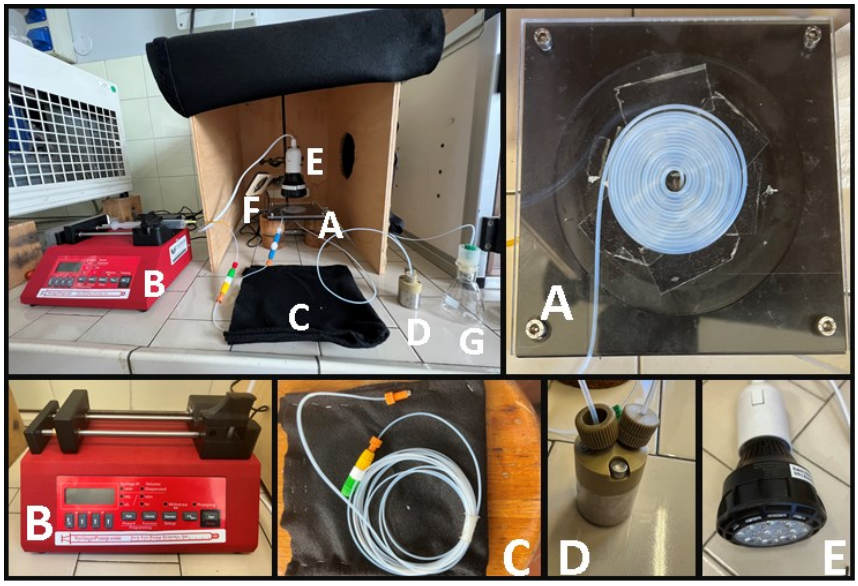

Figure S8. (A) Hand-made flow system. PTFE microreactor. (B) Syringe pump. (C) PTFE precoil. (D) Back pressure valve. (E) Evoluchem Lamp (405 nm, 18W). (F) Fan to avoid overheating due to light irradiation. (G) Erlenmeyer flask as a collector.

2.6 Characterization data.

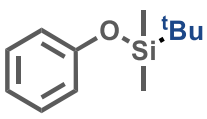

***tert*-Butyldimethyl(phenoxy)silane (2.1a).**

Dimethyl-*tert*butyl-chlorosilane (801 mg, 5.31 mmol 1.0 equiv.) was added dropwise to a stirred solution of phenol (500 mg, 5.31 mmol, 1 equiv.) and DBU (930 mg, 6.11 mmol, 1.15 equiv.) in DCM (5 mL). Purification by flash column chromatography yielded **2.1a** (colorless oil, 1 g, 90%). Spectroscopic data of **2.1a** are in accordance with the literature.[42]

2.1a. ^{1}H NMR (300 MHz, $(CD_3)_2CO$) δ 7.30–7.15 (m, 2H), 6.99–6.93 (m, 1H), 6.90–6.79 (m, 2H), 0.99 (d, *J* = 0.8 Hz, 9H), 0.21 (d, *J* = 0.8 Hz, 6H). ^{13}C NMR (75 MHz, $(CD_3)_2CO$) δ 156.6, 130.3, 122.2, 120.9, 26.0, 18.8, -4.3.

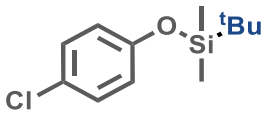

***tert*-Butyl(4-chlorophenoxy)dimethylsilane (2.1b).**

Dimethyl-*tert*butyl-chlorosilane (586 mg, 3.89 mmol 1.0 equiv.) was added dropwise to a stirred solution of 4-chlorophenol (500 mg, 3.89 mmol, 1 equiv.) and DBU (680 mg, 4.47 mmol, 1.15 equiv.) in DCM (4 mL). Purification by flash column chromatography yielded **2.1b** (colorless oil, 810 mg, 99% yield). Spectroscopic data of **2.1b** are in accordance with the literature.[43]

2.1b. ^{1}H NMR (300 MHz, $(CD_3)_2CO$) δ 7.32–7.19 (m, 2H), 6.96–6.81 (m, 2H), 0.99 (s, 9H), 0.22 (s, 6H). ^{13}C NMR (75 MHz, $(CD_3)_2CO$) δ 155.5, 130.2, 126.7, 122.5, 29.1, 26.0, -4.4.

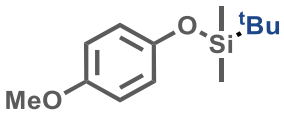

***tert*-Butyl(4-methoxyphenoxy)dimethylsilane (2.1c).**

Dimethyl-*tert*butyl-chlorosilane (607 mg, 4.03 mmol 1.0 equiv.) was added dropwise to a stirred solution of 4-methoxy phenol (500 mg, 4.03 mmol, 1 equiv.) and DBU (705 mg, 4.63 mmol, 1.15 equiv.) in DCM (4 mL). Purification by flash column chromatography yielded **2.1c** (colorless oil, 816 mg, 85%). Spectroscopic data of **2.1c** are in accordance with the literature.[44]

2.1c. ^{1}H NMR (300 MHz, $(CD_3)_2CO$) δ 6.99–6.54 (m, 4H), 3.73 (s, 3H), 1.18–0.69 (m, 9H), 0.17 (s, 6H). ^{13}C NMR (75 MHz, $(CD_3)_2CO$) δ 155.3, 150.1, 121.4, 115.3, 55.8, 26.1, 18.7, -4.4.

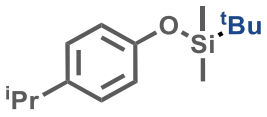

***tert*-Butyl(4-isopropylphenoxy)dimethylsilane (2.1d).**

Dimethyl-*tert*butyl-chlorosilane (553 mg, 3.67 mmol 1.0 equiv.) was added dropwise to a stirred solution of 4-isopropylphenol (500 mg, 3.67 mmol, 1 equiv.) and DBU (1.02 g, 4.22 mmol, 1.15 equiv.) in DCM (5 mL). Purification by flash column chromatography yielded **2.1d** (colorless oil, 841 mg, 92%). Spectroscopic data of **2.1d** are in accordance with the literature.[45]

2.1d. ^{1}H NMR (300 MHz, $(CD_3)_2CO$) δ 7.19–7.03 (m, 2H), 6.83–6.72 (m, 2H), 2.84 (hept, *J* = 6.8 Hz, 1H), 1.20 (d, *J* = 6.8 Hz, 6H), 0.99 (s, 9H), 0.19 (s, 6H). ^{13}C NMR (75 MHz, $(CD_3)_2CO$) δ 154.4, 142.5, 128.0, 120.6, 34.0, 26.1, 24.5, 18.7, -4.3.

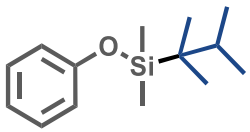

(2,3-Dimethylbutan-2-yl)dimethyl(phenoxy)silane (2.1e).

(2,3-Dimethylbutan-2-yl)dimethyl-chlorosilane (960 mg, 5.37 mmol 1.0 equiv.) was added dropwise to a stirred solution of phenol (500 mg, 5.37 mmol, 1 equiv.) and DBU (940 mg, 6.18 mmol, 1.15 equiv.) in DCM (5 mL). Purification by flash column chromatography yielded **2.1e** (colorless oil, 1.02 g, 81%). Spectroscopic data of **2.1e** are in accordance with the literature.[46]

2.1e. ^{1}H NMR (300 MHz, $(CD_3)_2CO$) δ 7.31–7.19 (m, 2H), 6.99–6.80 (m, 3H), 1.83–1.68 (m, 1H), 1.01–0.93 (m, 12H), 0.24 (s, 6H). ^{13}C NMR (75 MHz, $(CD_3)_2CO$) δ 156.4, 130.3, 122.2, 121.0, 35.0, 25.7, 20.6, 18.9, -2.3.

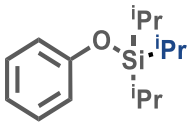

Triisopropyl(phenoxy)silane (2.1f).

Chlorotriisopropylsilane (1.02 g, 5.31 mmol, 1 equiv.) was added dropwise to a stirred solution of phenol (500 mg, 5.31 mmol, 1 equiv.) and DBU (930 mg, 5.31 mmol, 1.15 equiv.) in DCM (5 mL) Purification by flash column chromatography

yielded **2.1f** (colorless oil, 1.03 g, 77%). Spectroscopic data of **1f** are in accordance with the literature.[47]

2.1f. ^{1}H NMR (300 MHz, $(CD_3)_2CO$) δ 7.31–7.17 (m, 2H), 6.98–6.86 (m, 3H), 1.36–1.19 (m, 3H), 1.11 (d, *J* = 7.2 Hz, 18H). ^{13}C NMR (75 MHz, $(CD_3)_2CO$) δ 156.9, 130.3, 122.0, 120.7, 18.3, 13.4.

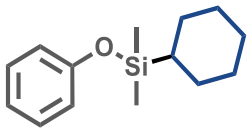

Cyclohexyldimethyl(phenoxy)silane (2.1g).

Chloro(cyclohexyl)dimethylsilane (0.94 g, 5.31 mmol, 1 equiv.) was added to a stirred solution of phenol (500 mg, 5.31 mmol, 1 equiv.) and DBU (930 mg, 5.31 mmol, 1.15 equiv.) in DCM (5 mL). Purification by flash column chromatography yielded **2.1g** (colorless oil, 0.88 g, 70%).

2.1g. ^{1}H NMR (300 MHz, $(CD_3)_2CO$) δ 7.30–7.16 (m, 2H), 7.00–6.89 (m, 1H), 6.90–6.78 (m, 2H), 1.87–1.64 (m, 6H), 1.33–1.16 (m, 5H), 0.19 (s, 6H). ^{13}C NMR (75 MHz, $(CD_3)_2CO$) δ 156.4, 130.3, 122.2, 120.8, 27.6, 27.3, -3.2. GC-MS (*m/z*) = 234 (25), 151 (100), 137 (10).

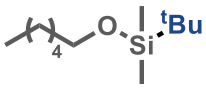

***tert*-Butyldimethyl(hexyloxy)silane (2.1h).**

tert-Butylchlorodimethylsilane (321.0 mg, 2.13 mmol 1.0 equiv.) was added to a stirred solution of hexan-1-ol (217 mg, 2.13 mmol, 1 equiv.) and DBU (372 mg, 2.45 mmol, 1.15 equiv.) in DCM (2.5 mL). Compound **2.1h** (colorless oil, 460 mg, 99%) was isolated without further purification. Spectroscopic data of **2.1h** are in accordance with the literature.[48]

2.1h. ^{1}H NMR (300 MHz, $(CD_3)_2CO$) δ 3.63 (t, *J* = 6.3 Hz, 2H), 1.56–1.44 (m, 2H), 1.32 (dtt, *J* = 11.0, 8.4, 4.5 Hz, 6H), 0.89 (s, 12H), 0.05 (s, 6H).^{13}C NMR (75 MHz, $(CD_3)_2CO$) δ 63.6, 33.6, 32.4, 26.3, 26.3, 23.4, 18.8, 14.3, -5.2.

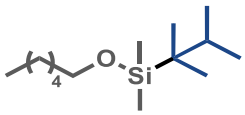

(2,3-Dimethylbutan-2-yl)dimethyl(hexyloxy)silane (2.1i).

Chloro(2,3-dimethylbutan-2-yl) dimethylsilane (347 mg, 1.96 mmol 1.0 equiv.) was added to a stirred solution of hexan-1-ol (200 mg, 1.96 mmol, 1 equiv.) and DBU (342 mg, 2.25 mmol, 1.15 equiv.) in DCM (3 mL). Compound **2.1i** (colorless oil, 479 mg, 99%) was isolated without further purification.

2.1i. ^{1}H NMR (300 MHz, $CDCl_3$) δ 3.57 (t, *J* = 6.6 Hz, 2H), 1.69–1.56 (m, 1H), 1.55–1.43 (m, 2H), 1.37–1.22 (m, 6H), 0.94–0.85 (m, 9H), 0.84 (s, 6H), 0.08 (s, 6H). ^{13}C NMR (75 MHz, $CDCl_3$) δ 63.2, 34.4, 33.0, 31.8, 25.7, 25.3, 22.8, 20.5, 18.6, 14.2, -3.2. GC-MS (*m/z*) = 159 (100), 89 (30), 84 (38), 75 (100), 73 (20).

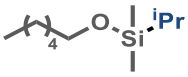

***iso*-Propyldimethyl(hexyloxy)silane (2.1j).**

Chloro(isopropyl)dimethylsilane (314 mg, 2.30 mmol 1.0 equiv.) was added to a stirred solution of hexan-1-ol (235 mg, 2.30 mmol, 1 equiv.) and DBU (402 mg, 2.64 mmol, 1.15 equiv.) in DCM (3 mL). Compound **2.1j** (colorless oil, 460 mg, 99%) was isolated without further purification.

2.1j. ^{1}H NMR (300 MHz, $(CD_3)_2CO$) δ 3.60 (t, *J* = 6.4 Hz, 2H), 1.56–1.43 (m, 2H), 1.41–1.20 (m, 6H), 0.96 (d, *J* = 6.8 Hz, 7H), 0.92–0.85 (m, 3H), 0.04 (s, 6H). ^{13}C NMR (75 MHz, $(CD_3)_2CO$) δ 63.3, 33.6, 32.4, 26.3, 23.3, 17.3, 15.4, 14.3, -4.3. GC-MS (*m/z*) = 159 (86), 89 (30), 75 (100), 59 (19).

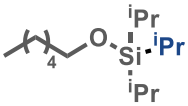

Triisopropyl(hexyloxy)silane (1k).

Chlorotriisopropylsilane (377 mg, 1.96 mmol 1.0 equiv.) was added to a stirred solution of hexan-1-ol (200 mg, 1.96 mmol, 1 equiv.) and DBU (342 mg, 2.25 mmol, 1.15 equiv.) in DCM (3 mL). Compound **2.1k** (colorless oil, 510 mg, 99%) was isolated without further purification. Spectroscopic data of **2.1k** are in accordance with the literature.[49]

2.1k. ^{1}H NMR (300 MHz, $CDCl_3$) δ 3.67 (t, *J* = 6.6 Hz, 2H), 1.64–1.49 (m, 2H), 1.39–1.22 (m, 6H), 1.14-0.95 (m, 21H), 0.92–0.85 (m, 3H). ^{13}C NMR (75 MHz, $CDCl_3$) δ 63.7, 33.2, 31.9, 25.7, 22.8, 18.2, 17.85, 14.2, 12.2. GC-MS (*m/z*) = 215 (100), 187 (45), 159 (30), 145 (23), 83 (30), 75 (45), 61 (30), 59 (20).

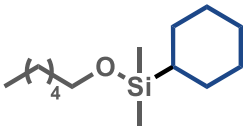

Cyclohexyldimethyl(hexyloxy)silane (2.1l).

Chloro(cyclohexyl)dimethylsilane (1.03 g, 5.87 mmol 1.0 equiv.) was added to a stirred solution of hexan-1-ol (600 mg, 5.87 mmol, 1 equiv.) and DBU (1.03 g, 1.15 mmol, 1.15 equiv.) in DCM (5 mL). Compound **2.1l** (colorless oil, 1.33 g, 94%) was isolated without further purification.

2.1l. ^{1}H NMR (300 MHz, $(CD_3)_2CO$) δ 3.59 (t, *J* = 6.4 Hz, 2H), 1.78-1.65 (d, *J* = 9.3 Hz, 6H), 1.55-1.40 (m, 2H), 1.38–1.04 (m, 11H), 0.95–0.83 (m, 3H), 0.02 (s, 6H). ^{13}C NMR (75 MHz, $(CD_3)_2CO$) δ 63.2, 33. 6, 32.4, 28.6, 27.6, 27.6, 26.3, 23.4, 14.3, -3.4. GC-MS (*m/z*) = 159 (100), 89 (24), 83 (26), 75 (72).

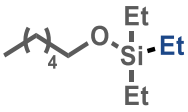

Triethyl(hexyloxy)silane (2.1m).

Chlorotriethylsilane (295 mg, 1.96 mmol 1.0 equiv.) was added to a stirred solution of hexan-1-ol (200 mg, 1.96 mmol, 1 equiv.) and DBU (342 mg, 2.25 mmol, 1.15 equiv.) in DCM (3 mL). Compound **2.1m** (colorless oil, 420 mg, 99%) was isolated without further purification. Spectroscopic data of **2.1m** are in accordance with the literature.[50]

2.1m. ^{1}H NMR (300 MHz, $(CD_3)_2CO$) δ 3.57-3.47 (m, 2H), 1.55–1.44 (m, 2H), 1.39–1.21 (m, 6H), 0.96 (t, *J* = 7.9 Hz, 9H), 0.91–0.83 (m, 3H), 0.66–0.49 (m, 6H). ^{13}C NMR (75 MHz, $(CD_3)_2CO$) δ 62.5, 33.8, 32.5, 26.4, 23.4, 14.3, 7.1, 5.1.

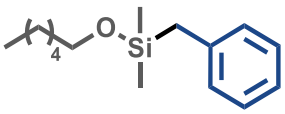

Benzyldimethyl(hexyloxy)silane (2.1n).

Benzylchlorodimethylsilane (1.81 g, 9.78 mmol 1.0 equiv.) was added to a stirred solution of hexan-1-ol (1 g, 9.78 mmol, 1 equiv.) and DBU (1.87 g, 11.25 mmol, 1.15 equiv.) in DCM (10 mL). Compound **2.1n** (colorless oil, 1.91 g, 78%) was isolated without further purification.

2.1n. ^{1}H NMR (300 MHz, $CDCl_3$) δ 7.25–7.17 (m, 2H), 7.12–7-02 (m, 3H), 3.57 (t, *J* = 6.7 Hz, 2H), 2.18 (s, 2H), 1.44–1.59 (m, 2H), 1.33–1.25 (m, 6H), 0.86–0.93 (m, 3H), 0.08 (s, 6H). ^{13}C NMR (75 MHz, $CDCl_3$) δ 139.3, 128.5, 128.3, 124.4, 63.3, 32.8, 31.8, 26.4, 25.6, 22.8, 14.2, -2.3. GC-MS (*m/z*) = 250 (M^+), 159 (100), 89 (20), 75 (100).

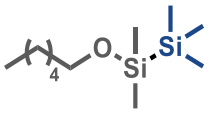

1,1,1,2,2-Pentamethyl-2-hexyloxydisilane (2.1o).

1-Chloro-1,1,2,2,2-pentamethyldisilane (979 mg, 5.87 mmol 1.0 equiv.) was added to a stirred solution of hexan-1-ol (600 mg, 5.87 mmol, 1 equiv.) and DBU (1.03 g, 6.75 mmol, 1.15 equiv.) in DCM (5 mL). Compound **2.1o** (colorless oil, 1.30 g, 95%) was isolated without further purification.

2.1o. ^{1}H NMR (300 MHz, $(CD_3)_2CO$) δ 3.58 (t, *J* = 6.4 Hz, 2H), 1.59–1.42 (m, 2H), 1.42 – 1.19 (m, 6H), 0.94 – 0.82 (m, 3H), 0.18 (s, 6H), 0.09 (s, 9H). ^{13}C NMR (75 MHz, $(CD_3)_2CO$) δ 13C NMR (75 MHz, $(CD_3)_2CO$) δ 64.0, 33.6, 32.4, 26.3, 23.3, 14.3, -0.60, -1.88. GC-MS (*m/z*) = 232 (M^+), 217 (5), 159 (13), 147 (100), 133 (25), 75 (50).

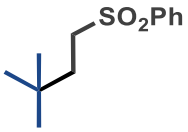

((3,3-Dimethylbutyl)sulfonyl)benzene (2.3)

10-methyl-9-mesitylacridinium (10.0 mg, 0.03 mmol, 10 mol%), $LiClO_4$ (5.0 mg, 0.50 mmol, 0.2 equiv.), biphenyl (19.3 mg, 0.12 mmol, 0.5 equiv.) and **2.2a** (42.0 mg, 0.25 mmol, 1.0 equiv.) were added to a solution of **2.1h** (81.2 mg, 0.375 mmol, 1.5 equiv.) in acetonitrile (5 mL). Purification by flash column chromatography (SiO_2,

DCM/MeOH from 100/0 to 95:5) gave the desired compound **2.3** (pale yellowish oil, 36.2 mg, 64%). When **2.1a** (78.1 mg, 0.375 mmol, 1.5 equiv.) was used as radical precursor, **2.3** was obtained in 94% yield. When **2.1h** (78.1 mg, 0.375 mmol, 10 mol %) was used as radical precursor and the reaction was performed under flow conditions, compound **2.3** was obtained in 99% yield (pale yellowish oil, 56.0 mg). Spectroscopic data of **2.3** are in accordance with the literature.[51]

2.3. ^{1}H NMR (300 MHz, $CDCl_3$) δ 7.91 (m, 2H), 7.74–7.50 (m, 3H), 3.15–3.0 (m, 2H), 1.65–1.55 (m, 2H), 0.87 (s, 9H). ^{13}C NMR (75 MHz, $CDCl_3$) δ 139.4, 133.8, 129.4, 128.2, 53.1, 35.8, 30.2, 29.1.

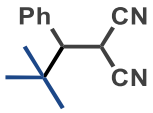

2-(2,2-Dimethyl-1-phenylpropyl)malononitrile (2.4)

10-methyl-9-mesitylacridinium (10.0 mg, 0.03 mmol, 10 mol%), $LiClO_4$ (5.0 mg, 0.50 mmol, 0.2 equiv.), biphenyl (19.3 mg, 0.12 mmol, 0.5 equiv.) and **2.2b** (38.5 mg, 0.25 mmol, 1.0 equiv.) were added to a solution of **2.1h** (81.2 mg, 0.375 mmol, 1.5 equiv.) in acetonitrile (5 mL). Purification by flash column chromatography (SiO_2, Cyclohexane/AcOEt from 100/0 to 90:10) yielded compound **2.4** (white powder, 24,4 mg, 46%). When **2.1a** (78.1 mg, 0.375 mmol, 1.5 equiv.) was used as radical precursor, compound **2.4** was obtained in 76% yield. Spectroscopic data of **2.4** are in accordance with the literature.[52]

2.4.^{1}H NMR (300 MHz, $CDCl_3$) δ 7.39 (m, 5H), 4.22 (d, J = 5.7 Hz, 1H), 3.01 (d, J = 5.7 Hz, 1H), 1.11 (s, 9H). ^{13}C NMR (75 MHz, $CDCl_3$) δ 136.4, 129.4, 128.9, 113.2, 56.9, 35.1, 28.6, 25.2.

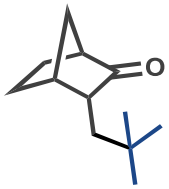

3-Neopentylbicyclo[2.2.1]heptan-2-one (2.5).

10-methyl-9-mesitylacridinium (10.0 mg, 0.03 mmol, 10 mol%), $LiClO_4$ (5.0 mg, 0.50 mmol, 0.2 equiv.), biphenyl (19.3 mg, 0.12 mmol, 0.5 equiv.) and **2.2c** (30.5 mg, 0.25 mmol, 1.0 equiv.) were added to a solution of **2.1h** (81.2 mg, 0.375 mmol, 1.5 equiv.) in acetonitrile (5 mL). Purification by flash column chromatography (SiO_2,

Cyclohexane/AcOEt from 100/0 to 90:10) gave compound **2.5** (pale yellowish oil, 29.7 mg, 66%). When **2.1a** (78.1 mg, 0.375 mmol, 1.5 equiv.) was used as radical precursor, compound **2.5** was obtained in 98% yield as the *endo* isomer.[53] Spectroscopic data of **2.5** are in accordance with the literature.[54]

2.5. ^{1}H NMR (300 MHz, $CDCl_3$) δ 2.66-2.62 (m, 1H), 2.61-2.55 (m, 1H), 2.58-1.94 (m, 1H), 1.83–1.53 (m, 6H), 1.40–1.28 (m, 1H), 1.20–1.09 (m, 1H), 0.90 (s, 9H). ^{13}C NMR (75 MHz, $CDCl_3$) δ 220.7, 51.6, 50.0, 40.5, 39.4, 37.5, 30.7, 29.9, 25.4, 21.5.

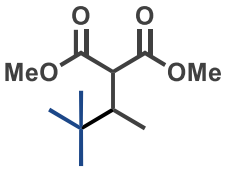

Dimethyl 2-(3,3-dimethylbutan-2-yl)malonate (2.6).

10-methyl-9-mesitylacridinium (10.0 mg, 0.03 mmol, 10 mol%), $LiClO_4$ (5.0 mg, 0.50 mmol, 0.2 eq), biphenyl (19.3 mg, 0.12 mmol, 0.5 equiv.) and **2.2d** (35 μL, 0.25 mmol, 1.0 equiv.) were added to a solution of **2.1h** (81.2 mg, 0.375 mmol, 1.5 equiv.) in acetonitrile (5 mL). Purification by flash column chromatography (SiO_2, Cyclohexane/AcOEt from 100/0 to 80:20) yielded compound **2.6** (pale yellow oil, 24.3 mg, 45%). When **2.1a** (78.1 mg, 0.375 mmol, 1.5 equiv.) was used as radical precursor, compound **2.6** was obtained in 95% yield. Spectroscopic data of **2.6** are in accordance with the literature.[55]

2.6 ^{1}H NMR (300 MHz, $CDCl_3$) δ 3.84–3.64 (m, 6H), 3.56 (d, *J* = 5.3 Hz, 1H), 2.25 (m, 1H), 1.00 (d, *J* = 7.0 Hz, 3H), 0.89 (s, 9H). ^{13}C NMR (75 MHz, $CDCl_3$) δ 170.7, 170.1, 53.2, 52.7, 52.2, 43.1, 33.7, 27.6, 12.2.

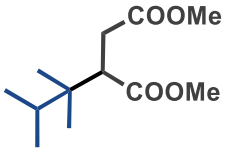

Dimethyl 2-(2,3-dimethylbutan-2-yl)succinate (2.7).

10-methyl-9-mesitylacridinium (10.0 mg, 0.03 mmol, 10 mol%), $LiClO_4$ (5.0 mg, 0.50 mmol, 0.2 equiv.), biphenyl (19.3 mg, 0.12 mmol, 0.5 equiv.) and **2.2e** (31 μL, 0.25 mmol, 1.0 equiv.) were added to a solution of **2.1i** (91.7 mg, 0.375 mmol, 1.5 equiv.) in acetonitrile (5 mL). Purification by flash column chromatography (SiO_2, Cyclohexane/AcOEt from 100/0 to 80:20) afforded compound **2.7** (colourless oil,

27.6 mg, 48%). When **2.1e** (88.7 mg, 0.375 mmol, 1.5 equiv.) was used as radical precursor, compound **2.7** was obtained in 40% yield.

2.7. ^{1}H NMR (300 MHz, $CDCl_3$) δ 3.68 (d, *J* = 1.2 Hz, 3H), 3.65 (d, *J* = 1.3 Hz, 3H), 2.97-2.90 (m, 1H), 2.82-2.69 (m, 1H), 2.50-2.40 (m, 1H), 1.68–1.48 (m, 1H), 0.94–0.78 (m, 12H). ^{13}C NMR (75 MHz, $CDCl_3$) δ 174.6, 173.4, 51.9, 51.5, 48.6, 37.8, 34.4, 32.3, 20.9, 20.7, 17.5, 17.5. HRMS (EI) m/z: $[M+Na]^+$ calculated for $C_{12}H_{22}O_4$ 253.1410, found 253.1407.

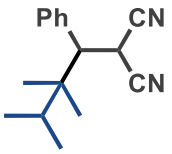

2-(2,2,3-Trimethyl-1-phenylbutyl)malononitrile (2.8).

10-methyl-9-mesitylacridinium (10.0 mg, 0.03 mmol, 10 mol%), $LiClO_4$ (5.0 mg, 0.50 mmol, 0.2 equiv.), biphenyl (19.3 mg, 0.12 mmol, 0.5 equiv.) and benzylidenemalononitrile (38.5 mg, 0.25 mmol, 1.0 equiv.) were added to a solution of **2.1i** (91.7 mg, 0.375 mmol, 1.5 equiv.) in acetonitrile (5 mL). Purification by flash column chromatography (SiO_2, Cyclohexane/AcOEt from 100/0 to 90:10) gave compound **2.8** (colourless oil, 44.5 mg, 74%). When **2.1e** (88.7 mg, 0.375 mmol, 1.5 equiv.) was used as radical precursor, compound **2.8** was obtained in 41% yield. Spectroscopic data of **2.8** are in accordance with the literature.[56]

2.8. ^{1}H NMR (300 MHz, $CDCl_3$) δ 7.47–7.34 (m, 5H), 4.20 (d, *J* = 5.1 Hz, 1H), 3.28 (d, *J* = 5.1 Hz, 1H), 1.70–1.53 (m, 1H), 1.12 (s, 3H), 0.98–0.77 (m, 9H). ^{13}C NMR (75 MHz, $CDCl_3$) δ 136.2, 129.9, 128.8, 128.7, 113.5, 113.3, 53.5, 40.0, 34.2, 25.1, 21.7, 21.0, 17.6, 17.3.

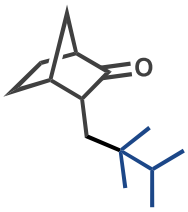

3-(2,2,3-Trimethylbutyl)bicyclo[2.2.1]heptan-2-one (2.9).

10-methyl-9-mesitylacridinium (10.0 mg, 0.03 mmol, 10 mol%), $LiClO_4$ (5.0 mg, 0.50 mmol, 0.2 equiv.), biphenyl (19.3 mg, 0.12 mmol, 0.5 equiv.) and **2.2c** (30.5 mg, 0.25 mmol, 1.0 equiv.) were added to a solution of **2.1i** (91.7 mg, 0.375 mmol, 1.5 equiv.) in acetonitrile (5 mL). Purification by flash column chromatography (SiO_2,

Cyclohexane/AcOEt from 100/0 to 90:10) yielded compound **2.9** (pale yellow oil, 46.9 mg, 90%) as the *endo* isomer.[55] When **2.1e** (88.7 mg, 0.375 mmol, 1.5 equiv.) was used as radical precurser, compound **2.9** was obtained in 82% yield.

2.9. ^{1}H NMR (300 MHz, $CDCl_3$) δ 2.70–2.54 (m, 2H), 2.06–1.94 (m, 1H), 1.89–1.73 (m, 1H), 1.73–1.59 (m, 4H), 1.50–1.38 (m, 2H), 1.38–1.23 (m, 1H), 1.21-1.12 (m, 1H), 0.98–0.69 (m, 12H). ^{13}C NMR (75 MHz, $CDCl_3$) δ 218.8, 51.1, 50.1, 40.8, 38.1, 36.2, 35.5, 35.4, 25.6, 24.6, 24.5, 21.7, 17.7, 17.6. HRMS (EI) m/z: $[M+H]^+$ calculated for $C_{14}H_{24}O$ 209.1900, found 209.1898.

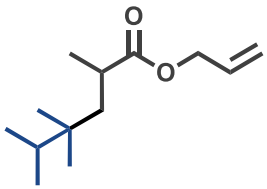

Allyl 2,4,4,5-tetramethylhexanoate (2.10).

10-methyl-9-mesitylacridinium (10.0 mg, 0.03 mmol, 10 mol%), $LiClO_4$ (5.0 mg, 0.50 mmol, 0.2 equiv.), biphenyl (19.3 mg, 0.12 mmol, 0.5 equiv.) and **2.2d** (33 mL, 0.25 mmol, 1.0 equiv.) were added to a solution of **2.1i** (91.7 mg, 0.375 mmol, 1.5 equiv.) in acetonitrile (5 mL). Purification by flash column chromatography (SiO_2, Cyclohexane/AcOEt from 100/0 to 80:20) afforded compound **2.10** (colourless oil, 22.8 mg, 43%). When **2.1e** (88.7 mg, 0.375 mmol, 1.5 equiv.) was used as radical precursor, compound **2.10** was obtained in 44% yield.

2.10. ^{1}H NMR (300 MHz, $CDCl_3$) δ 6.05–5.83 (m, 1H), 5.45–5.18 (m, 2H), 4.65–4.44 (m, 2H), 2.65–2.44 (m, 1H), 2.00–1.78 (m, 1H), 1.57–1.38 (m, 2H), 1.22–1.16 (m, 3H), 0.95–0.74 (m, 12H). ^{13}C NMR (75 MHz, $CDCl_3$) δ 177.8, 132.5, 118.2, 65.1, 43.9, 36.2, 35.8, 35.2, 27.1, 24.4, 23.7, 20.7, 17.6. HRMS (EI) m/z: $[M+H]^+$ calculated for $C_{13}H_{24}O_2$ 213.1849, found 213.1848.

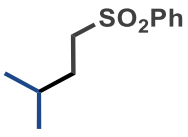

(*iso*-Pentylsulfonyl)benzene (2.11).

10-methyl-9-mesitylacridinium (10.0 mg, 0.03 mmol, 10 mol%), $LiClO_4$ (5.0 mg, 0.50 mmol, 0.2 equiv.), biphenyl (19.3 mg, 0.12 mmol, 0.5 equiv.) and **2.1a** (42.05 mg,

0.25 mmol, 1.0 equiv.) were added to a solution of **2.1j** (75.9 mg, 0.375 mmol, 1.5 equiv.) or in acetonitrile (5 mL). Purification by flash column chromatography (SiO_2, DCM/MeOH from 100/0 to 95:5) yielded compound **2.11** (pale yellowish oil, 39.8 mg, 75%). When **2.1k** (96.9 mg, 0.375 mmol, 1.5 equiv.) was used as radical precursor, compound **2.11** was obtained in 36%. Spectroscopic data of **2.11** are in accordance with the literature.[57]

2.11. ^{1}H NMR (300 MHz, $CDCl_3$) δ 7.97–7.85 (m, 2H), 7.71–7.62 (m, 1H), 7.57 (t, *J* = 6.5, 1.8 Hz, 2H), 3.15–3.01 (m, 2H), 1.66–1.55 (m, 3H), 0.87 (d, *J* = 6.2 Hz, 6H). ^{13}C NMR (75 MHz, $CDCl_3$) δ 139.4, 133.7, 129.4, 128.2, 54.9, 31.1, 27.4, 22.1.

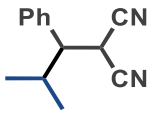

2-(2-Methyl-1-phenylpropyl)malononitrile (2.12).

10-methyl-9-mesitylacridinium (10.0 mg, 0.03 mmol, 10 mol%), $LiClO_4$ (5.0 mg, 0.50 mmol, 0.2 equiv.), biphenyl (19.3 mg, 0.12 mmol, 0.5 equiv.) and **2.2b** (38.5 mg, 0.25 mmol, 1.0 equiv.) were added to a solution of **2.1j** (75.9 mg, 0.375 mmol, 1.5 equiv.) in acetonitrile (5 mL). Purification by flash column chromatography (SiO_2, Cyclohexane/AcOEt from 100/0 to 90:10) gave compound **2.12** (white powder, 37.7 mg, 76%). When **2.1k** (96.9 mg, 0.375 mmol, 1.5 equiv.) was used as radical precursor, compound **2.12** was obtained in 43% yield Spectroscopic data of **2.12** are in accordance with the literature.[58]

2.12. ^{1}H NMR (300 MHz, $CDCl_3$) δ 7.45–7.34 (m, 3H), 7.36–7.27 (m, 2H), 4.16 (d, *J* = 5.6 Hz, 1H), 2.84 (dd, *J* = 9.7, 5.6 Hz, 1H), 2.50–2.29 (m, 1H), 1.14 (d, *J* = 6.6 Hz, 3H), 0.83 (d, *J* = 6.6 Hz, 3H). ^{13}C NMR (75 MHz, $CDCl_3$) δ 136.7, 129.3, 128.9, 128.4, 112.3, 112.0, 53.6, 30.4, 27.9, 21.1, 20.5.

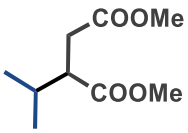

Dimethyl 2-isopropylsuccinate (2.13).

10-methyl-9-mesitylacridinium (10.0 mg, 0.03 mmol, 10 mol%), $LiClO_4$ (5.0 mg, 0.50 mmol, 0.2 equiv.), biphenyl (19.3 mg, 0.12 mmol, 0.5 equiv.) and **2.2e** (31 mL, 0.25 mmol, 1.0 equiv.) were added to a solution of **2.1j** (75.9 mg, 0.375 mmol, 1.5 equiv.)

in acetonitrile (5 mL). Purification by flash column chromatography (SiO_2, Cyclohexane/AcOEt from 100/0 to 80:20) to yield the desired compound **2.13** (colourless oil, 35.8 mg, 76%). When **2.1k** (96.9 mg, 0.375 mmol, 1.5 equiv.) was used as radical precursor, compound **2.13** was obtained in 95% yield. Spectroscopic data of **2.13** are in accordance with the literature.[59]

2.13. ^{1}H NMR (300 MHz, $CDCl_3$) δ 3.68 (d, *J* = 8.6 Hz, 6H), 2.77–2.66 (m, 2H), 2.51–2.33 (m, 1H), 2.07–1.89 (m, 1H), 0.99–0.85 (m, 6H). ^{13}C NMR (75 MHz, $CDCl_3$) δ 175.0, 173.1, 51.9, 51.7, 47.6, 33.0, 30.2, 20.2, 19.7.

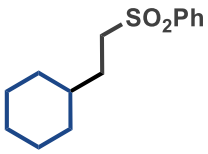

((2-Cyclohexylethyl)sulfonyl)benzene (2.14).

10-methyl-9-mesitylacridinium (10.0 mg, 0.03 mmol, 10 mol%), $LiClO_4$ (5.0 mg, 0.50 mmol, 0.2 equiv.), biphenyl (19.3 mg, 0.12 mmol, 0.5 equiv.) and **2.2a** (42.05 mg, 0.25 mmol, 1.0 equiv.) were added to a solution of **2.1l** (90.9 mg, 0.375 mmol, 1.5 equiv.) in acetonitrile (5 mL). Purification by flash column chromatography (SiO_2, DCM/MeOH from 100/0 to 95:5) afforded compound **2.14** (yellowish oil, 46.7 mg, 74%). Spectroscopic data of **2.14** are in accordance with the literature.[60]

2.14. ^{1}H NMR (300 MHz, $(CD_3)_2CO$) δ 7.99–7.85 (m, 2H), 7.78–7.58 (m, 3H), 3.25–3.11 (m, 2H), 1.72–1.45 (m, 7H), 1.35–1.05 (m, 4H), 0.94–0.76 (m, 2H). ^{13}C NMR (75 MHz, $(CD_3)_2CO$) δ 141.1, 134.5, 130.4, 130.3, 129.0, 37.4, 33.6, 30.8, 27.2, 26.9.

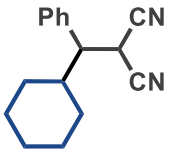

2-(Cyclohexyl(phenyl)methyl)malononitrile (2.15)

10-methyl-9-mesitylacridinium (10.0 mg, 0.03 mmol, 10 mol%), $LiClO_4$ (5.0 mg, 0.50 mmol, 0.2 equiv.), biphenyl (19.3 mg, 0.12 mmol, 0.5 equiv.) and benzylidenemalononitrile (38.5mg, 0.25 mmol, 1.0 equiv.) were added to a solution of **2.1l** (90.9 mg, 0.375 mmol, 1.5 equiv.) in acetonitrile (5 mL). Purification by flash column chromatography (SiO_2, Cyclohexane/AcOEt from 100/0 to 90:10) gave

compound **2.15** (white powder, 44.7 mg, 75%). Spectroscopic data of **2.15** are in accordance with the literature.[60]

2.15. ^{1}H NMR (300 MHz, $CDCl_3$) δ 7.47–7.35 (m, 3H), 7.34–7.27 (m, 2H), 4.19 (d, *J* = 5.5 Hz, 1H), 2.88 (dd, *J* = 9.7, 5.5 Hz, 1H), 2.12–1.77 (m, 3H), 1.74–1.60 (m, 2H), 1.50-1.25 (m, 2H), 1.20–0.99 (m, 3H), 0.96–0.74 (m, 1H). ^{13}C NMR (75 MHz, $CDCl_3$) δ 136.8, 129.3, 128.9, 128.4, 112.3, 112.1, 51.8, 39.4, 31.3, 30.7, 27.2, 26.0, 25.9, 25.9.

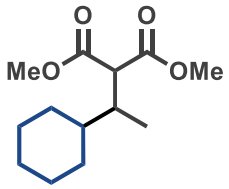

Dimethyl 2-(1-cyclohexylethyl)malonate (2.16).

10-methyl-9-mesitylacridinium (10.0 mg, 0.03 mmol, 10 mol%), $LiClO_4$ (5.0 mg, 0.50 mmol, 0.2 equiv.), biphenyl (19.3 mg, 0.12 mmol, 0.5 equiv.) and **2.2d** (35 mL, 0.25 mmol, 1.0 equiv.) were added to a solution of **2.1l** (90.9 mg, 0.375 mmol, 1.5 equiv.) in acetonitrile (5 mL). Purification by flash column chromatography (SiO_2, Cyclohexane/AcOEt, from 100/0 to 90:10) yielded compound **2.16** (pale yellowish oil, 10.3 mg, 30%). Spectroscopic data of **2.16** are in accordance with the literature.[61]

2.16.^{1}H NMR (300 MHz, $CDCl_3$) δ 3.73 (d, *J* = 3.2 Hz, 6H), 3.44 (d, *J* = 9.1 Hz, 1H), 2.28–2.09 (m, 1H), 1.77–1.50 (m, 5H), 1.35–1.06 (m, 6H), 0.93–0.86 (m, 3H). ^{13}C NMR (75 MHz, $CDCl_3$) δ 169.9, 169.6, 55.6, 52.5, 52.4, 40.5, 38.8, 31.6, 27.6, 26.8, 26.7, 26.6, 13.1.

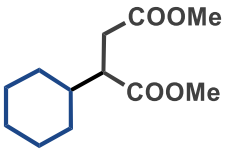

Dimethyl 2-cyclohexylsuccinate (2.17).

10-methyl-9-mesitylacridinium (10.0 mg, 0.03 mmol, 10 mol%), $LiClO_4$ (5.0 mg, 0.50 mmol, 0.2 equiv.), biphenyl (19.3 mg, 0.12 mmol, 0.5 equiv.), and **2.2e** (31 mL, 0.25 mmol, 1.0 equiv.) were added to a solution of **2.1l** (90.9 mg, 0.375 mmol, 1.5 equiv.) in acetonitrile (5 mL). Purification by flash column chromatography (SiO_2, Cyclohexane/AcOEt, from 100/0 to 80:20) gave compound **2.17** (colourless oil, 16.0 mg, 28%). Spectroscopic data of **2.17** are in accordance with the literature.[59]

2.17. ^{1}H NMR (300 MHz, $CDCl_3$) δ 3.69 (s, 3H), 3.66 (s, 3H), 2.84–2.61 (m, 2H), 2.55–2.38 (m, 1H), 1.85–1.60 (m, 5H), 1.40–0.93 (m, 6H). ^{13}C NMR (75 MHz, $CDCl_3$) δ 175.1, 173.1, 51.9, 51.7, 47.2, 40.1, 33.4, 30.8, 30.3, 26.5, 26.3.

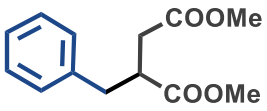

Dimethyl 2-benzylsuccinate (2.19).

10-methyl-9-mesitylacridinium (10.0 mg, 0.03 mmol, 10 mol%), $LiClO_4$ (5.0 mg, 0.50 mmol, 0.2 equiv.), biphenyl (19.3 mg, 0.12 mmol, 0.5 equiv.), and dimethyl maleate (31 mL, 0.25 mmol, 1.0 equiv.) were added to a solution of **2.1n** (93.9 mg, 0.375 mmol, 1.5 equiv.) in acetonitrile (5 mL). Purification by flash column chromatography (SiO_2, Cyclohexane/AcOEt, from 100/0 to 85:15) gave compound **2.19** (pale yellowish oil, 47.8 mg, 81%). Spectroscopic data of **2.19** are in accordance with the literature.[62]

2.19. ^{1}H NMR (300 MHz, $CDCl_3$) δ 7.38–7.28 (m, 2H), 7.23–7.10 (m, 3H), 3.67 (s, 3H), 3.64 (s, 3H), 3.22–2.93 (m, 2H), 2.85–2.56 (m, 2H), 2.41 (dd, *J* = 16.8, 4.8 Hz, 1H). ^{13}C NMR (75 MHz, $CDCl_3$) δ 174.8, 172.4, 138.3, 129.2, 128.7, 126.9, 52.1, 51.9, 43.2, 37.9, 35.1.

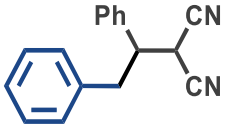

2-(1,2-Diphenylethyl)malononitrile (2.20).

10-methyl-9-mesitylacridinium (10.0 mg, 0.03 mmol, 10 mol%), $LiClO_4$ (5.0 mg, 0.50 mmol, 0.2 equiv.), biphenyl (19.3 mg, 0.12 mmol, 0.5 equiv.), and **2.2b** (38.5 mg, 0.25 mmol, 1.0 equiv.) were added to a solution of **2.1n** (93.9 mg, 0.375 mmol, 1.5 equiv.) in acetonitrile (5 mL). Purification by flash column chromatography (SiO_2, Cyclohexane/AcOEt, from 100/0 to 85:15) afforded the desired compound **2.20** (white powder, 31.4 mg, 51%). Spectroscopic data of **2.20** are in accordance with the literature.[62]

2.20. ^{1}H NMR (300 MHz, $CDCl_3$) δ 7.48–7.37 (m, 5H), 7.37–7.27 (m, 3H), 7.23–7.15 (m, 2H), 3.85 (d, *J* = 5.1 Hz, 1H), 3.47 (td, *J* = 7.8, 5.0 Hz, 1H), 3.27 (dd, *J* = 7.7, 1.8 Hz,

2H). ^{13}C NMR (75 MHz, $CDCl_3$) δ 136.8, 136.6, 129.3, 129.3, 129.2, 129.1, 128.2, 127.7, 112.2, 111.6, 48.5, 38.7, 28.7.

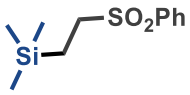

Trimethyl(2-(phenylsulfonyl)ethyl)silane (2.21).

10-methyl-9-mesitylacridinium (10.0 mg, 0.03 mmol, 10 mol%), $LiClO_4$ (5.0 mg, 0.50 mmol, 0.2 equiv.), biphenyl (19.3 mg, 0.12 mmol, 0.5 equiv.), and **2.2a** (42.05 mg, 0.25 mmol, 1.0 equiv.) were added to a solution of **2.1o** (91.7 mg, 0.375 mmol, 1.5 equiv.) in acetonitrile (5 mL). Purification by flash column chromatography (SiO_2, Cyclohexane/MeOH, from 100/0 to 95:5) yielded the compound **2.21** (pale yellowish powder, 12.1 mg, 20%). Spectroscopic data of **2.21** are in accordance with the literature.[63]

2.21. ^{1}H NMR (300 MHz, $CDCl_3$) δ 7.93 (s, 2H), 7.77–7.47 (m, 3H), 3.18–2.83 (m, 2H), 1.04–0.78 (m, 2H), 0.26– -0.17 (m, 9H). ^{13}C NMR (75 MHz, $CDCl_3$) δ 138.9, 133.7, 129.4, 128.4, 52.9, 9.3, -1.9.

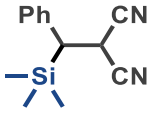

2-(Phenyl(trimethylsilyl)methyl)malononitrile (2.22).

10-methyl-9-mesitylacridinium (10.0 mg, 0.03 mmol, 10 mol%), $LiClO_4$ (5.0 mg, 0.50 mmol, 0.2 equiv.), biphenyl (19.3 mg, 0.12 mmol, 0.5 equiv.), and **2.2b** (30.5 mg, 0.25 mmol, 1.0 equiv.) were added to a solution of **2.1o** (91.7 mg, 0.375 mmol, 1.5 equiv.) in acetonitrile (5 mL). Purification by flash column chromatography (SiO_2, Cyclohexane/AcOEt, from 100/0 to 90:10) gave **2.22** (white powder, 15.4 mg, 27%). Spectroscopic data of **2.22** are in accordance with the literature.[64]

22. ^{1}H NMR (300 MHz, $CDCl_3$) δ 7.42–7.33 (m, 2H), 7.32–7.27 (m, 1H), 7.22–7.14 (m, 2H), 4.08 (d, *J* = 7.8 Hz, 1H), 2.65 (d, *J* = 7.8 Hz, 1H), 0.17 (s, 9H). ^{13}C NMR (75 MHz, $CDCl_3$) δ 137.3, 129.3, 128.0, 127.5, 113.4, 113.3, 38.0, 25.4, -2.0.

2.7 References.

1) (*a*) Ravelli, D., Protti, S., Fagnon,i M. and Albini, A. Visible Light Photocatalysis. A Green Choice? *Curr. Org. Chem.* **2013**, *17*, 2366; (*b*) Ravelli, D., Protti, S. and Fagnoni, M. Carbon–Carbon Bond Forming Reactions via Photogenerated Intermediates, *Chem. Rev.* **2016**, *116*, 9850; (*c*) Goddard, J.-P., Ollivier, C. and Fensterbank, L. Photoredox Catalysis for the Generation of Carbon Centered Radicals, *Acc. Chem. Res.* **2016**, *49*, 1924; (*d*) *Visible Light Photocatalysis in Organic Chemistry,* Eds: Stephenson, C. R. J., Yoon, T. P. and MacMillan, D. W. C. Wiley-VCH, Weinheim, Germany **2018**; (*e*) Fagnoni, M., Protti, S. and Ravelli, D .*Photoorganocatalysis in organic synthesis,* World Scientific Publishing Europe Ltd., Singapore, **2019**; (*f*) Pitre, S. P., Weires, N. A. and Overman, L. E. Forging C(sp^3)–C(sp^3) Bonds with Carbon-Centered Radicals in the Synthesis of Complex Molecules. *J. Am. Chem. Soc.* **2019**, *141*, 2800; (*g*) Crespi, S. and Fagnoni, M. Generation of Alkyl Radicals: From the Tyranny of Tin to the Photon Democracy, *Chem. Rev.* **2020**, *120*, 9790; (*h*) *Chemical Photocatalysis. 2nd ed.*; Ed König, B. De Gruyter, 2020. (*i*) Fagnoni, M., Ravelli, D. and Protti, S. in *Science of Synthesis: Free Radicals: Fundamentals and Applications in Organic Synthesis*, Eds Fensterbank, L. and Ollivier, C. Thieme: Stuttgart, **2021**, Vol. 2, pp 339–357; (*j*) Capaldo, L., Ravelli, D. and Fagnoni, M. Direct Photocatalyzed Hydrogen Atom Transfer (HAT) for Aliphatic C–H Bonds Elaboration, *Chem. Rev.* **2022**, *121*, 1875.
2) *(a)* Steinmetz, M. G. Organosilane Photochemistry, *Chem. Rev.,* **1995**, *95*, 1527; *(b)* Postigo, A. In: *Photochemistry Research Progress* Sánchez A. and Gutierrez, S. J. Eds. Nova Science Publishers, Inc. **2008**.
3) *(a)* Baguley, P. A. and Walton, J. C. Flight from the Tyranny of Tin: The Quest for Practical Radical Sources Free from Metal Encumbrances, *Angew. Chem., Int. Ed.*, **1998**, *37*, 3072; *(b) Sax's Dangerous Properties of Industrial Materials*; Lewis, R. J. Ed.; John Wiley & Sons, Inc.: Hoboken, NJ, USA, **2004**; *(c)* Davies, A. G. *Organotin Chemistry, Second, Completely Revised and Updated ed*.; John Wiley & Sons, Ltd, **2004**.

4) Juliá, F., Constantin, T. and Leonori, D. Applications of Halogen-Atom Transfer (XAT) for the Generation of Carbon Radicals in Synthetic Photochemistry and Photocatalysis, *Chem. Rev.,* **2022**, *122*, 2292.
5) Lind, F., Markelov, K. and Studer, A. Benzoyldiisopropylchlorosilane: a visible light photocleavable alcohol protecting group, *Chem. Sci.,* **2023**, *14*, 12615.
6) *(a)* Li, Q., Li, X., Ling, Y., Liu, J. and Yang, J. Photoinduced Base-Metal Catalyzed sp^3-C-Si Bond Activation of Organosilanols to Generate sp^3-Carbon-Centered Radicals, *ACS Catal.,* **2023** *13*, 6879; *(b)* Feng, L., Chen, X., Guo, N., Zhou, Y., Lin, L., Cao, W. and Feng, X. Visible-light-induced chemo-, diastereo- and enantioselective α-C(sp^3)–H functionalization of alkyl silanes, *Chem. Sci.,* **2023**, *14*, 4516.
7) *(a)* Yoshida, J.-i. *Electrochemical reactions of organosilicon compounds*. In: E. Steckhan, (eds) Electrochemistry V. Topics in Current Chemistry, vol 170. Springer, Berlin, Heidelberg, **1994**; *(b)* Jouikov, V. V Electrochemical reactions of organosilicon compounds, *Russ. Chem. Rev.,* **1997**, *66***,** 509; *(c)* Yoshida, J.-i. and Nishiwaki, K. Redox selective reactions of organo-silicon and -tin compounds, *J. Chem. Soc., Dalton Trans.,* **1998**, 2589; *(d)* Yoshida, J.-i., Kataoka, K., Horcajada, R. and Nagaki, A. Modern Strategies in Electroorganic Synthesis, *Chem. Rev.,* **2008**, *108*, 2265.
8) *(a)* Mella, M., Fagnoni, M., Freccero, M., Fasani, E. and Albini, A. New synthetic method via cation fragmentation, *Chem. Soc. Rev.,* **1998**, *27*, 81; *(b)* Corcé, V., Ollivier, C., Fensterbank, L. Boron, silicon, nitrogen and sulfur-based contemporary precursors for the generation of alkyl radicals by single electron transfer and their synthetic utilization, *Chem. Soc. Rev.*, **2022**, *51*, 1470.
9) *(a)* Gutenberger, G., Steckhan, E. and Blechert, S. α-Silyl Ethers as Hydroxymethyl Anion Equivalents in Photoinduced Radical Electron Transfer Additions, *Angew. Chem., Int. Ed.,* **1998**, *37*, 660; *(b)* Kang, Y. W., Kim, R. H., Atriardi, S. R. and Woo, S. K. Visible-Light Photoredox-Catalyzed Giese Reaction of α-Silyl Ethers with Various Michael Acceptors, *J. Org. Chem.,* **2023**, *88*, 3555.

10) *(a)* Yoon, U. C. and Mariano, P. S. The Synthetic Potential of Phthalimide SET Photochemistry, *Acc. Chem. Res.* **2001**, *34*, 523; *(b)* Lim, S. H., Yi, J., Moon, G. M., Ra, C. S., Nahm, K., Cho, D. W., Kim, K., Hyung, T. G., Yoon, U. C., Lee, G. Y., Kim, S., Kim, J. and Mariano, P. S. Method for the Synthesis of Amine-Functionalized Fullerenes Involving SET-Promoted Photoaddition Reactions of α-Silylamines, *J. Org. Chem.,* **2014**, *79*, 6946; *(c)* Balu Atar, A. A Photocatalyst-Free, SET-Mediated Photochemical Approach for the Synthesis of Dumbbell-Like Amine-Functionalized Bis-C_{60} Fullerene through C–C Bond Formation, *Synlett,* **2019**, *30*, 1462.

11) *(a)* Mella, M., Fasani, E. and Albini, A. The Photochemical Reaction between Aromatic Nitriles and Allylsilane, *J. Org. Chem.,* **1992**, *57*, 6210; *(b)* Liu, R., Chia, S. P. M., Goh, Y. Y, Cheo, H. W. B., Fan, Li, R., Zhou, R. and Wu, J. Visible-Light-Mediated Regioselective Allylation, Benzylation, and Silylation of Methylene-Malononitriles via Photoredox-Induced Radical Cation Fragmentation, *Eur. J. Org. Chem.,* **2020**, 1459; *(c)* Berger, M., Carboni, D. and Melchiorre, P. Photochemical Organocatalytic Regio- and Enantioselective Conjugate Addition of Allyl Groups to Enals, *Angew. Chem. Int. Ed.,* **2021**, *60*, 26373; *(d)* Lal, N., Shirsath, S. B., Singh, D. P., and Shaikh, A. C. Allylsilane as a versatile handle in photoredox catalysis, *Chem. Commun.,* **2024**, *60*, 4633.

12) *(a)* Cermenati, L., Freccero, M., Venturello, P. and Albini, A. SET and Exciplex Pathways in the Photochemical Reactions between Aromatic Ketones and Benzylsilane and Stannane Derivatives, *J. Am. Chem. Soc.,* **1995**, *117*, 7869; *(b)* Montanaro, S., Ravelli, D., Merli, D., Fagnoni, M. and Albini, A. Decatungstate as photoredox catalyst: benzylation of electron-poor olefins, *Org. Lett.* **2012**, *14*, 4218; *(c)* Silvi, M., Verrier, C., Rey, Y. P., Buzzetti, L. and Melchiorre, P. Visible-light excitation of iminium ions enables the enantioselective catalytic β-alkylation of enals, *Nat. Chem.,* **2017**, *9*, 868; *(d)* Feng, L., Chen, X., Guo, N., Zhou, Y., Lin, L., Cao, W. and Feng, X. Visible-light-induced chemo-, diastereo- and enantioselective a-C(sp^3)–H functionalization of alkyl silanes, *Chem. Sci.,* **2023**, *14*, 4516.

13) *(a)* Capaldo, L., Riccardi, R., Ravelli, D. and Fagnoni, M. Acyl Radicals from Acylsilanes: Photoredox Catalyzed Synthesis of Unsymmetrical Ketones, *ACS Catal.,* **2018**, *8*, 304; *(b)* Guo, N., Luo, Y., Feng, L., Liu, Z., Cao, W. and Feng, X.

Radical Conjugate Addition of Acylsilane Enabled by Synergistic Photoredox and Lewis Acid Catalysis, *Asian J. Org. Chem.*, **2023**, *12*, e202300164.

14) Klingler, R. J. and Kochi, J. K., Heterogeneous Rates of Electron Transfer. Application of Cyclic Voltammetric Techniques to Irreversible Electrochemical Processes, *J. Am. Chem. Soc.*, **1980**, *102*, 4790.
15) Kyushin, S., Nakadaira, Y. and Ohashi, M. Photoalkylation of Pyrylium Salt with Group 14 Metal-Carbon σ Donors via Electron Transfer**,** *Chem. Lett.,* **1990**, 2191.
16) *(a)* Kyushin, S., Masuda, Y., Matsuhita, K., Nakadaira, Y. and Ohashi, M. Novel alkylation of aromatic nitriles via photo-induced electron transfer of group 14 metal-carbon σ donors, *Tetrahedron Lett.,* **1990**, *31*, 6395; *(b)* Fagnoni, M., Mella, M. and Albini, A. Scope and mechanism of the electron transfer photoinduced alkylation of an aromatic nitrile, *Tetrahedron,* **1994**, *50*, 6401.
17) Bonesi, S. and Fagnoni, M. The aromatic carbon-carbon ipso-substitution reaction, *Chem. Eur. J.,* **2010**, *16*, 13572.
18) *(a)* Corcé, V., Chamoreau, L.-M., Derat, E., Goddard, J.-P., Ollivier, C. and Fensterbank, L. Silicates as Latent Alkyl Radical Precursors: Visible-Light Photocatalytic Oxidation of Hypervalent Bis-Catecholato Silicon Compounds, *Angew. Chem. Int. Ed.*, **2015**, *54*, 11414; *(b)* Jouffroy, M., Primer, D. N. and Molander, G. A. Base-Free Photoredox/Nickel Dual-Catalytic Cross-Coupling of Ammonium Alkylsilicates, *J. Am. Chem. Soc.,* **2016**, *138*, 475; *(c)* Lévêque, C., Chenneberg, L., Corcé, V., Ollivier, C. and Fensterbank, L. Organic photoredox catalysis for the oxidation of silicates: applications in radical synthesis and dual catalysis, *Chem. Commun.,* **2016**, *52*, 9877.
19) *(a)* Morofuji, T., Matsui, Y, Ohno, M., Ikarashi, G. and Kano, N. Photocatalytic Giese-Type Reaction with Alkylsilicates Bearing C,O-Bidentate Ligands, *Chem. Eur. J.,* **2021**, *27*, 6713; *(b)* Abdellaoui, M., Deis, T., Wiethoff, M.-A., Bahri, C., Lemière, G., Ollivier, C. and Fensterbank, L. Martin Silicates as Partners in Photoredox/Ni Dual Catalysis for the Installation of CH_3, CH_2D, CD_2H, CD_3 and $^{13}CH_3$ Groups onto (Hetero)Arenes, *Adv. Synth. Catal.*, **2023**, *365*, 884.
20) *(a)* Puskar, L., Barran, P. E., Duncombe, B. J., Chapman, D. and Stace, A. J. Gas-Phase Study of the Chemistry and Coordination of Lead(II) in the Presence

of Oxygen-, Nitrogen-, Sulfur-, and Phosphorus-Donating Ligands, *J. Phys. Chem. A,* **2005,** *109,* 273. *(b)* The value was obtained from its ionization potential. See for details:. Miller, L. L., Nordblom, G. D. and Mayeda, E. A. A Simple, Comprehensive Correlation of Organic Oxidation and Ionization Potentials, *J. Org. Chem.,* **1972**, *37*, 916.

21) Gassman, P. G. The addition of methyllithium to 2,2,4,4-tetramethylcyclobutan-1-one-3-thione. The generation and capture of a bishomoenolate anion, *Tetrahedron Lett.*, **1980**, *21*, 2219.
22) Yu, W.-L., Luo, Y.-C., Yan, L., Liu, D., Wang, Z.-Y. and Xu, P.-F. Dehydrogenative Silylation of Alkenes for the Synthesis of Substituted Allylsilanes by Photoredox, Hydrogen-Atom Transfer, and Cobalt Catalysis, *Angew. Chem. Int. Ed.*, **2019**, *58*, 10941.
23) Liang, H., Wang, L.-J., Ji, Y.-X., Wang, H. and Zhang, B. Selective Electrochemical Hydrolysis of Hydrosilanes to Silanols via Anodically Generated Silyl Cations, *Angew. Chem. Int. Ed.*, **2021**, *60*, 1839.
24) *(a)* Luguera Ruiz, A., La Mantia, M., Merli, D., Protti, S. and Fagnoni, M. Alkyl Radical Generation via C-C Bond Cleavage in 2-Substituted Oxazolidines, *ACS Catal.,* **2022**, *12*, 12469; *(b)* Luguera Ruiz, A., Mariani, E., Protti, S. and Fagnoni, M. Photoredox Catalyzed Release of Carbon-based Radicals from 2-Substituted-1,3-imidazolidines, *Org. Chem. Front.,* **2024**, *11*, 661.
25) Yue, G. and Liu, B. The photoinduced electron transfer (PET) reactions of silyl ethers and their application, *Tetrahedron Chem* **2024**, *9*, 100067.
26) Chen, M.-Y., Lu, K.-C., Shih-Yuan Lee, A. and Lin, C.-C. Chemoselective deprotection of primary tert-butyldimethylsilyl ethers on carbohydrate molecules in the presence of secondary silyl ethers, *Tetrahedron Lett.*, **2002**, *43*, 2777.
27) Wuts, P. G. M. *Greene's Protective Groups in Organic Synthesis*, 5th ed.; John Wiley & Sons: Hoboken, **2014**.
28) Mella, M., d'Alessandro, N., Freccero, M. and Albini, A. Photochemical reaction of arenecarbonitriles in the presence of alkylsilanes, silyl ethers and silyl amines, *J. Chem. Soc. Perkin Trans. 2*, **1993**, 515.

29) Fagnoni, M., Mella, M. and Albini, A. Alkylation of alkenes by radicals generated through photoinduced single electron transfer, *Tetrahedron*, **1995**, *51*, 859.

30) Joshi-Pangu, A., Lévesque, F., Roth, H. G., Oliver, S. F., Campeau, L. C., Nicewicz, D. and DiRocco, D. A. Acridinium-Based Photocatalysts: A Sustainable Option in Photoredox Catalysis, *J. Org. Chem.* **2016**, *81*, 7244.

31) Guirado, G., Fleming, C. N., Lingenfelter, T. G., Williams, M. L., Zuilhof, H. and Dinnocenzo, J. P. Nanosecond Redox Equilibrium Method for Determining Oxidation Potentials in Organic Media, *J. Am. Chem. Soc.,* **2004**, *126*, 14086.

32) Bonesi, S. M. and Postigo, A. *Photoorganocatalysis in Organic Synthesis.* Eds Fagnoni, M., Protti, S. and Ravelli, D. World Scientific Publishing Europe Ltd, **2018**, Vol. 18, pp 183-242.

33) For related quenching experiments on acridinium salts see: *(a)* Motz, R. N., Sun, A. C., Lehnherr, D. and Ruccolo, S. High-Throughput Determination of Stern–Volmer Quenching Constants for Common Photocatalysts and Quenchers, *ACS Org. Inorg. Au* ***2023***, *3*, 266; *(b)* Margrey, K. A., Czaplyski, W. L., Nicewicz, D. A. and Alexanian, E. J. A General Strategy for Aliphatic C–H Functionalization Enabled by Organic Photoredox Catalysis, *J. Am. Chem. Soc.* **2018**, *140*, 4213.

34) Fagnoni, M., Mella, M. and Albini, A. Radical Addition to Alkenes via Electron Transfer Photosensitization, *J. Am. Chem. Soc.,* **1995**, *117*, 7877.

35) *(a)* Capaldo, L., Buzzetti, L., Merli, D., Fagnoni, M. and Ravelli, D. Smooth Photocatalyzed Benzylation of Electrophilic Olefins via Decarboxylation of Arylacetic Acids, *J. Org. Chem.,* **2016**, **81**, 7102; *(b)* Tanaka, Y., Kubosaki, S., Osaka, K., Yamawaki, M., Morita, T. and Yoshimi, Y. Two Types of Cross-Coupling Reactions between Electron-Rich and Electron-Deficient Alkenes Assisted by Nucleophilic Addition Using an Organic Photoredox Catalyst. *J. Org. Chem.,* **2018**, *83*, 13625; *(c)* Yoshimi, Y. Organic Photoredox Reactions in Two-Molecule Photoredox System*, Chem. Rec.* **2023**, e202300326.

36) Gould, I. R., Ege, D., Moser, J. E. and Farid, S. Efficiencies of Photoinduced Electron-Transfer Reactions: Role of the Marcus Inverted Region in Return Electron Transfer within Geminate Radical-Ion Pairs, *J. Am. Chem. Soc.*, **1990**, *112*, 4290.

37) Warzecha, K.-D., Demuth, M. and Görner, H. Photocyclization of terpenoid polyalkenes upon electron transfer to a triphenylpyrylium salt. A time-resolved study, *J. Chem. Soc., Faraday Trans.*, **1997**, *93*, 1523.

38) *(a)* Stewart, R. F. and Miller, L. L. The electrochemical oxidation of trialkylsiloxybenzene derivatives, *J. Am. Chem. Soc.* **1980**, *102*, 4999; *(b)* Swenton, J. S., Carpenter, K., Chen, Y., Kerns, M. L. and Morrow, G. W. *J. Org. Chem.*, **1993**, *58*, 3308.

39) Lovering, F., Bikker, J. and Humblet. C. Escape from flatland: increasing saturation as an approach to improving clinical success, *J. Med. Chem.,* **2009**, *52*, 6752.

40) *(a)* Tuazon, E. C., Aschmann, S. M. and Atkinson, R. Atmospheric Degradation of Volatile Methyl-Silicon Compounds, *Environ. Sci. Technol.,* **2000**, *34*, 1970; *(b)* Rücker, C. and Kümmerer, K. Environmental Chemistry of Organosiloxanes, *Chem. Rev.,* **2015**, *115*, 466; *(c)* Alton, M. W. and Browne, E. C. Atmospheric Degradation of Cyclic Volatile Methyl Siloxanes: Radical Chemistry and Oxidation Products, *ACS Environ. Au*, **2022**, *2*, 263; *(d)* Sarai, N. S., Fulton, T. J., O'Meara, R. L., Johnston, K. E., Brinkmann-Chen, S., Maar, R. R., Tecklenburg, R. E., Roberts, J. M., Reddel, J. C. T., Katsoulis, D. E. and Arnold, F. H. Directed evolution of enzymatic silicon-carbon bond cleavage in siloxanes, *Science,* **2024**, *383*, 438.

41) Di Terlizzi, L., Roncari, F., Crespi, S., Protti, S. and Fagnoni, M. Aryl–Cl vs heteroatom–Si bond cleavage on the route to the photochemical generation of σ,π-heterodiradicals, *Photochem. Photobiol. Sci*. **2022**, *21*, 667.

42) Jirgensons A. and Lielpetere, A. Friedel–Crafts Alkylation with Carbenium Ions Generated by Electrochemical Oxidation of Stannylmethyl Ethers, *Eur. J. Org. Chem*., **2020**, *29*, 4510.

43) Blechta, V., Šabata, S., Sýkora, J., Hetflejš, J., Soukupová, L. and Schraml, J. The effect of solvent accessible surface on Hammett-type dependencies of infinite dilution ^{29}Si and ^{13}C-NMR shifts in ring substituted silylated phenols dissolved in chloroform and acetone, *Magn. Reason. Chem.,* **2012**, *50*, 128.

44) Caldora, H., Zhang, Z., Tilby, M. J, Turner, O. and Leonori, D. Dual photochemical H-atom transfer & cobalt catalysis for the desaturative

synthesis of phenols from cyclohexanones*, Angew. Chem. Int. Ed.,* **2023**, *62*, e202301656

45) Melnick, M., Reich, S. H., Lewis, K. K., Mitchell, L. J., Nguyen, Jr. D., Trippe, A. J., Dawson, H., Davies, J. F., Appelt, II, K., Wu, B.W., Musick, L., Gehlhaar, D. K., Webber, S., Shetty, B., Kosa, M., Kahil, D. and Andrada, D. Bis Tertiary Amide Inhibitors of the HIV-1 Protease Generated via Protein Structure-Based Iterative Design, *J. Med. Chem.* **1996**, *39*, 2795.

46) Seyferth, D., Annarelli, D. C., Shannon, M. L., Escudie, J. and Duncan, D. P. Hexamethylsilirane: II. Ring-opening reactions with some simple reagents, *J. Organomet. Chem.,* **1982**, *225*, 177.

47) De Lucia, N. A., Das, N. and Vannucci, A. K. Mild synthesis of silyl ethers via potassium carbonate catalyzed reactions between alcohols and hydrosilanes, *Org. Biomol. Chem.,* **2018**, *16*, 3415.

48) Han, B., Ren, C. and Wu, L. Titanium-Catalyzed Hydrodehalogenation of Alkyl Halides, *Organometallics*, **2023**, *42*, 1248.

49) Davies, J. S., Higginbotham, L. C., Tremeer, E. J., Brown, C. and Treadgold, R. C. Protection of hydroxy groups by silylation: use in peptide synthesis and as lipophilicity modifiers for peptides*, J. Chem. Soc., Perkin Trans. 1*, **1992**, *22*, 3043.

50) Park, S. and Brookhart, M. Hydrosilylation of epoxides catalyzed by a cationic η1-silane iridium(iii) complex, *Chem. Commun*., **2011**, *47*, 3643.

51) Yang, X., Sun, R., Li, R., Zheng, X., Yuan, M., Xu, B., Jiang, W., Chen, H., Fu, H. and Li, R. Regioselective Direct C–H Trifluoromethylation of Pyridine. *Org. Lett*. **2020**, *22*, 7108.

52) Beato, E., Spinnato, D., Zhou, W. and Melchiorre, P. A General Organocatalytic System for Electron Donor–Acceptor Complex Photoactivation and Its Use in Radical Processes*, J. Am. Chem. Soc.* **2021**, *143*, 12304.

53) Liao, K., Chan, C. Y., Liu, S., Zhang, X., Che, J. and Huang, Y. Photoredox Cleavage of a Csp^3–Csp^3 Bond in Aromatic Hydrocarbons, *J. Am. Chem. Soc.* **2023**, *145*, 12284.

54) The assignment of the endo or exo configuration in 3-alkyl-substituted 2-norbornanones can be estimated by comparing the C-5 and C-6 ^{13}C-NMR spectroscopic chemical shifts, see: Ravelli, D., Zema, M., Mella, M., Fagnoni,

M. and Albini, A. Benzoyl Radicals from (Hetero)aromatic Aldehydes. Decatungstate Photocatalyzed Synthesis of Substituted Aromatic Ketones, *Org. Biomol. Chem.* **2010**, *8*, 4158.

55) Petrier, C., De Souza Barbosa, J., Dupuy, C. and Luche, J. L. Ultrasound in organic synthesis. 7. Preparation of organozinc reagents and their nickel-catalyzed reactions with α,β-unsaturated carbonyl compounds*, J. Org. Chem*. **1985**, *50*, 5761.

56) Luguera Ruiz, A., La Mantia, M., Merli, D., Protti, S. and Fagnoni, M. Alkyl Radical Generation via C–C Bond Cleavage in 2-Substituted Oxazolidines, *ACS Catal.* **2022**, *12*, 12469.

57) Jia, P., Li, Q., Poh, W. C., Jiang, H., Liu, H., Deng, H. and Wu, J. Light-Promoted Bromine-Radical-Mediated Selective Alkylation and Amination of Unactivated C(sp^3)–H Bonds, *Chem*., **2020***, 6*, 1766.

58) Luguera Ruiz, A., Mariani, E., Protti, S. and Fagnoni, M. Photoredox Catalyzed Release of Carbon-based Radicals from 2-Substituted-1,3-Imidazolidines. *Org. Chem. Front.*, **2024**, *11*, 661.

59) Liao, K., Chan, C. Y., Liu, S., Zhang, X., Chen, J. and Huang, Y. Photoredox Cleavage of a Csp3–Csp3 Bond in Aromatic Hydrocarbons, *J. Am. Chem. Soc.* **2023,** *145*, 12284.

60) Hayakawa, M., Shimizu, R., Omori, H., Shirota, H., Uchida, K., Mashimo, H., Xu, H., Yamada, R., Niino, S., Wakame, Y., Liu, C., Aoyam,a T. and Ouchi, A. Photochemical addition of cyclic ethers/acetals to olefins using tBuOOtBu: Synthesis of masked ketones/aldehydes and diols, *Tetrahedron*, **2020**, *76*, 131557.

61) Wan, T., Capaldo, L., Ravelli, D, Vitullo, W., de Zwart, F. J., de Bruin, B. and Noël, T. Photoinduced Halogen-Atom Transfer by N-Heterocyclic Carbene-Ligated Boryl Radicals for C(sp^3)–C(sp^3) Bond Formation, *J. Am. Chem. Soc.* **2023**, *145*, 991.

62) Capaldo, L., Merli, D., Fagnoni, M. and Ravelli, D. Visible Light Uranyl Photocatalysis: Direct C–H to C–C Bond Conversion, *ACS Catal*., **2019**, *9*, 3054.

63) Montanaro, S., Ravelli, D., Merli, D., Fagnoni, M. and Albini, A. Decatungstate as Photoredox Catalyst: Benzylation of Electron-Poor Olefins, *Org. Lett,.* **2012**, *14*, 4218.

64) Iannazzo, L. and Molander, G. A. Activation of Si–Si Bonds for Copper(I)-Catalyzed Conjugate Silylation, *Eur. J. Org. Chem*., **2012**, 4923.

Chapter 3

Metal-free Photocatalytic Cross-Electrophile Coupling enables C1 Homologation and Alkylation of Carboxylic Acids with Aldehydes

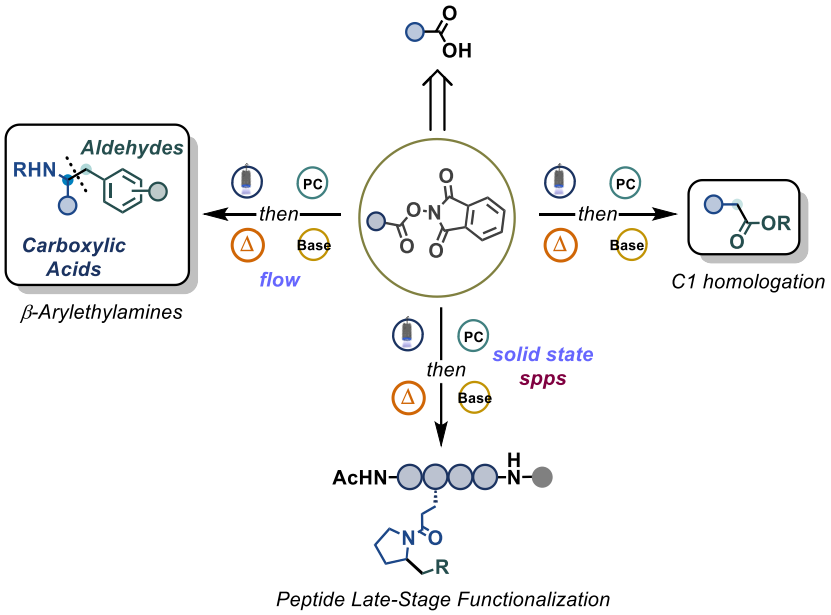

This chapter is based on:

Bonciolini S.; Pulcinella A.; Leone M.; Schiroli D.; **Luguera Ruiz A.**; Sorato A.; Maryne A.; Dubois, J.; Gopalakrishnan, R.; Masson, G.; Della Ca', N.; Protti, S.; Fagnoni, M.; Zysman-Colman, E.; Johansson, M.; Noël, T. Metal-free Photocatalytic Cross-Electrophile Coupling enables C1 Homologation and Alkylation of Carboxylic Acids with Aldehydes. *Nat Commun*. **2024**, *15*, 1509-1517.

3.1 Introduction.

In drug discovery, the 3D structure of proteins is crucial for the success of drugs. The increased use of sp^3-hybridized carbon atoms (Fsp^3) is key, as it correlates with a drug's effectiveness and safety.[1] This trend, known as 'Escape from Flatland',[2] involves increasing Fsp^3 in drugs for better alignment with protein structures, enhancing selectivity and efficacy.[3] This strategy improves target interaction and reduces side effects, balancing effective treatment with minimal negative effects.

Historically, classical cross-coupling reactions have been a linchpin in synthetic chemistry, enabling the straightforward construction of $C(sp^2)–C(sp^2)$ bonds and thereby propelling the production of planar, biaryl structures. This entrenched reliance on cross-coupling has inadvertently sculpted a discernible bias in small molecule drug design, steering the generation of libraries that predominantly feature structurally analogous, two-dimensional compounds.[4] While there have been laudable strides made within the domain of $C(sp^3)–C(sp^3)$ cross-coupling, contemporary methodologies are oftentimes plagued by several pragmatic limitations.[5,6] They typically necessitate sizable excesses of one coupling partner and frequently hinge upon non-abundant starting materials, such as air- and moisture-sensitive alkyl organometallics, thereby constraining the reaction scope and practicality in a drug discovery context. Consequently, the quest for alternative strategies that circumvent these limitations while facilitating the construction of three-dimensional molecular structures persists as an imperative in medicinal chemistry research.[7]

In recent years, nickel-mediated cross-electrophile (XEC) coupling has emerged as a potent strategy for constructing $C(sp^3)–C(sp^3)$ bonds, utilizing various native and bench-stable aliphatic coupling entities, thus circumventing the use of moisture-sensitive organometallic species.[8–16] Despite substantial strides within this sphere, exploiting varied, ubiquitous functional groups such as aldehydes as coupling partners has lingered in a state of underdevelopment. Traditionally, aldehydes have been harnessed as carbonyl electrophiles with Mg or Li-based organometallic species or within Nozaki–Hiyama–Kishi (NHK) type reactivity to yield alcohols,[17,18] yet their employment to forge $C(sp^3)–C(sp^3)$ bonds via a reductive deoxygenative

pathway remains, to our knowledge, uncharted. A pioneering approach, that enables the direct coupling of sp^2 and sp^3 electrophiles, such as aldehydes and carboxylic acids, heralds an attractive disconnection in the cross-electrophile coupling domain (Figure 3.1a). Aryl sulfonyl hydrazones are considered as a bench-stable, activated form of aldehydes due to their known propensity to undergo both radical and polar addition, ultimately yielding deoxygenated, cross-coupled products upon thermal decomposition of alkylated hydrazide intermediates (Figure 3.1b).[19–28] Utilizing abundant aliphatic carboxylic acids activated as NHPI-based redox-active esters (RAEs) to serve as sp^3 electrophiles, and employing visible light-mediated decarboxylation to yield carbon-centered radicals,[29–32] we envisioned a trapping mechanism with aldehyde sulfonyl hydrazones to, upon sulfinate and dinitrogen extrusion, afford the coveted product (Figure 3.1c). In this study, we realize such a metal-free cross-electrophile coupling, leveraging Eosin Y as an economical organophotocatalyst under visible light irradiation.[33]

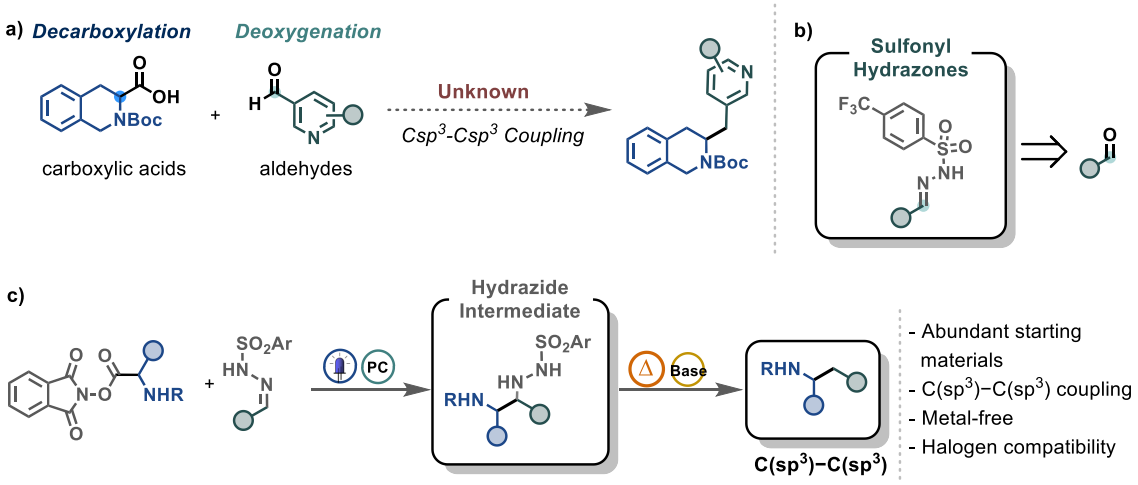

Figure 3.1. Design and applications of the cross-electrophile coupling of carboxylic acids with aldehydes. a) Elusive cross-electrophile coupling between carboxylic acids and aldehydes. b) Fast and scalable activation of aldehydes. c) Our strategy: visible light promoted coupling of activated carboxylic acids and sulfonyl hydrazones.

Illustrating the potential of our synthetic strategy becomes particularly appealing when reflecting upon the strategic C1 homologation of carboxylic acids, traditionally achieved through the Arndt-Eistert reaction.[34–37] Although this protocol, developed in the 1950s, bears chemical reliability, significant limitations persist, particularly those pertaining to the generation, purification, and utilization of toxic and explosive

diazomethane, hindering its widespread adoption and applicability. While flow technology has provided a partial answer to these safety challenges,[38] a truly general and practical alternative for such transformation has been elusive.[39] Indeed, polar variants such as the Kowalsky Ester homologation suffer from the use of organolithium bases, strongly limiting the substrate scope of the transformation and its scalability.[40,41] For seminal radical variants, Barton proposed a photoinduced C1 homologation of *N*-hydroxy-2-thiopyridone esters, although this strategy suffered from low functional group compatibility, a narrow scope, and requisite lengthy synthetic sequences.[42,43]

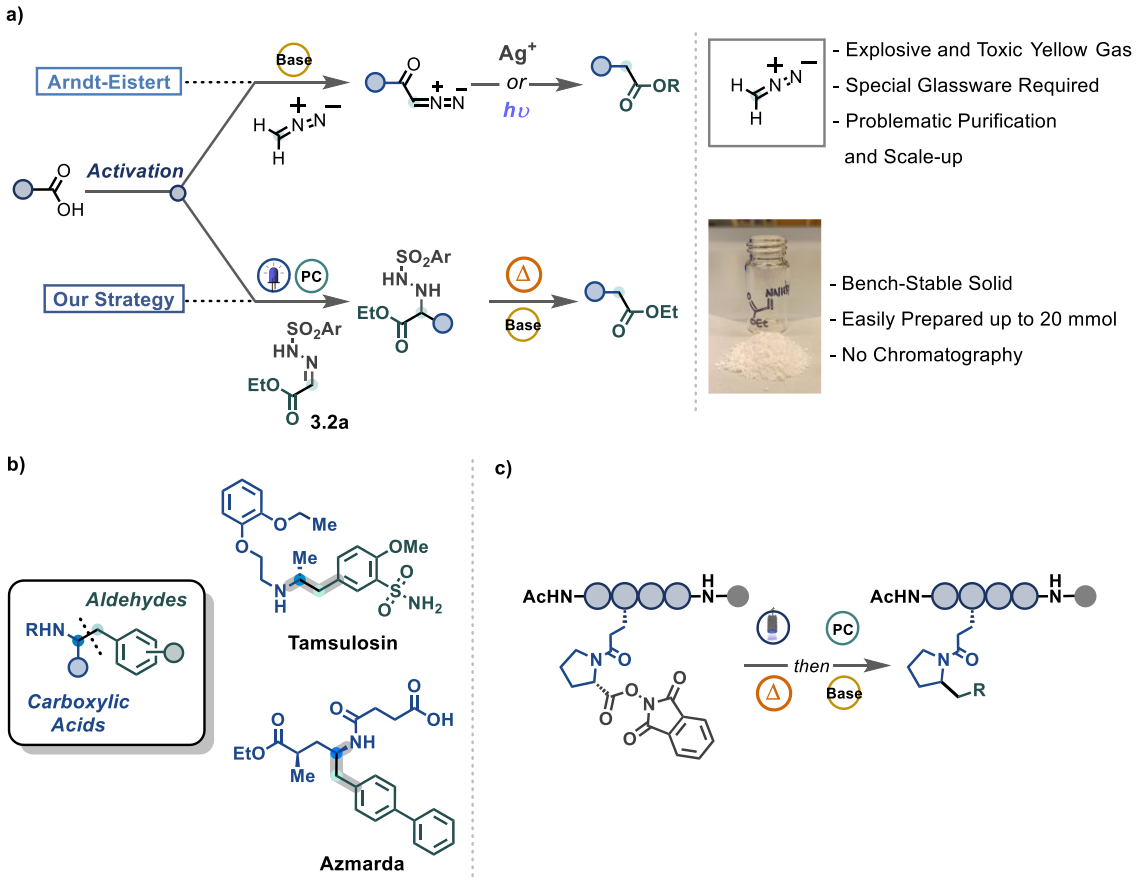

Figure 3.2. Design and applications of the cross-electrophile coupling of carboxylic acids with aldehydes. a) Application: alternative approach to the classical Arndt-Eistert C1-homologation. b) Application: retrosynthetic strategy for the synthesis of arylethylamines. c) Late-stage alkylation of peptides on resin.

In this context, we present the utilization of ethyl glyoxalate-derived sulfonyl hydrazone **3.2a** as a bench-stable and easy-to-handle crystalline radical acceptor to realize the C1 homologation of carboxylic acids under mild conditions (Figure 3.2a). As a subsequent, potent application of this synthetic paradigm, our attention was

drawn by the synthesis of β-arylethylamines, a prevalent structural motif within numerous drugs and natural products.[44] Although various synthetic routes have been delineated, an intuitive retrosynthetic strategy entailing a cross-coupling reaction between a benzyl electrophile and α-amino nucleophile has remained underrepresented.[44–46] We posit that the advanced cross-electrophile coupling between NHPI esters and aldehyde sulfonyl hydrazones will provide a straightforward and direct route for the efficient preparation of substituted cyclic and acyclic *β*-arylethylamines (Figure 3.2b). Concluding with a third robust synthetic application of this strategy, the methodology demonstrates significant utility in the late-stage functionalization (LSF) of peptides on solid-phase, enabling the modification of complex peptides under mild conditions instead of proceeding via classical *de-novo* synthesis (Figure 3.2c).[47–49]

3.2 Results and discussions.

We initially commenced to develop a direct decarboxylative C1 homologation, beginning with *N*-Boc (*L*)-Proline, but we were met with failure to produce the desired product **3.3**. This result was linked to the noted sensitivity of aldehyde sulfonyl hydrazones to bases, which are indispensable to promote the decarboxylation process.[21,50] Consequently, our investigation focused on the use of well-established *N*-(acyloxy)phthalimides (NHPI-based esters) as redox-active esters (RAEs) in an effort to sidestep the necessity for bases during the decarboxylative generation of nucleophilic carbon radicals. An exhaustive screening of all reaction parameters (Table 3.1) led us to discover that the targeted homologated product **3.3** could be obtained in excellent yields (Table 3.1, entry 1, 90% yield) when a dichloromethane (0.1 M) solution composed of ethyl glyoxalate-derived 4-trifluoromethyl-phenyl sulfonyl hydrazone **3.2a** (1.0 equiv.) as the radical acceptor, *N*-Boc (*L*)-Proline RAE **3.1a** (1.0 equiv.) as the radical precursor, Hantzsch ester (HE, 1.5 equiv.) as the reductive quencher, and disodium Eosin Y ($EYNa_2$, 10 mol%) as the photocatalyst was irradiated with blue LEDs (40W Kessil, 456 nm, PR160L) for 12 hours. The yield reflects the one obtained for the final product **3.3**, achieved when the hydrazinyl intermediate was swiftly subjected to cleavage conditions in ethanol, according to our previous report.[27] Evaluating a two-step one-pot procedure, with trifluorotoluene as the solvent, revealed diminished yields of

3.3 (Table 1, entry 27). Surprisingly, an excess of radical acceptor **3.2a** did not markedly influence the reactivity (Table 1, entry 11). Noteworthy is the underperformance of more expensive organophotoredox catalysts like 4CzIPN, $3DPA_2FBN$ or the widely used transition-metal based photocatalyst $Ru(bpy)_3PF_6$ (Table 1, entries 2-7, 26-29).[51,52] HE played a major role in the transformation, as other reductive quenchers, such as DABCO, DIPEA, or tetramethylguanidine entirely inhibited the reaction (Table 3.1, entries 18-22). Remarkably, incorporating acidic additives, such as HFIP, TFA, and various amino acids, did not substantially impact the reactivity (Tables 3.1 entries 16, 17). Control experiments conducted to explore the formation of donor-acceptor complexes between RAE **3.1a** and HE, performed at 456 and 390 nm without $EYNa_2$, either yielded no product or achieved lower yields (Table 3.1, entries 30, 31), underscoring the crucial role of the photocatalyst in photoinitiating the reaction, thus securing higher yields.[53,54] Running the reaction in the dark resulted in the quantitative recovery of all starting materials (Table 3.1, entry 32). Notably, applying the optimized conditions to the less electrophilic 4-CF_3-benzaldehyde-derived sulfonyl hydrazone **3.2c** as the radical acceptor yielded the corresponding β-arylethylamine product **3.46** in a 58% NMR yield.

Table 3.1. Optimization of the photochemical step for the C1 homologation of RAE **3.1a**.

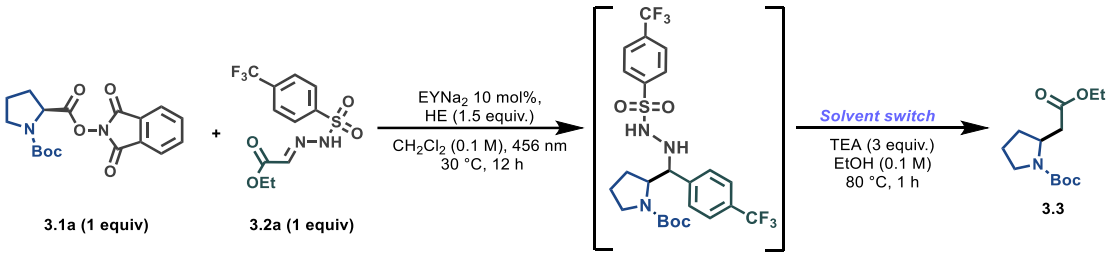

Entry	Deviations from the standard conditions	3.3 (% Yield)[a]
1	None	90
2	$Ru(bpy)_3(PF_6)_2$ (1 mol%)	65
3	$Ru(bpy)_3(PF_6)_2$ (1 mol%), 3.1a (2.0 equiv.)	44
4	$Ru(bpy)_3(PF_6)_2$ (1 mol%), HE (2.0 equiv.)	67
5	$Ir(ppy)_3$ (1 mol%)	30
6	4CzIPN (5 mol%)	64
7	$3DPA_2FBN$ (5 mol%)	54
8	Eosyn Y $(Na)_2$ (5 mol%)	70

Table 3.1. Table continues.

Entry	Deviations from the standard conditions	3.3 (% Yield)[a]
9	Eosyn Y $(Na)_2$ (10 mol%)	81
10	Eosyn Y (10 mol%)	75
11	DCM as solvent, 3.2a (2.0 equiv.)	81
12	DCE as solvent	54
13	Toluene as solvent	68
14	THF as solvent	Traces
15	Acetone, 3.2a (1.0 equiv.)	25
16	DCM, TFA (20 mol%)	90
17	DCM, HFIP (20 mol%)	84
18	DABCO as reductive quencher	-
19	Tetramethylguanidine as reductive quencher	-
20	DIPEA as reductive quencher	-
21	No reductive quencher	-
22	HE as reductive quencher	90
23	EtOH as solvent	Messy crude
24	DMF as solvent	Messy crude
25	ACN as solvent	Messy crude
26	$Ru(bpy)_3(PF_6)_2$ (1 mol%), ACN	Messy crude
27	$Ru(bpy)_3(PF_6)_2$ (1 mol%), TFT	64
28	$Ru(bpy)_3(PF_6)_2$ (1 mol%), DMF	71
29	$Ru(bpy)_3(PF_6)_2$ (1 mol%), DMF. Cleavage EtOH/DMF 1:1 (0.05 M)	63
30	No PC	-
31	No PC, 390 nm	40
32	No light	-

[a]The yields were determined by ^{1}H-NMR using trichloroethylene as external standard (0.2 mmol scale, 0.1 M).

Having established optimal reaction conditions, we next investigated the scope of the photochemical C1 homologation of RAEs derived from readily available carboxylic acids (Figure 3.2). As expected, *N*-Boc protected cyclic amino acids afforded the desired products (**3.3-3.5**) in good yields. Moreover, linear proteogenic amino acids underwent homologation to the respective ethyl esters (**3.6-3.13**) under the standardized reaction conditions. Noteworthy is the performance of

challenging substrates, such as the redox-sensitive methionine and thiophene-derived amino acid, which, despite providing the target compounds (**3.8** and **3.10**), did so in somewhat attenuated yields.

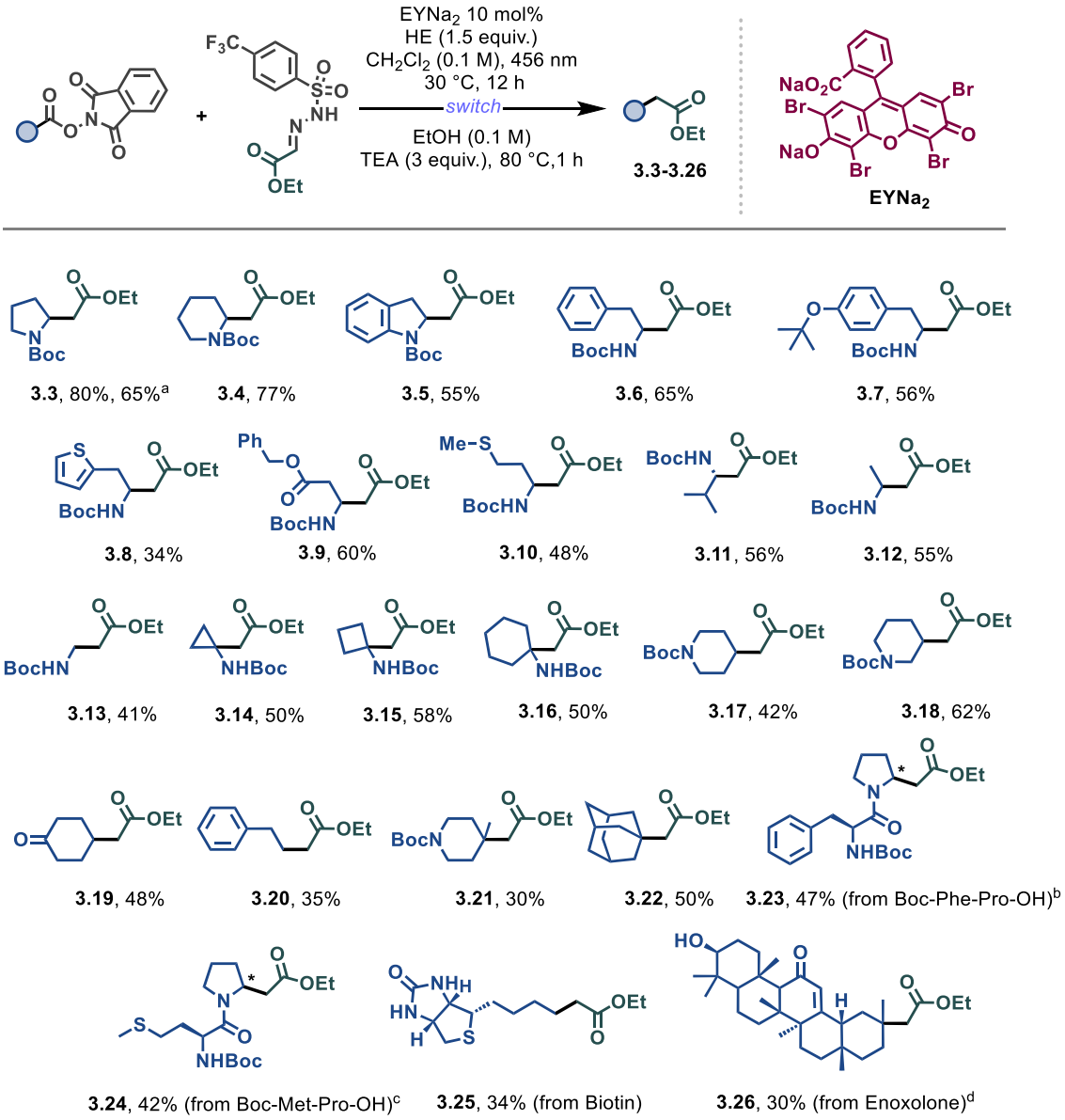

Figure 3.3. Scope of the C1 homologation. Coupling of carboxylic acid-derived redox-active esters (RAEs) with ethyl glyoxylate-derived 4-trifluoromethylphenyl sulfonyl hydrazones **3.2a**. Reaction conditions: redox active ester (0.3 mmol, 1 equiv.), **3.2a** (1 equiv.), Hantzsch ester (1.5 equiv.) and $EYNa_2$ (0.10 equiv.) in 3 mL of CH_2Cl_2 (0.1 M). [a]1mmol reaction. [b]> 20:1 d.r. [c]3:1 d.r. [d]2.5:1 d.r.

The protocol's generality was highlighted through the homologation of sterically hindered cyclic tertiary amino acids, producing the target products in synthetically useful yields (**3.14**-**3.16**). A subsequent examination of various inactivated primary, secondary, and tertiary RAEs revealed that all coupled with glyoxalate-derived

sulfonyl hydrazones **3.2a**, presenting moderate to good yields (**3.17**-**3.22**). In a particularly notable development, two dipeptides underwent photochemical homologation, yielding the targeted homoproline-analogues (**3.23-3.24**).[55] Importantly, the mild conditions of this photocatalytic C1 homologation protocol facilitated the conversion of natural products like biotin and enoxolone—each harboring different sensitive functional groups—to their corresponding ethyl esters (**3.25**-3.**26**), not accessible by the aforementioned methods.

We next aimed to explore further the generality of our developed reaction conditions, applying them to the cross-electrophile coupling of RAEs, derived from a diverse set of carboxylic acids, with various aldehyde-derived sulfonyl hydrazones (Figure 3.4). We envisioned providing streamlined access to cyclic and acyclic *β*-arylethylamines, thereby presenting a new, intuitive radical disconnection for practitioners in the field.[44] The reaction was optimized adopting the previous found conditions for the C1 homologation process.

Table 3.2. Optimization of the photochemical step for the alkylation reaction. [a]External standard: dodecane.

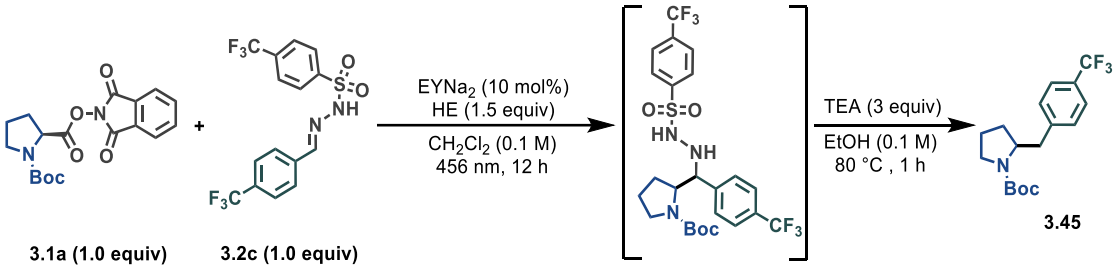

Entry	Deviations from the standard conditions	3.45 (% GC-Yield)[a]
1	None	57
2	Acetone as solvent	43
3	EtOAc as solvent	37
4	ACN as solvent	50
5	Toluene as solvent	21
6	DCM + 20 equiv. H_2O as solvent	56
7	DCM + 50 equiv. H_2O as solvent	56
8	DCM (no degass)	54
9	Eosyn Y(H_2) (10 mol%)	55
10	Eosyn Y(H_2) (10 mol%), **3.2b** (1.0 equiv.)	61

Table 3.2. Table continues.

Entry	Deviations from the standard conditions	3.45 (% GC-Yield)[a]
11	Green light 525 nm	57
12	0.05 M	58
13	Eosyn Y(Na_2) (20 mol%)	45
14	**3.2a** (2.0 equiv.)	52
15	Eosyn Y(Na_2) (20 mol%), 3.2a (2.0 equiv.)	58
16	HE (1.0 equiv.)	45
17	HE (2.0 equiv.)	38
18	(L)-Boc-Phe-OH (1.0 equiv.) as additive	50
19	**3.2p** (1.0 equiv.)	25
21	**3.1a** (2.0 equiv.), 3.2p (1.0 equiv.)	50

Regarding the scope of the α-amino RAEs, a myriad of medicinally pertinent cyclic structures—encompassing azetidine, piperazine, indoline, and isoquinoline—were successfully coupled, achieving synthetically useful yields in all cases (**3.27-3.33**).[56]

Such methodology enabled the conversion of even challenging tertiary RAEs, facilitating the creation of quaternary centers, albeit with somewhat reduced yields (**3.34-3.36**). Beyond cyclic structures, the protocol also exhibited proficiency with a range of linear amino acids, yielding the corresponding β-arylethylamines in moderate to good isolated yields (**3.37-3.41**). Noteworthily, the metal-free nature of the protocol tolerated halogenated arenes and heterocycles, providing convenient handles for subsequent synthetic elaboration (**3.30**, **3.47**, **3.48**, **3.50-3.53**). A noticeable limitation of the scope was observed: electron-rich sulfonyl hydrazones yielded only traces of the desired product, with a notable reduction of the carboxylic acid. Additionally, under slightly modified reaction conditions, Eosin Y(H2) (10 mol%) and **3.2b** (1.0 equiv.), unactivated aliphatic aldehyde-derived sulfonyl hydrazones acted as effective coupling partners, delivering alkylated secondary amines in synthetically useful yields, and underlining the method's simplicity and versatility (**3.54-3.58**).

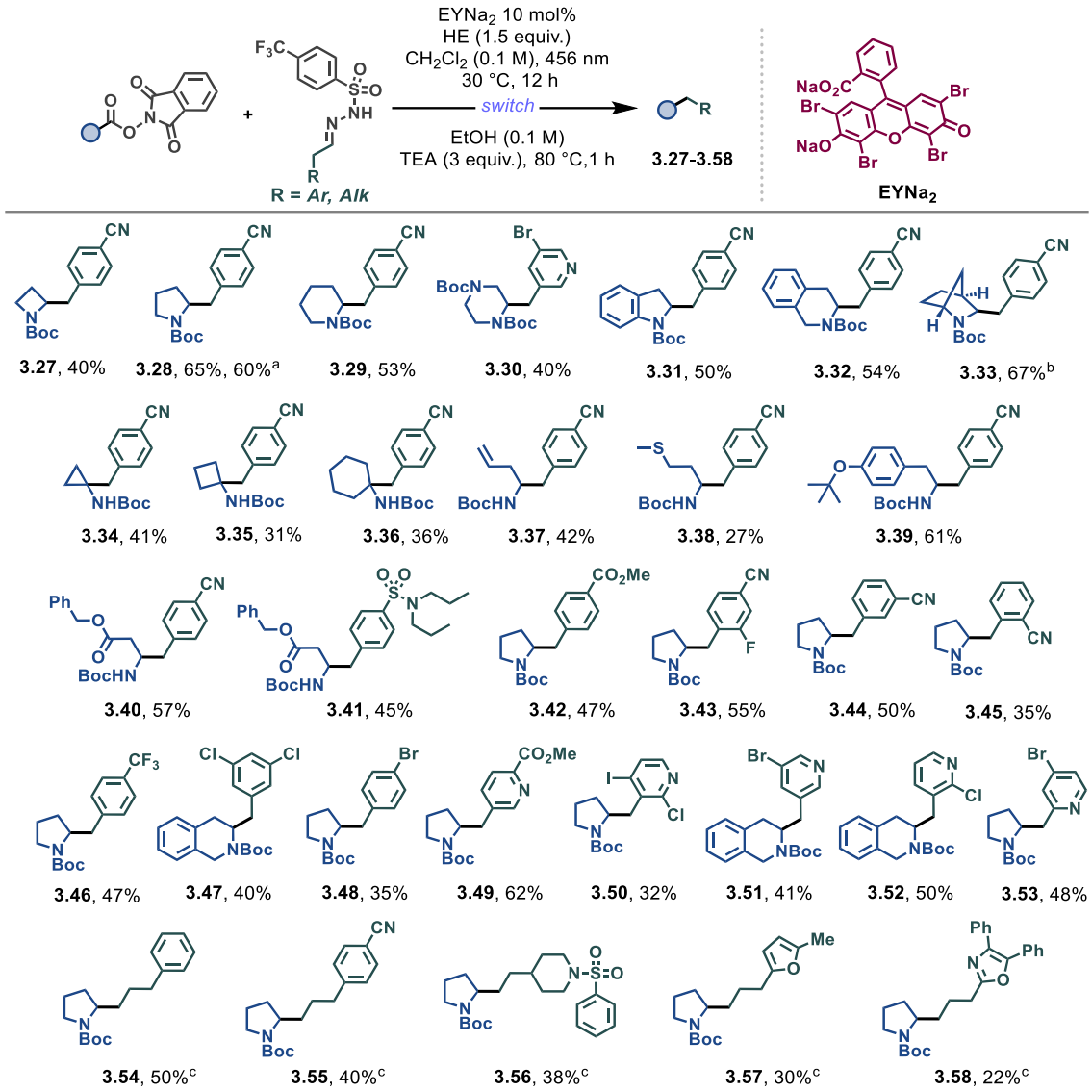

Figure 3.4. Scope of the alkylation. Cross-electrophile coupling of RAEs with aromatic and aliphatic aldehyde-derived sulfonyl hydrazones. Reaction conditions: RAE (0.3 mmol, 1 equiv.), Sulfonyl Hydrazone (1 equiv.), Hantzsch ester (1.5 equiv.) and $EYNa_2$ (0.10 equiv.) in 3 mL of CH_2Cl_2 (0.1 M). [a]1mmol scale. [b]1:1.4 d.r. [c]2 equiv. of *N*-Boc (L)-Proline RAE **3.1a** was used.

Having demonstrated the generality of the photochemical cross-electrophile coupling between sulfonyl hydrazones and RAEs, we turned our inquiry toward the potential extension of this protocol to facilitate the late-stage functionalization (LSF) of more complex molecules, such as peptides. Given the increasing prominence of peptides as therapeutic modalities, the development of methods capable of functionalizing extensive amino acid sequences directly on resin becomes especially valuable, enabling the generation of diversity without necessitating the development of *de-novo* synthetic methods.[57,58] Moreover, on-resin modification

brings forth substantial practical advantages, addressing key challenges related to purification and solubility that are often encountered in peptide chemistry in solution. Specifically, considering the well-documented compatibility of redox-active ester synthesis with solid-phase approaches,[47,59,60] and the mild basic condition of our two-step protocol, we hypothesized that adapting this photochemical transformation to heterogeneous conditions on resin would be an attainable objective.

At the outset of our investigation, a sensitivity/robustness screening was undertaken to determine which amino acids would be compatible with the reaction conditions and, consequently, could be possibly incorporated into the peptide sequence (Table 3.3).

Table 3.3. Sensitivity assessment of the C1 homologation reaction.

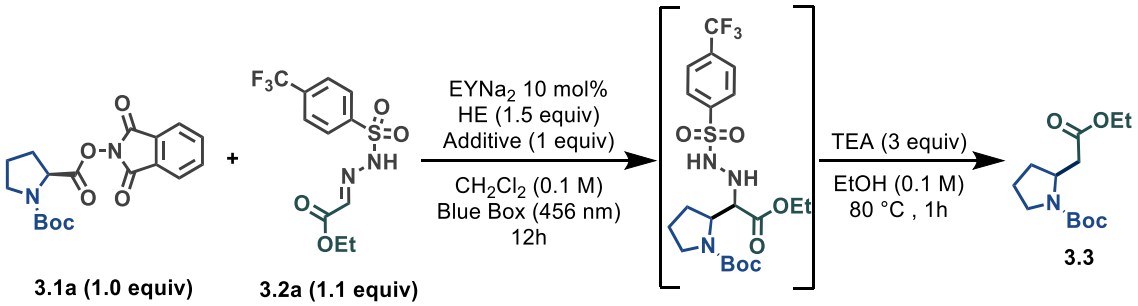

Entry	Deviations from the standard conditions	3.3 (% Yield)[a]
1	None	91
2	Boc-Ph-OH	95
3	Fmoc-Ph-OH	95
4	Fmoc-Ala-OH	90
5	Fmoc-Lys(Boc)-OH	93
6	Fmoc-Arg(Pbf)-OH	70
7	Fmoc-Trp(Boc)-OH	88
8	Fmoc-Cys(Trt)-OH	77
9	Fmoc-Met-OH	82
10	Fmoc-Lys(Boc)-OH	93
11	Fmoc-Hyst(Trt)-OH	75

[a]The yields were determined by ^{1}H-NMR using trichloroethylene as external standard. The corresponding aa was employed as an additive (1.0 equiv.).

In the experiments, we opted for Fmoc-protected amino acids bearing fully protected side chains due to their availability and low price. Despite Fmoc removal was envisioned during the fragmentation of the intermediate, the goal of the assessment was to evaluate the compatibility of the functional groups of amino acids side chains, that being redox active, could disrupt the desired reactivity.

Pleasingly, all screened amino acid residues, when added as additives, did not interfere with the model reaction and it could be readily engaged in the photocatalytic alkylation (Figure 3.5). Illustratively, heptapeptide **3.P1** was subjected to LSF, yielding the corresponding homoproline-containing analogue **3.59** in a 28% isolated yield after 21 steps from resin loading (74% LCAP for the decarboxylative alkylation step, with LCAP defined as LC Area % of the product peak in the ultra-performance liquid chromatography (UPLC) chromatogram of the reaction crude, General procedure 3.6 and 3.7, Figure ES3.2-3.8). Highlighting the efficacy of our method, a 28% yield robustly demonstrates the potential of our cross-electrophile coupling for synthesizing complex structures with high selectivity and notable yield conservation. Similarly, a late-stage incorporation of a benzylic unit was accomplished efficiently, demonstrating utility in the context of lipophilicity modulation (**3.60**) (72% LCAP for the decarboxylative alkylation step, with LCAP defined as LC Area % of the product peak in the ultra-performance liquid chromatography (UPLC) chromatogram of the reaction crude).

To our delight, a derivative of afamelanotide—a therapeutic peptide indicated for patients affected by erythropoietic protoporphyria—was also successfully engaged in the protocol, affording derivative **3.61** in an overall 9% yield from resin loading (71% LCAP for the decarboxylative alkylation step.[61]

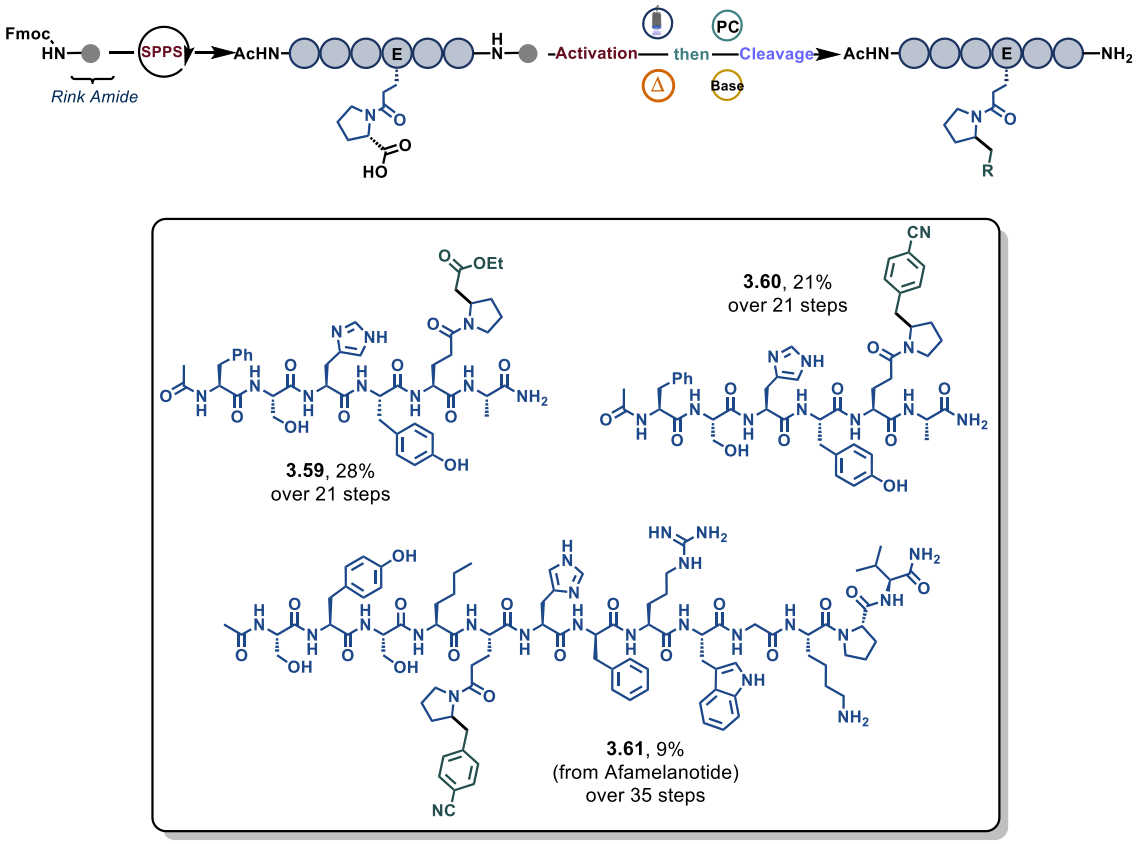

Figure 3.5. Scope of the cross-electrophile coupling of peptide RAEs on resin. Reaction conditions: RAE (0.03 mmol, 1 equiv.), Sulfonyl Hydrazone (3 equiv.), Hantzsch ester (4.5 equiv.) and $EYNa_2$ (0.30 equiv.) in CH_2Cl_2 (33 mM).

Additionally, we demonstrate the scalability of our photochemical C1 homologation using flow technology (Figure 3.6). In batch settings above 1 mmol, the heterogeneous reaction mixture led to a significant drop in yield of the desired product **3.3**. Suspecting non-uniform irradiation and limited light penetration at larger scales, we transitioned the photochemical alkylative step to continuous flow.[68–70]

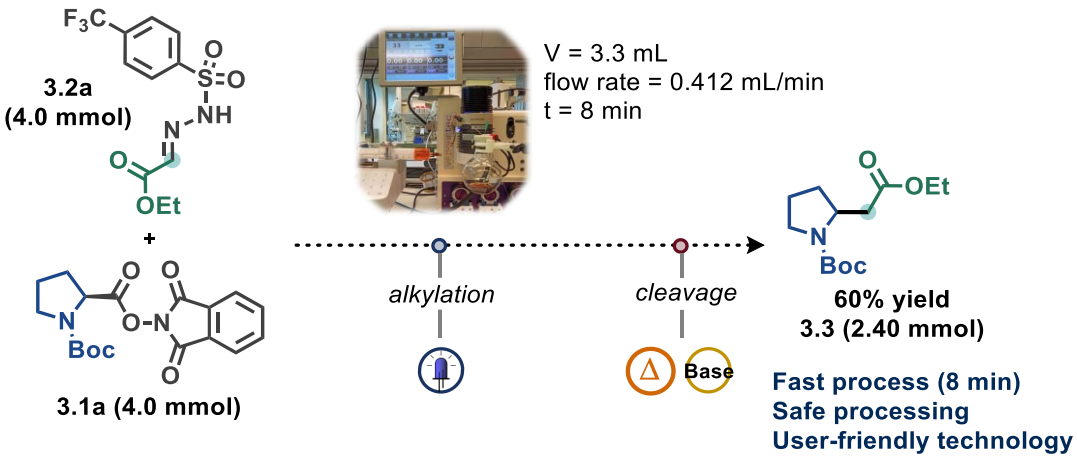

Figure 3.6. Scale-up C1 homologation of **3.1a** in continuous flow.

After an extensive optimization conducted at 0.2 mmol scale (Table 3.4), we established conditions for the protocol using a Vapourtec UV-150 photochemical flow reactor (ID: 0.8 mm; V = 3.33 mL, flow rate = 0.412 mL min^{-1}, t = 8 min) set at 30 °C, irradiated with 60 W 450 nm LEDs. Subsequent thermal cleavage of the alkylated hydrazide intermediate yielded the targeted C1 homologated product in 60% isolated yield.

Table 3.4. Sensitivity assessment of the C1 homologation reaction.

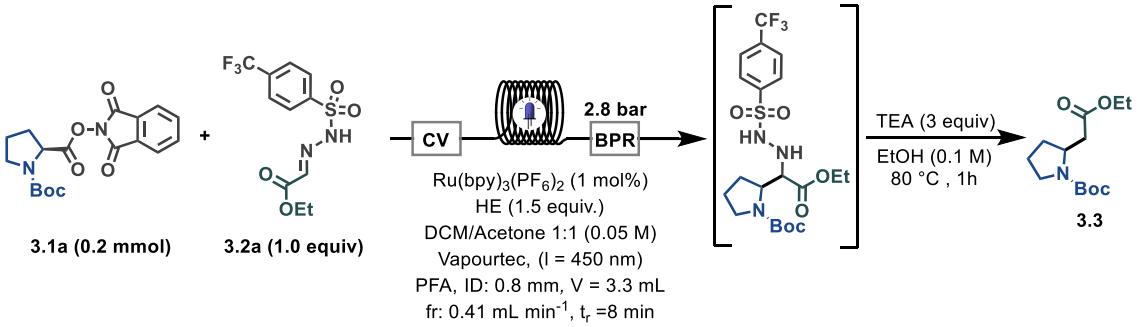

Entry	Deviations from the standard conditions	3.3 (% Yield)[a]
1	**None**	**65**
2	Eosyn Y(Na_2) (10 mol%), DCM (0.1 M), tr: 10 min	Not soluble
3	Eosyn Y(Na_2) (10 mol%), DCM (0.05 M), tr: 10 min	Not soluble
4	Eosyn Y(H_2) (10 mol%), DCM (0.05 M), tr: 10 min	Not soluble
5	Eosyn Y(H_2) (10 mol%), DCM/DMSO (3:1) (0.1 M), tr: 10 min	Messy crude
6	Eosyn Y(H_2) (10 mol%), DCM/THF (1:1) (0.1 M), tr: 10 min	Messy crude
7	Eosyn Y(H_2) (10 mol%), DCM/Acetone (8:1) (0.05 M), tr: 10 min	45
8	Eosyn Y(H_2) (10 mol%), DCM/Acetone (1:1) (0.05 M), tr: 10 min	Messy crude
9	$Ru(bpy)_3(PF_6)_2$ (1 mol%), DMF (0.1 M), tr: 2.5 min	<10[b]
10	$Ru(bpy)_3(PF_6)_2$ (1 mol%), DMF (0.1 M), tr: 8 min	50[b]
11	$Ru(bpy)_3(PF_6)_2$ (1 mol%), DMF (0.1 M), tr: 15 min	<10[b]
12	$Ru(bpy)_3(PF_6)_2$ (1 mol%), DMF/EtOH (1:1) (0.1 M), tr: 8 min	40[b]
13	$Ru(bpy)_3(PF_6)_2$ (1 mol%), DMF/Acetone (1:1) (0.1 M), tr: 8 min	Not soluble

[a]The yields were determined by ^{1}H-NMR using trichloroethylene as external standard. The corresponding aa was employed as an additive (1.0 equiv.). [b]Cleavage conditions: Solvent switch to EtOH (0.1 M), TEA (3 equiv.), 80 °C.

In our pursuit to elucidate the mechanism, we executed a series of experiments to explore the radical pathway and identify the catalytic species facilitating the photochemical transformation. Confirmation of the radical nature of the reaction

was achieved through radical trapping and radical clock experiments (Figure 3.7).[62] Indeed, ESI-HRMS analysis substantiated the formation of TEMPO adduct **3.62**, while GC-MS analysis convincingly demonstrated carbon radical formation through the production of **3.64** via a 5-exo-trig radical cyclization.

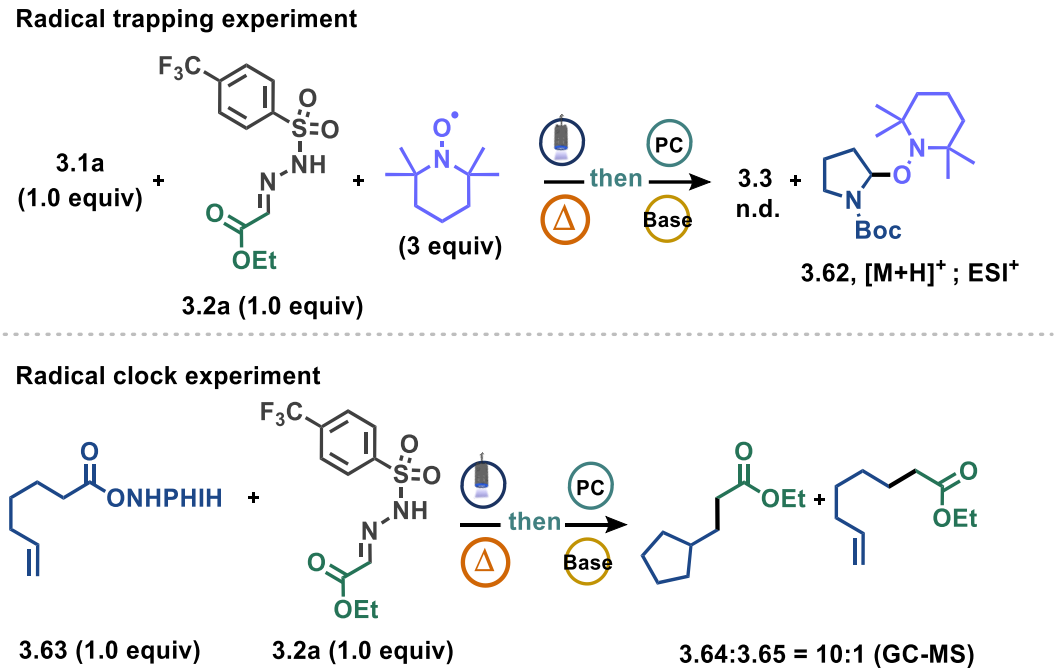

Figure 3.7. Radical trapping and radical clock experiments.

In light of these observations and based on the reported Single Electron Transfer (SET) mechanism of $EYNa_2$, we propose the ensuing catalytic cycle (Figure 3.8).[63,64] Upon absorption of visible light, the triplet excited state of $EYNa_2$ is reductively quenched by the sacrificial electron donor HE to generate $HE^{+\cdot}$. Following the findings of Overmann and König,[65–67] the redox-active ester is subsequently reduced by the $EYNa_2$ radical anion**,** thereby completing the catalytic cycle and yielding the nucleophilic alkyl radical **3.66** upon decarboxylation. The emergent alkyl radical is then captured by the electrophilic site of sulfonyl hydrazone, resulting in the formation of the hydrazinyl radical intermediate **3.67**. Finally, a plausible Hydrogen Atom Transfer (HAT) step from $HE^{+\cdot}$ or neutral HE to **3.67** is considered, generating the pyridium co-product **3.68** and the targeted product **3.69**.

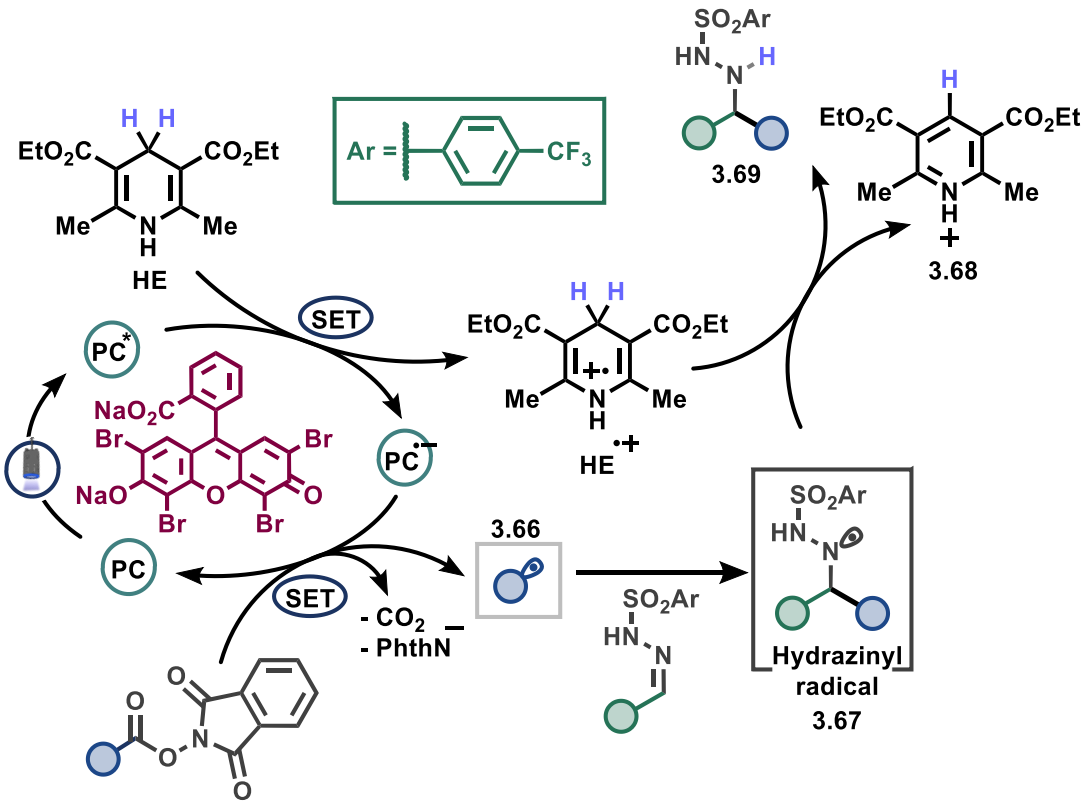

Figure 3.8. Proposed mechanism.

3.3 Mechanistic studies.

3.3.1 UV-Vis characterization.

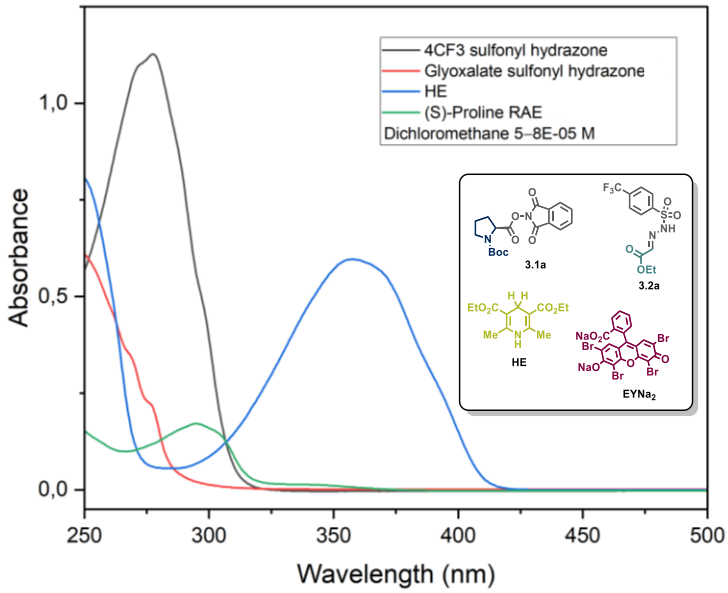

Figure 3.9: Absorption spectra of each reaction component. The spectra were recorded $5 \cdot 10^{-5}$-$8 \cdot 10^{-5}$ M in dichlomethane (quartz cuvettes, optical path: 1 cm) with a bandwidth of 5 nm and a data pitch of 1 nm. Scan rate: medium.

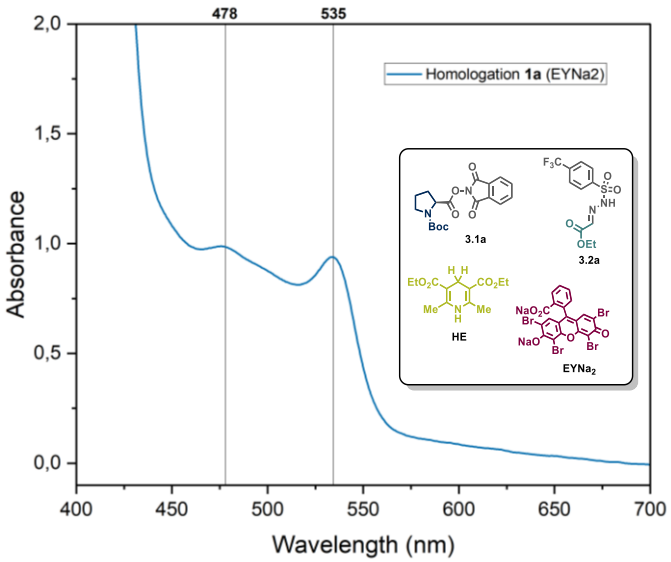

Figure 3.10: Absorption spectrum of the optimized reaction condition for the C1 homologation of **3.1a** with glyoxalate-derived sulfonyl hydrazone **3.2a** using **EYNa$_2$** as PC. The spectrum was recorded in dichloromethane (after filtration of the non-soluble components) in quartz cuvettes (optical path: 1 cm) with a bandwidth of 5 nm and a data pitch of 1 nm. Scan rate: medium.

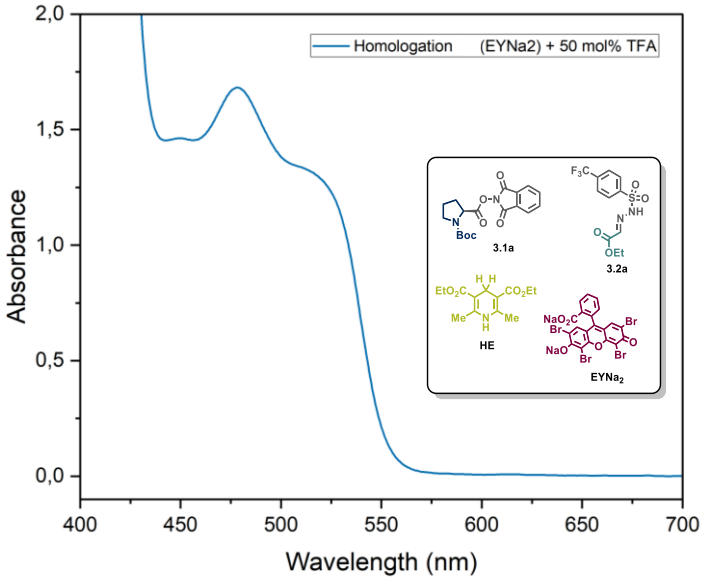

Figure 3.11: Absorption spectrum of the reaction mixture for the C1 homologation of **3.1a** with glyoxalate-derived sulfonyl hydrazone **3.2a** using **EYNa$_2$** as PC in presence of 50 mol% TFA. The spectrum was recorded in dichloromethane (after filtration of the non-soluble components) in quartz cuvettes (optical path: 1 cm) with a bandwidth of 5 nm and a data pitch of 1 nm. Scan rate: medium.

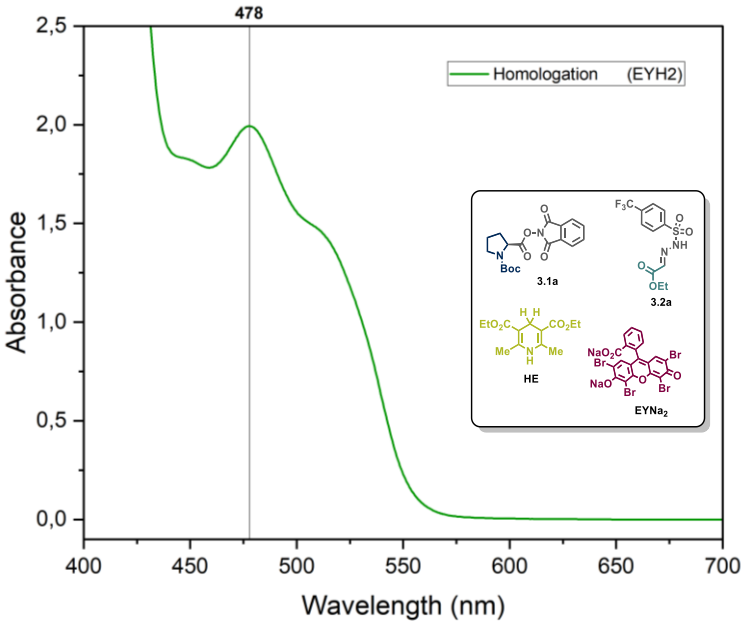

Figure 3.12: Absorption spectrum of the reaction mixture for the C1 homologation of **3.1a** with glyoxalate-derived sulfonyl hydrazone **3.2a** using **EYH_2** as PC. The spectrum was recorded in dichloromethane (after filtration of the non-soluble components) in quartz cuvettes (optical path: 1 cm) with a bandwidth of 5 nm and a data pitch of 1 nm. Scan rate: medium.

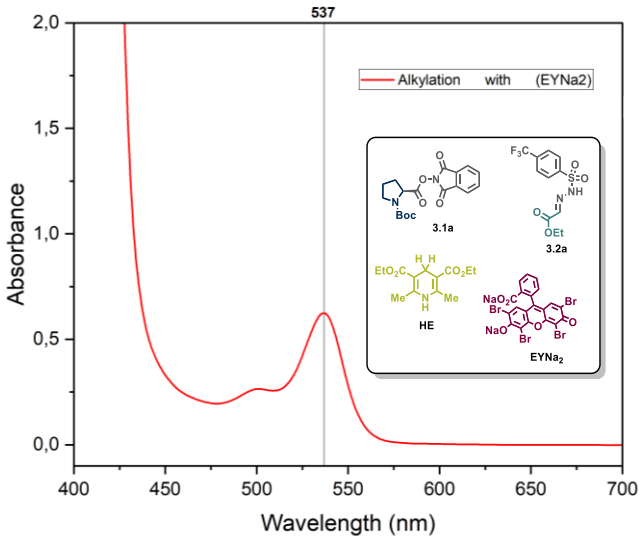

Figure 3.13: Absorption spectrum of the reaction mixture for the alkylation of **3.1a** with arylsulfonyl hydrazone **3.2c** using **$EYNa_2$** as PC. The spectrum was recorded in dichloromethane (after filtration of the unsoluble components) in quartz cuvettes (optical path: 1 cm) with a bandwidth of 5 nm and a data pitch of 1 nm. Scan rate: medium.

3.3.2 TEMPO trapping experiment.

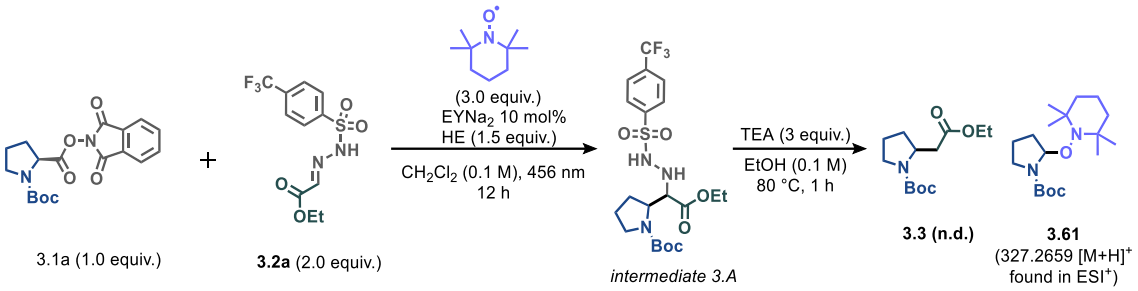

To an oven-dried 7 mL vial equipped with a stirring bar were added **3.1a** (0.300 mmol, 1.0 equiv.), **3.2a** (0.300 mmol, 1.0 equiv.), Hantzsch Ester (1.5 equiv.), **EYNa$_2$** (10 mol%) and TEMPO (3.0 equiv.) and the vial was sealed with a rubber septum. Subsequently, dry and degassed dichloromethane (3 mL) was added under N_2 atmosphere (0.1 M). The vial was stirred and irradiated in the UFO photochemical reactor for 12 h. The temperature was maintained at 30 °C during the course of the reaction. Then, the vial was removed from the photochemical reactor and the solvent was evaporated under reduced pressure. The obtained crude mixture was then dissolved in 3 mL of ethanol (0.1 M), TEA was added (3.0 equiv.) and the vial was placed in an oil bath at 80 °C for 1 h. The reaction mixture was cooled to r.t. and the solvent was removed under reduced pressure. The obtained crude was diluted with diethyl ether and washed with 1 M HCl. The combined organic layers were dried over Na_2SO_4, filtered and the solvent was removed under reduced pressure. The final crude reaction mixture was analyzed via ^{1}H-NMR using trichloroethylene as external standard and ESI-HRMS.

3.3.3 Radical Clock experiment.

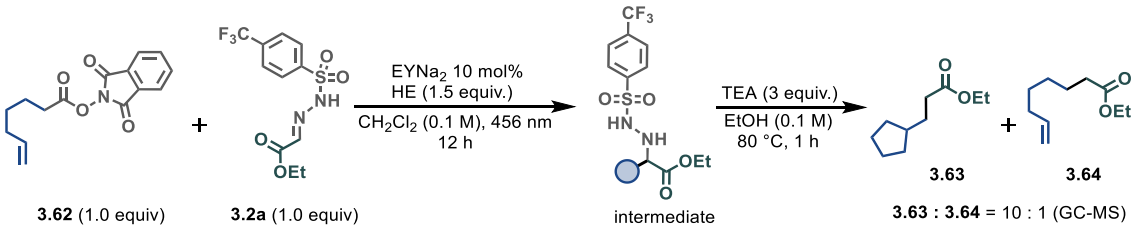

To an oven-dried 7 mL vial equipped with a stirring bar were added **3.62** (0.300 mmol, 1.0 equiv.), **3.2a** (0.300 mmol, 1.0 equiv.), Hantzsch Ester (1.5 equiv.), **EYNa$_2$** (10 mol%) and the vial was sealed with a rubber septum. Subsequently, dry and degassed dichloromethane (3 mL) was added under N_2 atmosphere (0.1 M). The vial

was stirred and irradiated in the UFO photochemical reactor for 12 h. The temperature was maintained at 30 °C during the course of the reaction. Then, the vial was removed from the photochemical reactor and the solvent was evaporated under reduced pressure. The obtained crude mixture was then dissolved in 3 mL of ethanol (0.1 M), TEA was added (3.0 equiv.) and the vial was placed in an oil bath at 80° C for 1 h. The reaction mixture was cooled to r.t. and the solvent was removed under reduced pressure. The obtained crude was diluted with diethyl ether and washed with 1 M HCl. The combined organic layers were dried over Na_2SO_4, filtered and the solvent was removed under reduced pressure. The final crude reaction mixture was analyzed via ^{1}H-NMR using trichloroethylene as external standard and GC-MS.

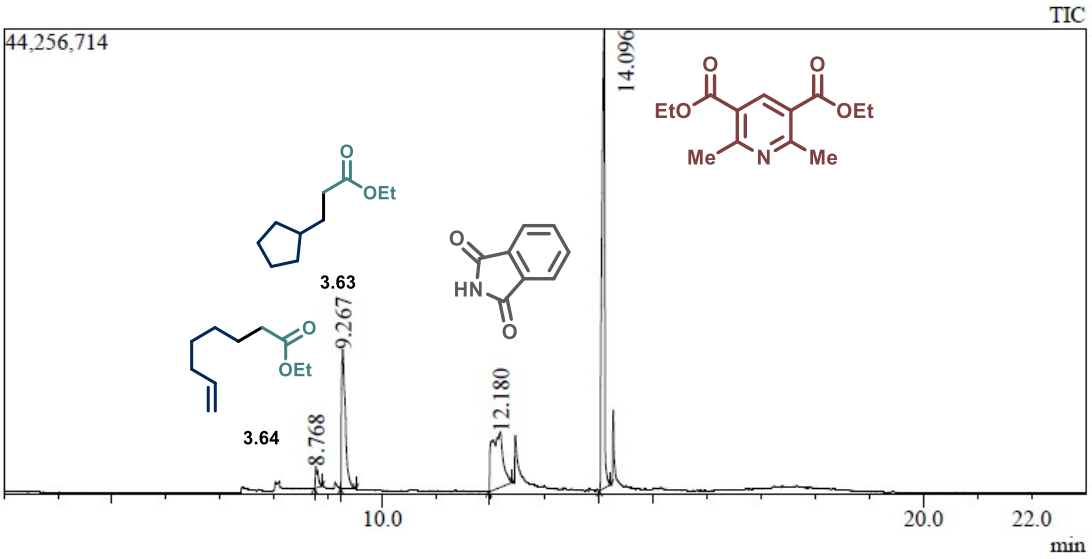

Figure 3.14: GC trace of the crude reaction (formation of **3.63** and **3.64**).

3.4 Conclusions.

In summary, we have developed a visible light mediated metal-free cross-electrophile coupling approach that stands as a powerful and versatile C(sp^3)–C(sp^3) cross-coupling platform. It combines carboxylic acid-derived redox-active esters with aldehyde sulfonyl hydrazones, utilizing Eosin Y as an efficient organophotocatalyst under visible light, leading to the desired cross-coupled products through subsequent fragmentation. Our approach provides a safer alternative to the traditional Arndt-Eistert reaction for C1 homologation of carboxylic acids and enables direct synthesis of cyclic and acyclic β-arylethylamines

using diverse aldehyde-derived sulfonyl hydrazones. Furthermore, the method proves also effective for late-stage functionalization (LSF) of peptides on solid-phase. Given these capabilities, we are confident our method will enable the exploration of sp^3-hybridized molecules in contemporary drug discovery and development.

3.5 Experimental section.

All reagents and solvents were used as received without further purification, unless stated otherwise. Reagents and solvents were bought from Sigma Aldrich, TCI, Fluorochem and Fisher Scientific and, if applicable, kept under argon atmosphere. Technical solvents were bought from VWR International and Biosolve and were used as received. Photocatalyst 4CzIPN and $3DPA_2FBN$ were prepared according to a published procedure.[71,72] Aldehydes (3a-3d) were prepared according to a published procedure.[73,74] Disposable syringes were purchased from Laboratory Glass Specialist. Product isolation was performed manually, using silica (P_{60}, SILICYCLE) or automatically, using Biotage® Isolation Four, with Biotage® SNAP KP-Sil 4 or 10 g flash chromatography cartridges. Polygoprep 60-50 C_{18} silica from Macherey-Nagel was used for reverse-phase chromatography. TLC analysis was performed using Silica on aluminum foils TLC plates (F254, Supelco Sigma-Aldrich™) with visualization under ultraviolet light (254 nm and 365 nm) or appropriate TLC staining (cerium ammonium molybdate or potassium permanganate).

^1H (400 MHz), ^{13}C (101 MHz), ^{19}F NMR (376 MHz) spectra were recorded unless stated otherwise at ambient temperature using a Bruker AV400 or a Bruker AV300. 1H NMR spectra are reported in parts per million (ppm) downfield relative to $CDCl_3$ (7.26 ppm) and all ^{13}C NMR spectra are reported in ppm relative to $CDCl_3$ (77.16 ppm) unless stated otherwise. The following abbreviations have been adopted to describe the multiplicity: bs (broad singlet), s (singlet), d (doublet), t (triplet), q (quartet), p (pentet), h (hextet), hept (heptet), m (multiplet), dd (double doublet), td (triple doublet), tt (triplet of triplets). Coupling constants (J) are reported in hertz (Hz). NMR data were processed using the MestReNova 14.1.0 software package. Known products were characterized through comparison with the corresponding ^1H-NMR and ^{13}C-NMR from literature.

High resolution mass spectra (HRMS) were collected on an AccuTOF LC, JMS-T100LP Mass spectrometer (JEOL, Japen. UV-Vis spectra were recorded with a double beam spectrophotometer Shimadzu UV2600 equipped with a deuterium lamp (190-350 nm), a halogen lamp (330-900 nm) and a photomultiplier (Hamamatsu R928). HPLC analyses were performed on a Shimadzu apparatus equipped with a diode array detector (DAD) and column temperature control module. Liquid chromatograph (LC-20AD); Autosampler (SIL-20A); Diode Array detector (SPD-M20A); Column oven (CTO-20AC); Degasser (DGU-20A5). The names of all products were generated using the PerkinElmer ChemBioDraw Ultra v.12.0.2 software package.

For the photochemical batch experiments and scale-up (1 mmol), a 3D-printed (PLA) reactor internally coated with aluminum foil and equipped with a specific 3D-printed (PLA) lid serving as vials holder and lamp holder was used (see section 4 for details).

3.5.1 Chart of starting materials.

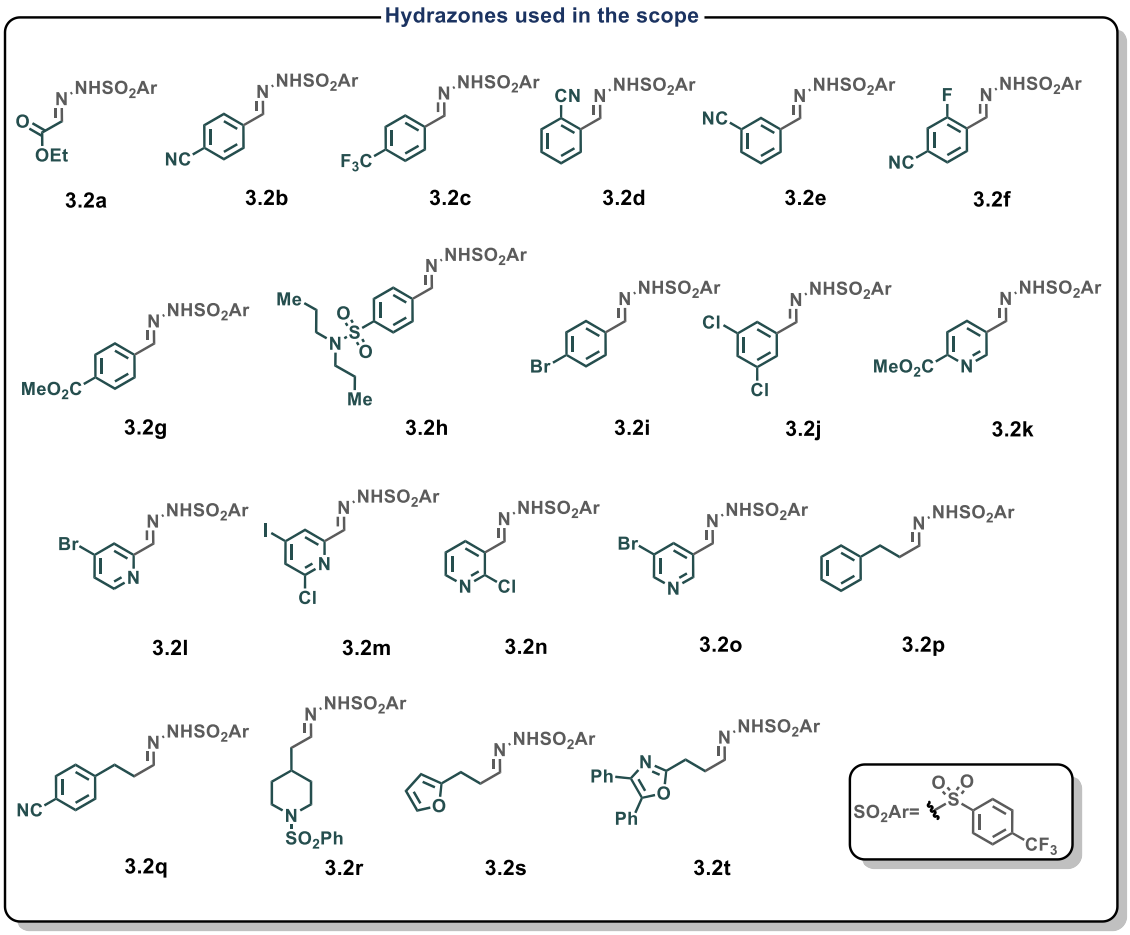

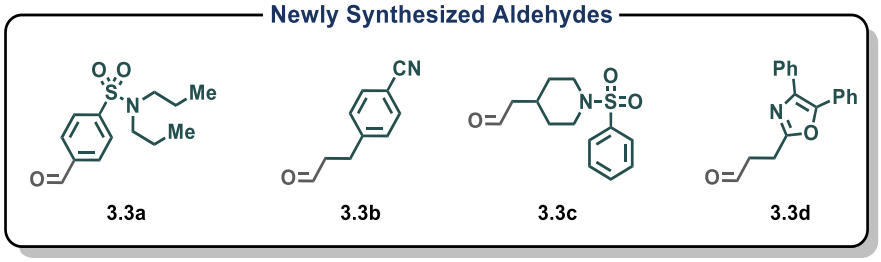

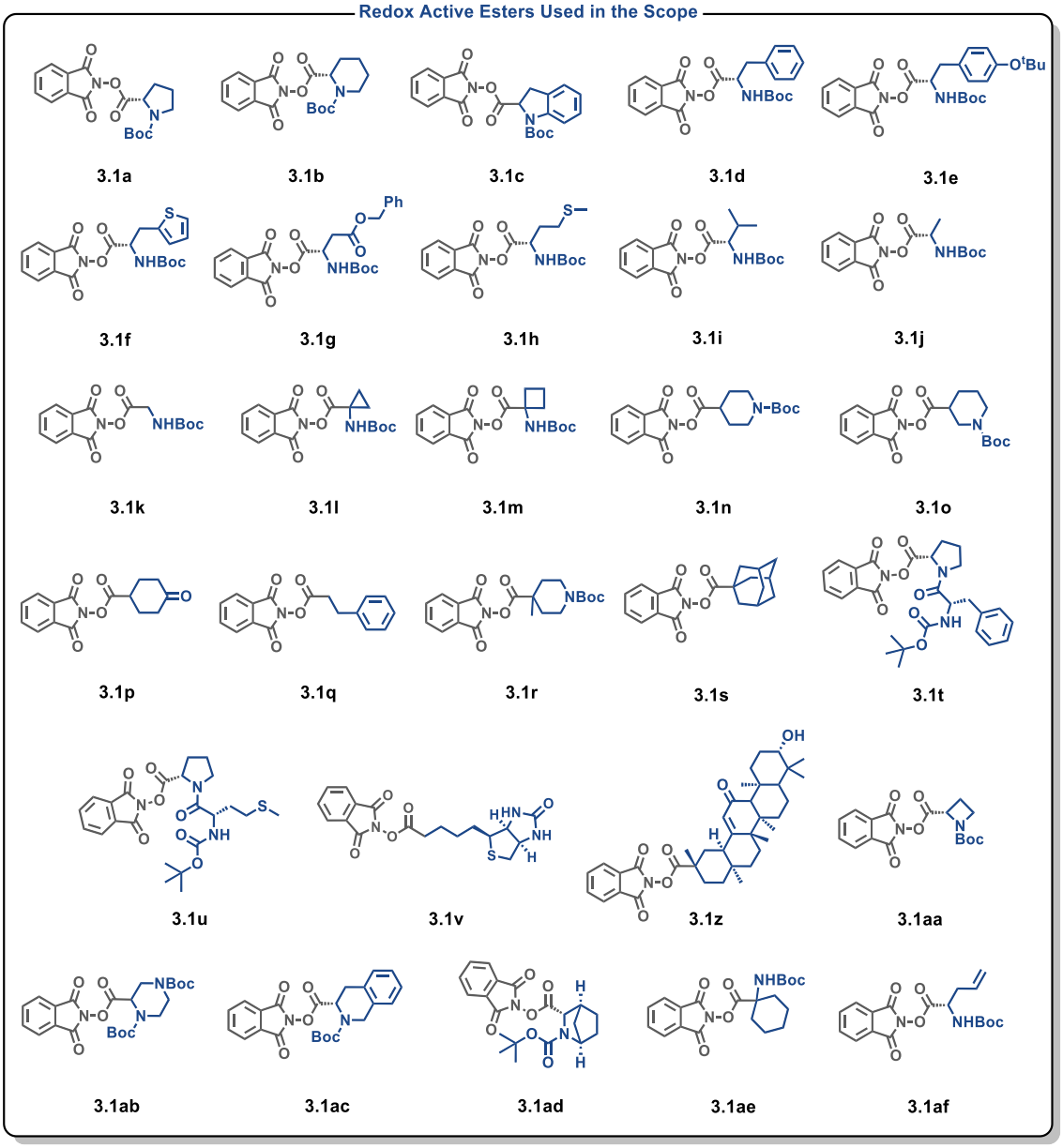

3.5.2 General procedures.

3.5.2.1 Synthesis of 4-(trifluoromethyl)benzenesulfonohydrazide.

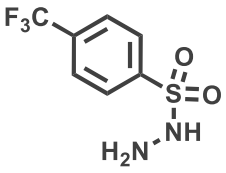

Hydrazine hydrate (108 mmol, 5.3 mL, 3 equiv.) was added dropwise to a solution of 4-(trifluoromethyl)benzenesulfonyl chloride (36 mmol, 8.81 g) in 180 mL of THF at 0 ◦ C and stirred for 30 minutes at the same temperature. The reaction mixture was then diluted with ethyl acetate and washed five times with brine. The organic

layer was dried over Na_2SO_4, filtered and the solvent was removed under reduced pressure to afford the desired compound as a white solid (8.20 g, 34.0 mmol., 95% yield).

^{1}H NMR (500 MHz, DMSO-*d*$_6$) δ 8.67 (bs, 1H), 8.04 (d, *J* = 8.3 Hz, 2H), 7.98 (d, *J* = 8.3 Hz, 2H), 4.29 (bs, 2H).^{13}C NMR (126 MHz, DMSO *d*$_6$) δ 142.5, 132.4 (q, *J* = 32.2 Hz), 128.7, 126.2 (q, *J* = 3.8 Hz), 123.6 (q, *J* = 272.8 Hz). ^{19}F NMR (470 MHz, DMSO *d*$_6$) δ -61.77. HRMS (ESI+) (m/z): $[M+H]^+$ calcd. for $C_7H_7F_3N_2O_2S$, 241.0259; found: 241.0269.

3.5.2.2 Synthesis of ethyl glyoxylate-derived 4-trifluoromethylphenyl sulfonyl hydrazone 3.2a.

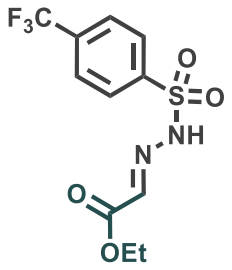

To a 0.3 M solution of 4-(trifluoromethyl)benzenesulfonohydrazide (1.20 g, 5.00 mmol, 1.0 equiv.) in dry ethanol, ethyl glyoxylate (50% soln. toluene, 1.02 g, 1.02 mL, 5.0 mmol, 1.0 equiv.) was added dropwise. The reaction mixture was stirred for 1.5 h, then the solvent was removed under vacuum. The resulting solid was washed with Pentane:Ethyl Acetate 10:1. **3.2a** was isolated as a white solid after filtration (1.45 g, 89% yield). The protocol can be extended to a 20 mmol scale (80% yield).

3.2a. ^{1}H NMR (400 MHz, $CDCl_3$) δ 12.2 (s, 1H), 8.1 (d, *J* = 8 Hz, 2H), 7.8 (d, *J* = 8 Hz, 2H), 6.8 (s, 1H), 4.3 (q, *J* = 7 Hz, 2H), 1.32 (t, *J* = 7 Hz, 3H). ^{13}C NMR (101 MHz, $CDCl_3$) δ 161.8, 141.9, 135.5 (q, *J* = 33 Hz), 129.2, 128.6, 126.5 (q, *J* = 4 Hz), 123.2 (q, *J* = 273 Hz), 62.2, 14.0. ^{19}F NMR (282 MHz, $CDCl_3$) δ -63.28.

3.5.2.3 General procedure 3.1. Preparation of (trifluoromethyl) benzenesulfonyl hydrazone compounds 3.2b-3.2o.

To a suspension of 4-(trifluoromethyl)benzenesulfonohydrazide (1.0 equiv.) in ethanol (0.8 M), the corresponding aldehyde (1.0 equiv.) was added portionwise and the reaction mixture was stirred at room temperature for 3-16 hours. In case a solid crashed out of the solution, it was filtered, washed with pentane and dried to afford

the desired aryl sulfonylhydrazone. For those compounds that did not precipitate, the solvent was removed under reduced pressure and the obtained solid was washed with pentane, filtered and dried to afford the desired aryl sulfonylhydrazone. For all newly reported benzenesulfonyl hydrazones see characterization data section. Aliphatic Sulfonyl Hydrazones **3.2p**-**3.2t** were prepared in accordance with a literature procedure and used without any further purification.

3.5.2.4 General procedure 3.2. Preparation of NHPI Redox Active Esters 3.1a-u, 3.1aa-af.

To a vigorous stirring solution of carboxylic acid (2.0-30 mmol, 1.0 equiv.), 4-dimethylaminopyridine (0.1 equiv.) and N-hydroxyphthalimide (1.0 equiv.) in CH_2Cl_2 (0.3 M), *N,N′*-Diisopropylcarbodiimide (1.0 equiv.) was added dropwise. Then, the reaction mixture was stirred overnight at room temperature. Upon completion, the mixture was filtered, and the solvent was removed under reduced pressure. Purification via silica gel column chromatography afforded the desired product. For all newly reported redox-active esters see section 10.2 for characterization data. RAEs **3.1v**, **3.1z** were prepared in accordance with literature procedures.

3.5.2.5 General procedure 3.3. Photochemical radical addition to benzenesulfonyl hydrazones and subsequent fragmentation of the benzenesulfonyl hydrazide.

In a typical experiment, to an oven-dried 7 mL vial equipped with a stirring bar were added 4-(trifluoromethyl)sulfonyl hydrazone (0.300 mmol, 1 equiv.), redox active ester (0.300 mmol, 1.0 equiv.), Hantzsch ester (114 mg, 0.450 mmol, 1.5 equiv.) and **EYNa$_2$** (20.8 mg, 10 mol%).and the vial was sealed with a rubber septum. Subsequently, dry and degassed dichloromethane (3 mL) was added under N_2 atmosphere (0.1 M). The vial was stirred and irradiated in the UFO photochemical reactor for 12 h. The temperature was maintained at 30 °C during the course of the reaction. The oven-dried 30 mL vial equipped with a stirring bar was irradiated using the photoreactor described below. A 40W Kessil PR160L-456 nm was used as LED lamp, while the temperature was maintained around 30 °C via a fan positioned under the reactor. The assembled set-up was placed behind UV-light shielding

amber acrylic for all duration of the reaction. 4 vials can be irradiated simultaneously to ensure a productivity of 4 mmol scale on a per-reactor basis.

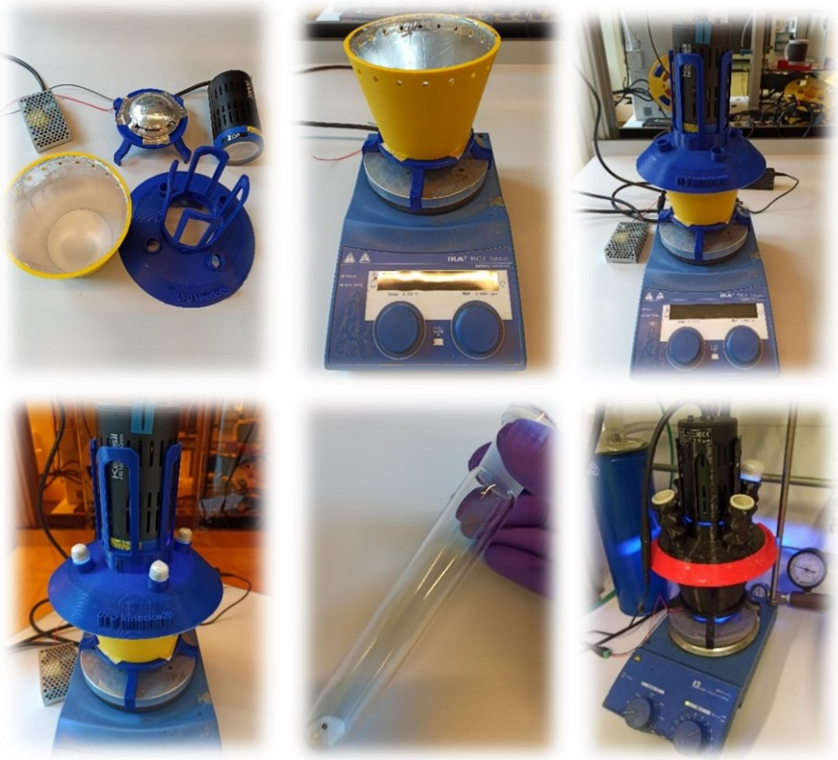

Figure ES3.1: Photoreactor used for the optimization and scope.

Then, the vial was removed from the photochemical reactor and the solvent was evaporated under reduced pressure. The obtained crude mixture was then dissolved in 3 mL of ethanol (0.1 M), TEA was added (3.0 equiv., 0.9 mmol, 125 µL) and the vial was placed in an oil bath at 80° C for 1 h. The reaction mixture was cooled to r.t. and the solvent was removed under reduced pressure. The obtained crude was diluted with diethyl ether and washed with 1 M HCl. The combined organic layers were dried over Na_2SO_4, filtered and the solvent was removed under reduced pressure. The crude reaction mixture was then purified by flash column chromatography on silica gel.

3.5.2.6 General procedure 3.4. Scale-up on the synthesis of 3.3 in flow.

In a typical experiment, to an oven-dried 7 mL vial equipped with a stirring bar were added 4-(trifluoromethyl)sulfonyl hydrazone **3.2a** (65 mg, 0.20 mmol, 1 equiv.), **3.1a** (72 mg, 0.20 mmol, 1.0 equiv.), Hantzsch Ester (76 mg, 0.30 mmol, 1.5 equiv.) and the indicated **PC** (10 mol% or 1 mol%).and the vial was sealed with a rubber

septum. Subsequently, dry and degassed solvent was added under N_2 atmosphere, and the corresponding solution was taken up with a syringe. Finally, the syringe was mounted on a syringe pump and pushed into a Vapourtec UV-150 equipped blue LEDs (l =450 nm, 60 W) for the required residence time. The outflow was collected in a 10 mL round-bottom flask. Then, the solvent was evaporated under reduced pressure. The obtained crude mixture was dissolved in 2 mL of ethanol (0.1 M), TEA was added (3.0 equiv.) and the vial was placed in an oil bath at 80° C for 1 h. The reaction mixture was cooled to r.t. and the solvent was removed under reduced pressure. The obtained crude was diluted with diethyl ether and washed with 1 M HCl. The combined organic layers were dried over Na_2SO_4, filtered and the solvent was removed under reduced pressure. The final crude reaction mixture was analyzed via ^{1}H-NMR using trichloroethylene as external standard.

3.5.2.7 General procedure 3.5. Solid Phase Synthesis of Peptides and Purification.

The peptides were synthesized via Fmoc solid-phase peptide synthesis using a Biotage® Initiator+ AlstraTM automated peptide synthesizer. Peptide syntheses were monitored by reversed-phase (RP) UPLC-MS. Analytical RP-UPLC-MS was performed on a Waters Acquity UPLC system (PDA, sample manager, sample organizer, column oven modules) and Waters SQD2 mass spectrometer using the following column: Waters Acquity CSH C18 column, 130Å, 1.7 µm, 50 × 2.1 mm at a flow rate of 0.5 mL/min at 45 °C.

A linear gradient of mobile phase: A=H_2O + 10 mM formic acid, 1 mM ammonia and 0.03% TFA and B=acetonitrile/H_2O 95/5 v/v + 10 mM formic acid, 1 mM ammonia and 0.03% TFA was used with detection from 210 - 350 nm.

High resolution mass spectra of the purified peptides (HRMS) were collected using a Water Synapt G2Si QTOF Mass Spectrometer. Column: Aquity UPLC CSH C19 100 mm x 2.1 mm, 1.7 µm particles. Mobile Phases: 1mM ammonium formate, 10 mM formic acid, 0.03 % TFA, pH=3, in MilliQ (A) and MeCN (B), respectively. Flow Rate: 0.5 mL/min. Purity: Relative absorbance at 214 nm.

Water was purified using a Millipore MilliQ water purification system. Peptides were synthesized using standard Fmoc SPPS. Fmoc-amino acids were purchased

from Chem-Impex International, Inc., with the following side-chain protection: Fmoc-Arg(Pbf)-OH, Fmoc-Asn(Trt)-OH, Fmoc-Asp(OtBu)-OH, Fmoc-Cys(Trt)-OH, Fmoc-Gln(Trt)-OH, Fmoc-Glu(OtBu)-OH, Fmoc-His(Trt)-OH, Fmoc-Lys(Boc)-OH, Fmoc-Ser(tBu)-OH, Fmoc-Thr(tBu)-OH, Fmoc-Trp(Boc)-OH, Fmoc-Tyr(tBu)-OH amd Fmoc-(D)-Phe-OH. Oxyma was purchased from Chem-Impex International, Inc., DIPEA and FITC from Sigma-Aldrich. Acetic anhydride was purchased from Acros Organics.

Peptide synthesis

General Protocol for SPPS. The peptides were synthesized via Fmoc solid-phase peptide. The peptide chains were then assembled following **method A** and then *N*-terminal acetylation was performed according to **method B** before being cleaved from the resin, deprotected according to **method C** and purified.

Method A: Automated Fmoc SPPS, Biotage® Initiator+ AlstraTM automated microwave peptide synthesizer. Rink Amide MBHA resin (final loading 0.77 mmol/g) was swollen in CH_2Cl_2 for 10 min and then the solvent was drained. The Fmoc N-protecting group was removed with 20% piperidine in DMF (2 x 5 min) at room temperature. The amino acids (4 equiv.) dissolved in DMF (0.2 M) were repeatedly coupled with DIC (4 equiv.) in DMF (2 M) and OXYMA (4 equiv.) in DMF (0.5 M) at 40 degrees for 10 min. Washing of the resin between the coupling steps was performed with EtOAc.DMSO (9:1). The resin was finally washed with CH_2Cl_2 (2 x 5 mL).

Method B: Acetylation of the N terminal position. After the final Fmoc deprotection, the resin was swollen with CH_2Cl_2 (2 x 5 mL) and drained. A solution of NMP: acetic anhydride: 2,6 Lutidine 90:5:5, (9 mL) was added to the resin and stirred at room temperature for 60 min before the mixture was drained. This procedure was repeated twice, and the resin was washed with DMF (3 x 5 mL) and CH_2Cl_2 (3 x 5 mL).

Method C: Cleavage from resin/side-chain deprotection. A solution of TFA/water/DODT/TIS 90:2.5:2.5:5 (10 mL) was added to the dry resin. The

reaction mixture was shaken at room temperature for 2 h. The resin was rinsed with TFA (2 x 0.3 mL) and the TFA solution collected in a flask and concentrated under reduced pressure to reduce the total volume. The solution was then poured in cold diethyl ether. The precipitated peptide was centrifuged, and the crude peptide was lyophilized from acetonitrile-water.

General method for Alloc deprotection

The resin bound peptide was suspended in anhydrous CH_2Cl_2 followed by the addition of phenylsilane (25 equiv.) and $Pd[(C_6H_5)_3P]_4$ (0.25 equiv.) and the suspension was shaken for 1 h followed by removal of the liquid and the addition of fresh reagents. After 1 h, the peptidyl resin was drained and washed with CH_2Cl_2 (3 x 5 mL), DMF (3 x 5 mL).

Synthetic Route to Peptide 3.P0

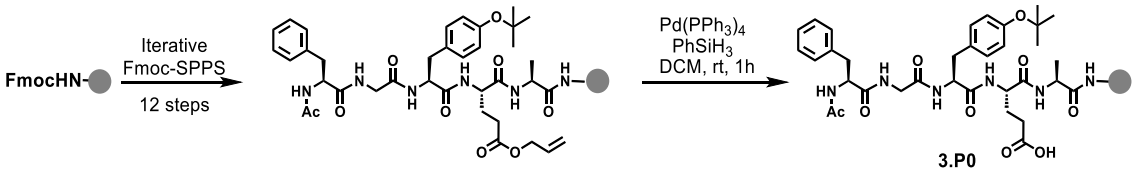

Figure ES3.2: Synthesis of peptide **3.P0**.

Synthetic Route to Peptide 3.P1.

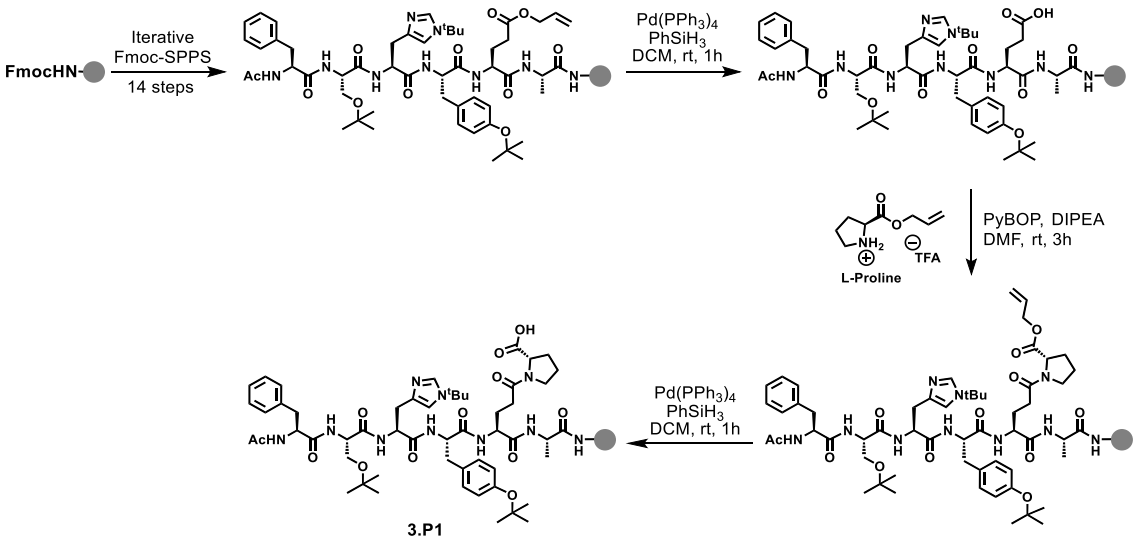

Figure ES3.3. Synthesis of peptide **3.P1**.

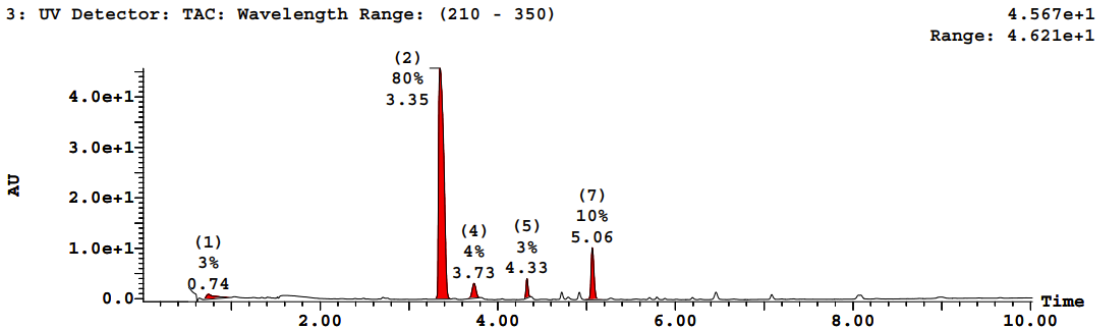

Figure ES3.4: UPLC-MS Trace of the resin-bound crude peptide 3.P1. Analyzed by cleavage of a fraction of resin beads by treatment with TFA/DODT/Water/TIS (90: 2.5: 2.5: 5, v/v) for 1 h at rt. Conditions: (3 to 43 % B over 10 min).

Synthetic Route to Peptide 3.P2.

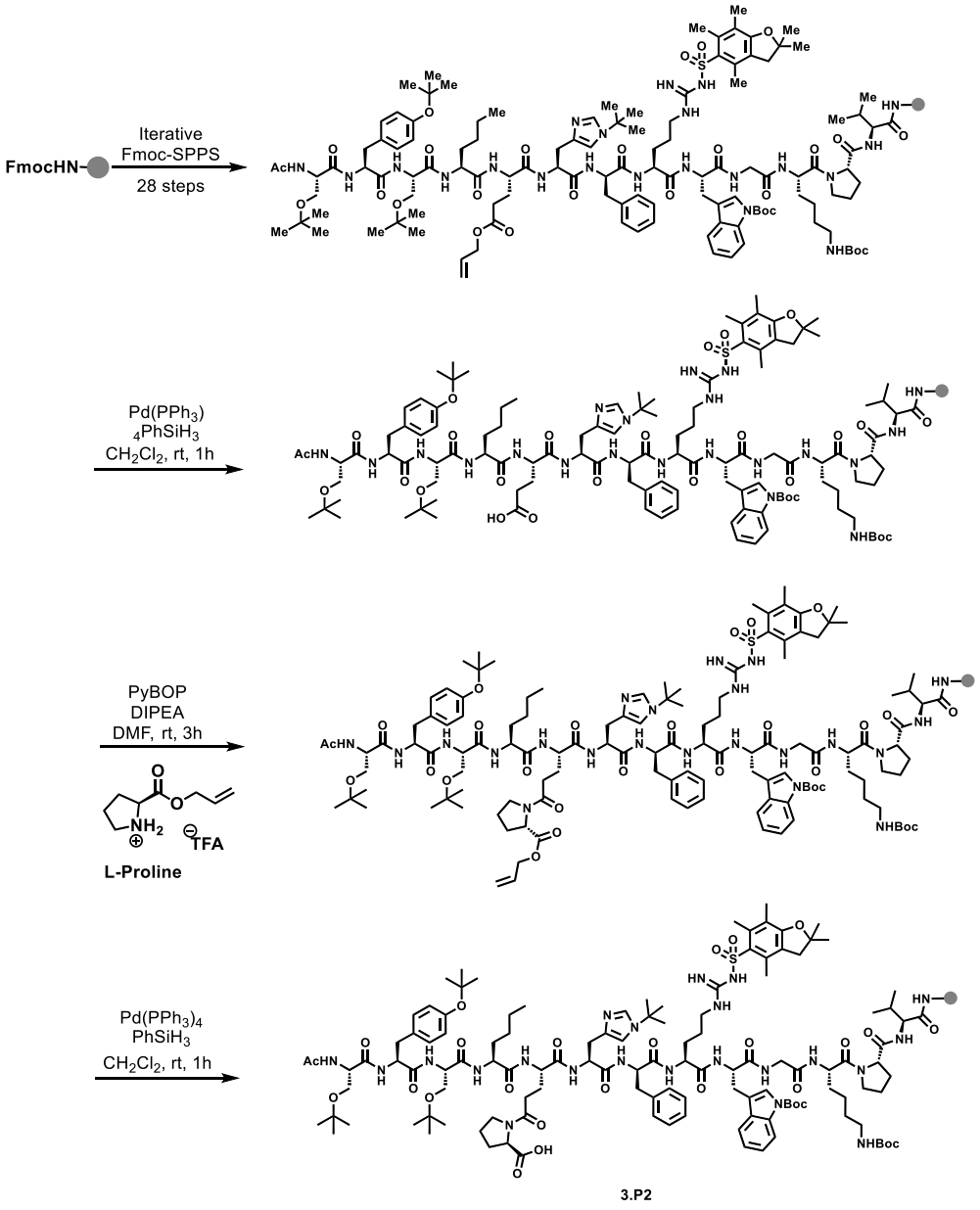

Figure ES3.5: Synthesis of peptide **3.P2**.

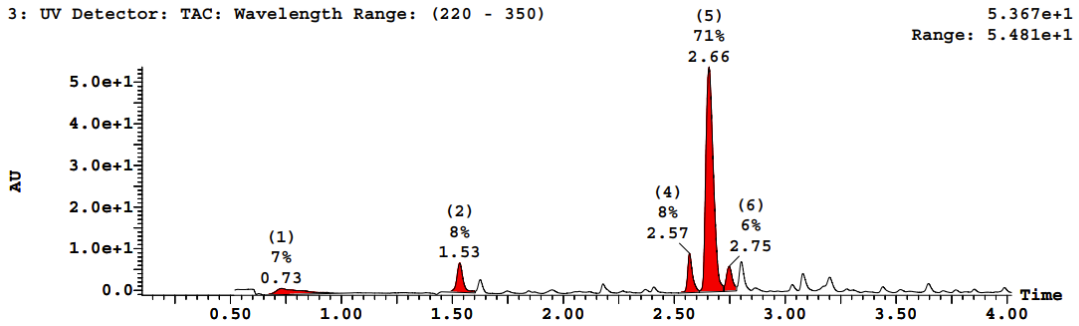

Figure ES3.6: UPLC-MS Trace of the resin-bound crude peptide 3.P2. Analyzed by cleavage of a fraction of resin beads by treatment with TFA/DODT/Water/TIS (90: 2.5: 2.5: 5, v/v) for 1 h at rt. Conditions: (3 to 43 % B over 4 min).

3.5.2.8 General procedure 3.6. Synthesis of Redox Active Esters (RAEs) on resin.

The resin-bound peptide (30 µmol), N-hydroxyphthalimide (NHPI) (98 mg, 0.6 mmol, 20.0 equiv.) and DMAP (7.3 mg, 0.06 mmol, 2.0 equiv.) were added to the the fritted syringe. Then, a solution of DIC (94 µL, 0.6 mmol, 20.0 equiv.) in dry DMF (25-50 mM concentration with respect to the resin-bound peptide) was withdrawn with the syringe containing the solids. The syringe containing the resin and all the activating agents was capped, sealed with Teflon tape, located in a plastic casing. Then, was placed in a falcon tube containing water and agitated on a orbital shaker at the indicated temperature for 2h. The activation solution was then drained, and the resin washed with dry DMF (5 x 3 mL), dry CH_2Cl_2 (3 x 5 mL).

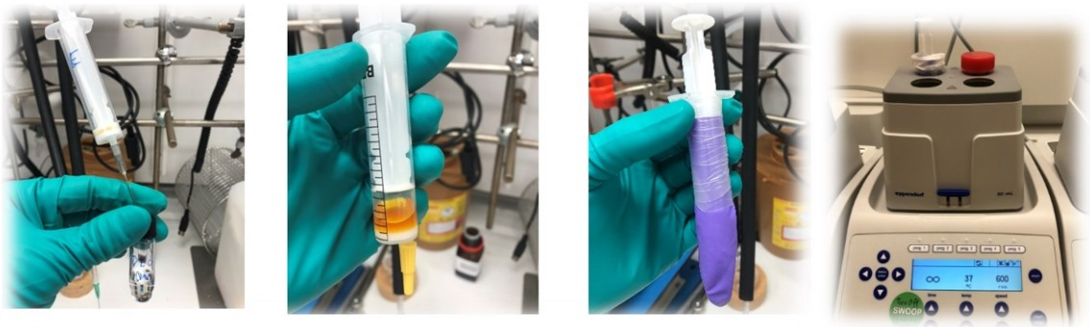

Figure ES3.7: Graphical procedure for the synthesis of redox active esters on resins.

3.5.2.9 General procedure 3.7. On resin photochemical radical addition to Aryl Sulfonyl Hydrazones 3.2a and 3.2b.

After the activation step (general procedure 3.6), the resin-bound peptide was subjected to the photochemical coupling without any purification. After drying, the resin (30 μmol, 1 equiv.) was transferred to an oven-dried 7 mL vial equipped with a stirring bar. Then, 4-(trifluoromethyl) sulfonyl hydrazone **3.2a** or **3.2b** (29 mg, 90 μmol, 3 equiv.), Hantzsch Ester (34 mg, 135 μmol, 4.5 equiv.) and **EYNa$_2$** (6.2 mg, 9 μmol, 0.3 equiv.) were added. The vial was sealed and 90 μL of dry CH_2Cl_2 were added (33 mM concentration in respect to the resin bound peptide) and stirred for 12h in the Blue Box photochemical reactor.

Reactions for the On Resin Photochemical LSF of peptides carried out in AstraZeneca were irradiated using the photoreactor described below. A 40W Kessil PR160L-456 nm was used as LED lamp, while the temperature was maintained below 30 °C via a fan positioned under the reactor. The assembled set-up was placed behind UV-light shielding amber acrylic for all duration of the reaction.

Then, the suspension containing the resin-bound peptide was transferred to a frittered syringe, drained and washed with DMF (5 x 3 mL) and CH_2Cl_2 (5 x 3 mL). After drying the resin, it was transferred to a falcon tube and a 90 mL (1:1 v:v) solution of EtOH-DMF was added (33 mM final concentration) followed by the addition of TEA (38 μL, 9 equiv., 270 μmol). The tube was closed and agitated on a orbital shaker for 2 h at 80 ◦ C degrees. Next, the solution was transferred to a frittered syringe, and the resin was drained, washed with dry DMF (5 x 3 mL) and dry CH_2Cl_2 (5 x 3 mL). The reaction was analyzed by cleavage of a fraction of resin beads by treatment with TFA/DODT/Water/TIS (90: 2.5: 2.5: 5, v/v) for 1 h at rt and analysis by UPLC-MS.

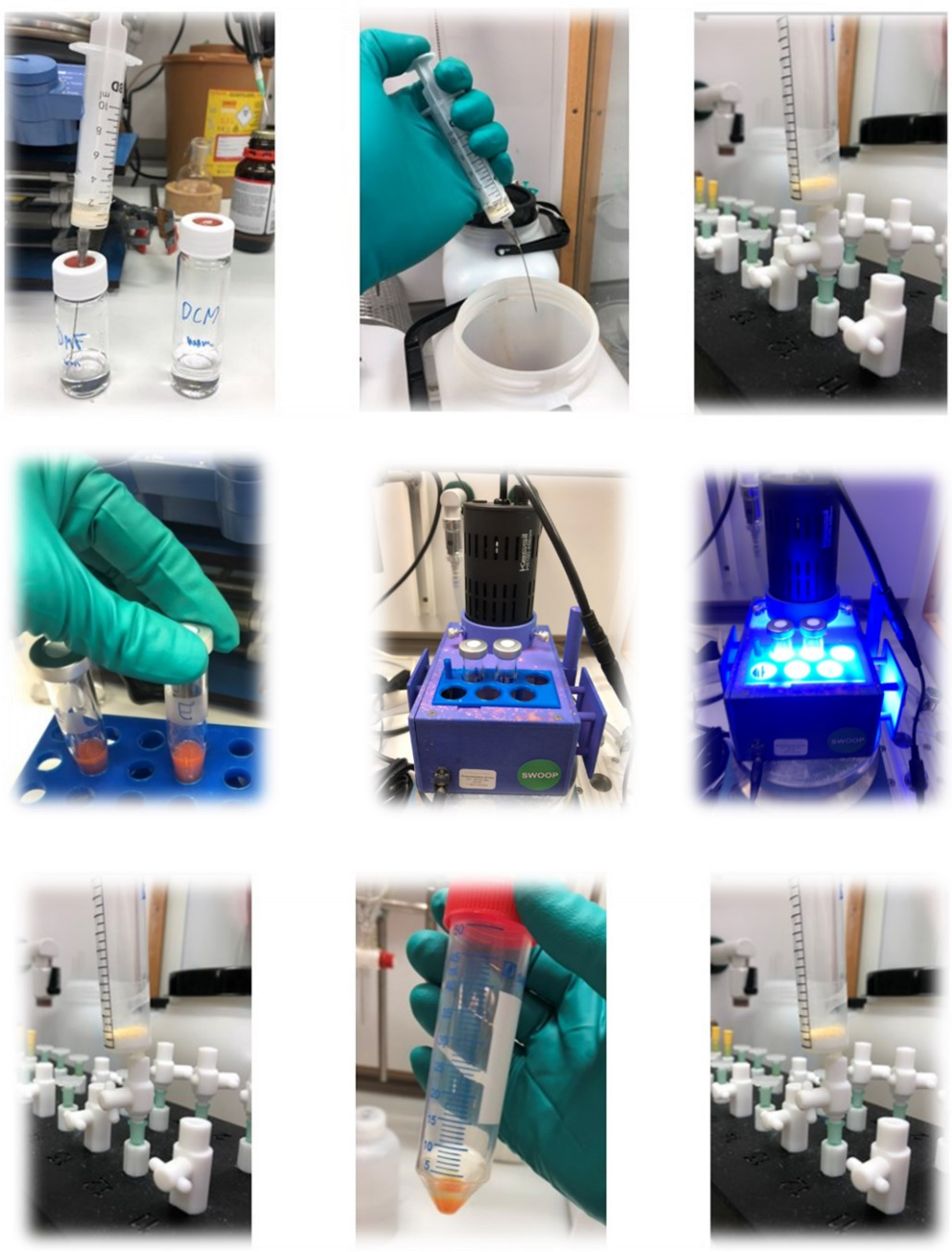

Figure ES3.8: Graphical procedure for the photochemical step on resin.

3.5.2.10 General procedure 3.8. Scale-up of the C1 homologation process in flow.

In a typical experiment, to an oven-dried 7 mL vial equipped with a stirring bar were added 4-(trifluoromethyl)sulfonyl hydrazone **3.2a** (65 mg, 0.20 mmol, 1 equiv.), **3.1a** (72 mg, 0.20 mmol, 1.0 equiv.), Hantzsch Ester (76 mg, 0.30 mmol, 1.5 equiv.) and the indicated **PC** (10 mol% or 1 mol%).and the vial was sealed with a rubber septum. Subsequently, dry and degassed solvent was added under N_2 atmosphere,

and the corresponding solution was taken up with a syringe. Finally, the syringe was mounted on a syringe pump and pushed into a Vapourtec UV-150 equipped blue LEDs (l =450 nm, 60 W) for the required residence time. The outflow was collected in a 10 mL round-bottom flask. Then, the solvent was evaporated under reduced pressure. The obtained crude mixture was dissolved in 2 mL of ethanol (0.1 M), TEA was added (3.0 equiv.) and the vial was placed in an oil bath at 80◦ C for 1 h. The reaction mixture was cooled to r.t. and the solvent was removed under reduced pressure. The obtained crude was diluted with diethyl ether and washed with 1 M HCl. The combined organic layers were dried over Na_2SO_4, filtered and the solvent was removed under reduced pressure. The final crude reaction mixture was analyzed via ^{1}H-NMR using trichloroethylene as external standard.

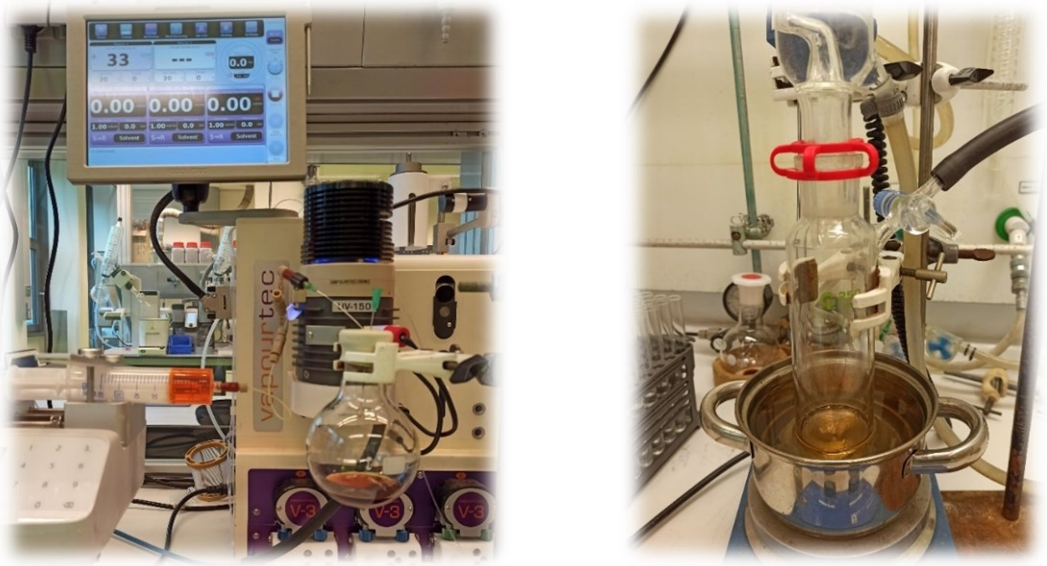

Figure ES3.9. Photochemical step of the C1 homologation in Flow (450 nm, Vapourtec reactor). Thermal cleavage step in batch (80 ◦ C).

3.5.3 Characterization data.

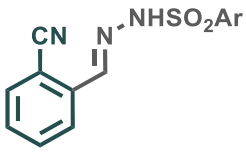

***N*'-(2-cyanobenzylidene)-4-(trifluoromethyl)benzenesulfonohydrazide** (**3.2d**).

Prepared according to GP1 using 4-(trifluoromethyl)benzenesulfonohydrazide (480 mg, 2.0 mmol, 1.0 equiv.) and 2-formylbenzonitrile (262 mg, 2.0 mmol, 1.0 equiv.). Isolated as a pale brown solid after filtration (1.53 mmol, 77% yield).

3.2d. ^{1}H NMR (400 MHz, DMSO-d_6) δ 12.29 (s, 1H), 8.21 (s, 1H), 8.13 (d, *J* = 8.2 Hz, 2H), 8.01 (d, *J* = 8.2 Hz, 2H), 7.87 (dd, *J* = 7.9, 4.1 Hz, 2H), 7.73 (t, *J* = 7.7 Hz, 1H), 7.58 (t, *J* = 7.6 Hz, 1H). ^{13}C NMR (101 MHz, DMSO-d_6) δ 143.3, 142.6, 135.6, 133.7, 133.5, 132.9 (q, *J* = 32.3 Hz), 130.6, 128.3, 126.6 (q, *J* = 3.7 Hz), 126.4, 123.4 (q, *J* = 273.0 Hz), 116.9, 110.3. ^{19}F NMR (282 MHz, DMSO-d_6) δ -56.98. HRMS (ESI+) (m/z): $[M+H]^+$ calcd. for $C_{15}H_{10}F_3N_3O_2S$, 354.0524; found: 354.0515.

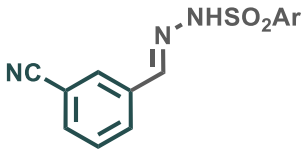

***N*'-(3-cyanobenzylidene)-4-(trifluoromethyl)benzenesulfonohydrazide** (3.**2e**). Prepared according to GP1 using 4-(trifluoromethyl)benzenesulfonohydrazide (480 mg, 2.0 mmol, 1.0 equiv.) and 3-formylbenzonitrile (262 mg, 2.0 mmol, 1.0 equiv.). Isolated as a white solid after filtration (600 mg, 85% yield).

3.2e. ^{1}H NMR (400 MHz, DMSO-d_6) δ 12.06 (s, 1H), 8.13 (d, J = 8.2 Hz, 2H), 8.00 (dd, J = 5.6, 2.8 Hz, 4H), 7.92 (dt, J = 8.0, 1.4 Hz, 1H), 7.84 (dt, J = 7.9, 1.4 Hz, 1H), 7.59 (t, J = 7.8 Hz, 1H). ^{13}C NMR (101 MHz, DMSO-d_6) δ 145.7, 142.7, 134.7, 133.5, 132.8 (q, J = 32.4 Hz), 130.8, 130.6, 130.1, 128.2, 126.6 (q, J = 3.9 Hz), 123.4 (q, J = 272.9 Hz), 118.3, 112.0. ^{19}F NMR (282 MHz, DMSO-d_6) δ -61.76. HRMS (FD+) (m/z): $[M]^+$ calcd. for $C_{15}H_{10}F_3N_3O_2S$, 353.0446; found: 353.0436.

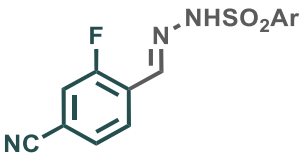

***N'*-(4-cyano-2-fluorobenzylidene)-4-(trifluoromethyl)benzenesulfonohydrazide (3.2f).**

Prepared according to GP1 using 4-(trifluoromethyl)benzenesulfonohydrazide (480 mg, 2.0 mmol, 1.0 equiv.) and 3-fluoro-4-formylbenzonitrile (298 g, 2.0 mmol, 1.0 equiv.). Isolated as a white solid after filtration (620 g, 84% yield).

3.2f. ^{1}H NMR (300 MHz, DMSO-d_6) δ 12.05 (s, 1H), 8.17 – 8.07 (m, 3H), 8.05 – 7.94 (m, 4H), 7.55 (t, J = 9.0 Hz, 1H). ^{13}C NMR (101 MHz, DMSO-d_6) δ 163.1 (d, J = 259.2 Hz), 144.8, 142.7, 133.6 (d, J = 9.1 Hz), 132.8 (q, J = 32.3 Hz), 132.4, 131.2 (d, J = 3.4 Hz), 128.3, 126.6 (q, J = 3.8 Hz), 123.4 (q, J = 272.9 Hz), 117.3 (d, J = 20.2 Hz), 113.5, 100.9 (d, J = 16.0 Hz). ^{19}F NMR (282 MHz, DMSO-d_6) δ -61.73, -106.35. HRMS (ESI+) (m/z): $[M+H]^+$ calcd. for $C_{15}H_9F_4N_3O_2S$, 372.0430; found: 372.0426.

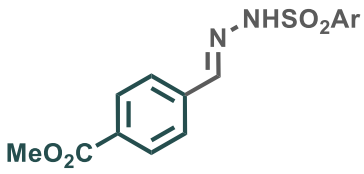

Methyl (E)-5-((2-((4(trifluoromethyl)phenyl)sulfonyl)hydrazineylidene)methyl) picolinate (3.2g).

Prepared according to GP1 using 4 (trifluoromethyl)benzenesulfonohydrazide (360 mg, 1.5 mmol, 1.0 equiv.) and methyl 5-formylpicolinate (248 mg, 1.5 mmol, 1.0 equiv.). Isolated as a white solid after filtration (535 mg, 92% yield). **3.2g.** ^{1}H NMR (500 MHz, DMSO-d_6) δ 12.25 (bs, 1H), 8.86 (d, J = 2.1 Hz, 1H), 8.21 – 7.93 (m, 7H), 3.87 (s, 3H). ^{13}C NMR (126 MHz, DMSO-d_6) δ 164.7, 148.4, 147.9, 144.1, 142.6, 134.6, 132.8 (q, J = 32.5 Hz), 132.3, 128.2, 126.6 (q, J = 3.8 Hz), 124.9, 123.4 (d, J = 272.9 Hz), 52.5. ^{19}F NMR (470 MHz, DMSO-d_6) δ -61.78. HRMS (ESI+) (m/z): $[M+H]^+$ calcd. for $C_{15}H_{12}F_3N_3O_4S$, 388.0579; found: 388.0571.

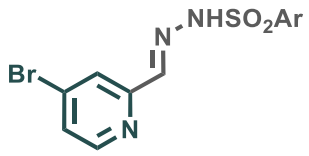

***N′*-((4-bromopyridin-2-yl)methylene)-4-(trifluoromethyl)benzenesulfonohydrazide (3.2l).**

Prepared according to GP1 using 4-(trifluoromethyl)benzenesulfonohydrazide (480 mg, 2.0 mmol, 1.0 equiv.) and 4-bromopicolinaldehyde (372 mg, 2.0 mmol, 1.0 equiv.). Isolated as a pale pink solid after filtration (432 mg, 53% yield).

3.2l. ^{1}H NMR (400 MHz, DMSO-d_6) δ 12.31 (s, 1H), 8.44 (d, J = 5.3 Hz, 1H), 8.12 (d, J = 8.2 Hz, 2H), 8.02 (d, J = 8.3 Hz, 2H), 7.93 (s, 1H), 7.88 (d, J = 1.9 Hz, 1H), 7.67 (dd, J = 5.3, 2.0 Hz, 1H). **^{13}C NMR** (101 MHz, DMSO-d_6) δ 153.6, 150.8, 146.3, 142.6, 132.9 (q, J = 32.4 Hz), 132.8, 128.2, 127.5, 126.71 (q, J = 3.8 Hz), 123.3 (q, J = 273.0 Hz) 122.5. **^{19}F NMR** (282 MHz, DMSO-d_6) δ -61.76. **HRMS** (ESI+) (m/z): $[M+H]^+$ calcd. for $C_{13}H_9BrF_3N_3O_2S$, 409.9609; found: 409.9593.

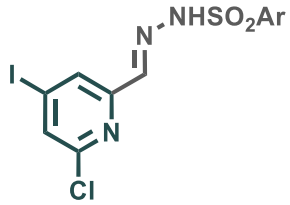

***(E)-N′*-((2-chloro-4-iodopyridin-3-yl)methylene)-4 (trifluoromethyl) benzenesulfonohydrazide (3.2m).**

Prepared according to GP1 using 4-(trifluoromethyl)benzenesulfonohydrazide (360 mg, 1.5 mmol, 1.0 equiv.) and 2-chloro-4-iodonicotinaldehyde (401 mg, 1.5 mmol, 1.0 equiv.). Isolated as a white solid after filtration (624 mg, 85% yield).

(3.2m). ^{1}H NMR (400 MHz, DMSO-d_6) δ 12.33 (s, 1H), 8.10 (d, J = 8.3 Hz, 2H), 8.02 (d, J = 7.9 Hz, 2H), 8.00 – 7.93 (m, 3H). ^{13}C NMR (101 MHz, DMSO-d_6) δ 149.5, 148.3, 145.9, 142.9, 134.4, 132.9 (q, J = 32 Hz), 131.5, 128.4, 126.6 (q, J = 4 Hz), 123.4 (q, J = 273 Hz). 111.6. ^{19}F NMR (282 MHz, DMSO-d_6) δ -61.70. HRMS (ESI+) (m/z): $[M+H]^+$ calcd. for $C_{13}H_8ClF_3IN_3O_2S$, 489.9101; found: 489.9109.

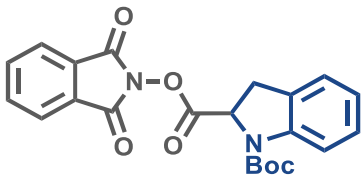

1-(*tert*-Butyl) 2-(1,3-dioxoisoindolin-2-yl) (*S*)-indoline-1,2-dicarboxylate (3.1c).

Prepared according to GP2 from (S)-1-(tert-butoxycarbonyl)indoline-2-carboxylic acid (526 mg, 2.0 mmol, 1.0 equiv.), 2-hydroxyisoindoline-1,3-dione (326 mg, 2 mmol, 1.0 equiv.), N,N-dimethylpyridin-4-amine (24.4 mg, 0.2 mmol, 0.1 equiv.) and diisopropylmethanediimine (313 µL, 2.0 mmol, 1.0 equiv.). Purified via flash column chromatography on silica gel (from Heptane to Heptane:Ethyl Acetate 3:1) to afford the product as a white solid (768 mg, 94% yield).

3.1c. ^{1}H NMR (500 MHz, $CDCl_3$) δ 7.98 – 7.78 (m, 5H), 7.32 – 7.19 (m, 2H), 7.03 (t, *J* = 7.5 Hz, 1H), 5.26 (dd, *J* = 11.8, 4.5 Hz, 1H), 3.77 (dd, *J* = 16.8, 11.8 Hz, 1H), 3.57 (dd, *J* = 16.9, 4.6 Hz, 1H), 1.65 (s, 9H). ^{13}C NMR (126 MHz, $CDCl_3$) δ 168.5, 161.7, 151.2, 142.2, 135.0, 128.9, 128.2, 127.3, 124.7, 124.1, 123.0, 114.8, 82.8, 58.5, 33.1, 28.1. HRMS (ESI+) (m/z): $[M+H]^+$ calcd. for $C_{22}H_{20}N_2O_6$, 409.1400; found: 409.1401

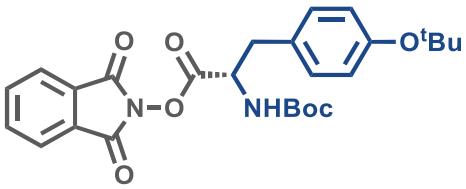

1, 3-Dioxoisoindolin-2-yl (S)-2-((*tert*-butoxycarbonyl)amino)-3-(thiophen-2-yl) propanoate (3.1e).

Prepared according to GP2 from 3-(4-(tert-butoxy)phenyl)-2-((tert-butoxycarbonyl)amino)propanoic acid (1.69 g, 5.0 mmol, 1.0 equiv.), 2-hydroxyisoindoline-1,3-dione (816 mg, 5.0 mmol, 1.0 equiv.), N,N-dimethylpyridin-4-amine (61.1 mg, 0.5 mmol, 0.1 equiv.) and diisopropylmethanediimine (783 µL, 5.0 mmol, 1.0 equiv.). Purified via flash column chromatography on silica gel (from Pentane:Ethyl Acetate 20:1 to 3:1) to afford the product as a white solid (1.95 g, 81% yield).

3.1e. ^{1}H NMR (400 MHz, $CDCl_3$) δ 7.88 (dd, *J* = 5.5, 3.1 Hz, 2H), 7.78 (dd, *J* = 5.5, 3.1 Hz, 2H), 7.20 (d, *J* = 8.4 Hz, 2H), 6.95 (d, *J* = 8.5 Hz, 2H), 5.08 – 4.57 (m, 2H), 3.38 –

3.03 (m, 2H), 1.41 (s, 9H), 1.32 (s, 9H). ^{13}C NMR (101 MHz, $CDCl_3$) δ 168.8, 161.5, 154.8, 134.9, 130.3, 129.6, 128.9, 124.3, 124.1, 80.5, 78.5, 52.8, 37.7, 28.9, 28.3. HRMS (ESI+) (m/z): $[M+H]^+$ calcd. for $C_{26}H_{30}N_2O_7$, 483.2131; found: 483.2134.

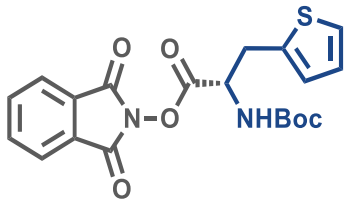

1, 3-Dioxoisoindolin-2-yl (S)-2-((*tert*-butoxycarbonyl)amino)-3-(thiophen-2-yl)propanoate (3.1f).

Prepared according to GP2 from (S)-2-((*tert*-butoxycarbonyl)amino)-3-(thiophen-2-yl)propanoic acid (543 mg, 2.0 mmol, 1.0 equiv.), 2-hydroxyisoindoline-1,3-dione (326 mg, 2.0 mmol, 1.0 equiv.), *N,N*-dimethylpyridin-4-amine (24.4 mg, 0.2 mmol, 0.1 equiv.) and diisopropylmethanediimine (313 µL, 2.0 mmol, 1.0 equiv.). Purified via flash column chromatography on silica gel (from Pentane:Ethyl Acetate 10:1 to 2:1) to afford the product as a white solid (566 mg, 68% yield).

3.1f. ^{1}H NMR (400 MHz, $CDCl_3$) δ 7.87 (dd, *J* = 5.5, 3.1 Hz, 2H), 7.78 (dd, *J* = 5.6, 3.1 Hz, 2H), 7.20 (d, *J* = 5.1 Hz, 1H), 7.07 (d, *J* = 3.5 Hz, 1H), 6.98 (dd, *J* = 5.2, 3.5 Hz, 1H), 5.21 – 4.61 (m, 2H), 3.65 – 3.23 (m, 2H), 1.44 (s, 9H). ^{13}C NMR (101 MHz, $CDCl_3$) δ 168.3, 161.5, 154.7, 136.1, 135.0, 128.8, 127.7, 127.4, 125.3, 124.1, 80.7, 52.8, 32.4, 28.3. HRMS Failed to find the mass due to instability of the NHPI redox active ester.

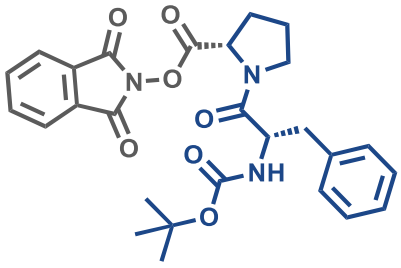

1,3-Dioxoisoindolin-2-yl (*tert*-butoxycarbonyl)-L-methionyl-L-prolinate (3.1t).

Prepared according to GP2 from (tert-butoxycarbonyl)-L-phenylalanyl-L-prolineproline (1.14 g, 1.0 mmol, 1.0 equiv.), 2-hydroxyisoindoline-1,3-dione (163 mg, 1.0 mmol, 1.0 equiv.), N,N-dimethylpyridin-4-amine (12.2 mg, 0.1 mmol, 0.1 equiv.) and diisopropylmethanediimine (157 µL, 1.0 mmol, 1.0 equiv.). Purified via

flash column chromatography on silica gel (Dichloromethane:MeOH 95:5 to 90:10) to afford the product as a white solid (238 mg, 47% yield).

3.1t. ^{1}H NMR (400 MHz, $CDCl_3$) δ 7.35 (dd, *J* = 5.5, 3.1 Hz, 2H), 7.26 – 7.20 (m, 2H), 6.72 – 6.57 (m, 5H), 4.84 (d, *J* = 8.9 Hz, 1H), 4.30 (dd, *J* = 8.6, 4.6 Hz, 1H), 4.08 (t, *J* = 7.8 Hz, 1H), 3.05 (dt, *J* = 9.8, 7.3 Hz, 1H), 2.57 – 2.45 (m, 2H), 2.39 (dd, *J* = 13.6, 6.3 Hz, 1H), 1.85 – 1.63 (m, 2H), 1.50 – 1.38 (m, 2H), 0.84 (s, 9H). ^{13}C NMR (101 MHz, $CDCl_3$) δ 171.2, 168.4, 161.7, 155.4, 136.3, 134.9, 129.8, 129.1, 128.6, 126.9, 124.2, 79.9, 57.1, 53.6, 46.8, 39.5, 29.5, 28.5, 25.1. HRMS (ESI+) (m/z): $[M+H]^+$ calcd. for $C_{27}H_{29}N_3O_7$, 508.2084; found: 508.2081

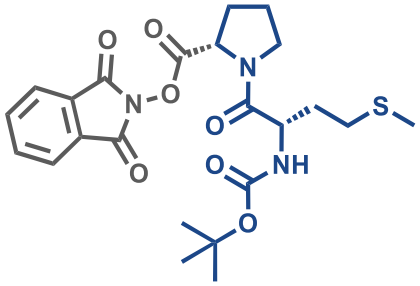

1,3-Dioxoisoindolin-2-yl(*tert*-butoxycarbonyl)-L-methionyl-L-prolinate (3.1u).

Prepared according to GP2 from (tert-butoxycarbonyl)-L-methionyl-L-proline (1.14 g, 3.3 mmol, 1.0 equiv.), 2-hydroxyisoindoline-1,3-dione (537 mg, 3.3 mmol, 1.0 equiv.), N,N-dimethylpyridin-4-amine (40.2 mg, 0.33 mmol, 0.1 equiv.) and diisopropylmethanediimine (510 µL, 3.3 mmol, 1.0 equiv.). Purified via flash column chromatography on silica gel (gradient from Dichloromethane:MeOH 100:0 to 98:2) to afford the product as a yellow solid (924 mg, 57% yield).

3.1u. ^{1}H NMR (400 MHz, $CDCl_3$) δ 7.86 (dd, *J* = 5.5, 3.1 Hz, 2H), 7.78 (dd, *J* = 5.5, 3.1 Hz, 2H), 5.41 (d, *J* = 8.9 Hz, 1H), 4.89 (dd, *J* = 8.6, 4.8 Hz, 1H), 4.69 – 4.56 (m, 1H), 3.89 – 3.71 (m, 2H), 2.56 (t, *J* = 7.2 Hz, 2H), 2.49 – 2.28 (m, 2H), 2.27 – 2.07 (m, 2H), 2.06 (s, 3H), 2.05 – 1.96 (m, 1H), 1.94 – 1.81 (m, 1H), 1.41 (s, 9H). ^{13}C NMR (101 MHz, $CDCl_3$) δ 171.3, 168.5, 161.6, 155.7, 134.9, 129.0, 124.1, 80.0, 57.0, 51.0, 47.1, 32.4, 29.9, 29.4, 28.4, 25.2, 15.7. HRMS (ESI+) (m/z): $[M+H]^+$ calcd. for $C_{23}H_{29}N_3O_7S$, 492.1804; found: 492.1794.

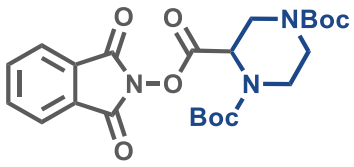

1,4-Di-*tert*-butyl 2-(1,3-dioxoisoindolin-2-yl) piperazine-1,2,4-tricarboxylate (3.1ab). Prepared according to GP2 from 1,4-bis(tert-butoxycarbonyl)piperazine-2-carboxylic acid (1.35 g, 4.1 mmol, 1.0 equiv.), 2-hydroxyisoindoline-1,3-dione (667 mg, 4.1 mmol, 1.0 equiv.), N,N-dimethylpyridin-4-amine (50.0 mg, 0.41 mmol, 0.1 equiv.) and diisopropylmethanediimine (633 µL, 4.1 mmol, 1.0 equiv.). Purified via flash column chromatography on silica gel (gradient Dichloromethane:Diethyl Ether) to afford the product (mixture of rotamers) as a white solid (856 mg, 44% yield).

3.1ab. ^{1}H NMR (400 MHz, $CDCl_3$) δ 7.89 – 7.81 (m, 2H), 7.81 – 7.73 (m, 2H), 5.21 & 4.97 (rotameric m, 1H), 4.79 – 4.54 (m, 1H), 4.25 – 3.76 (m, 2H), 3.37 – 3.12 (m, 2H), 3.10 – 2.69 (m, 1H), 1.54 – 1.40 (m, 18H). ^{13}C NMR (101 MHz, $CDCl_3$) δ 167.2 & 166.9 (rotameric signals), 161.3, 155.0 & 154.7 (rotameric signals), 154.2, 134.9, 129.0, 124.0, 81.9, 80.8, 53.7 & 52.4 (rotameric signals), 44.3 & 43.4 (rotameric signals), 42.2 & 41.7 (rotameric signals), 40.4, 28.3, 28.1. HRMS (ESI+) (m/z): $[M+H]^+$ calcd. for $C_{23}H_{29}N_3O_8$, 476.2033; found: 476.2036.

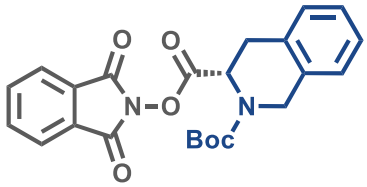

2-(*tert*-Butyl) 3-(1,3-dioxoisoindolin-2-yl) (*S*)-3,4-dihydroisoquinoline-2,3(1H)-dicarboxylate (3.1ac).

Prepared according to GP2 from (S)-2-(tert-butoxycarbonyl)-1,2,3,4-tetrahydroisoquinoline-3-carboxylic acid (1.14 g, 4.1 mmol, 1.0 equiv.), 2-hydroxyisoindoline-1,3-dione (667 mg, 4.1 mmol, 1.0 equiv.), N,N-dimethylpyridin-4-amine (50.0 mg, 0.41 mmol, 0.1 equiv.) and diisopropylmethanediimine (633 µL, 4.1 mmol, 1.0 equiv.). Purified via flash column chromatography on silica gel (gradient Dichloromethane:Diethyl Ether) to afford the product (mixture of rotamers) as a white solid (814 mg, 47% yield).

3.1ac. ^{1}H NMR (400 MHz, $CDCl_3$) δ 7.88 – 7.78 (m, 2H), 7.78 – 7.69 (m, 2H), 7.33 – 7.10 (m, 4H), 5.54 & 5.10 (rotameric t, J_{minor} = 4.8 Hz, J_{major} = 5.7 Hz, 1H), 4.81 – 4.58 (m, 2H), 3.45 – 3.27 (m, 2H), 1.57 – 1.52 (m, 9H). ^{13}C NMR (101 MHz, $CDCl_3$) δ 168.9 & 168.3 (rotameric signals), 161.6 & 161.5 (rotameric signals), 155.0 & 154.5 (rotameric signals), 134.9 & 134.8 (rotameric signals), 134.4 & 132.8 (rotameric signals), 131.7 & 131.2 (rotameric signals), 129.0 & 128.8 (rotameric signals), 128.0, 127.5 & 127.2 (rotameric signals), 127.5 & 127.1 (rotameric signals), 126.4 & 126.3 (rotameric signals), 124.0, 82.0 & 81.4 (rotameric signals), 53.4 & 51.6 (rotameric signals), 44.7 & 44.1 (rotameric signals), 32.2 & 31.5 (rotameric signals), 28.5 & 28.3 (rotameric signals). HRMS Failed to find the mass due to instability of the NHPI redox active ester.

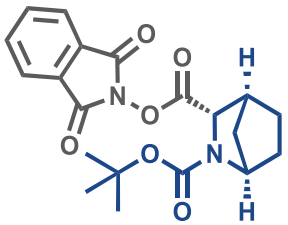

2-(*tert*-Butyl)3-(1,3-dioxoisoindolin-2-yl)(1R,3S,4S)-2-azabicyclo[2.2.1]-heptane-2,3-dicarboxylate (3.1ad).

Prepared according to GP2 from (1R,3S,4S)-2-(tert-Butoxycarbonyl)-2-azabicyclo[2.2.1]heptane-3-carboxylic acid (1.00 g, 4.1 mmol, 1.0 equiv.), 2-hydroxyisoindoline-1,3-dione (667 mg, 4.1 mmol, 1.0 equiv.), N,N-dimethylpyridin-4-amine (50.0 mg, 0.41 mmol, 0.1 equiv.) and diisopropylmethanediimine (633 µL, 4.1 mmol, 1.0 equiv.). Purified via flash column chromatography on silica gel (gradient Dichloromethane:Diethyl Ether) to afford the product (mixture of rotamers) as a pale brown solid (1.33 mg, 83% yield).

3.1ad. ^{1}H NMR (400 MHz, $CDCl_3$) δ 7.91 – 7.83 (m, 2H), 7.82 – 7.73 (m, 2H), 4.40 & 4.24 (rotameric s, 1H), 4.22 & 4.10 (rotameric s, 1H), 3.05 – 2.97 (m, 1H), 2.05 – 1.96 (m, 1H), 1.92 – 1.74 (m, 2H), 1.74 – 1.51 (m, 2H), 1.48 & 1.46 (rotameric s, 9H), 1.44 – 1.33 (m, 1H). ^{13}C NMR (101 MHz, $CDCl_3$) δ 167.6 & 167.5 (rotameric signals), 161.8 & 161.7 (rotameric signals), 154.1 & 153.0 (rotameric signals), 134.9 & 134.8 (rotameric signals), 129.1 & 129.0 (rotameric signals), 124.1 & 124.0 (rotameric signals), 81.1 & 80.4 (rotameric signals), 62.4 & 62.2 (rotameric signals), 57.7 & 56.5 (rotameric signals), 43.6 & 42.7 (rotameric signals), 35.9 & 35.1 (rotameric signals), 30.6 & 30.3 (rotameric signals), 28.5 & 28.3 (rotameric signals), 28.0 & 27.7

(rotameric signals). HRMS (ESI+) (m/z): $[M+H]^+$ calcd. for $C_{20}H_{22}N_2O_6$, 387.1556; found: 387.1554.

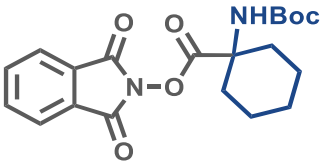

1,3-Dioxoisoindolin-2-yl-1-((*tert*-butoxycarbonyl)amino)cyclohexane-1-carboxylate (3.1ae).

Prepared according to GP2 from 1-((tert-butoxycarbonyl)amino)cyclohexane-1-carboxylic acid (1.00 g, 4.1 mmol, 1.0 equiv.), 2-hydroxyisoindoline-1,3-dione (667 mg, 4.1 mmol, 1.0 equiv.), N,N-dimethylpyridin-4-amine (50.0 mg, 0.41 mmol, 0.1 equiv.) and diisopropylmethanediimine (633 µL, 4.1 mmol, 1.0 equiv.). Purified via flash column chromatography on silica gel (gradient Dichloromethane:Diethyl Ether) to afford the product as a white solid (1.12 g, 70% yield).

3.1ae. ^{1}H NMR (400 MHz, $CDCl_3$) δ 7.85 (dd, *J* = 5.5, 3.1 Hz, 2H), 7.76 (dd, *J* = 5.5, 3.1 Hz, 2H), 4.94 (s, 1H), 2.20 – 2.02 (m, 4H), 1.77 – 1.64 (m, 2H), 1.64 – 1.55 (m, 2H), 1.51 (s, 9H), 1.46 – 1.32 (m, 1H). ^{13}C NMR (101 MHz, $CDCl_3$) δ 170.8, 161.9, 154.5, 134.7, 129.2, 123.9, 80.8, 58.5, 33.3, 28.3, 25.2, 21.2. HRMS (ESI+) (m/z): $[M+H]^+$ calcd. for $C_{20}H_{24}N_2O_6$, 389.1713; found: 389.1705.

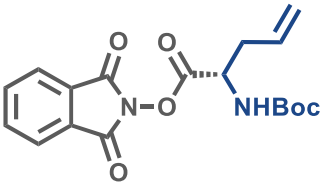

1,3-Dioxoisoindolin-2-yl-(*S*)-2-((*tert*-butoxycarbonyl)amino)pent-4-enoate (3.1af). Prepared according to GP2 from (S)-2-((tert-butoxycarbonyl)amino)pent-4-enoic acid (431 mg, 2.0 mmol, 1.0 equiv.), 2-hydroxyisoindoline-1,3-dione (326 mg, 2 mmol, 1.0 equiv.), N,N-dimethylpyridin-4-amine (24.4 mg, 0.2 mmol, 0.1 equiv.) and diisopropylmethanediimine (313 µL, 2.0 mmol, 1.0 equiv.). Purified via flash column chromatography on silica gel (from Heptane to Heptane:Ethyl Acetate 6:1) to afford the product (mixture of rotamers) as a white solid (504 mg, 70% yield).

3.1af. ^{1}H NMR (500 MHz, $CDCl_3$) δ 7.88 (dd, *J* = 5.5, 3.1 Hz, 2H), 7.79 (dd, *J* = 5.5, 3.1 Hz, 2H), 5.92 – 5.80 & 5.78 – 5.69 (rotameric m, 1H), 4.85 – 4.77 (m, 4H), 2.76 – 2.70

& 2.63 – 2.47 (rotameric m, 2H), 1.54 – 1.36 (m, 9H).^{13}C NMR (126 MHz, $CDCl_3$) δ 168.88, 161.60, 154.93, 134.98, 131.24, 128.96, 124.15, 120.70, 82.19 & 80.72 (rotameric signals), 52.77 & 51.45 (rotameric signals), 36.98 & 36.33 (rotameric signals), 28.38 & 28.12 (rotameric signals). HRMS Failed to find the mass due to instability of the NHPI redox active ester.

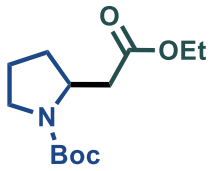

***tert*-Butyl 2-(2-ethoxy-2-oxoethyl)pyrrolidine-1-carboxylate (3.3).**

Prepared according to GP3 from **3.1a** (108 mg, 0.3 mmol, 1.0 equiv.) and **3.2a** (97 mg, 0.3 mmol, 1.0 equiv.). Purified via flash column chromatography on silica gel (Pentane:Ethyl Acetate 40:1) to afford the product (mixture of rotamers) as a colorless oil (62 mg, 80% yield).

Flow reaction: An oven dried 250 mL Schlenk flask, equipped with a magnetic stirring bar, was charged 4-(trifluoromethyl)sulfonyl hydrazone **3.2a** (1.30 g, 4.0 mmol, 1 equiv.), **3.1a** (1.44 g, 4.0 mmol, 1.0 equiv.), hantzsch ester (1.52 g, 6.0 mmol, 1.5 equiv.) and $Ru(bpy)_3(PF_6)_2$ (34 mg, 0.04 mmol, 1 mol%) and sealed with a rubber septum. Subsequently, dry and degassed CH_2Cl_2 (40 mL) and acetone (40 mL) were added under nitrogen atmosphere to prepare a 0.05 M solution (both the solvents were sparged with nitrogen for 20 min before the addition). The solution was taken up with a 60 mL syringe, mounted on a syringe pump and pushed into a Vapourtec UV-150 equipped blue LEDs (l =450 nm, 60 W) for the required residence time. The outflow was collected in a 250 mL round-bottom flask.Then, the solvent was evaporated under reduced pressure. The obtained crude mixture was dissolved in 40 mL of ethanol (0.1 M) in a flask equipped with a reflux condenser. TEA was added (3.0 equiv.) and the vessel was placed under stirring in an oil bath at 80 °C for 1 h (set-up connected to the schlenk line. The reaction mixture was cooled to r.t. and the solvent was removed under reduced pressure. The obtained crude was diluted with diethyl ether and washed with 1 M HCl. The combined organic layers were dried over Na_2SO_4, filtered and the solvent was removed under reduced pressure. The residue was purified via flash column chromatography on silica gel (Pentane:Ethyl

Acetate 30:1) to afford the product as a colorless oil (620 mg, 60% yield).Characterization data are in accordance with literature.

3.3. ^{1}HNMR (400 MHz, $CDCl_3$) δ 4.11 (d, *J* = 7.2 Hz, 3H), 3.42 – 3.23 (m, 2H), 3.01 – 2.70 (m, 1H), 2.28 (dd, *J* = 15.0, 9.9 Hz, 1H), 2.11 – 1.96 (m, 1H), 1.88 – 1.67 (m, 3H), 1.45 (s, 9H), 1.24 (t, *J* = 7.1 Hz, 3H). ^{13}C NMR (101 MHz, $CDCl_3$) δ 171.7, 154.4, 79.7 & 79.4 (rotameric signals), 60.5, 54.2, 46.7 & 46.3 (rotameric signals), 39.5 & 38.7 (rotameric signals), 31.4 & 30.6 (rotameric signals), 28.6, 23.6 & 22.9 (rotameric signals), 14.3.

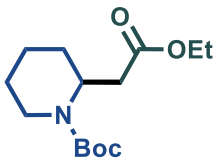

***tert*-Butyl 2-(2-ethoxy-2-oxoethyl)piperidine-1-carboxylate (3.4).**

Prepared according to GP3 from **3.1b** (112 mg, 0.3 mmol, 1.0 equiv.) and **3.2a** (97 mg, 0.3 mmol, 1.0 equiv.). Purified via flash column chromatography on silica gel (from Pentane:Ethyl Acetate 40:1 to 15:1) to afford the product as a colorless oil (63 mg, 77% yield).

3.4. ^{1}H NMR (500 MHz, $CDCl_3$) δ 4.68 (d, *J* = 8.1 Hz, 1H), 4.10 (q, *J* = 7.1 Hz, 2H), 3.97 (d, *J* = 13.2 Hz, 1H), 2.76 (t, *J* = 13.3 Hz, 1H), 2.61 – 2.49 (m, 2H), 1.61 (d, *J* = 12.2 Hz, 4H), 1.54 – 1.35 (m, 11H), 1.23 (t, *J* = 7.1 Hz, 3H). ^{13}C NMR (126 MHz, $CDCl_3$) δ 171.5, 154.8, 79.6, 60.6, 48.0, 39.3, 35.4, 28.5, 28.3, 25.4, 19.0, 14.3.

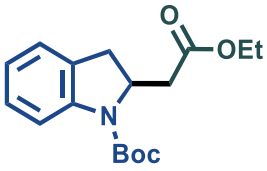

***tert*-Butyl 2-(2-ethoxy-2-oxoethyl)indoline-1-carboxylate (3.5).**

Prepared according to GP3 from **3.1c** (123 mg, 0.3 mmol, 1.0 equiv.) and **3.2a** (97 mg, 0.3 mmol, 1.0 equiv.). Purified via flash column chromatography on silica gel (from Pentane:Ethyl Acetate 20:1 to 10:1) to afford the product as a colorless oil (50 mg, 55% yield).

3.5. ^{1}H NMR (500 MHz, $CDCl_3$) δ 7.87 – 7.33 (m, 1H), 7.19 – 7.10 (m, 2H), 6.94 (t, *J* = 7.5 Hz, 1H), 4.86 – 4.68 (m, 1H), 4.16 – 4.05 (m, 2H), 3.40 (dd, *J* = 16.4, 9.7 Hz, 1H), 2.94 – 2.77 (m, 2H), 2.51 (dd, *J* = 15.2, 9.9 Hz, 1H), 1.57 (s, 9H), 1.22 (t, *J* = 7.1 Hz, 3H). ^{13}C NMR (126 MHz, $CDCl_3$) δ 171.2, 152.1, 141.8, 129.8, 127.6, 125.1, 122.7, 115.4,

81.4, 60.7, 56.2, 39.3, 34.0, 28.6, 14.3. HRMS (GC-FI+) (m/z): $[M+H]^+$ calcd. for $C_{17}H_{23}NO_4$, 305.1627; found: 305.1640.

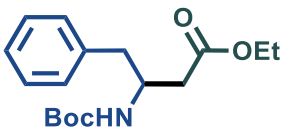

Ethyl 3-((*tert*-butoxycarbonyl)amino)-4-phenylbutanoate (3.6).

Prepared according to GP3 from **3.1d** (123 mg, 0.3 mmol, 1.0 equiv.) and **3.2a** (97.3 mg, 0.3 mmol, 1.0 equiv.). Purified via flash column chromatography on silica gel (gradient from Pentane:Ethyl Acetate 98:2 to 90:10) to afford the product as a white solid (60 mg, 65% yield).

3.6. ^{1}H NMR (400 MHz, $CDCl_3$) δ 7.29 (dd, *J* = 8.1, 6.6 Hz, 2H), 7.24 – 7.15 (m, 3H), 5.05 (s, 1H), 4.22 – 4.09 (m, 3H), 2.91 (d, *J* = 6.6 Hz, 1H), 2.81 (dd, *J* = 13.4, 7.6 Hz, 1H), 2.46 (qd, *J* = 15.8, 5.7 Hz, 2H), 1.40 (s, 9H), 1.26 (t, *J* = 7.2 Hz, 3H). ^{13}C NMR (101 MHz, $CDCl_3$) δ 171.8, 155.2, 137.9, 129.5, 128.6, 126.7, 79.4, 60.7, 49.0, 40.5, 37.9, 28.5, 14.3.

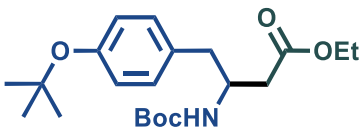

Ethyl 4-(4-(*tert*-butoxy)phenyl)-3-((*tert*-butoxycarbonyl)amino)butanoate (3.7).

Prepared according to GP3 from **3.1e** (145 mg, 0.3 mmol, 1.0 equiv.) and **3.2a** (97.3 mg, 0.3 mmol, 1.0 equiv.). Purified via flash column chromatography on silica gel (gradient from Pentane:Ethyl Acetate 98:2 to 90:10)) to afford the product as a white solid (64 mg, 56% yield).

3.7. ^{1}H NMR (400 MHz, $CDCl_3$) δ 7.09 – 7.02 (m, 2H), 6.94 – 6.86 (m, 2H), 5.14 – 4.84 (m, 1H), 4.18 – 4.08 (m, 3H), 2.90 – 2.69 (m, 2H), 2.48 (dd, *J* = 15.7, 5.5 Hz, 1H), 2.40 (dd, *J* = 15.7, 5.9 Hz, 1H), 1.39 (s, 9H), 1.31 (s, 9H), 1.25 (t, *J* = 7.1 Hz, 3H). ^{13}C NMR (101 MHz, $CDCl_3$) δ 171.8, 155.2, 154.1, 132.7, 129.9, 124.3, 79.4, 78.4, 60.7, 49.0, 39.8, 38.0, 28.9, 28.5, 14.3. HRMS (ESI+) (m/z): [M+H]+ calcd. for $C_{21}H_{33}NO_5$, 380.2437; found: 380.2428.

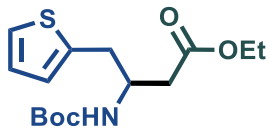

Ethyl 3-((*tert*-butoxycarbonyl)amino)-4-(thiophen-2-yl)butanoate (3.8).

Prepared according to GP3 from **3.1f** (125 mg, 0.3 mmol, 1.0 equiv.) and **3.2a** (97.3 mg, 0.3 mmol, 1.0 equiv.). Purified via flash column chromatography on silica gel (gradient from Pentane:Ethyl Acetate 98:2 to 90:10) to afford the product as a colorless oil (32 mg, 34% yield).

3.8. ^{1}H NMR (400 MHz, $CDCl_3$) δ 7.16 (dd, *J* = 5.1, 1.2 Hz, 1H), 6.93 (dd, *J* = 5.2, 3.4 Hz, 1H), 6.82 (dd, *J* = 3.5, 1.0 Hz, 1H), 5.22 – 4.85 (m, 1H), 4.21 – 4.09 (m, 3H), 3.21 – 2.96 (m, 2H), 2.58 – 2.42 (m, 3H), 1.42 (s, 9H), 1.26 (t, *J* = 7.2 Hz, 3H). ^{13}C NMR (101 MHz, $CDCl_3$) δ 171.6, 155.2, 139.7, 127.1, 126.4, 124.4, 79.6, 60.8, 48.8, 37.7, 34.3, 28.5, 14.3. HRMS (ESI+) (m/z): [M+H]+ calcd. for $C_{15}H_{23}NO_4S$, 314.1426; found: 314.1429

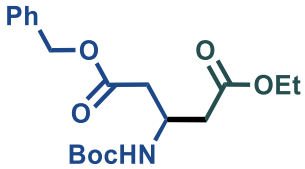

1-Benzyl 5-ethyl 3-((*tert*-butoxycarbonyl)amino)pentanedioate (3.9).

Prepared according to GP3 from **3.1g** (141 mg, 0.3 mmol, 1.0 equiv.) and **3.2a** (97 mg, 0.3 mmol, 1.0 equiv.). Purified via flash column chromatography on silica gel (from Pentane:Ethyl Acetate 60:1 to 20:1) to afford the product as a colorless oil (66 mg, 60% yield).

3.9. ^{1}H NMR (400 MHz, $CDCl_3$) δ 7.39 – 7.32 (m, 5H), 5.39 – 5.25 (m, 1H), 5.12 (s, 2H), 4.40 – 4.29 (m, 1H), 4.12 (q, *J* = 7.1 Hz, 2H), 2.80 – 2.53 (m, 4H), 1.42 (s, 9H), 1.24 (t, *J* = 7.1 Hz, 3H). ^{13}C NMR (101 MHz, $CDCl_3$) δ 171.3, 171.2, 155.1, 135.7, 128.7, 128.5, 128.4, 79.7, 66.7, 60.8, 44.6, 38.3 (2C), 28.5, 14.3. HRMS (ESI+) (m/z): $[M+H]^+$ calcd. for $C_{19}H_{27}N_2O_6$, 366.1917; found: 366.1929

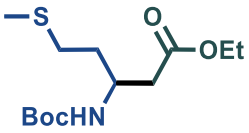

Ethyl 3-((*tert*-butoxycarbonyl)amino)-5-(methylthio)pentanoate (3.10).

Prepared according to GP3 from **3.1h** (118 mg, 0.3 mmol, 1.0 equiv.) and **3.2a** (97.3 mg, 0.3 mmol, 1.0 equiv.). Purified via flash column chromatography on silica gel (gradient from Pentane:Ethyl Acetate 98:2 to 90:10) to afford the product as a colorless oil (42 mg, 48% yield).

3.10. ^{1}H NMR (400 MHz, $CDCl_3$) δ 5.16 – 4.70 (m, 1H), 4.11 (q, *J* = 7.1 Hz, 2H), 4.06 – 3.89 (m, 1H), 2.59 – 2.41 (m, 4H), 2.06 (s, 3H), 1.86 – 1.70 (m, 2H), 1.40 (s, 9H), 1.23 (t, *J* = 7.1 Hz, 3H). ^{13}C NMR (101 MHz, $CDCl_3$) δ 171.6, 155.4, 79.4, 60.7, 47.0, 39.2, 34.2, 30.8, 28.4, 15.6, 14.3. HRMS (ESI+) (m/z): [M+Na]+ calcd. for $C_{13}H_{25}NO_4S$, 314.1402; found: 314.1400.

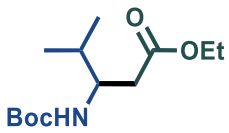

Ethyl 3-((*tert*-butoxycarbonyl)amino)-4-methylpentanoate (3.11).

Prepared according to GP3 from **3.1i** (109 mg, 0.3 mmol, 1.0 equiv.) and **3.2a** (97.3 mg, 0.3 mmol, 1.0 equiv.). Purified via flash column chromatography on silica gel (gradient from Pentane:Ethyl Acetate 98:2 to 90:10) to afford the product as a colorless oil (44 mg, 56% yield).

3.11. ^{1}H NMR (400 MHz, $CDCl_3$) δ 4.87 (d, *J* = 9.7 Hz, 1H), 4.11 (q, *J* = 7.1 Hz, 2H), 3.80 – 3.68 (m, 1H), 2.53 – 2.37 (m, 2H), 1.84 – 1.71 (m, *J* = 7.8, 7.0 Hz, 1H), 1.40 (s, 9H), 1.23 (t, *J* = 7.1 Hz, 3H), 0.89 (d, *J* = 6.8 Hz, 6H). ^{13}C NMR (101 MHz, $CDCl_3$) δ 172.0, 155.6, 79.2, 60.6, 53.1, 37.5, 32.0, 28.5, 19.4, 18.6, 14.3. HRMS (FI+) (m/z): $[M]^+$ calcd. for $C_{13}H_{25}NO_4$, 259.1784; found: 259.1785.

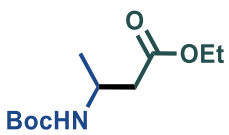

Ethyl 3-((*tert*-butoxycarbonyl)amino)butanoate (3.12).

Prepared according to GP3 from **3.1j** (100 mg, 0.3 mmol, 1.0 equiv.) and **3.2a** (97.3 mg, 0.3 mmol, 1.0 equiv.). Purified via flash column chromatography on silica gel

(gradient from Pentane:Ethyl Acetate 98:2 to 90:10) to afford the product as a colorless oil (38 mg, 55% yield).

3.12. ^{1}H NMR (400 MHz, $CDCl_3$) δ 4.94 (s, 1H), 4.10 (q, *J* = 7.1 Hz, 2H), 4.05 (s, 1H), 2.53 – 2.37 (m, 2H), 1.40 (s, 9H), 1.22 (t, *J* = 7.1 Hz, 3H), 1.17 (d, *J* = 6.7 Hz, 3H). ^{13}C NMR (101 MHz, $CDCl_3$) δ 171.6, 155.2, 79.3, 60.5, 43.6, 40.9, 28.5, 20.5, 14.3.

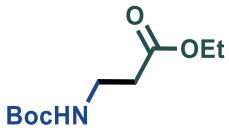

Ethyl 3-((*tert*-butoxycarbonyl)amino)propanoate (3.13). Prepared according to GP3 from **3.1k** (96 mg, 0.3 mmol, 1.0 equiv.) and **3.2a** (97 mg, 0.3 mmol, 1.0 equiv.). Purified via flash column chromatography on silica gel (from Pentane:Ethyl Acetate 10:1 to 5:1) to afford the product as a colorless oil (27 mg, 41% yield).

3.13. ^{1}H NMR (400 MHz, $CDCl_3$) δ 5.03 (s, 1H), 4.13 (q, *J* = 7.1 Hz, 2H), 3.37 (t, *J* = 6.1 Hz, 2H), 2.49 (t, *J* = 6.1 Hz, 2H), 1.42 (s, 9H), 1.25 (t, *J* = 7.1 Hz, 3H). ^{13}C NMR (101 MHz, $CDCl_3$) δ 172.6, 155.9, 79.4, 60.7, 36.2, 34.8, 28.5, 14.3.

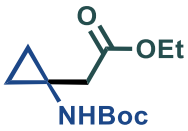

Ethyl 2-(1-((*tert*-butoxycarbonyl)amino)cyclopropyl)acetatecarboxylate (3.14).

Prepared according to GP3 from **3.1l** (104 mg, 0.3 mmol, 1.0 equiv.) and **3.2a** (97 mg, 0.3 mmol, 1.0 equiv.). Purified via flash column chromatography on silica gel (Pentane:Ethyl Acetate 10:1) to afford the product as a colorless oil (36 mg, 50% yield).

3.14. ^{1}H NMR ^{1}H NMR (500 MHz, $CDCl_3$) δ 5.23 (s, 1H), 4.14 (q, *J* = 7.1 Hz, 2H), 2.53 (s, 2H), 1.41 (s, 9H), 1.25 (t, *J* = 7.1 Hz, 3H), 0.89 – 0.80 (m, 2H), 0.74 – 0.63 (m, 2H). ^{13}C NMR (126 MHz, $CDCl_3$) δ 172.2, 155.7, 79.5, 60.5, 41.3, 30.1, 28.5, 14.4, 13.9. HRMS (GC-FI+) (m/z): $[M+H]^+$ calcd. for $C_{12}H_{21}NO_4$, 243.1471; found: 243.1480.

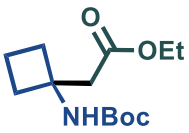

Ethyl 2-(1-((*tert*-butoxycarbonyl)amino)cyclobutyl)acetate (3.15). Prepared according to GP3 from **3.1m** (108 mg, 0.3 mmol, 1.0 equiv.) and **3.2a** (97.3 mg, 0.3 mmol, 1.0 equiv.). Purified via flash column chromatography on silica gel (gradient from Pentane:Ethyl Acetate 98:2 to 90:10) to afford the product as a colorless oil (45 mg, 58% yield).

3.15. ^{1}H NMR (400 MHz, $CDCl_3$) δ 5.04 (s, 1H), 4.10 (q, *J* = 7.1 Hz, 2H), 2.81 (s, 2H), 2.32 – 2.20 (m, 2H), 2.17 – 2.06 (m, 2H), 1.99 – 1.84 (m, 1H), 1.84 – 1.71 (m, 1H), 1.40 (s, 9H), 1.23 (t, *J* = 7.1 Hz, 3H). ^{13}C NMR (101 MHz, $CDCl_3$) δ 171.6, 154.5, 79.2, 60.3, 54.4, 41.6, 33.0, 28.5, 14.8, 14.3. HRMS (ESI+) (m/z): [M+Na]+ calcd. for $C_{13}H_{23}NO_4$, 280.1525; found: 280.1529.

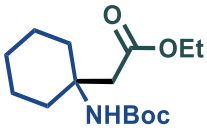

Ethyl 2-(1-((*tert*-butoxycarbonyl)amino)cyclohexyl)acetate (3.16).

Prepared according to GP3 from **3.1ae** (117 mg, 0.3 mmol, 1.0 equiv.) and **3.2a** (97 mg, 0.3 mmol, 1.0 equiv.). Purified via flash column chromatography on silica gel (from Pentane:Ethyl Acetate 40:1 to 20:1) to afford the product as a colorless oil (33 mg, 50% yield).

3.16. ^{1}H NMR (400 MHz, $CDCl_3$) δ 4.49 (s, 1H), 4.09 (q, *J* = 7.1 Hz, 2H), 2.72 (s, 2H), 2.05 (dd, *J* = 11.1, 5.2 Hz, 2H), 1.56 – 1.38 (m, 16H), 1.23 (t, *J* = 7.1 Hz, 4H). ^{13}C NMR (101 MHz, $CDCl_3$) δ 171.4, 154.7, 79.0, 60.2, 53.5, 42.8, 35.2, 28.6, 25.6, 21.6, 14.4. HRMS (ESI+) (m/z): $[M+H]^+$ calcd. for $C_{15}H_{27}NO_4$, 286.2018; found: 286.2011.

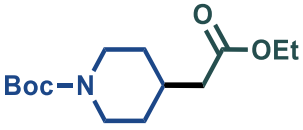

***tert*-Butyl 4-(2-ethoxy-2-oxoethyl)piperidine-1-carboxylate (3.17).**

Prepared according to GP3 from **3.1n** (112 mg, 0.3 mmol, 1.0 equiv.) and **3.2a** (97.3 mg, 0.3 mmol, 1.0 equiv.). Purified via flash column chromatography on silica gel

(gradient from Pentane:Ethyl Acetate 100:0 to 90:10) to afford the product as a pale yellow oil (34 mg, 42% yield).

3.17. ^{1}H NMR (400 MHz, $CDCl_3$) δ 4.10 (p, *J* = 7.0 Hz, 4H), 2.69 (t, *J* = 12.6 Hz, 2H), 2.20 (d, *J* = 7.1 Hz, 2H), 1.90 (ttt, *J* = 11.1, 7.2, 3.7 Hz, 1H), 1.70 – 1.61 (m, 2H), 1.42 (d, *J* = 0.9 Hz, 9H), 1.23 (t, *J* = 7.1, 3H), 1.13 (qd, *J* = 12.4, 4.3 Hz, 2H). ^{13}C NMR (101 MHz, $CDCl_3$) δ 172.5, 154.9, 79.4, 60.4, 43.8, 41.2, 33.2, 31.9, 28.5, 14.4.

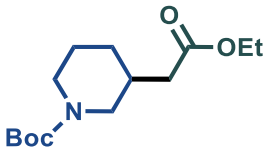

***tert*-Butyl 3-(2-ethoxy-2-oxoethyl)piperidine-1-carboxylate (3.18).** Prepared according to GP3 from **3.1o** (112 mg, 0.3 mmol, 1.0 equiv.) and **3.2a** (97.3 mg, 0.3 mmol, 1.0 equiv.). Purified via flash column chromatography on silica gel (gradient from Pentane:Ethyl Acetate 100:0 to 90:10) to afford the product as a pale yellow oil (50 mg, 62% yield).

3.18. ^{1}H NMR (400 MHz, $CDCl_3$) δ 4.11 (q, *J* = 7.2 Hz, 2H), 4.05 – 3.70 (m, 2H), 2.90 – 2.73 (m, 1H), 2.74 – 2.40 (br m, 1H), 2.23 (dd, *J* = 15.1, 7.0 Hz, 1H), 2.14 (dd, *J* = 15.1, 7.3 Hz, 1H), 2.04 – 1.88 (m, 1H), 1.87 – 1.76 (m, 1H), 1.68 – 1.56 (m, 1H), 1.42 (s, 10H), 1.24 (t, *J* = 7.1 Hz, 3H), 1.21 – 1.09 (m, 1H). ^{13}C NMR (101 MHz, $CDCl_3$) δ 172.3, 154.9, 79.5, 60.5, 49.4, 43.9, 38.4, 32.9, 30.6, 28.5, 24.6, 14.4. HRMS (FI+) (m/z): $[M]^+$ calcd. for $C_{14}H_{25}NO_4$, 271.1784; found: 271.1781.

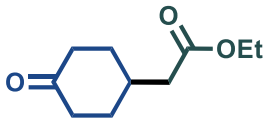

Ethyl 2-(4-oxocyclohexyl)acetate (3.19).

Prepared according to GP3 from **3.1p** (86mg, 0.3 mmol, 1.0 equiv.) and **3.2a** (97 mg, 0.3 mmol, 1.0 equiv.). Purified via flash column chromatography on silica gel (from Pentane:Acetone 12:1) to afford the product as a colorless oil (27 mg, 48% yield).

3.19. ^{1}H NMR (400 MHz, $CDCl_3$) δ 4.15 (q, *J* = 7.1 Hz, 2H), 2.38 (dd, *J* = 8.8, 4.6 Hz, 4H), 2.33 – 2.22 (m, 3H), 2.12 – 2.05 (m, 2H), 1.54 – 1.43 (m, 2H), 1.29 – 1.21 (m, 3H). ^{13}C NMR (101 MHz, $CDCl_3$) δ 211.4, 172.5, 60.6, 40.7, 40.4, 33.2, 32.5, 14.4. HRMS (GC-FI+) (m/z): $[M]^+$ calcd. for $C_{10}H_{16}O_3$, 184.1099; found: 184.1099.

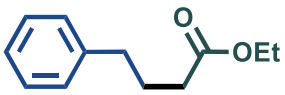

Ethyl 4-phenylbutanoate (3.20).

Prepared according to GP3 from **3.1q** (88.6 mg, 0.3 mmol, 1.0 equiv.) and **3.2a** (97.3 mg, 0.3 mmol, 1.0 equiv.). Purified via flash column chromatography on silica gel (gradient from Pentane:Ethyl Acetate 100:0 to 95:5) to afford the product as a colorless oil (20 mg, 35% yield).

3.20. ^{1}H NMR (400 MHz, $CDCl_3$) δ 7.32 – 7.26 (m, 2H), 7.24 – 7.14 (m, 3H), 4.13 (q, *J* = 7.1 Hz, 2H), 2.70 – 2.59 (m, 2H), 2.32 (t, *J* = 7.5 Hz, 2H), 1.96 (p, *J* = 7.6 Hz, 2H), 1.26 (t, *J* = 7.2 Hz, 3H). ^{13}C NMR (101 MHz, $CDCl_3$) δ 173.7, 141.6, 128.6, 128.5, 126.1, 60.4, 35.3, 33.8, 26.7, 14.4.

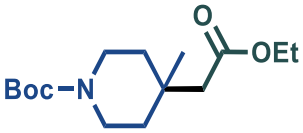

***tert*-Butyl 4-(2-ethoxy-2-oxoethyl)-4-methylpiperidine-1-carboxylate (3.21).**

Prepared according to GP3 from **3.1r** (117 mg, 0.3 mmol, 1.0 equiv.) and **3.2a** (97.3 mg, 0.3 mmol, 1.0 equiv.). Purified via flash column chromatography on silica gel (gradient from Pentane:Ethyl Acetate 100:0 to 95:5) to afford the product as a colorless oil (26 mg, 30% yield).

3.21. ^{1}H NMR (400 MHz, $CDCl_3$) δ 4.11 (q, *J* = 7.1 Hz, 2H), 3.49 (ddd, *J* = 13.7, 6.7, 4.1 Hz, 2H), 3.29 (ddd, *J* = 13.7, 8.5, 3.8 Hz, 2H), 2.25 (s, 2H), δ 1.55 – 1.47 (m, 2H), 1.44 (s, 9H), 1.43 – 1.35 (m, 2H), 1.25 (t, *J* = 7.1 Hz, 3H), 1.07 (s, 3H). ^{13}C NMR (101 MHz, $CDCl_3$) δ 171.8, 155.1, 79.5, 60.2, 45.5, 39.8, 36.9, 31.9, 28.6, 24.2, 14.4. HRMS (ESI+) (m/z): [M+H]+ calcd. for $C_{15}H_{27}NO_4$, 286.2018; found: 286.2015.

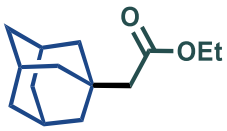

Ethyl (adamantan-1-yl)acetate (3.22).

Prepared according to GP3 from **3.1s** (97.6 mg, 0.3 mmol, 1.0 equiv.) and **3.2a** (97.3 mg, 0.3 mmol, 1.0 equiv.). Purified via flash column chromatography on silica gel

(gradient from Pentane:Ethyl Acetate 100:0 to 95:5) to afford the product as a colorless oil (33 mg, 50% yield).

3.22. ^{1}H NMR (400 MHz, $CDCl_3$) δ 4.10 (q, *J* = 7.1 Hz, 2H), 2.05 (s, 2H), 1.99 – 1.92 (m, 3H), 1.74 – 1.57 (m, 12H), 1.25 (t, *J* = 7.1 Hz, 3H). ^{13}C NMR (101 MHz, $CDCl_3$) δ 172.0, 59.9, 49.1, 42.5, 36.9, 32.9, 28.8, 14.5.

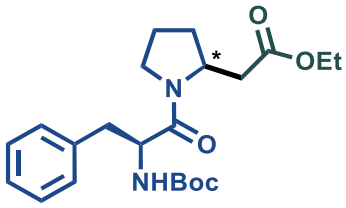

Ethyl 3-((*tert*-butoxycarbonyl)amino)propanoate (3.23).

Prepared according to GP1 from **3.1t** (152 mg, 0.3 mmol, 1.0 equiv.) and **3.2a** (97 mg, 0.3 mmol, 1.0 equiv.). Purified via flash column chromatography on silica gel (Pentane:Ethyl Acetate 4:1) to afford the product as a white solid (57 mg, 47% yield). *d.r.* ratio of **3.23** was determined via ^{1}H NMR to be > 20:1.

3.23. ^{1}H NMR (400 MHz, $CDCl_3$) δ 7.22 – 7.12 (m, 5H), 5.30 (d, *J* = 9.0 Hz, 1H), 4.52 – 4.41 (m, 1H), 4.20 (ddt, *J* = 10.2, 6.9, 3.2 Hz, 1H), 4.09 – 3.98 (m, 2H), 3.34 – 3.23 (m, 1H), 2.99 – 2.82 (m, 3H), 2.46 (dt, *J* = 9.8, 7.1 Hz, 1H), 2.16 (dd, *J* = 15.5, 9.9 Hz, 1H), 1.76 – 1.49 (m, 3H), 1.35 (s, 9H), 1.26 – 1.09 (m, 4H). ^{13}C NMR (101 MHz, $CDCl_3$) δ 171.4, 170.2, 155.2, 136.6, 129.5, 128.5, 127.0, 79.7, 60.5, 54.3, 53.9, 46.6, 40.2, 37.4, 29.8, 28.4, 23.4, 14.3. HRMS (ESI+) (m/z): $[M+H]^+$ calcd. for $C_{22}H_{32}N_2O_5$, 405.2389; found: 405.2380.

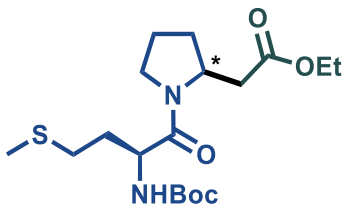

Ethyl 2-(1-((*tert*-butoxycarbonyl)-L-methionyl)pyrrolidin-2-yl)acetate (3.24).

Prepared according to GP3 from **3.1u** (148 mg, 0.3 mmol, 1.0 equiv.) and **3.2a** (97.3 mg, 0.3 mmol, 1.0 equiv.). Purified via flash column chromatography on silica gel (gradient from Pentane:Ethyl Acetate 80:20 to 60:40) to afford the two

diastereomers as an inseparable mixture as a colorless oil (49 mg, 42% yield). *d.r.* ratio of **3.24** was determined via ^{1}H NMR to be 3:1.

3.24. ^{1}H NMR (400 MHz, $CDCl_3$) δ 5.36 & 5.32 (diastereomeric d, *J* = 8.8, 1H), 4.56 – 4.46 (m, 1H), 4.45 – 4.32 (m, 1H), 4.20 – 4.03 (m, 2H), 3.73 – 3.63 (m, 1H), 3.58 – 3.41 (m, 1H), 2.99 & 2.81 (diastereomeric dd, *J* = 15.4, 3.7 Hz, 1H), 2.59 – 2.48 (m, 2H), 2.41 & 2.29 (diastereomeric dd, *J* = 15.5, 9.8 Hz, 1H), 2.09 & 2.08 (diastereomeric s, 3H), 2.08 – 1.86 (m, 4H), 1.86 – 1.74 (m, 2H), 1.42 & 1.41 (diastereomeric s, 9H), 1.23 (diastereomeric t, *J* = 7.1 Hz, 3H). ^{13}C NMR (101 MHz, $CDCl_3$) δ 171.4 & 171.3 (diastereomeric signals), 170.6 & 170.3 (diastereomeric signals), 155.6, 79.8, 60.6 & 60.6 (diastereomeric signals), 54.6 & 54.3 (diastereomeric signals), 51.4 & 51.3 (diastereomeric signals), 47.2 & 46.8 (diastereomeric signals), 37.6 & 37.5 (diastereomeric signals), 33.1 & 32.7 (diastereomeric signals), 30.3 & 30.2 (diastereomeric signals), 30.0 & 29.9 (diastereomeric signals), 28.4, 24.3 & 23.8 (diastereomeric signals), 15.8 &15.8 (diastereomeric signals), 14.3. HRMS (ESI+) (m/z): $[M+H]^+$ calcd. for $C_{18}H_{32}N_2O_5S$, 389.2110; found: 389.2111.

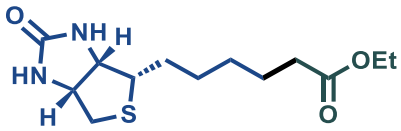

Ethyl 6-((3aS,4S,6aR)-2-oxohexahydro-1H-thieno[3,4-d]imidazol-4-yl)hexanoate (3.25).

Prepared according to GP3 from **3.1v** (117 mg, 0.3 mmol, 1.0 equiv.) and **3.2a** (97.3 mg, 0.3 mmol, 1.0 equiv.). Purified via flash column chromatography on silica gel (gradient from Dichloromethane:Methanol 98:2 to 95:5) to afford the product as a pale yellow oil (29 mg, 34% yield).

3.25. ^{1}H NMR (400 MHz, $CDCl_3$) δ 5.94 (s, 1H), 5.63 (s, 1H), 4.49 (dd, *J* = 7.8, 5.0 Hz, 1H), 4.33 – 4.25 (m, 1H), 4.11 (q, *J* = 7.1 Hz, 2H), 3.20 – 3.08 (m, 1H), 2.95 – 2.85 (m, 1H), 2.72 (d, *J* = 12.8 Hz, 1H), 2.28 (t, *J* = 7.5 Hz, 2H), 1.77 – 1.54 (m, 4H), 1.48 – 1.30 (m, 4H), 1.24 (t, *J* = 7.1 Hz, 3H). ^{13}C NMR (101 MHz, $CDCl_3$) δ 174.0, 163.9, 62.2, 60.5, 60.3, 55.9, 40.7, 34.4, 29.2, 28.8, 28.5, 24.7, 14.4. HRMS (ESI+) (m/z): $[M+H]^+$ calcd. for $C_{13}H_{22}N_2O_3S$, 287.1429; found: 287.1423.

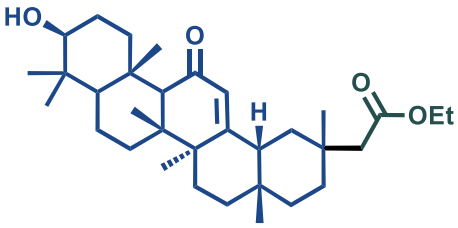

Ethyl (enoxolone)acetate (3.26).

Prepared according to GP3 from **3.1z** (123 mg, 0.2 mmol, 1.0 equiv.) and **3.2a** (65 mg, 0.3 mmol, 1.0 equiv.). Purified via flash column chromatography on silica gel (gradient from Pentane:Ethyl Acetate 90:10 to 80:20) to afford the product with a minor aromatic impurity. Further purification via reverse-phase column chromatrography (gradient from Acetonitrile:Water 50:50 to 80:20) followed by extraction with ethyl acetate yielded the pure product as an inseparable mixture as a white solid (31 mg, 30% yield). *d.r.* ratio of **26** was determined via ^{1}H NMR to be 2.5:1.

3.26. ^{1}H NMR (400 MHz, $CDCl_3$) δ 5.58 (s, 1H), 4.10 (q, *J* = 7.2 Hz, 3H), 3.22 (dd, *J* = 10.8, 5.5 Hz, 1H), 2.77 (dt, *J* = 13.5, 3.6 Hz, 1H), 2.32 (s, 1H), 2.20 – 1.99 (m, 5H), 1.94 – 1.74 (m, 2H), 1.72 – 1.53 (m, 3H), 1.53 – 1.37 (m, 4H), 1.35 (s, 3H), 1.34 – 1.27 (m, 3H), 1.27 – 1.21 (m, 4H), 1.21 – 1.14 (m, 2H), 1.14 – 1.10 (m, 5H), 1.02 – 0.98 (m, 6H), 0.97 – 0.92 (m, 1H), 0.90 – 0.83 (m, 3H), 0.79 (s, 3H), 0.72 – 0.64 (m, 1H). ^{13}C NMR (101 MHz, $CDCl_3$) δ 200.4, 171.9, 170.0, 128.5, 78.9, 61.9, 60.2, 55.1, 49.7, 47.2, 45.6, 43.5, 42.7, 39.3, 37.2, 36.0, 34.1, 32.9, 32.5, 32.2, 29.8, 28.7, 28.2, 27.4, 26.5, 26.5, 23.5, 21.7, 18.8, 17.6, 16.5, 15.7, 14.5.

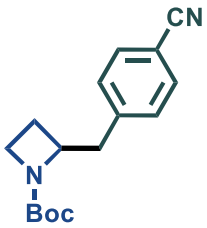

***tert*-Butyl 2-(4-cyanobenzyl)azetidine-1-carboxylate (3.27)**.

Prepared according to GP3 from **3.1aa** (104 mg, 0.3 mmol, 1.0 equiv.) and **3.2b** (106 mg, 0.3 mmol, 1.0 equiv.). Purified via flash column chromatography on silica gel (gradient from Pentane:Ethyl Acetate 98:2 to 90:10) to afford the product as a white solid (33 mg, 40% yield).

3.27. ^{1}H NMR (400 MHz, $CDCl_3$) δ 7.59 (d, *J* = 8.11, 2H), 7.30 (d, *J* = 8.11, 2H), 4.48 – 4.36 (m, 1H), 3.79 (td, *J* = 8.8, 6.7 Hz, 1H), 3.61 (td, *J* = 8.8, 5.2 Hz, 1H), 3.18 (dd, *J* =

13.6, 4.2 Hz, 1H), 3.02 (dd, *J* = 13.6, 8.0 Hz, 1H), 2.23 – 2.10 (m, 1H), 1.90 – 1.77 (m, 1H), 1.44 (s, 9H).^{13}C NMR (101 MHz, $CDCl_3$) δ 156.5, 143.3, 132.3, 130.4, 119.1, 110.5, 79.7, 61.7, 46.4, 41.1, 28.6, 21.1.HRMS (ESI+) (m/z): $[M+H]^+$ calcd. for $C_{16}H_{20}N_2O_2$, 273.1603; found: 273.1616.

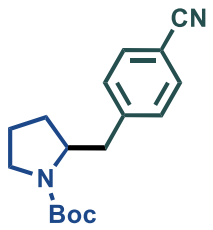

***tert*-Butyl 2-(4-cyanobenzyl)pyrrolidine-1-carboxylate (3.28).**

Prepared according to GP3 from **3.1a** (108 mg, 0.3 mmol, 1.0 equiv.) and **3.2b** (106 mg, 0.3 mmol, 1.0 equiv.). Purified via flash column chromatography on silica gel (Pentane:Ethyl Acetate 10:1) to afford the product (mixture of rotamers) as a colorless oil (56 mg, 65% yield).

3.28. ^{1}H NMR (400 MHz, $CDCl_3$) δ 7.61 – 7.53 (m, 2H), 7.36 – 7.25 (m, 2H), 4.12 – 3.87 (m, 1H), 3.47 – 3.00 (m, 3H), 2.74 – 2.56 (m, 1H), 1.91 – 1.68 (m, 3H), 1.66 – 1.58 (m, 1H), 1.48 (s, 9H). ^{13}C NMR (101 MHz, $CDCl_3$) δ 154.7 & 154.5 (rotameric signals), 145.0 & 144.6 (rotameric signals), 132.3 & 132.2 (rotameric signals), 130.4 & 130.3 (rotameric signals), 119.1, 110.2, 79.7 & 79.5 (rotameric signals), 58.51, 46.92 & 46.43 (rotameric signals), 41.0 & 40.1 (rotameric signals), 30.0 & 29.2 (rotameric signals), 28.3, 23.6 & 22.8 (rotameric signals).

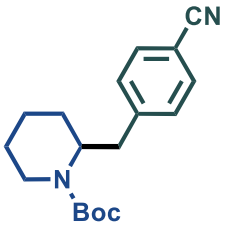

***tert*-Butyl 2-(4-cyanobenzyl)piperidine-1-carboxylate (3.29).**

Prepared according to GP3 from **3.1b** (112 mg, 0.3 mmol, 1.0 equiv.) and **3.2b** (106 mg, 0.3 mmol, 1.0 equiv.). Purified via flash column chromatography on silica gel (gradient from Pentane:Ethyl Acetate 96:4 to 90:10) to afford the product as a white solid (48 mg, 53% yield).

3.29. ^{1}H NMR (400 MHz, $CDCl_3$) δ 7.55 (d, *J* = 8.0 Hz, 2H), 7.28 (d, *J* = 7.7 Hz, 2H), 4.44 (s, 1H), 4.04 (s, 1H), 2.99 (dd, *J* = 13.3, 8.2 Hz, 1H), 2.87 (td, *J* = 13.2, 2.6 Hz, 1H), 2.77 (dd, *J* = 13.4, 7.2 Hz, 1H), 1.73 – 1.36 (m, 6H), 1.29 (s, 9H). ^{13}C NMR (101 MHz, $CDCl_3$) δ 154.8, 145.3, 132.2, 130.2, 119.1, 110.1, 79.5, 52.0, 39.1, 36.5, 28.4, 27.9, 25.6, 19.1. HRMS (ESI+) (m/z): $[M+H]^+$ calcd. for $C_{18}H_{24}N_2O_2$, 301.1916; found: 301.1928.

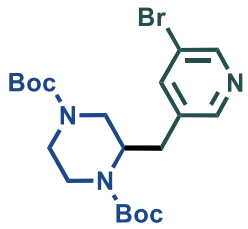

Di-*tert*-butyl-2-((5-bromopyridin-3-yl)0ethyl)piperazine-1,4-dicarboxylate (3.30).

Prepared according to GP3 from **3.1ab** (95.1 mg, 0.2 mmol, 1.0 equiv.) and **3.2o** (81.6 mg, 0.2 mmol, 1.0 equiv.). Purified via flash column chromatography on silica gel (gradient from Pentane:Ethyl Acetate 90:10 to 70:30) to afford the product (mixture of rotamers) as a white solid (55 mg, 40% yield).

3.30. ^{1}H NMR (400 MHz, $CDCl_3$) δ 8.54 (s, 1H), 8.39 (s, 1H), 7.85 – 7.58 (m, 1H), 4.53 – 3.68 (m, 4H), 3.14 – 2.99 (m, 1H), 2.91 (dd, *J* = 13.6, 3.9 Hz, 1H), 2.86 – 2.68 (m, 3H), 1.48 (s, 9H), 1.40 (s, 9H). ^{13}C NMR (101 MHz, $CDCl_3$) δ 155.1, 154.4, 149.2, 148.9, 139.5, 135.7, 120.8, 80.6 (2C), 53.1 & 51.5 (rotameric signals), 45.0 & 42.9 (rotameric signals), 39.8 & 38.5 (rotameric signals), 32.6, 29.8, 28.5, 28.4. HRMS (ESI+) (m/z): $[M+H]^+$ calcd. for $C_{20}H_{30}BrN_3O_4$, 456.1498; found: 456.1493.

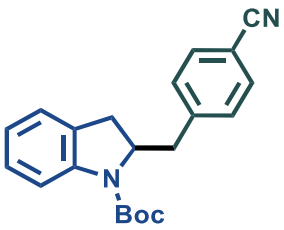

***tert*-Butyl 2-(4-cyanobenzyl)indoline-1-carboxylate (3.31).**

Prepared according to GP3 from **3.1c** (123 mg, 0.3 mmol, 1.0 equiv.) and **3.2b** (106 mg, 0.3 mmol, 1.0 equiv.). Purified via flash column chromatography on silica gel (gradient from Pentane:Ethyl Acetate 98:2 to 85:15) to afford the product as a pale yellow oil (50 mg, 50% yield).

3.31. ^{1}H NMR (400 MHz, $CDCl_3$) δ 7.94 – 7.40 (br s, 1H), 7.58 (d, *J* = 7.9 Hz, 2H), 7.32 (d, *J* = 7.8 Hz, 2H), 7.17 (t, *J* = 7.7 Hz, 1H), 7.11 (d, *J* = 7.4 Hz, 1H), 6.94 (t, *J* = 7.4 Hz, 1H), 4.65 (s, 1H), 3.23 (d, *J* = 13.2 Hz, 1H), 3.15 (dd, *J* = 16.2, 9.4 Hz, 1H), 2.77 – 2.63 (m, 2H), 1.57 (s, 9H).^{13}C NMR (101 MHz, $CDCl_3$) δ 152.2, 143.6, 141.7, 132.3, 130.4, 129.6, 127.7, 125.1, 122.8, 119.0, 115.5, 110.5, 81.4, 60.1, 40.5, 32.7, 28.5. HRMS (ESI+) (m/z): $[M+H]^+$ calcd. for $C_{21}H_{22}N_2O_2$, 335.1760; found: 335.1750.

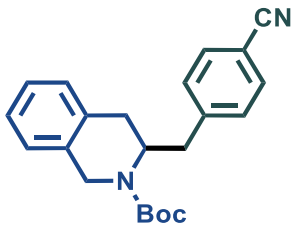

***tert*-Butyl-3-(4-cyanobenzyl)-3,4-dihydroisoquinoline-2(1H)-carboxylate (3.32).**

Prepared according to GP3 from **3.1ac** (127 mg, 0.3 mmol, 1.0 equiv.) and **3.2b** (106 mg, 0.3 mmol, 1.0 equiv.). Purified via flash column chromatography on silica gel (gradient from Pentane:Ethyl Acetate 100:0 to 80:20) to afford the product (mixture of rotamers) as a white solid (56 mg, 54% yield).

3.32. ^{1}H NMR (400 MHz, $CDCl_3$) δ 7.60 – 7.53 (m, 2H), 7.30 – 7.07 (m, 6H), 4.86 – 4.49 (m, 2H), 4.34 (br t, *J* = 13.7 Hz, 1H), 3.00 (dd, *J* = 15.9, 5.5 Hz, 1H), 2.83 (dd, *J* = 13.4, 7.3 Hz, 1H), 2.64 – 2.52 (m, 2H), 1.47 – 1.37 (m, 9H). ^{13}C NMR (101 MHz, $CDCl_3$) δ 154.7 & 154.6 (rotameric signals), 144.6, 132.8, 132.6, 132.3, 130.1, 129.3 & 129.0 (rotameric signals), 127.0, 126.7, 126.5 & 126.3 (rotameric signals), 119.0, 110.3, 80.1, 51.7 & 50.1 (rotameric signals), 43.7 & 43.1 (rotameric signals), 39.1 & 38.5 (rotameric signals), 32.8 & 32.1 (rotameric signals), 28.4. HRMS (FD+) (m/z): $[M]^+$ calcd. for $C_{22}H_{24}N_2O_2$, 348.1838; found: 348.1835.

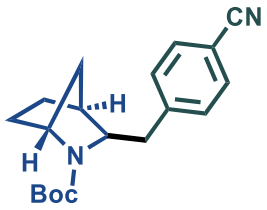

***tert*-Butyl (1R,4S)-3-(4-cyanobenzyl)-2-a0zabicyclo[2.2.1]heptane-2-carboxylate (3.33).**

Prepared according to GP3 from **3.1ad** (116 mg, 0.3 mmol, 1.0 equiv.) and **3.2b** (147 mg, 0.3 mmol, 1.0 equiv.). Purified via flash column chromatography on silica gel (from Pentane:Ethyl Acetate 20:1 to 10:1) to afford the two diastereomers as an inseparable mixture as a colorless oil (63 mg, 67% yield). *d.r.* ratio of **3.33** was determined via ^{1}H NMR to be 2.5:1.

3.33. ^{1}H NMR (400 MHz, $CDCl_3$) δ 7.61 – 7.52 (m, 2H), 7.34 & 7.27 (diastereomeric d, *J* = 7.9 Hz, 2H), 4.21 – 4.18 & 4.11 – 4.06 (diastereomeric m, 1H), 3.39 & 3.15 (diastereomeric dd, *J* = 13.2, 3.3 Hz, 1H), 3.30 – 3.22 (m, 1H), 2.50 – 2.40 (m, 1H), 2.21 – 2.14 (m, 1H), 1.83 – 1.52 (m, 4H), 1.49 & 1.47 (diastereomeric s, 9H), 1.28 – 1.19 (m, 2H). ^{13}C NMR (101 MHz, $CDCl_3$) δ 155.2 & 154.6 (diastereomeric signals), 145.2 & 145.1 (diastereomeric signals), 132.4 & 132.3 (diastereomeric signals), 130.3 & 130.1 (diastereomeric signals), 119.2 & 119.0 (diastereomeric signals), 110.3 & 110.1 (diastereomeric signals), 79.7 & 79.4 (diastereomeric signals), 65.7 & 65.6 (diastereomeric signals), 58.0 & 57.2 (diastereomeric signals), 40.7 & 40.1 (diastereomeric signals), 40.0 & 39.4 (diastereomeric signals), 34.7 & 33.9 (diastereomeric signals), 30.4 & 29.9 (diastereomeric signals), 28.7 & 28.7 (diastereomeric signals), 27.8 & 27.7(diastereomeric signals). HRMS (ESI+) (m/z): $[M+H]^+$ calcd. for $C_{19}H_{24}N_2O_2$, 313.1916; found: 313.1912.

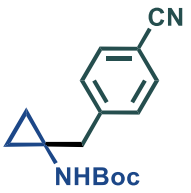

***tert*-Butyl (1-(4-cyanobenzyl)cyclopropyl)carbamate (3.34).**

Prepared according to GP3 from **3.1l** (104 mg, 0.3 mmol, 1.0 equiv.) and **3.2b** (106 mg, 0.3 mmol, 1.0 equiv.). Purified via flash column chromatography on silica gel

(from Pentane:Ethyl Acetate 40:1 to 15:1) to afford the product as a colorless oil (33 mg, 41% yield).

3.34. ^{1}H NMR (500 MHz, $CDCl_3$) δ 7.59 (d, *J* = 8.2 Hz, 2H), 7.29 (d, *J* = 8.0 Hz, 2H), 4.75 – 4.48 (m, 1H), 2.95 – 2.79 (m, 2H), 1.47 – 1.36 (m, 9H), 0.83 – 0.74 (m, 4H). ^{13}C NMR (126 MHz, $CDCl_3$) δ 155.5, 145.1, 132.2, 130.3, 119.1, 110.5, 79.7, 41.9, 34.1, 28.5, 13.8. HRMS (GC-FI+) (m/z): $[M+H]^+$ calcd. for $C_{16}H_{20}N_2O_2$, 272.1525; found: 272.1522.

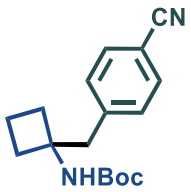

***tert*-Butyl (1-(4-cyanobenzyl)cyclobutyl)carbamate (3.35).** Prepared according to GP3 from **3.1m** (108 mg, 0.3 mmol, 1.0 equiv.) and **3.2b** (106 mg, 0.3 mmol, 1.0 equiv.). Purified via flash column chromatography on silica gel (gradient from Pentane:Ethyl Acetate 100:0 to 70:30) to afford the product as a white solid (27 mg, 31% yield).

3.35. ^{1}H NMR (400 MHz, $CDCl_3$) δ 7.57 (d, *J* = 8.20 Hz, 2H), 7.25 (d, *J* = 8.20 Hz, 2H), 4.46 (s, 1H), 3.29 – 3.03 (m, 2H), 2.22 – 2.09 (m, 2H), 2.09 – 1.92 (m, 3H), 1.92 – 1.77 (m, 1H), 1.46 (s, 9H). ^{13}C NMR (101 MHz, $CDCl_3$) δ 154.3, 144.1, 131.9, 130.9, 119.1, 110.3, 79.4, 56.9, 42.6, 33.1, 28.6, 15.1. HRMS (FI+) (m/z): $[M]^+$ calcd. for $C_{17}H_{22}N_2O_2$, 286.1681; found: 286.1676.

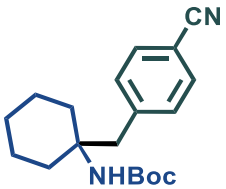

***tert*-Butyl (1-(4-cyanobenzyl)cyclohexyl)carbamate (3.36).**

Prepared according to GP3 from **3.1ae** (117 mg, 0.3 mmol, 1.0 equiv.) and **3.2b** (106 mg, 0.3 mmol, 1.0 equiv.). Purified via flash column chromatography on silica gel (gradient from Pentane:Ethyl Acetate 98:2 to 90:10) to afford the product as a white solid (34 mg, 36% yield).

3.36. ^{1}H NMR (400 MHz, $CDCl_3$) δ 7.57 – 7.50 (d, *J* = 8.1 Hz, 2H), 7.23 (d, *J* = 8.1 Hz, 2H), 4.05 (s, 1H), 3.05 (s, 2H), 1.89 (d, *J* = 12.1 Hz, 2H), 1.64 – 1.50 (m, 3H), 1.46 (s,

9H), 1.43 – 1.17 (m, 5H). ^{13}C NMR (101 MHz, $CDCl_3$) δ 154.5, 143.8, 131.6, 131.4, 119.2, 110.1, 79.1, 54.9, 44.3, 35.2, 28.6, 25.7, 21.5. HRMS (FD+) (m/z): $[M]^+$ calcd. for $C_{19}H_{26}N_2O_2$, 315.2073; found: 315.2065.

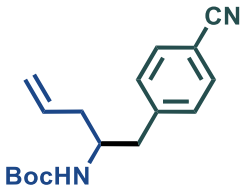

***tert*-Butyl (1-(4-cyanophenyl)pent-4-en-2-yl)carbamate (3.37).**

Prepared according to GP3 from **3.1af** (108 mg, 0.3 mmol, 1.0 equiv.) and **3.2b** (106 mg, 0.3 mmol, 1.0 equiv.). Purified via flash column chromatography on silica gel (from Pentane:Ethyl Acetate 30:1 to 10:1) to afford the product as a colorless oil (36 mg, 42% yield).

3.37. ^{1}H NMR (500 MHz, $CDCl_3$) δ 7.57 (d, *J* = 7.8 Hz, 2H), 7.30 (d, *J* = 7.8 Hz, 2H), 5.83 – 5.71 (m, 1H), 5.16 – 5.07 (m, 2H), 4.46 – 4.32 (m, 1H), 4.01 – 3.82 (m, 1H), 2.86 – 2.81 (m, 2H), 2.24 (dt, *J* = 13.3, 6.4 Hz, 1H), 2.13 (dt, *J* = 14.4, 7.3 Hz, 1H), 1.37 (s, 9H). ^{13}C NMR (126 MHz, $CDCl_3$) δ 155.3, 144.2, 133.9, 132.2, 130.3, 119.1, 118.7, 110.4, 79.6, 51.0, 41.0, 38.5, 28.4. HRMS (GC-FI+) (m/z): $[M+H]^+$ calcd. for $C_{17}H_{22}N_2O_2$, 286.1681; found: 286.1686.

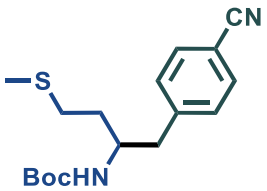

***tert*-Butyl (1-(4-cyanophenyl)-4-(methylthio)butan-2-yl)carbamate (3.38).**

Prepared according to GP3 from **3.1h** (118 mg, 0.3 mmol, 1.0 equiv.) and **3.2b** (106 mg, 0.3 mmol, 1.0 equiv.). Purified via flash column chromatography on silica gel (gradient from Pentane:Ethyl Acetate 100:0 to 70:30) to afford the product as a white solid (26 mg, 27% yield).

3.38. ^{1}H NMR (400 MHz, $CDCl_3$) δ 7.58 (d, *J* = 8.0 Hz, 2H), 7.30 (d, *J* = 8.0 Hz, 2H), 4.44 – 4.29 (m, 1H), 4.0 – 3.84 (br s, 1H), 2.85 (d, *J* = 6.8 Hz, 2H), 2.63 – 2.44 (m, 2H), 2.06 (s, 3H), 1.84 – 1.71 (m, 1H), 1.71 – 1.57 (m, 1H), 1.38 (s, 9H). ^{13}C NMR (101 MHz, $CDCl_3$) δ 155.4, 144.0, 132.3, 130.3, 119.0, 110.5, 79.7, 51.1, 41.9, 34.2, 30.9, 28.4, 15.8. HRMS (FD+) (m/z): $[M]^+$ calcd. for $C_{17}H_{24}N_2O_2S$, 320.1558; found: 320.1547.

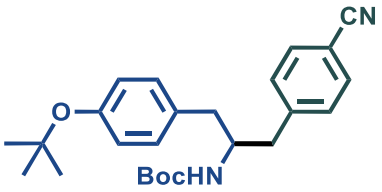

***tert*-Butyl (1-(4-(*tert*-butoxy)phenyl)-3-(4-cyanophenyl)propan-2-yl)carbamate (3.39).**

Prepared according to GP3 from **3.1e** (145 mg, 0.3 mmol, 1.0 equiv.) and **3.2b** (106 mg, 0.3 mmol, 1.0 equiv.). Purified via flash column chromatography on silica gel (Pentane:Ethyl Acetate 10:1) to afford the product as a colorless oil (75 mg, 61% yield).

3.39. ^{1}H NMR (400 MHz, $CDCl_3$) δ 7.56 (d, *J* = 8.1 Hz, 2H), 7.27 (d, *J* = 8.3 Hz, 2H), 7.05 (d, *J* = 8.4 Hz, 2H), 6.92 (d, *J* = 8.4 Hz, 2H), 4.35 (s, 1H), 4.20 – 4.01 (m, 1H), 2.87 (dd, *J* = 13.8, 5.7 Hz, 1H), 2.73 (d, *J* = 6.4 Hz, 3H), 1.32 (s, 18H). ^{13}C NMR (101 MHz, $CDCl_3$) δ 155.2, 154.2, 144.4, 132.5, 132.2, 130.2, 129.8, 124.4, 119.1, 110.4, 79.5, 78.5, 52.6, 40.9, 40.2, 28.9, 28.4. HRMS (ESI+) (m/z): $[M+H]^+$ calcd. for $C_{25}H_{32}N_2O_3$, 409.2491; found: 409.2490.

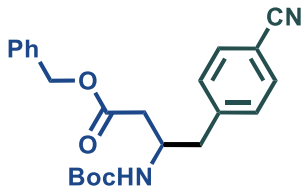

Benzyl 3-((*tert*-butoxycarbonyl)amino)-4-(4-cyanophenyl)butanoate (3.40).

Prepared according to GP3 from **3.1g** (140 mg, 0.3 mmol, 1.0 equiv.) and **3.2b** (106 mg, 0.3 mmol, 1.0 equiv.). Purified via flash column chromatography on silica gel (gradient from Cyclohexane:Ethyl Acetate 100:0 to 80:20) to afford the product as a white solid (67 mg, 57% yield).

3.40. ^{1}H NMR (400 MHz, $CDCl_3$) δ 7.54 (d, *J* = 8.1 Hz, 2H), 7.43 – 7.30 (m, 5H), 7.24 (d, *J* = 8.1 Hz, 2H), 5.24 – 5.00 (m, 3H), 4.24 – 4.06 (m, 1H), 2.95 (dd, *J* = 13.6, 7.4 Hz, 1H), 2.85 (dd, *J* = 13.4, 7.0 Hz, 1H), 2.58 (dd, *J* = 16.1, 5.5 Hz, 1H), 2.49 (dd, *J* = 16.1, 5.5 Hz, 1H), 1.37 (s, 9H). ^{13}C NMR (101 MHz, $CDCl_3$) δ 171.3, 155.1, 143.7, 135.6, 132.4, 130.2, 128.8, 128.7, 128.5, 119.0, 110.7, 79.8, 66.8, 48.6, 40.6, 37.9, 28.4. HRMS (ESI+) (m/z): $[M+H]^+$ calcd. for $C_{23}H_{26}N_2O_4$, 395.1971; found: 395.1995.

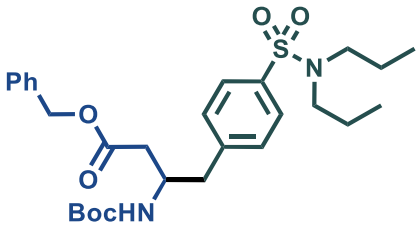

Benzyl 3-((*tert*-butoxycarbonyl)amino)-4-(4-(*N,N*-dipropylsulfamoyl) phenyl)butanoate (3.41).

Prepared according to GP3 from **3.1g** (141 mg, 0.3 mmol, 1.0 equiv.) and **3.2h** (147 mg, 0.3 mmol, 1.0 equiv.). Purified via flash column chromatography on silica gel (from Hexane:Ethyl Acetate 5:1 to 2:1) to afford the product as a colorless oil (72 mg, 45% yield).

3.41. ^{1}H NMR (400 MHz, $CDCl_3$) δ 7.69 (d, *J* = 8.1 Hz, 2H), 7.40 – 7.34 (m, 5H), 7.27 – 7.21 (m, 2H), 5.22 – 4.99 (m, 3H), 4.22 – 3.95 (m, 1H), 3.10 – 3.01 (m, 4H), 3.01 – 2.82 (m, 2H), 2.57 (dd, *J* = 16.1, 5.4 Hz, 1H), 2.48 (dd, *J* = 16.1, 5.6 Hz, 1H), 1.55 (dt, *J* = 15.1, 7.8 Hz, 4H), 1.39 (s, 9H), 0.86 (t, *J* = 7.4 Hz, 6H). ^{13}C NMR (101 MHz, $CDCl_3$) δ 171.4, 155.1, 142.8, 138.6, 135.7, 130.0, 128.8, 128.6, 128.5, 127.4, 79.7, 66.7, 50.2, 40.2, 37.8, 29.8, 28.5, 22.2, 11.3. HRMS (ESI+) (m/z): $[M+H]^+$ calcd. for $C_{28}H_{40}N_2O_6S$, 533.2685; found: 533.2671

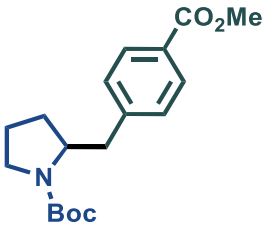

***tert*-Butyl 2-(4-(methoxycarbonyl)benzyl)pyrrolidine-1-carboxylate (3.42).**

Prepared according to GP3 from **3.1a** (108 mg, 0.3 mmol, 1.0 equiv.) and **3.2g** (116 mg, 0.3 mmol, 1.0 equiv.). Purified via flash column chromatography on silica gel (gradient from Pentane:Ethyl Acetate 98:2 to 90:10) to afford the product (mixture of rotamers) as a colorless oil (45 mg, 47% yield).

3.42. ^{1}H NMR (400 MHz, $CDCl_3$) δ 7.95 (d, *J* = 7.7 Hz, 2H), 7.25 (q, *J* = 7.5 Hz, 2H), 4.11 – 3.92 (m, 1H), 3.89 (s, 3H), 3.43 – 3.22 (m, 2H), 3.22 – 3.03 (m, 1H), 2.69 – 2.55 (m, 1H), 1.85 – 1.59 (m, 4H), 1.49 (s, 9H). ^{13}C NMR (101 MHz, $CDCl_3$) δ 167.2, 154.6, 144.8, 129.8 & 129.7 (rotameric signals), 129.7 & 129.5 (rotameric signals), 128.4 & 128.2 (rotameric signals), 79.6 & 79.3 (rotameric signals), 58.7 & 58.5 (rotameric

signals), 52.1, 46.9 & 46.4 (rotameric signals), 40.8 & 39.8 (rotameric signals), 29.8, 28.7, 23.6 & 22.8 (rotameric signals).

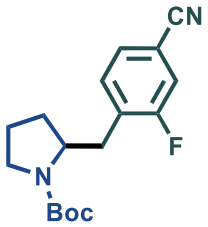

***tert*-Butyl 2-(4-cyano-2-fluorobenzyl)pyrrolidine-1-carboxylate (3.43).**

Prepared according to GP3 from **3.1a** (108 mg, 0.3 mmol, 1.0 equiv.) and **3.2f** (111 mg, 0.3 mmol, 1.0 equiv.). Purified via flash column chromatography on silica gel (gradient from Pentane:Ethyl Acetate 98:2 to 90:10) to afford the product (mixture of rotamers) as a white solid (50 mg, 55% yield).

3.43. ^{1}H NMR (300 MHz, $CDCl_3$) δ 7.56 – 7.30 (m, 2H), 7.18 – 7.06 (m, 1H), 4.07 – 3.80 (m, 1H), 3.53 – 3.16 (m, 2H), 3.04 (t, *J* = 15.8 Hz, 1H), 2.74 – 2.45 (m, 1H), 1.93 – 1.53 (m, 4H), 1.47 (s, 9H). ^{13}C NMR (75 MHz, $CDCl_3$) δ 162.0 (d, *J* = 257.7 Hz), 154.7, 136.4 (d, *J* = 3.8 Hz), 136.2, 134.0, 116.5, 114.1, 101.4, 79.8 &79.6 (rotameric signals), 58.5 & 58.4 (rotameric signals), 46.9 & 46.5 (rotameric signals), 39.6 & 38.7 (rotameric signals), 29.9 & 29.3 (rotameric signals), 28.7, 23.6 & 22.8 (rotameric signals). ^{19}F NMR (282 MHz, $CDCl_3$) δ -110.1 & -110.5 (rotameric signals). HRMS (ESI+) (m/z): $[M+H]^+$ calcd. for $C_{17}H_{21}FN_2O_2$, 305.1665; found: 305.1661.

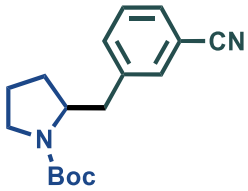

***tert*-Butyl 2-(3-cyanobenzyl)pyrrolidine-1-carboxylate (3.44).**

Prepared according to GP3 from **3.2a** (108 mg, 0.3 mmol, 1.0 equiv.) and **3.2e** (106 mg, 0.3 mmol, 1.0 equiv.). Purified via flash column chromatography on silica gel (gradient from Pentane:Ethyl Acetate 98:2 to 90:10) to afford the product (mixture of rotamers) as a pale yellow oil (43 mg, 50% yield).

3.44. ^{1}H NMR (400 MHz, $CDCl_3$) δ 7.58 – 7.30 (m, 4H), 4.05 – 3.83 (m, 1H), 3.47 – 3.18 (m, 2H), 3.17 – 2.95 (m, 1H), 2.72 – 2.50 (m, 1H), 1.86 – 1.53 (m, 4H), 1.47 (s, 9H). ^{13}C NMR (101 MHz, $CDCl_3$) δ 154.7 & 154.5 (rotameric signals), 140.8, 134.2 &

134.0 (rotameric signals), 133.1 & 132.9 (rotameric signals), 130.1, 129.4 & 129.2 (rotameric signals), 119.0, 112.6 & 112.4 (rotameric signals), 79.7 & 79.5 (rotameric signals), 58.6 & 58.3 (rotameric signals), 46.9 & 46.4 (rotameric signals), 40.4 & 39.4 (rotameric signals), 29.9 & 29.2 (rotameric signals), 28.7, 23.6 & 22.8 (rotameric signals).

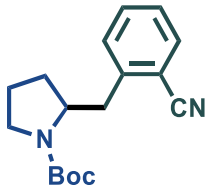

***tert*-Butyl 2-(2-cyanobenzyl)pyrrolidine-1-carboxylateacetate (3.45).**

Prepared according to GP3 from **3.1a** (108 mg, 0.3 mmol, 1.0 equiv.) and **3.2d** (106 mg, 0.3 mmol, 1.0 equiv.). Purified via flash column chromatography on silica gel (gradient from Pentane:Ethyl Acetate 98:2 to 90:10) to afford the product (mixture of rotamers) as a white solid (30 mg, 35% yield).

3.45. ^{1}H NMR (400 MHz, $CDCl_3$) δ 7.61 (t, *J* = 9.4 Hz, 1H), 7.52 (td, *J* = 7.6, 1.3 Hz, 1H), 7.48 – 7.27 (m, 2H), 4.16 – 4.06 (m, 1H), 3.49 – 3.05 (m, 3H), 2.94 (dd, *J* = 13.3, 8.3 Hz, 1H), 1.97 – 1.67 (m, 4H), 1.42 (rotameric s, 9H). ^{13}C NMR (101 MHz, $CDCl_3$) δ 154.7 & 154.6 (rotameric signals), 143.5 & 143.4 (rotameric signals), 132.9, 132.6, 130.8, 127.0 & 126.8 (rotameric signals), 118.4, 113.4 & 113.3 (rotameric signals), 79.6 & 79.3 (rotameric signals), 58.7 & 58.4 (rotameric signals), 46.8 & 46.3 (rotameric signals), 38.9 & 38.1 (rotameric signals), 30.3 & 29.4 (rotameric signals), 28.6, 23.7 & 22.8. (rotameric signals) HRMS (ESI+) (m/z): $[M+H]^+$ calcd. for $C_{17}H_{22}N_2O_2$, 287.1760; found: 287.1752.

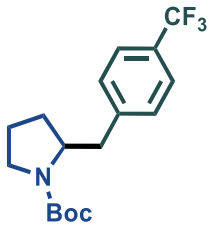

***tert*-Butyl 2-(4-(trifluoromethyl)benzyl)pyrrolidine-1-carboxylate (3.46).**

Prepared according to GP3 from **3.1a** (108 mg, 0.3 mmol, 1.0 equiv.) and **3.2c** (119 mg, 0.3 mmol, 1.0 equiv.). Purified via flash column chromatography on silica gel (Pentane:Ethyl Acetate 30:1) to afford the product as a colorless oil (46 mg, 47% yield).

3.46. ^{1}H NMR (400 MHz, $CDCl_3$) δ 7.53 (d, *J* = 8.0 Hz, 2H), 7.32 – 7.26 (m, 2H), 4.02 – 3.98 (m, 1H), 3.40 – 3.24 (m, 2H), 3.18 – 3.07 (m, 1H), 2.63 (dd, *J* = 13.0, 9.1 Hz, 1H), 1.87 – 1.60 (m, 4H), 1.49 (s, 9H). ^{13}C NMR (101 MHz, $CDCl_3$) δ 154.6, 143.5 (q, *J* = 2 Hz), 129.9, 128.7 (q, *J* = 33 Hz), 125.4 (q, *J* = 4 Hz), 124.4 (q, *J* = 273 Hz), 79.5, 58.6, 46.7, 40.4, 29.6, 28.7, 23.2. ^{19}F NMR (282 MHz, $CDCl_3$) δ -62.4.

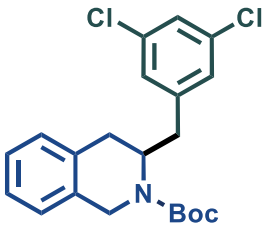

***tert*-Butyl 3-(3,5-dichlorobenzyl)-3,4-dihydroisoquinoline-2(1H)-carboxylate (3.47).**

Prepared according to GP3 from **3.1ac** (127 mg, 0.3 mmol, 1.0 equiv.) and **3.2j** (119 mg, 0.3 mmol, 1.0 equiv.). Purified via flash column chromatography on silica gel (Pentane:Ethyl Acetate 4:1) to afford the product with a minor impurity. Further purification via a second flash column chromatography on silica gel (Dichloromethane) yielded the pure product (mixture of rotamers) as a colorless oil (47 mg, 40% yield).

3.47. ^{1}H NMR (400 MHz, $CDCl_3$) δ 7.37 (s, 1H), 7.25 – 7.10 (m, 5H), 7.03 – 6.83 (m, 1H), 4.98 – 4.68 (m, 2H), 4.38 (d, *J* = 17.3 Hz, 1H), 3.07 (dd, *J* = 16.2, 5.6 Hz, 1H), 2.84 – 2.70 (m, 2H), 2.66 (dd, *J* = 15.9, 2.1 Hz, 1H), 1.47 – 1.26 (m, 9H). ^{13}C NMR (101 MHz, $CDCl_3$) δ 154.8, 135.4, 135.3, 133.1, 132.7, 132.3, 129.3, 127.1, 126.8, 126.6, 126.4, 80.0, 49.3 & 49.0 (rotameric signals), 43.6 & 42.9 (rotameric signals), 36.1 & 35.3 (rotameric signals), 33.5 & 32.6 (rotameric signals), 28.3. HRMS (ESI+) (m/z): $[M+H]^+$ calcd. for $C_{21}H_{23}Cl_2NO_2$, 392.1184; found: 392.1179.

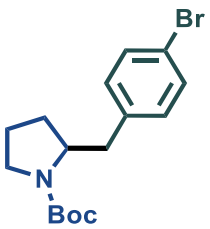

***tert*-Butyl 2-(4-bromobenzyl)pyrrolidine-1-carboxylate (3.48).**

Prepared according to GP3 from **3.1a** (108 mg, 0.3 mmol, 1.0 equiv.) and **3.2i** (119 mg, 0.3 mmol, 1.0 equiv.). Purified via flash column chromatography on silica gel (Pentane:Ethyl Acetate 40:1) to afford the product (mixture of rotamers) as a colorless oil (36 mg, 35% yield).

3.48. ^{1}H NMR (400 MHz, $CDCl_3$) δ 7.39 (d, *J* = 7.9 Hz, 2H), 7.10 – 6.99 (m, 2H), 4.03 – 3.88 (m, 1H), 3.43 – 3.22 (m, 2H), 3.15 – 2.91 (m, 1H), 2.52 (d, *J* = 12.3 Hz, 1H), 1.84 – 1.61 (m, 4H), 1.49 (s, 9H). ^{13}C NMR (101 MHz, $CDCl_3$) δ 154.6, 138.3, 131.6 & 131.4 (rotameric signals), 131.2, 120.2, 79.5 & 79.3 (rotameric signals), 58.7, 46.9 & 46.5 (rotameric signals), 40.1 & 39.1 (rotameric signals), 29.8, 28.7, 23.6 & 22.8 (rotameric signals).

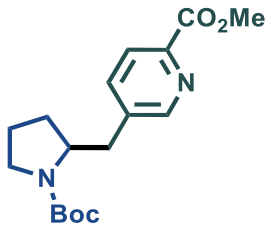

Methyl 6-((1-(*tert*-butoxycarbonyl)pyrrolidin-2-yl)methyl)nicotinate (3.49).

Prepared according to GP3 from **3.1a** (108 mg, 0.3 mmol, 1.0 equiv.) and **3.2k** (116 mg, 0.3 mmol, 1.0 equiv.). Purified via flash column chromatography on silica gel (Pentane:Ethyl Acetate 5:1) to afford the product (mixture of rotamers) as a colorless oil (60 mg, 62% yield).

3.49. ^{1}H NMR (500 MHz, $CDCl_3$) δ 8.51 (d, *J* = 9.7 Hz, 1H), 8.02 (d, *J* = 8.0 Hz, 1H), 7.68 – 7.53 (m, 1H), 4.05 – 3.86 (m, 4H), 3.41 – 3.13 (m, 2H), 3.13 – 3.00 (m, 1H), 2.85 – 2.58 (m, 1H), 1.84 – 1.50 (m, 4H), 1.44 (s, 9H). ^{13}C NMR (126 MHz, $CDCl_3$) δ 165.8, 154.7 & 154.4 (*rotameric signals*), 150.7, 146.1 & 146.0 (*rotameric signals*), 138.7, 138.1 & 137.7 (*rotameric signals*), 124.9, 79.7 & 79.5 (*rotameric signals*), 58.4 & 57.9 (*rotameric signals*), 52.9, 46.9 & 46.4 (*rotameric signals*), 38.0 & 36.7 (*rotameric signals*), 30.0 & 29.2 (*rotameric signals*), 28.6, 23.6 & 22.8 (*rotameric signals*). HRMS (GC-FI+) (m/z): $[M+H]^+$ calcd. for $C_{17}H_{24}N_2O_4$, 320.1736; found: 320.1734.

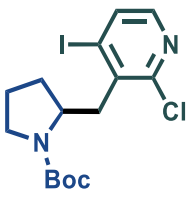

***tert*-Butyl 2-((2-chloro-4-iodopyridin-3-yl)methyl)pyrrolidine-1-carboxylate (3.50).**

Prepared according to GP3 from **3.1a** (108 mg, 0.3 mmol, 1.0 equiv.) and **3.2m** (147 mg, 0.3 mmol, 1.0 equiv.). Purified via flash column chromatography on silica gel (Pentane:Ethyl Acetate 3:1) to afford the product (mixture of rotamers) as a colorless oil (40 mg, 32% yield).

3.50. ^{1}H NMR (400 MHz, $CDCl_3$) δ 7.86 – 7.59 (m,2H), 4.58 – 4.42 (m, 1H), 3.54 – 3.17 (m, 3H), 3.05 – 2.90 (m, 1H), 2.19 – 2.02 (m, 1H), 1.99 – 1.81 (m, 2H), 1.73 – 1.63 (m, 1H), 1.32 – 1.15 (m, 9H). ^{13}C NMR (101 MHz, $CDCl_3$) δ 154.5, 151.1, 147.1, 137.4 & 137.0 (rotameric signals), 134.1, 114.1 & 113.7 (rotameric signals), 79.4, 55.2 & 54.8 (rotameric signals), 46.5, 42.9 & 42.5 (rotameric signals), 31.3, 28.3, 23.7 & 22.9 (rotameric signals). HRMS (ESI+) (m/z): $[M+H]^+$ calcd. for $C_{15}H_{20}ClIN_2O_2$, 422.0336; found: 422.0327.

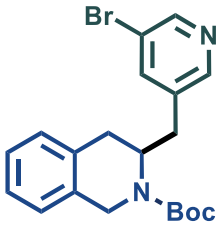

***tert*-Butyl 3-((5-bromopyridin-3-yl)methyl)-3,4-dihydroisoquinoline-2(1H)-carboxylate (3.51).**

Prepared according to GP3 from **3.1ac** (127 mg, 0.3 mmol, 1.0 equiv.) and **3.2o** (122 mg, 0.3 mmol, 1.0 equiv.). Purified via flash column chromatography on silica gel (gradient from Pentane:Ethyl Acetate 100:0 to 70:30) to afford the product (mixture of rotamers) as a white solid (50 mg, 41% yield).

3.51. ^{1}H NMR (400 MHz, $CDCl_3$) δ 8.52 (s, 1H), 8.29 – 8.21 (m, 1H), 7.77 – 7.50 (m, 1H), 7.25 – 7.19 (m, 2H), 7.19 – 7.08 (m, 2H), 4.88 – 4.49 (m, 2H), 4.32 (d, J = 17.0 Hz, 1H), 3.02 (d, J = 15.7 Hz, 1H), 2.73 (dd, J = 13.8, 7.4 Hz, 1H), 2.62 (dd, J = 15.9, 2.2 Hz, 1H), 2.56 – 2.46 (m, 1H), 1.46 – 1.39 (m, 9H). ^{13}C NMR (101 MHz, $CDCl_3$) δ 154.8 & 154.5 (rotameric signals), 149.0, 148.7, 139.3, 136.2 & 136.1 (rotameric signals), 132.8, 132.5 & 132.2 (rotameric signals), 129.3 & 129.0 (rotameric signals), 127.1, 126.8, 126.5 & 126.3 (rotameric signals), 120.7, 80.3, 51.5 & 49.9 (rotameric signals), 43.8 & 43.0 (rotameric signals), 35.8 & 35.1 (rotameric signals), 32.9 & 32.1

(rotameric signals), 28.5. HRMS (ESI+) (m/z): $[M+H]^+$ calcd. for $C_{20}H_{23}BrN_2O_2$, 405.1003; found: 405.1003.

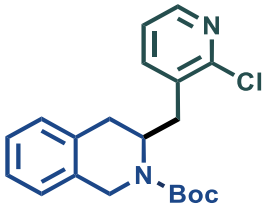

***tert*-Butyl 3-((2-chloropyridin-3-yl)methyl)-3,4-dihydroisoquinoline-2(1H)-carboxylate (3.52).**

Prepared according to GP3 from **3.1ac** (127 mg, 0.3 mmol, 1.0 equiv.) and **3.2h** (109 mg, 0.3 mmol, 1.0 equiv.). Purified via flash column chromatography on silica gel (Pentane:Ethyl Acetate 3:1) to afford the product (mixture of rotamers) as a colorless oil (54 mg, 50% yield).

3.52. ^{1}H NMR (400 MHz, $CDCl_3$) δ 8.35 – 8.21 (m, 1H), 7.57 – 7.28 (m, 1H), 7.25 – 7.10 (m, 5H), 4.98 – 4.64 (m, 2H), 4.37 (d, *J* = 17.3 Hz, 1H), 3.21 – 2.99 (m, 1H), 2.86 – 2.59 (m, 3H), 1.42 – 1.16 (m, 9H). ^{13}C NMR (101 MHz, $CDCl_3$) δ 154.8 & 154.5 (rotameric signals), 149.0, 148.7, 139.3, 136.2 & 136.1 (rotameric signals), 132.8, 132.5 & 132.2 (rotameric signals), 129.3 & 129.0 (rotameric signals), 127.1, 126.8, 126.5 & 126.3 (rotameric signals), 120.7, 80.3, 51.5 & 49.9 (rotameric signals), 43.8 & 43.0 (rotameric signals), 35.8 & 35.1 (rotameric signals), 32.9 & 32.1 (rotameric signals), 28.5. HRMS (ESI+) (m/z): $[M+H]^+$ calcd. for $C_{20}H_{23}ClN_2O_2$, 359.1521; found: 359.1516.

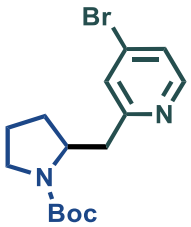

***tert*-Butyl 2-((4-bromopyridin-2-yl)methyl)pyrrolidine-1-carboxylate (3.53).**

Prepared according to GP3 from **3.1a** (108 mg, 0.3 mmol, 1.0 equiv.) and **3.2l** (122 mg, 0.3 mmol, 1.0 equiv.). Purified via flash column chromatography on silica gel

(from Pentane:Ethyl Acetate 10:1 to 2:1) to afford the product (mixture of rotamers) as a colorless oil (49 mg, 48% yield).

3.53. ^{1}H NMR (400 MHz, $CDCl_3$) δ 8.31 (d, *J* = 5.4 Hz, 1H), 7.47 – 7.27 (m, 1H), 4.12 (dd, *J* = 9.1, 4.7 Hz, 1H), 3.53 – 3.12 (m, 4H), 2.90 – 2.67 (m, 1H), 1.86 – 1.70 (m, 4H), 1.46 (s, 9H). ^{13}C NMR (101 MHz, $CDCl_3$) δ 161.3, 154.6, 150.0, 133.0, 127.2, 124.8, 79.4, 57.8, 46.9, 42.9 & 41.8 (*rotameric signals*), 30.3 & 29.4 (*rotameric signals*), 28.7, 23.6 & 22.9 (*rotameric signals*). HRMS (ESI+) (m/z): $[M+H]^+$ calcd. for $C_{15}H_{21}BrN_2O_2$, 265.1916; found: 165.1914.

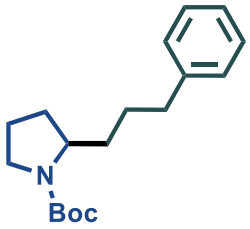

***tert*-Butyl 2-(3-phenylpropyl)pyrrolidine-1-carboxylate (3.54).**

Prepared according to GP3 from **3.1a** (216 mg, 0.6 mmol, 2.0 equiv.) and **3.2p** (107 mg, 0.3 mmol, 1.0 equiv.). Purified via flash column chromatography on silica gel (Pentane:Ethyl Acetate10:1) to afford the product (mixture of rotamers) as a colorless oil (43 mg, 50% yield).

3.54. ^{1}H NMR (400 MHz, $CDCl_3$) δ 7.31 – 7.23 (m, 2H), 7.21 – 7.13 (m, 3H), 3.70 (s, 1H), 3.48 – 3.17 (m, 2H), 2.62 (q, *J* = 9.8 Hz, 2H), 1.93 – 1.70 (m, 4H), 1.66 – 1.52 (m, 3H), 1.52 – 1.31 (m, 10H). ^{13}C NMR (101 MHz, $CDCl_3$) δ 154.8, 142.8 & 142.5 (rotameric signals), 128.5, 128.4, 125.8, 79.0, 57.3, 46.6 & 46.2 (rotameric signals), 36.1, 34.5 & 34.1 (rotameric signals), 30.8 & 29.8 (rotameric signals), 28.7, 28.2, 23.9 & 23.2(rotameric signals).

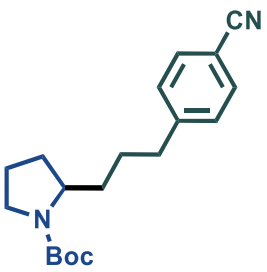

***tert*-Butyl 2-(3-(4-cyanophenyl)propyl)pyrrolidine-1-carboxylate (3.55).**

Prepared according to GP3 from **3.1a** (216 mg, 0.6 mmol, 2.0 equiv.) and **3.2q** (114 mg, 0.3 mmol, 1.0 equiv.). Purified via flash column chromatography on silica gel (gradient from Pentane:Ethyl Acetate 90:10 to 70:30) to afford the product (mixture of rotamers) as a colorless oil (38 mg, 40% yield).

3.55. ^{1}H NMR (300 MHz, $CDCl_3$) δ 7.55 (d, J = 7.9 Hz, 2H), 7.26 (d, J = 8.0 Hz, 2H), 3.89 – 3.58 (m, 1H), 3.48 – 3.18 (m, 2H), 2.76 – 2.60 (m, 2H), 1.99 – 1.71 (m, 4H), 1.65 – 1.50 (m, 3H), 1.49 – 1.29 (m, 10H). ^{13}C NMR (101 MHz, $CDCl_3$) δ 154.8, 148.5 &148.2 (rotameric signals), 132.2, 129.3, 119.2, 109.7, 79.1, 57.1, 46.5 & 46.2 (rotameric signals), 36.2, 34.3 & 34.0 (rotameric signals), 30.9 & 30.1 (rotameric signals), 28.6, 28.0 & 27.7 (rotameric signals), 23.9 & 23.2 (rotameric signals). HRMS (ESI+) (m/z): $[M+H]^+$ calcd. for $C_{19}H_{26}N_2O_2$, 314.1994; found: 314.2003.

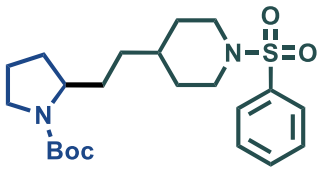

***tert*-Butyl 2-(2-(1-(phenylsulfonyl)piperidin-4-yl)ethyl)pyrrolidine-1-carboxylate (3.56).**

Prepared according to GP3 from **3.1a** (216 mg, 0.6 mmol, 2.0 equiv.) and **3.2r** (147 mg, 0.3 mmol, 1.0 equiv.). Purified via flash column chromatography on silica gel (gradient from Pentane:Ethyl Acetate 10:1 to 4:1) to afford the product as a pale yellow solid (48 mg, 38% yield).

3.56. ^{1}H NMR (400 MHz, $CDCl_3$) δ 7.78 – 7.70 (m, 2H), 7.61 – 7.55 (m, 1H), 7.51 (dd, *J* = 8.3, 6.6 Hz, 2H), 3.83 – 3.55 (m, 3H), 3.44 – 3.17 (m, 2H), 2.21 (td, *J* = 11.8, 2.6 Hz, 2H), 1.97 – 1.50 (m, 7H), 1.42 (s, 9H), 1.34 – 1.04 (m, 6H). ^{13}C NMR (101 MHz, $CDCl_3$) δ 154.7, 136.3, 132.7, 129.0, 127.7, 79.0, 57.3, 46.6, 46.2, 35.2, 32.7, 31.8 & 31.5 (rotameric signals), 31.1 & 30.7 (rotameric signals), 29.9, 28.7, 23.9 & 23.2 (rotameric signals). HRMS (ESI+) (m/z): $[M+H]^+$ calcd. for $C_{22}H_{34}N_2O_4S$, 423.2318; found: 423.2315.

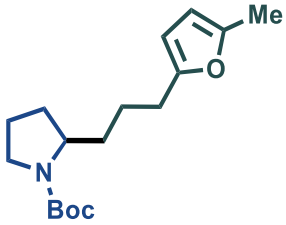

***tert*-Butyl 2-(3-(5-methylfuran-2-yl)propyl)pyrrolidine-1-carboxylate (3.57).**

Prepared according to GP3 from **3.1a** (216 mg, 0.6 mmol, 2.0 equiv.) and **3.2s** (108 mg, 0.3 mmol, 1.0 equiv.). Purified via flash column chromatography on silica gel (from Hexane:Ethyl Acetate 30:1 to 10:1) to afford the product as a colorless oil (26 mg, 30% yield).

3.57. ^{1}H NMR (400 MHz, $CDCl_3$) δ 5.83 (s, 2H), 3.85 – 3.67 (m, 1H), 3.40 – 3.22 (m, 2H), 2.57 (q, *J* = 6.9 Hz, 2H), 2.24 (s, 3H), 1.94 – 1.72 (m, 3H), 1.68 – 1.54 (m, 4H), 1.44 (s, 9H), 1.41 – 1.24 (m, 1H). ^{13}C NMR (101 MHz, $CDCl_3$) δ 154.8, 154.5, 150.3, 105.9, 105.4, 79.0, 57.2, 46.3, 34.3, 30.8, 28.7, 28.2, 25.2, 23.3, 13.6. HRMS (ESI+) (m/z): $[M+H]^+$ calcd. for $C_{17}H_{27}NO_3$, 294.2069; found: 294.2067

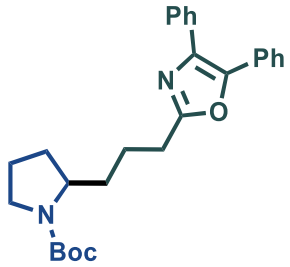

***tert*-Butyl 2-(3-(4,5-diphenyloxazol-2-yl)propyl)pyrrolidine-1-carboxylate (3.58).**

Prepared according to GP3 from **3.1a** (216 mg, 0.6 mmol, 1.0 equiv.) and **3.2t** (150 mg, 0.3 mmol, 1.0 equiv.). Purified via flash column chromatography on silica gel (gradient from Pentane:Ethyl Acetate 20:1 to 4:10) to afford the product (mixture of rotamers) as a colorless oil (28 mg, 22% yield).

3.58. ^{1}H NMR (400 MHz, $CDCl_3$) δ 7.66 – 7.60 (m, 2H), 7.60 – 7.54 (m, 2H), 7.42 – 7.26 (m, 6H), 3.93 – 3.67 (m, 1H), 3.48 – 3.23 (m, 2H), 2.92 – 2.78 (m, 2H), 2.04 – 1.75 (m, 6H), 1.75 – 1.65 (m, 1H), 1.51 – 1.35 (m, 10H). ^{13}C NMR (101 MHz, $CDCl_3$) δ 163.5, 154.8, 145.3, 135.2, 132.7, 129.3, 128.7, 128.7, 128.5, 128.1, 128.1, 126.6, 79.2 & 79.1 (rotameric signals), 57.1, 46.4, 34.5 & 34.0 (rotameric signals), 30.9, 28.7, 28.4, 24.2, 23.0. HRMS (ESI+) (m/z): $[M+H]^+$ calcd. for $C_{27}H_{32}N_2O_3$, 433.2491; found: 433.2493.

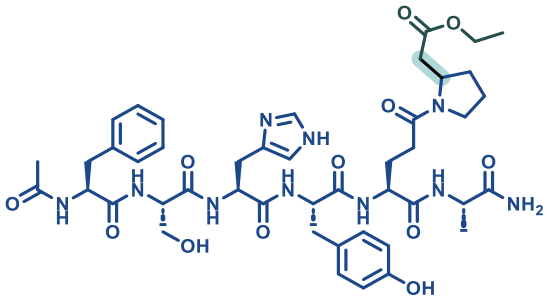

Peptide 3.59.

3.59 was prepared on a 30 µmol scale from resin-bound substrate **3.P1** following general procedure 3.6 for the synthesis of the corresponding RAE on resin, and P3.7 for the photocatalytic alkylation step and the thermal cleavage of the alkylated sulfonylhydrazide. After cleavage from the resin and ether precipitation, the crude peptide was purified by reverse phase HPLC (Shimadzu Preparative LCMS Nexera LC-40), (solvent system: A: MeCN and B: 5% TFA in H_2O), (20% B for 5 min, 20% to 60% B gradient over 16 min) and lyophilized to afford peptide **3.59** as a fluffy white solid (7.8 mg, 28% yield calculated from the original resin loading).

3.59. HRMS (ESI+) (m/z): $[M+2H]^{2+}$ calcd. for $C_{45}H_{62}N_{10}O_{12}$, 467.2274; found: 467.2274.

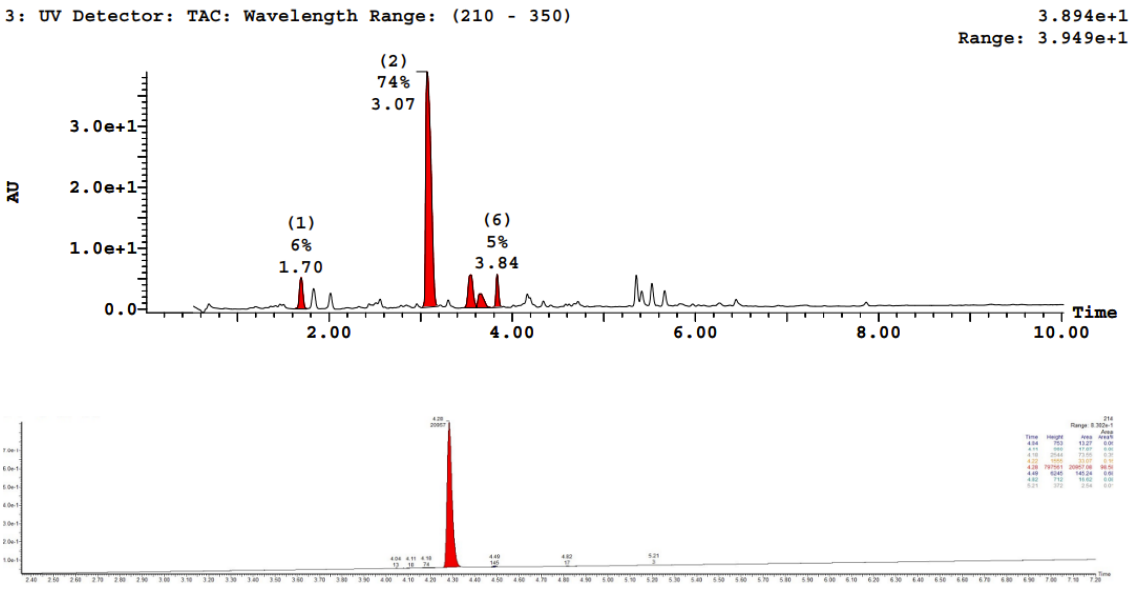

Figure ES3.10. Up: UPLC-MS Trace of the crude reaction mixture (product **3.59**) after full cleavage. Conditions: (10 to 50 % B over 10 min). Down: UPLC-MS Trace of the product 3.**59** after purification. Conditions: (10% MeCN 1 min; 10-60% 1-9 min; 60-95% 9-10 min).

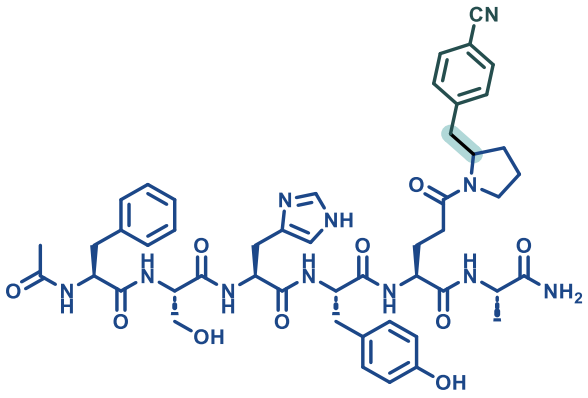

Peptide 3.60

3.60 was prepared on a 30 µmol scale from resin-bound substrate **3.P1** following general procedure 3.6 for the synthesis of the corresponding RAE on resin, and 3.7 for the photocatalytic alkylation step and the thermal cleavage of the alkylated sulfonylhydrazide. After cleavage from the resin and ether precipitation, the crude peptide was purified by reverse phase HPLC (Shimadzu Preparative LCMS Nexera LC-40), (solvent system: A: MeCN and B: 5% TFA in H_2O), (25% B for 5 min, 25% to 65% B gradient over 16 min) and lyophilized to afford peptide **3.60** as a fluffy white solid (6.1 mg, 21% yield calculated from the original resin loading).

3.60. HRMS (ESI+) (m/z): $[M+2H]^{2+}$ calcd. for $C_{49}H_{59}N_{11}O_{10}$, 481.7301; found: 481.7306.

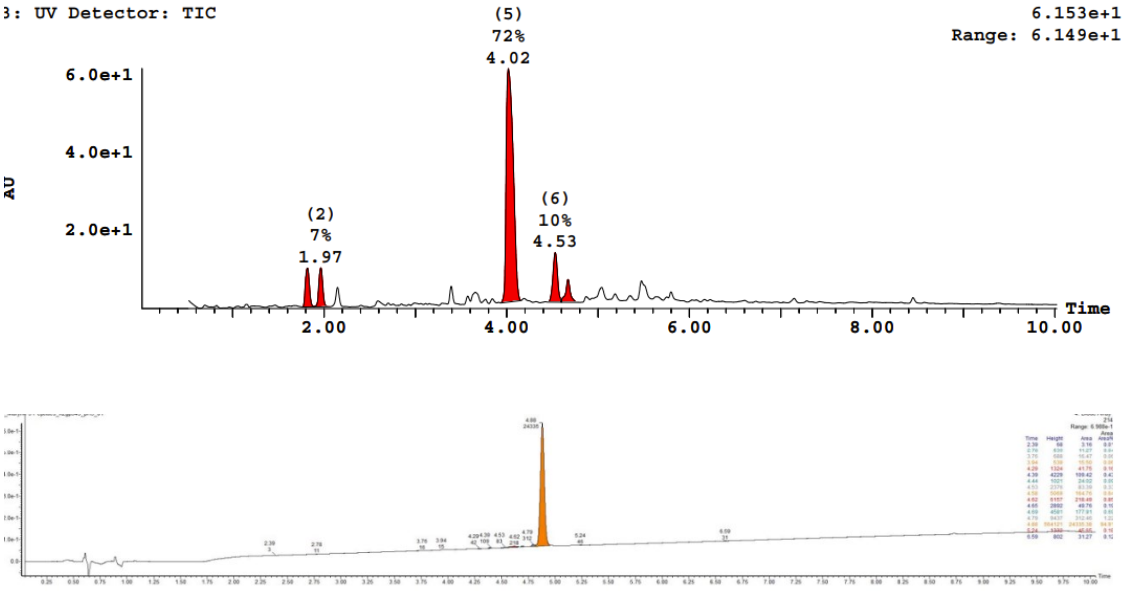

Figure ES3.11: Up: UPLC-MS Trace of the crude reaction mixture (product **3.60**) after full cleavage. Conditions: (10 to 50 % B over 10 min). Down: UPLC-MS Trace of the product **3.60** after purification. Conditions: (10% MeCN 1 min; 10-60% 1-9 min; 60-95% 9-10 min).

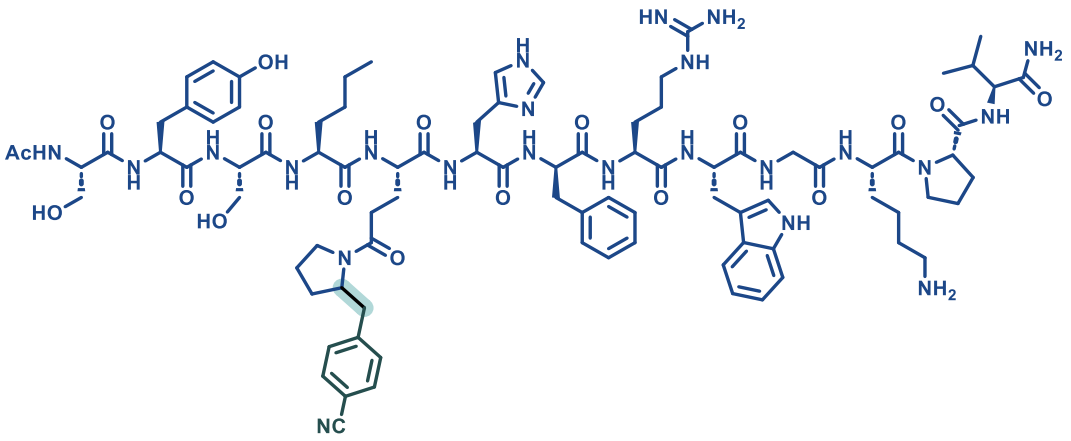

Peptide 3.61.

3.61 was prepared on a 30 µmol scale from resin-bound substrate **3.P2** following general procedure 3.6 for the synthesis of the corresponding RAE on resin and 3.7 for the photocatalytic alkylation step and thermal cleavage of the alkylated sulfonylhydrazide. After cleavage from the resin and ether precipitation, the crude peptide was purified by reverse phase HPLC (Shimadzu Preparative LCMS Nexera LC-40), (solvent system: A: MeCN and B: 5% TFA in H_2O), (25% B for 5 min, 25% to 75% B gradient over 16 min) and lyophilized to afford peptide **3.61** as a fluffy white solid (4.9 mg, 9% yield calculated from the original resin loading).

3.61. HRMS (ESI+) (m/z): $[M+3H]^{3+}$ calcd. for $C_{90}H_{123}N_{23}O_{18}$, 605.6550; found: 605.6567.

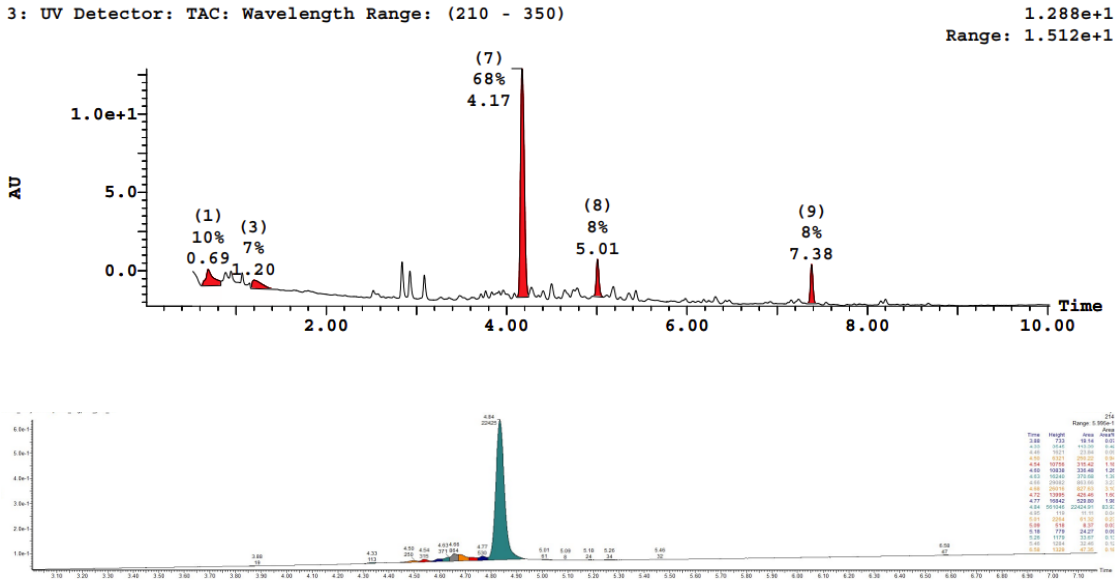

Figure 3.12: Up: UPLC-MS Trace of the crude reaction mixture (product **3.61**) after full cleavage. Conditions: (10 to 50 % B over 10 min). Down: UPLC-MS Trace of the product **3.61** after purification. Conditions: (10% MeCN 1min; 10-60% 1-9 min; 60-95% 9-10 min).

3.6 References.

1) Wei, W., Cherukupalli, S., Jing, L., Liu, X. & Zhan, P. Fsp3: A new parameter for drug-likeness. *Drug Discov Today,* **2020**, *25*, 1839–1845.
2) Lovering, F., Bikker, J. & Humblet, C. Escape from Flatland: Increasing Saturation as an Approach to Improving Clinical Success. *J. Med. Chem.* **2009**, *52*, 6752–6756.
3) Clemons, P. A. *et al.* Small molecules of different origins have distinct distributions of structural complexity that correlate with protein-binding profiles. *Proc. Natl. Acad. Sci.* **2010***, 107*, 18787–18792.
4) Brown, D. G. & Boström, J. Analysis of Past and Present Synthetic Methodologies on Medicinal Chemistry: Where Have All the New Reactions Gone? *J. Med. Chem.* **2016**, *59*, 4443–4458.
5) Tasker, S. Z., Standley, E. A. & Jamison, T. F. Recent advances in homogeneous nickel catalysis. *Nature,* **2014***, 509*, 299–309.
6) Choi, J. & Fu, G. C. Transition metal–catalyzed alkyl-alkyl bond formation: Another dimension in cross-coupling chemistry. *Science,* **2017***, 356,* eaaf7230.
7) Blakemore, D. C. *et al.* Organic synthesis provides opportunities to transform drug discovery. *Nat. Chem.* **2018**, *10*, 383–394.
8) Zhang, B. *et al.* Ni-electrocatalytic Csp^3–Csp^3 doubly decarboxylative coupling. *Nature,* **2022***, 606*, 313–318.
9) Hioki, Y. *et al.* Overcoming the limitations of Kolbe coupling with waveform-controlled electrosynthesis. *Science,* **2023**, *380*, 81–87.
10) Johnston, C. P., Smith, R. T., Allmendinger, S. & MacMillan, D. W. C. Metallaphotoredox-catalysed sp^3–sp^3 cross-coupling of carboxylic acids with alkyl halides. *Nature,* **2016**, *536*, 322–325.
11) Smith, R. T. *et al.* Metallaphotoredox-Catalyzed Cross-Electrophile Csp^3 –Csp^3 Coupling of Aliphatic Bromides. *J. Am. Chem. Soc.* **2018**, *140*, 17433–17438.
12) Liu, W., Lavagnino, M. N., Gould, C. A., Alcázar, J. & MacMillan, D. W. C. A biomimetic S_H2 cross-coupling mechanism for quaternary sp^3-carbon formation. *Science* **2021***, 374*, 1258–1263 (2021).
13) Lyon, W. L. & MacMillan, D. W. C. Expedient Access to Underexplored Chemical Space: Deoxygenative $C(sp^3)$–$C(sp^3)$ Cross-Coupling. *J. Am. Chem. Soc.* **145**, 7736–7742 (2023).

14) Kang, K. & Weix, D. J. Nickel-Catalyzed C(sp^3)–C(sp^3) Cross-Electrophile Coupling of In Situ Generated NHP Esters with Unactivated Alkyl Bromides. *Org. Lett.* **2022**, *24*, 2853–2857.

15) Douthwaite, J. L. *et al.* Formal Cross-Coupling of Amines and Carboxylic Acids to Form sp^3–sp^2 Carbon–Carbon Bonds. *J. Am. Chem. Soc.* **2023**, ***145***, 10930–10937 (2023).

16) Sakai, H. A. & MacMillan, D. W. C. Nontraditional Fragment Couplings of Alcohols and Carboxylic Acids: C(sp^3)–C(sp^3) Cross-Coupling via Radical Sorting. *J. Am. Chem. Soc.* **2022**, *144*, 6185–6192.

17) Xiao, J., Li, Z. & Montgomery, J. Nickel-Catalyzed Decarboxylative Coupling of Redox-Active Esters with Aliphatic Aldehydes. *J. Am. Chem. Soc.* **2021**, *143*, 21234–21240.

18) Gao, Y. *et al.* Electrochemical Nozaki–Hiyama–Kishi Coupling: Scope, Applications, and Mechanism. *J. Am. Chem. Soc.* **2021**, *143*, 9478–9488.

19) Yang, Y. *et al.* Practical and Modular Construction of C(sp^3)-Rich Alkyl Boron Compounds. *J. Am. Chem. Soc.* **2021**, *143*, 471–480.

20) Liu, Z. *et al.* Silver-catalyzed site-selective C(sp^3)−H benzylation of ethers with N-triftosylhydrazones. *Nat. Commun.* **2022**, *13*.

21) Wang, H., Wang, S., George, V., Llorente, G. & König, B. Photo-Induced Homologation of Carbonyl Compounds for Iterative Syntheses. *Angew. Chem. Int. Ed.* **2022**, *134.*

22) Dao, H. T., Li, C., Michaudel, Q., Maxwell, B. D. & Baran, P. S. Hydromethylation of Unactivated Olefins. *J. Am. Chem. Soc.* **2015**, *137*, 8046–8049.

23) Saladrigas, M., Bonjoch, J. & Bradshaw, B. Iron hydride radical reductive alkylation of unactivated alkenes. *Org. Lett.* **2020**, *22*, 684–688.

24) Kim, S. Radical cyclization involving the evolution of nitrogen. *Pure Appl. Chem.* **1996**, *68*, 623–626.

25) Wang, S., Cheng, B.-Y., Sršen, M. & König, B. Umpolung Difunctionalization of Carbonyls via Visible-Light Photoredox Catalytic Radical-Carbanion Relay. *J. Am. Chem. Soc.* **2020**, *142*, 7524–7531.

26) Kinsella, A. G., Tibbetts, J. D., Stead, D. & Cresswell, A. J. *N* -tosylhydrazones as acceptors for nucleophilic alkyl radicals in photoredox catalysis: A short case study on possible side reactions. *Synth. Commun.* **2022**, *52*, 413–423.

27) Pulcinella, A., Bonciolini, S., Lukas, F., Sorato, A. & Noël, T. Photocatalytic Alkylation of C(sp^3)−H Bonds Using Sulfonylhydrazones. *Angew. Chem. Int. Ed.* **2023**, *62*, e202215374.

28) Merchant, R. R. & Lopez, J. A. A General C(sp ^{3})–C(sp ^{3}) Cross-Coupling of Benzyl Sulfonylhydrazones with Alkyl Boronic Acids. *Org. Lett.* **2020**, *22*, 2271–2275.

29) Okada, Keiji., Okamoto, Kazushige. & Oda, Masaji. A new and practical method of decarboxylation: photosensitized decarboxylation of N-acyloxyphthalimides via electron-transfer mechanism. *J. Am. Chem. Soc.* **1988**, *110*, 8736–8738.

30) Okada, K., Okamoto, K., Morita, N., Okubo, K. & Oda, M. Photosensitized decarboxylative Michael addition through N-(acyloxy)phthalimides via an electron-transfer mechanism. *J. Am. Chem. Soc.* **1991**, *113*, 9401–9402.

31) Parida, S. K. *et al.* Single Electron Transfer-Induced Redox Processes Involving N-(Acyloxy)phthalimides. *ACS Catal.* **2021**, *11*, 1640–1683.

32) Murarka, S. *N* -(Acyloxy)phthalimides as Redox-Active Esters in Cross-Coupling Reactions. *Adv. Synth. Catal.* **2018**, *360*, 1735–1753.

33) Noël, T. & Zysman-Colman, E. The promise and pitfalls of photocatalysis for organic synthesis. *Chem Catal.* **2022**, *2*, 468–476.

34) Podlech, J. & Seebach, D. The Arndt–Eistert Reaction in Peptide Chemistry: A Facile Access to Homopeptides. *Angew. Chem. Int. Ed. Engl.* **1995**, *34*, 471–472.

35) Winum, J.-Y., Kamal, M., Leydet, A., Roque, J.-P. & Montero, J.-L. Homologation of carboxylic acids by arndt-eistert reaction under ultrasonic waves. *Tetrahedron Lett.* **1996**, *37*, 1781–1782.

36) Marti, R. E., Bleicher, K. H. & Bair, K. W. Solid Phase Synthesis of β-Peptides via Arndt-Eistert Homologation of Fmoc-Protected Amino Acid Diazoketones. *Tetrahedron Lett.* **1997**, *38*, 6145–6148.

37) Bernardim, B., Hardman-Baldwin, A. M. & Burtoloso, A. C. B. LED lighting as a simple, inexpensive, and sustainable alternative for Wolff rearrangements. *RSC Adv.* **2015**, *5*, 13311–13314.

38) Mastronardi, F., Gutmann, B. & Oliver Kappe, C. Continuous flow generation and reactions of anhydrous diazomethane using a teflon AF-2400 tube-in-tube reactor. *Org. Lett.* **2013**, *15*, 5590–5593.

39) Katritzky, A. R., Zhang, S. & Fang, Y. BtCH_2TMS-Assisted Homologation of Carboxylic Acids: A Safe Alternative to the Arndt–Eistert Reaction. *Org. Lett.* **2000**, *2*, 3789–3791.

40) Kowalski, C. J., Haque, M. S. & Fields, K. W. Ester homologation via α-bromo α-keto dianion rearrangement. *J. Am. Chem. Soc.* **1985***, 107*, 1429–1430.

41) Kowalski, C. J. & Reddy, R. E. Ester homologation revisited: a reliable, higher yielding and better understood procedure. *J. Org. Chem.* **1991**, *57*, 7194–7208.

42) Derek, H. R., Barton Ching-Yuh, C. & Joseph, J. Cs. Homologation of acids via carbon radicals generated from the acyl derivatives of N-hydroxy-2-thiopyridone. (The two-carbon problem). *Tetrahedron Lett.* **1991**, *32*, 3309–3312.

43) Barton, D. H. R., Ching-Yuh, C. & Jaszberenyi, J. Cs. Homologation of carboxylic acids by improved methods based on radical chain chemistry of acyl derivatives of N-hydroxy-2-thiopyridone. *Tetrahedron Lett.* **1992**, *33*, 5013–5016.

44) Pozhydaiev, V., Muller, C., Moran, J. & Lebœuf, D. Catalytic Synthesis of β-(Hetero)arylethylamines: Modern Strategies and Advances. *Angew. Chem. Int. Ed.* **2023**, *62*.

45) Bunescu, A., Abdelhamid, Y. & Gaunt, M. J. Multicomponent alkene azidoarylation by anion-mediated dual catalysis. *Nature* **2021**, *598*, 597–603.

46) Noten, E. A., McAtee, R. C. & Stephenson, C. R. J. Catalytic intramolecular aminoarylation of unactivated alkenes with aryl sulfonamides. *Chem. Sci.* **2022**, *13*, 6942–6949.

47) Qin, T. *et al.* A general alkyl-alkyl cross-coupling enabled by redox-active esters and alkylzinc reagents. *Science* **2016***, 352*, 801–805.

48) Noisier, A. F. M. *et al.* Late-Stage Functionalization of Histidine in Unprotected Peptides. *Angew. Chem. Int. Ed.* **2019**, *58*, 19096–19102.

49) Twitty, J. C. *et al.* Diversifying Amino Acids and Peptides via Deaminative Reductive Cross-Couplings Leveraging High-Throughput Experimentation. *J. Am. Chem. Soc.* **2023***, 145*, 5684–5695.

50) Barluenga, J., Tomás-Gamasa, M., Aznar, F. & Valdés, C. Metal-free carbon-carbon bond-forming reductive coupling between boronic acids and tosylhydrazones. *Nat. Chem.* **2009**, *1*, 494–499.

51) Prier, C. K., Rankic, D. A. & MacMillan, D. W. C. Visible Light Photoredox Catalysis with Transition Metal Complexes: Applications in Organic Synthesis. *Chem. Rev.* **2013***, 113*, 5322–5363.

52) Romero, N. A. & Nicewicz, D. A. Organic Photoredox Catalysis. *Chem. Rev.* **2016,** *116*, 10075–10166.

53) Kammer, L. M., Badir, S. O., Hu, R.-M. & Molander, G. A. Photoactive electron donor–acceptor complex platform for Ni-mediated $C(sp^3)$–$C(sp^2)$ bond formation. *Chem. Sci.* **2021**, *12*, 5450–5457.

54) Crisenza, G. E. M., Mazzarella, D. & Melchiorre, P. Synthetic Methods Driven by the Photoactivity of Electron Donor–Acceptor Complexes. *J. Am. Chem. Soc.* **2020***, 142*, 5461–5476.

55) Zhang, Y., Yin, Z. & Wu, X.-F. Copper-Catalyzed Carbonylative Synthesis of β-Homoprolines from *N*-Fluoro-sulfonamides. *Org. Lett.* **2020**, *22*, 1889–1893.

56) Vitaku, E., Smith, D. T. & Njardarson, J. T. Analysis of the Structural Diversity, Substitution Patterns, and Frequency of Nitrogen Heterocycles among U.S. FDA Approved Pharmaceuticals. *J. Med. Chem.* **2014**, *57*, 10257–10274.

57) White, A. M., Palombi, I. R. & Malins, L. R. Umpolung strategies for the functionalization of peptides and proteins. *Chem. Sci.* **2022**, *13*, 2809–2823.

58) Mackay, A. S., Payne, R. J. & Malins, L. R. Electrochemistry for the Chemoselective Modification of Peptides and Proteins. *J. Am. Chem. Soc.* **2021***, 144*, 23–41.

59) Qin, T. *et al.* Nickel-Catalyzed Barton Decarboxylation and Giese Reactions: A Practical Take on Classic Transforms. *Angew. Chem. Int. Ed.* **2017**, *129*, 266–271.

60) Pal, S., Openy, J., Krzyzanowski, A., Noisier, A. & 't Hart, P. On-Resin Photochemical Decarboxylative Arylation of Peptides. *Org. Lett.* **2023,** DOI:10.1021/acs.orglett.3c03070.

61) Langendonk, J. G. *et al.* Afamelanotide for Erythropoietic Protoporphyria. *N. Engl. J. Med.* **2015***, 373*, 48–59.

62) Buzzetti, L., Crisenza, G. E. M. & Melchiorre, P. Mechanistic Studies in Photocatalysis. *Angew. Chem. Int. Ed.* **2019***, 58*, 3730–3747.

63) Xu, R., Xu, T., Yang, M., Cao, T. & Liao, S. A rapid access to aliphatic sulfonyl fluorides. *Nat. Commun.* **2019**, *10*.

64) Zhang, M., Yu, M., Wang, Z., Liu, Y. & Wang, Q. Rapid Access to Aliphatic Sulfonamides. *Org. Lett.* **2022**, *24*, 3932–3937.

65) Pratsch, G., Lackner, G. L. & Overman, L. E. Constructing Quaternary Carbons from N -(Acyloxy)phthalimide Precursors of Tertiary Radicals Using Visible-Light Photocatalysis. *J. Org. Chem.* **2015**, *80*, 6025–6036.

66) Lackner, G. L., Quasdorf, K. W., Pratsch, G. & Overman, L. E. Fragment Coupling and the Construction of Quaternary Carbons Using Tertiary Radicals Generated from tert -Alkyl N -Phthalimidoyl Oxalates by Visible-Light Photocatalysis. *J. Org. Chem.* **2015**, *80*, 6012–6024.

67) Schwarz, J. & König, B. Metal-free, visible-light-mediated, decarboxylative alkylation of biomass-derived compounds. *Green Chem.* **2016**, *18*, 4743–4749.

68) Capaldo, L., Wen, Z. & Noël, T. A field guide to flow chemistry for synthetic organic chemists. *Chem. Sci.* **2023**, *14*, 4230–4247.

69) Capaldo, L., Bonciolini, S., Pulcinella, A., Nuño, M. & Noël, T. Modular allylation of C(sp^3)–H bonds by combining decatungstate photocatalysis and HWE olefination in flow. *Chem. Sci.* **2022**, *13*, 7325–7331.

70) Mazzarella, D., Pulcinella, A., Bovy, L., Broersma, R. & Noël, T. Rapid and Direct Photocatalytic C(sp^3)−H Acylation and Arylation in Flow. *Angew. Chem. Int. Ed.* **2021**, *60*, 21277–21282.

71) Garreau, M., Le Vaillant, F. & Waser, J. C-Terminal Bioconjugation of Peptides through Photoredox Catalyzed Decarboxylative Alkynylation. *Angew. Chem. Int. Ed.* **2019**, *58*, 8182–8186

72) Askey, H. E., Grayson, J. D., Tibbetts, J. D., Turner-Dore, J. C., Holmes, J. M., Kociok-Kohn, G., Wrigley, G. L. & Cresswell, A. J. Hydroaminoalkylation of Styrenes with Unprotected Primary Alkylamines. *J. Am. Chem. Soc.* **2021**, *143*, 15936–15945

73) Wang, Q. J. & May, A. Formation of β-Oxo-N-vinylimidates via Intermolecular Ester Incorporation in Huisgen Cyclization/Carbene Cascade Reactions *Org. Lett.* **2020**, *22*, 9579–9584.

74) Pulcinella, A., Bonciolini, S., Lukas, F., Sorato, A. & Noël, T. Alkylation of C(sp^3)-H Bonds Using Sulfonylhydrazones. *Angew. Chem. Int. Ed.* **2023**, *62*, e202215374.

Chapter 4

Alkyl Radical Generation via C–C Bond Cleavage in 2-Substituted Oxazolidines

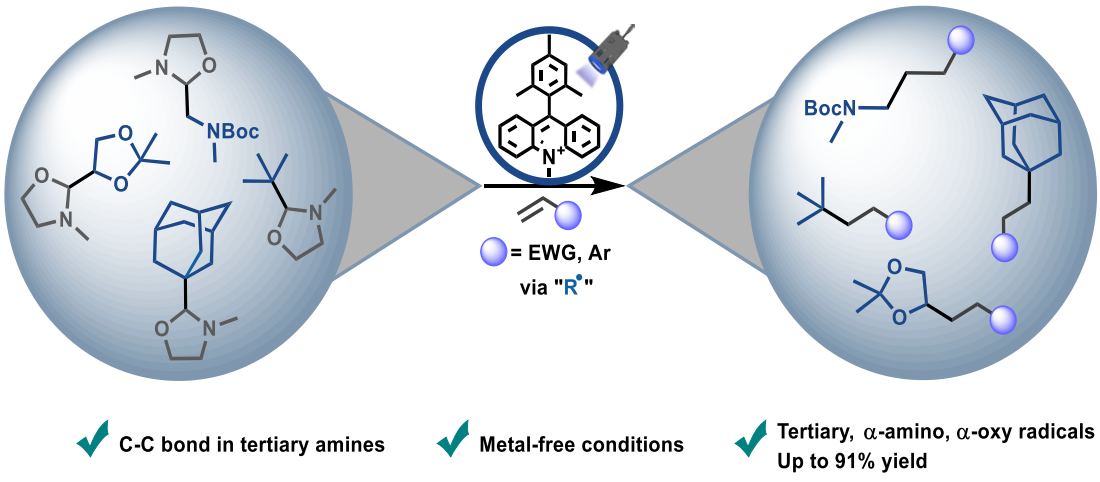

This chapter is based on:

Luguera Ruiz, A., La Mantia, M, Merli, D., Protti, S., Fagnoni, M. Alkyl Radical Generation via C–C Bond Cleavage in 2-Substituted Oxazolidines. *ACS Catal*. **2022**, *12*, 12469–12476. Highlighted in: List, B., Singh, V. K. *Synfacts.* **2022**, *18*, 1358.

4.1 Introduction.

The photochemical/photocatalyzed approach is nowadays the elective method for the generation of ground-state reactive intermediates[1] including carbon radicals that can be generated in a mild way using photons as traceless reagents.[2] In particular, great attention has been given, in the last decade, to the formation of C(sp^3)–C(sp^3) bonds via the generation of alkyl radicals,[3] and several precursors have been devised[3a–l] under tin-free conditions.[3e] In most cases, the alkyl radical is tethered to an electroauxiliary group (EA)[4] that acts as an electron donor/acceptor moiety. Upon photocatalytic oxidation/reduction, an electrofugal/nucleofugal group ($EA^{+/-}$) is released with the concomitant formation of the alkyl radical (Figure 4.1a).[3e] A charged precursor is usually required to facilitate such electron transfer reactions. As shown in Figure 1b, both anionic (e.g., alkyl carboxylates,[5] alkyl sulfinates,[6] alkyl trifluoroborates,[7] bis-catecholato silicates,[8] and alkyl oxalates[9]) or cationic (e.g., Katritzsky's salt)[3g,10] derivatives have been tested.

Due to solubility concerns, however, charged radical precursors can be used only in a limited range of solvents. Curiously, the development of uncharged, easily available radical precursors prone to be oxidized under photocatalyzed conditions is less common. In fact, apart from the case of 1,4-dihydropyridine derivatives (e.g., **A**) that exhibits a low E_{ox} value (1.05 V vs SCE),[11] other neutral donors such as tetraalkyl stannanes (**B**),[12] tetraalkyl silanes (**C**),[13] or 2,2-dialkyl 1,3-dioxolanes (**D**)[14] can be activated only under quite prohibitive conditions (E_{ox} up to 2.7 V vs SCE, Figure 4.1c).

The available literature points out that one of the elective classes for the design of new uncharged electron donors is certainly that of tertiary amines (E_{ox} = 0.83 V vs SCE for triethylamine).[5] Formerly, such a class of compounds has been largely employed as sacrificial electron donors in photoredox catalysis to reduce a species (or an intermediate) present in solution.[15] Nevertheless, the formation of acidic[16] amine radical cations has been extensively employed in synthesis[17] for the generation of other valuable reactive intermediates, as sketched in Scheme 4.1. Indeed, radical cation **4.II** often deprotonates to form a nucleophilic α-amino radical **4.III** (path *b*) that may, in turn, undergo oxidation to afford an iminium ion **4.IV**

(path *c*)[18] that upon the loss of a positively charged group leads to a 1,3-dipole **4.V** (path *d*).[18] In rare instances, the *α*-amino radical is photocatalytically reduced to the corresponding anion **4.VI** (path *e*).[19] If the carbons tethered to the nitrogen atom have no hydrogens, deprotonation from the N–H group may take place to give nitrogen-centered radical **4.VII** (path *f*).[20]

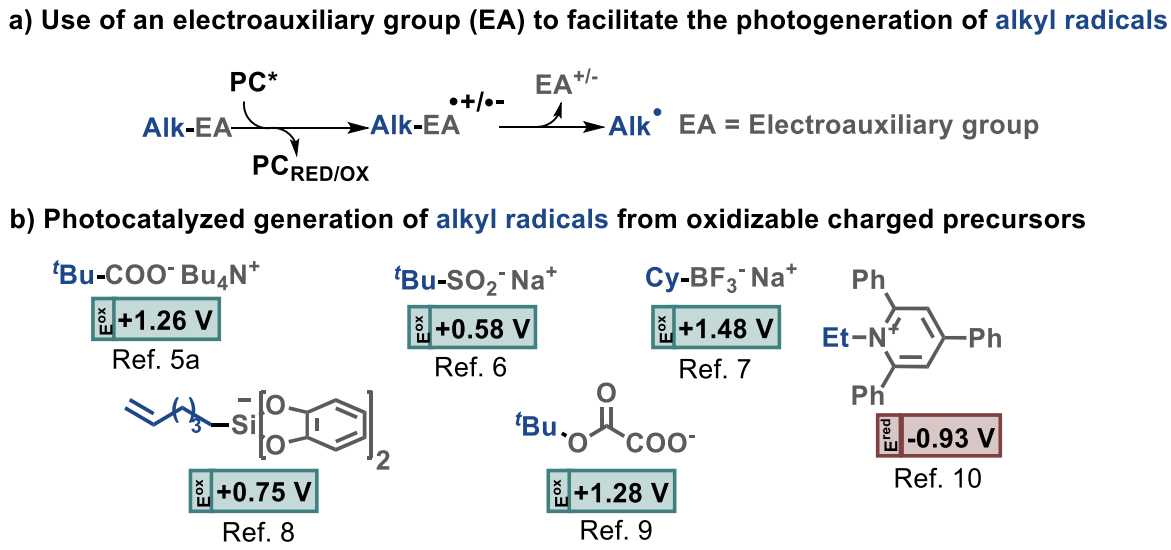

Figure 4.1. (a) Adoption of an electroauxiliary group (EA) to facilitate the generation of alkyl radicals. (b) Main classes of charged precursors used for photocatalyzed alkyl radical formation. (c) Uncharged precursors as electron donors tested for the release of alkyl radicals. *Oxidation and reduction potentials in V vs SCE.

On the other hand, when intermediate **4.II** is generated in a tertiary amine that reluctantly loses a proton (e.g., quinuclidine), this species acts instead as an efficient hydrogen atom abstractor (path *g*).[21] We were intrigued, however, by the possible C–C cleavage to form stable iminium ion **4.IX** along with a carbon radical (path *h*).[22] Examples of this cleavage are only rarely reported in the literature and point to the requirement of nitrogen containing heterocycles as ideal substrates.

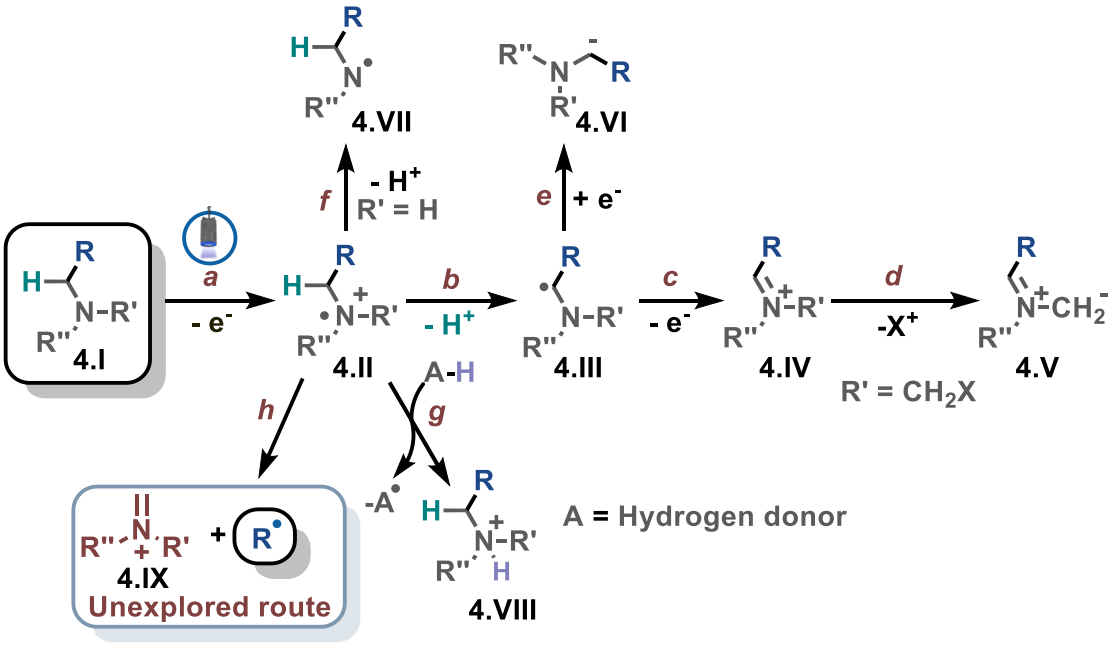

Scheme 4.1. Fate of the (photogenerated) amino radical cation **4.II**.

The photocatalyzed single-electron oxidation of (+)-catharanthine **4.X** indeed induces a C–C bond cleavage in the azabicyclo[2.2.2]oct-5-ene core (Scheme 4.2a), and the so-modified skeleton of the alkaloid is employed in the preparation of further natural compounds.[17a,23] In another instance, the cyclopropyl group in bicyclic cyclopropylamines **4.XI** was easily opened upon photocatalyzed oxidative conditions (Scheme 4.2b).[24] The oxidation of tetramethylethanediamine **4.XII** led to the generation of an iminium ion and an α-amino radical from the fragmentation of the resulting radical cation (Scheme 4.2c), but the thus obtained radical was applied exclusively to the polymerization of 2-hydroxyethylacrylate.[25]

To our knowledge, however, only dihydroquinazolinones (e.g., **4.XIII**, Scheme 4.2d) are used as nitrogen-based heterocycles for the generation of alkyl radicals by a reductive quenching catalytic cycle.[26] As for the above, a general method to generate (un)-substituted alkyl radicals by C–C cleavage from a tertiary amine is so far lacking. We have identified *N*-methyl oxazolidines (**4.XIV**, the nitrogen analogues of dioxolanes) as possible candidates to achieve this goal (Scheme 4.2e). Indeed, such compounds are oxidized easily (E_{ox} = 1.22 V vs SCE for 2,2,3-trimethyloxazolidine) and act as good electron donors.[27] We surmised that the driving force of the cleavage should be the stability of the resulting iminium ion **4.XV**.

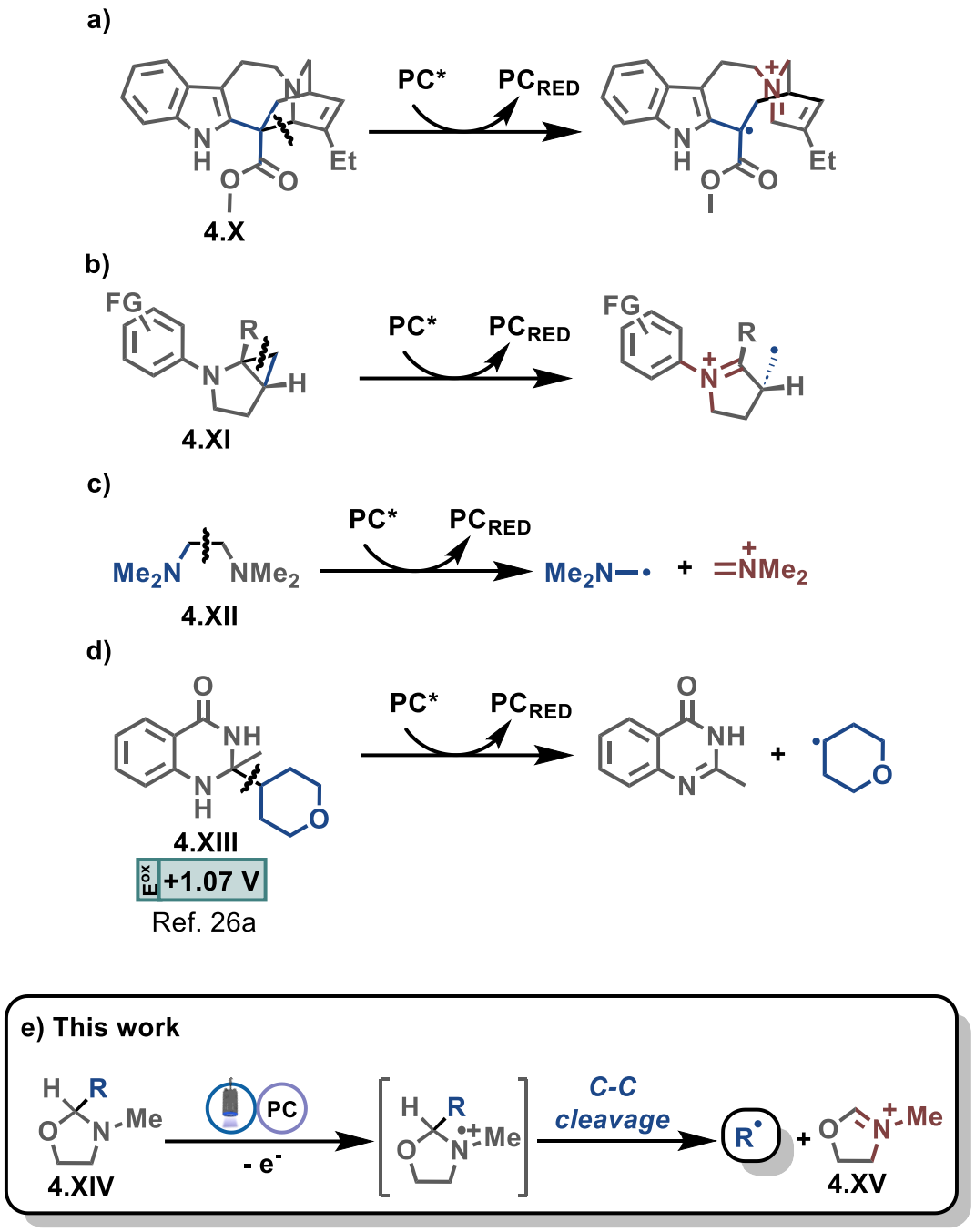

Scheme 4.2. Cleavage of a C–C Bond from a Radical Cation of an Amine.

The present approach represents a mild alternative route for the generation of radicals starting from nitrogen-based heterocycles easily prepared from widely available aldehydes. On these premises, we investigated 2-substituted *N*-methyl oxazolidines for the smooth generation of alkyl radicals to be used in C(sp^3)–C(sp^3) bond formation, as detailed in the following.

4.2 Results and discussion.

Oxazolidines **4.1a–f** have been easily prepared by treating the corresponding aldehydes with 2-(methylamino)ethanol. Related oxazole **4.1g** has been likewise prepared by the reaction of pivalaldehyde and 2-(methylamino)phenol (Figure 4.2). As shown in Figure 4.2 and Figures 4.3–4.6, compounds **4.1a–g** exhibited an oxidation potential in the 0.86–1.35 V (vs SCE) range. The E_{ox} of oxazolidines is quite independent of the presence of the (substituted) alkyl group, whereas the presence of the aromatic ring in oxazole **4.1g** made the oxidation of the heterocycle markedly easier (<1 V vs SCE). These low E_{ox} values allow us to test several (colored) photocatalysts (PCs) for the occurrence of the desired reaction.

The electrochemical characterization (CV) of compound **4.1a-g** was carried out by means of a Amel model 4330 module equipped with a 20 mL standard three-electrode cell with a glassy carbon (0.49 cm^2 geometrical area) working electrode, a platinum wire as auxiliary electrode and an Ag/AgCl, 3 M NaCl reference electrode, all obtained from BASi Electrochemistry. Acetonitrile containing 0.1 M lithium perchlorate were used as solvent and supporting electrolyte, scanning the potential in the range from 0 mV to + 2500 mV, with a 5 mM compound concentration and a scan speed of 50 mV/s.

The measured potentials were referred to the saturated calomel electrode (SCE) obtaining the corresponding results in Scheme 4.2 by applying the equation:

$$E_{ox}\ (SCE) = E_{ox}\ (Ag/AgCl, \text{3 M NaCl}) - 0.045\ \text{V}$$

according to the measured and plotted experimental results.

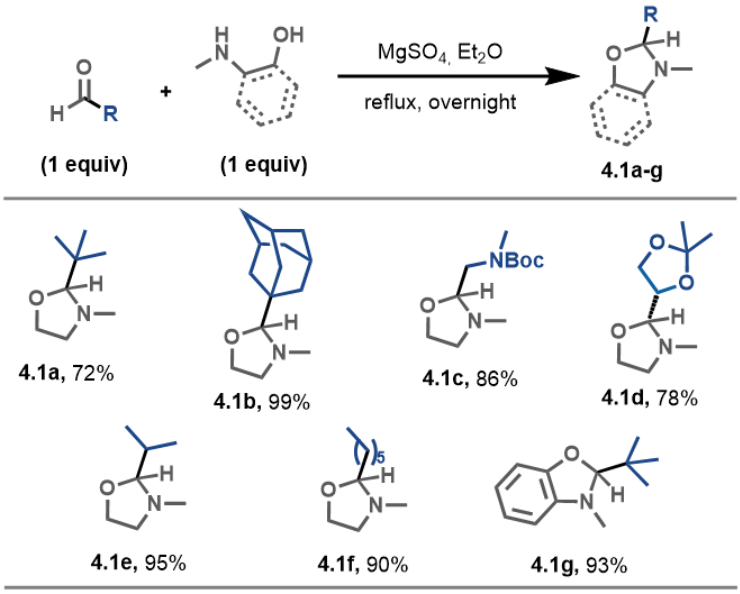

Compound	E_{ox} (V vs SCE)
4.1a	1.33
4.1b	1.26
4.1c	1.23
4.1d	1.22
4.1e	1.35
4.1f	1.19
4.1g	0,86

Figure 4.2. Synthesis of oxazolidines and their measured oxidation potential.

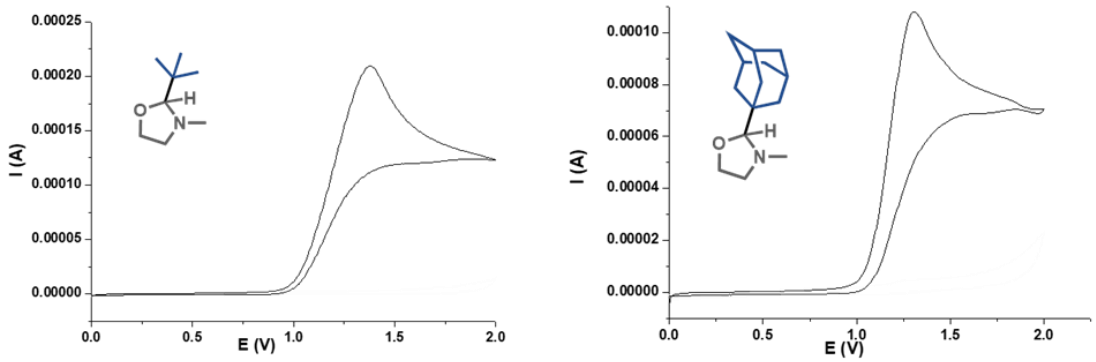

Figure 4.3. Cyclic voltammetry of oxazolidine **4.1a** and **4.1b**.

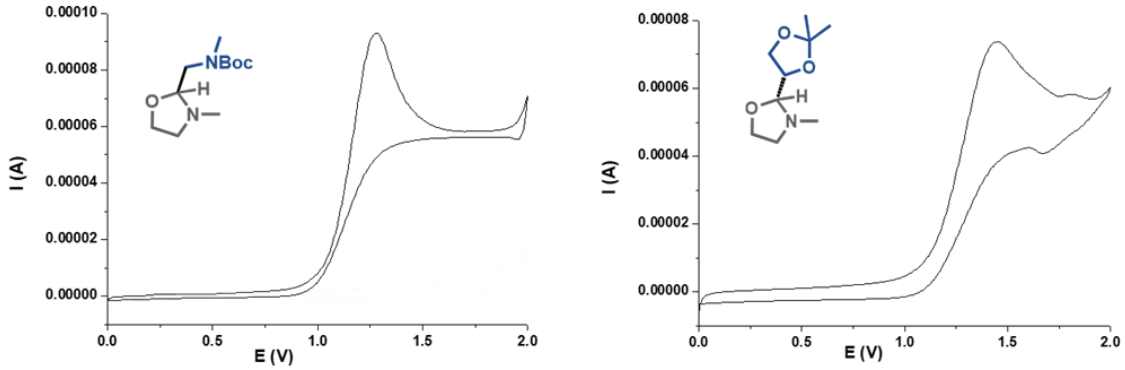

Figure 4.4. Cyclic voltammetry of oxazolidine **4.1c** and **4.1d**.

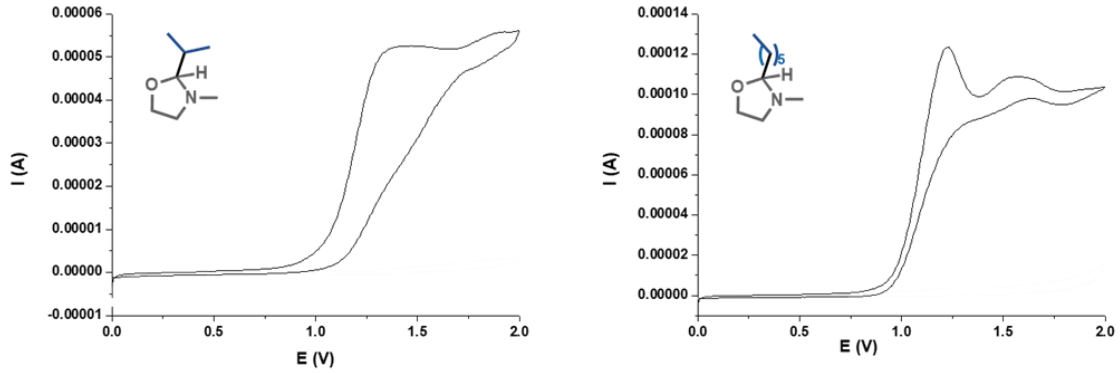

Figure 4.5. Cyclic voltammetry of oxazolidine **4.1e** and **4.1f**.

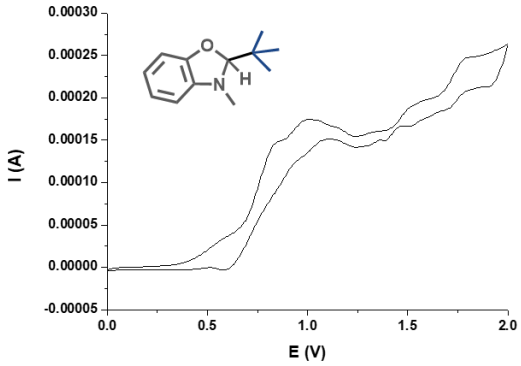

Figure 4.6. Cyclic voltammetry of oxazolidine **4.1g**.

To test our proposal, we then focused on the *tert*-butylation of dimethylmaleate **4.2a** using *N*-methyl-2-*tert*-butyl-oxazolidine **4.1a**. We then embarked on an extensive survey of reaction parameters by varying the PC employed (Ir(III)- and Ru(II)-based complexes as well as photoorgano catalysts), the reaction media, the stoichiometric ratio of the reactants, as well as the influence of oxygen in the reaction.

Table 4.1. Optimization of the photoredox catalyzed *tert*-butylation of olefin **4.2a** via oxazolidine **4.1a**. Deviation from standard conditions.

Entry	Deviations from the standard conditions	4.3 (% Yield)
1	**None**	**88**
2	4CzIPN (10 mol%), N_2 atmosphere	34
3	DCM as solvent	52
4	MeOH as solvent	5
5	N_2 atmosphere	71
6	No light	-
7	TEMPO (1 equiv.)	13
8	$Ir(ppy)_3$ (5 mol%), Ar	-
9	$Ir(ppy)_3$ (5 mol%)	11
10	$Ru(bpy)_3Cl_2$ (5 mol%)	5
11	$[Ph_3Pyrylium]^+$ $(BF_4)^-$ (10 mol%)	9
12	4CzIPN (10 mol%)	24
13	**4.1a** (1.3 equiv.)	66
14	$[Acr\text{-}Mes]^+$ $(BF_4)^-$ (5 mol%)	38
15	$CHCl_3$ as solvent	10
16	MeCN as solvent	-

Gratifyingly, by adopting the conditions described in Table 4.1 (entry 1), succinate **4.3** was isolated in an 88% yield. In detail, we found that the best reaction conditions were as follows: an air-equilibrated DCE solution of **4.2a** (0.05 M) in the presence of 1.5 equiv. of **4.1a**, $[Acr\text{-}Mes]^+$ $(BF_4)^-$ (10 mol %), irradiated at 405 nm for 24 h. Less satisfactory results were obtained when replacing $[Acr\text{-}Mes]^+$ $(BF_4)^-$ (E_{RED}^* > 1.88 V vs SCE)[28] with 4CzIPN (E_{RED}^* > 1.38 V vs SCE[28] in MeCN, entry 2) or other metal-free or metal-based PCs (entries 2, 8-12). The reaction carried out in neat protic solvents (entry 4) or in the absence of oxygen (entry 5) led to a decrease in the overall yield. Control experiments confirm the photochemical nature of the process (entry 6). The

alkylation yield dropped to 13% when the reaction was carried out in the presence of TEMPO (1 equiv., entry 7).

The scope of the reaction has been then extended to electron-poor alkenes **4.2b–h** and vinyl heteroarenes **4.2i** and **4.2j**. The results obtained have been depicted in Scheme 4.3. *tert*-Butylated derivatives **4.3–4.12** have been obtained in good to satisfactory yields. In one case (**4.4**), the reaction was repeated on a mmol scale. Allyl-methacrylate **4.2c** was regioselectivity *tert*-butylated on the electrophilic C=C bond, but ester **4.5** was isolated in only a 46% yield due to its volatility. The method shows a good tolerance in the presence of different functional groups including esters, nitriles, amides, carbonyls, and even heteroarenes. Similar satisfactory results have been obtained when using oxazolidines **4.1b–d**. In particular, **4.1b** was adopted to incorporate the adamantyl moiety into olefins, and the resulting adducts have been isolated in up to a 91% yield (e.g., for **4.14**). In this case, methanol (20% v/v) was added to completely dissolve **4.1b**. To our delight, we found that the release of substituted alkyl radicals such as α-amino (from **4.1c**) and α-oxy (from glyceraldehyde derivative **4.1d**) led to alkylated products **4.21–4.28** in the 43–90% range (Scheme 4.3). Unfortunately, no alkylation products were detected when **4.1e** and **4.1f** and aromatic derivative **4.1g** were used as the radical precursors.

This is an appealing approach for the generation of tertiary (e.g., ^{t}Bu and adamantyl) and α-oxy and α-amino carbon-centered radicals. The reaction took place upon visible light using a commercially available and widely employed organic dye ([Acr-Mes]$^{+}$ $(BF_4)^{-}$) as the photoredox catalyst and gives access to a large variety of alkylated compounds, including, among others, β-alkyl-amides, nitriles, and ketones, as well as functionalized nitrogen-based heterocycles via formation of a C(sp^3)–C(sp^3) bond. The preparation of **4.3–4.20** allows for the introduction of a quaternary carbon in an organic molecule by the forging of a C(sp^3)–C(sp^3) bond, a topic for which there is great interest in view of all-carbon quaternary scaffolds present in many biologically active compounds.[29] Moreover, the adamantylation of olefin is an important strategy to incorporate a moiety able to impart steric bulkiness, chemical inertness, rigidity, and lipophilicity to an organic compound, indeed, several adamantane-based drugs are known to take advantage of these

peculiarities.[30] The design of catalysts having the adamantane scaffold is also another hot topic.[31]

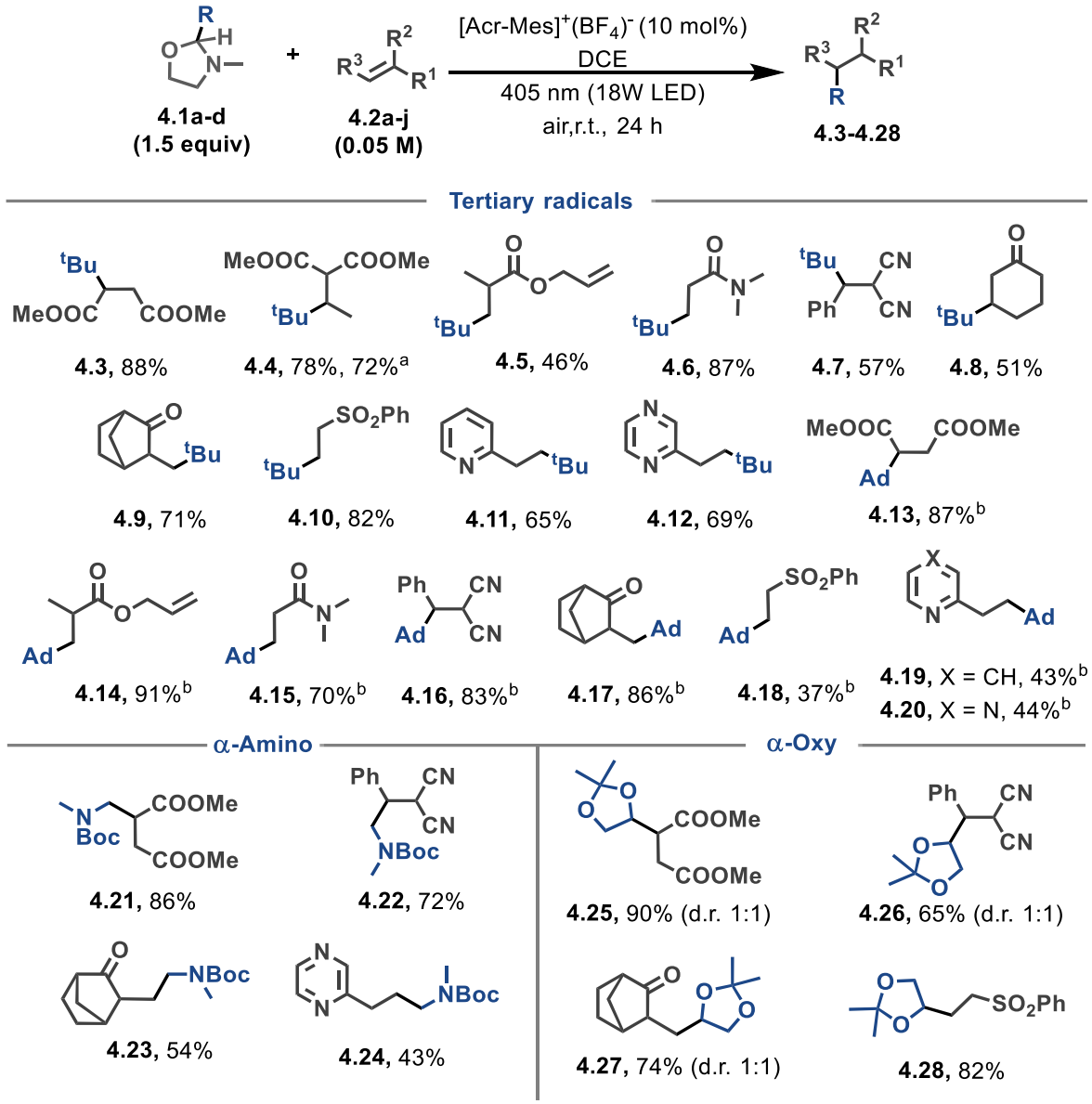

Scheme 4.3. Photoredox catalyzed alkylation of olefins **4.2a-j** via oxazolidine precursors **4.1a-d**. No product observed via **4.1e-g**. [a] Reaction carried out on 1 mmol scale. [b] The reaction was carried out in DCE-MeOH 5:1 mixture for solubility concerns.

As for the above, finding new methods for the formation of tertiary radicals and their application is of utmost importance.[3] The photogeneration of these radicals has been only sparsely reported using Barton esters,[32] *N*-(acyloxy)phthalimides,[33] alkyl *N*-phthalimidoyl oxalates,[34] and alkyl carboxylates.[5b] Thermal generation of these intermediates involved electrophiles such as alkyl halides[35] or alkylsulfones,[36]

despite that in some cases, the desired C(sp^3)–C(sp^3) bond formation failed to occur.[37]

A tentative mechanism for the process illustrated in the present manuscript is proposed in Scheme 4.4. Compounds **4.1a–4.1g** are radical precursors having an E_{ox} < 1.3 V vs SCE (Figure 4.2), comparable to that of other uncharged 1,4-dihydropyridine derivatives (Figure 4.1c).[11] The monoelectronic oxidation of **4.1a–4.1g** by the photoexcited acridinium catalyst [Acr-Mes]$^{+}$* to give the corresponding radical cations **4.1a$^{\bullet+}$–4.1g$^{\bullet+}$** is thus feasible (path a). At this stage, an unprecedented C–C cleavage in **4.1a$^{\bullet+}$–4.1d$^{\bullet+}$** took place, releasing a carbon-centered radical and a stable iminium ion (**4.29^{+}**, path b). The peculiar structure of the oxazolidines avoid the possible α-deprotonation at the radical cation stage from position 2 and 4 as well as from the *N*-Me group to give an α-amino radical (path b'). The driving force of such C–C cleavage is the stability of the tertiary, α-oxy, and α -amido radicals released.

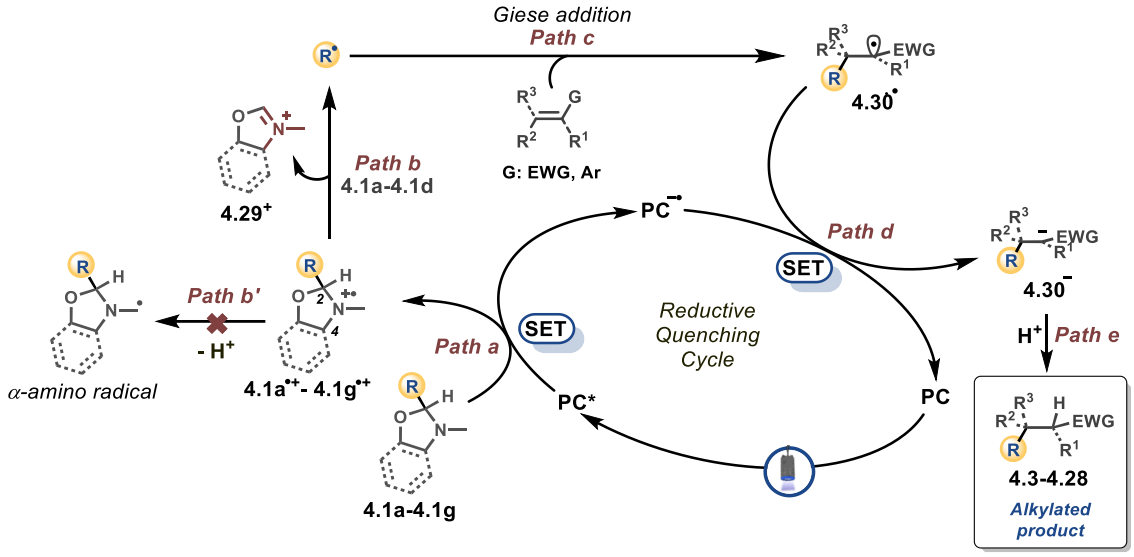

Scheme 4.4. Proposed mechanism.

In the case of oxazolidines **4.1e** and **4.1f** and oxazole **4.1g**, the formation of the corresponding radical cation led to an unproductive alkylation. In the former case, the release of a primary or a secondary radical is expected to be not so favored, and competitive paths may operate.[15]

The structure of compound **4.1g**, however, resembles that of an aniline derivative and may suffer, in analogy with *N,N*-dialkyl anilines, of competitive deprotonation[38] or the reactivity of **4.1g**$^{\bullet+}$ may not have a role due to the efficient back electron transfer with the reduced form of the PC.[39] The alkyl radicals derived from **4.1a**$^{\bullet+}$**–4.1d**$^{\bullet+}$ are, in turn, trapped by electron-poor olefins or vinyl (hetero)aromatics (path c). Back electron transfer from [Acr-Mes]$^{\bullet}$ to the adduct radical **4.30**$^{\bullet}$ (path d) followed by protonation (path e) led to the alkylated products while restoring the photoredox catalyst. This agrees with related conjugate radical additions promoted by the acridinium salt.[40] A hydrogen atom transfer from the solvent by **4.30**$^{\bullet}$ is safely excluded by the deuteration experiments. When the reaction is carried out in deuterated DCM-d^2 no deuterium incorporation was observed when analyzed by GC-MS, obtaining compound **4.3** (Figure 4.7) as when the reaction is performed in common DCM (Figure 4.8). The radical nature of the process is confirmed by the detrimental effect induced by the presence of a radical scavenger (TEMPO, see Table 4.1).

4.3 Mechanistic studies.

Deuteration experiments were carried out following general procedure 2 to discard hydrogen atom transfer processes between the radical adduct **4.30**$^{\bullet}$ and the solvent. Two experiments were performed in parallel, one in deuterated DCE while the second one was performed in DCE. The crude mixtures were analyzed by GC-MS demonstrating that no HAT processes are taking place during the process, as no deuterated product was detected (Figure 4.7-4.8).

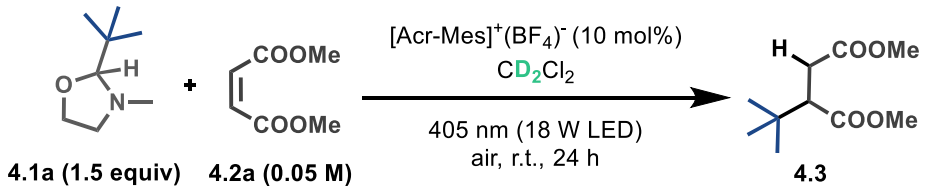

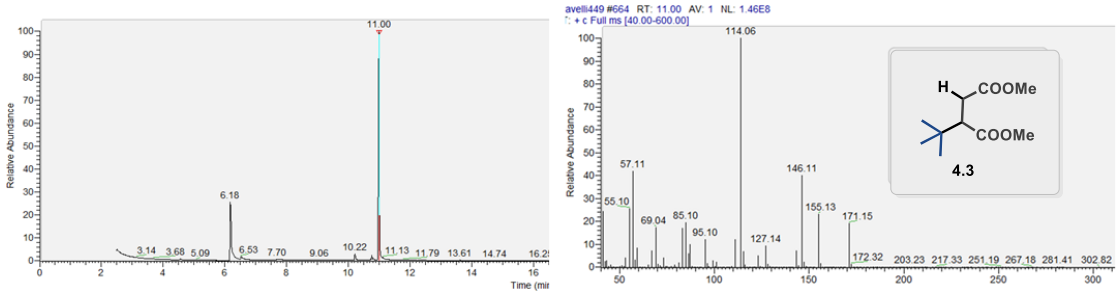

Figure 4.7. GC-MS fragmentation spectrum of compound **4.3**. Irradiation carried out in CD_2Cl_2.

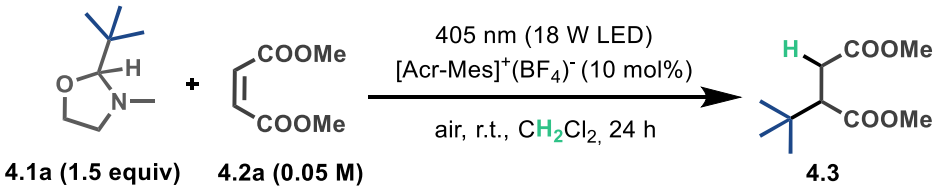

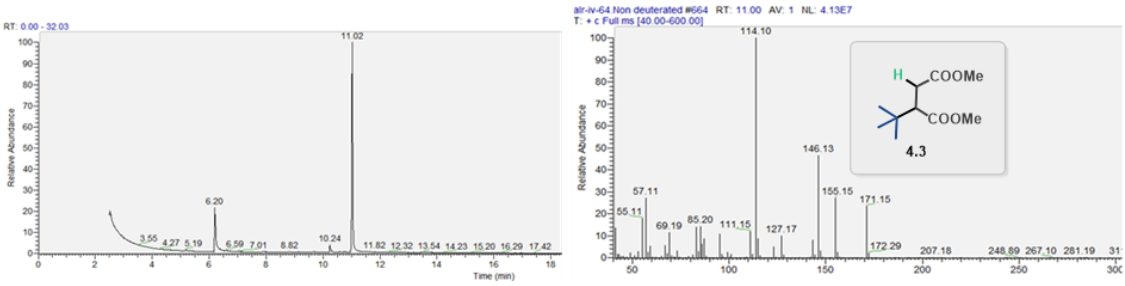

Figure 4.8. GC-MS fragmentation spectrum of compound **3**. Irradiation carried out in CH_2Cl_2.

4.4 Conclusions.

Summing up, we have designed a class of smoothly prepared uncharged precursors for the easy release of alkyl radicals (tertiary, α-oxy, and α-amido) under photoredox catalyzed conditions. This process relies on the unprecedented C–C cleavage in amine radical cations obtained by visible-light irradiation in the presence of commercially available $[Acr\text{-}Mes]^+$ $(BF_4)^-$ as a photo-organocatalyst. This approach was exploited for the introduction, among the others, of a quaternary carbon center via $C(sp^3)–C(sp^3)$ bond formation and for valuable adamantylations.

4.5 Experimental section.

^{1}H and ^{13}C NMR spectra were recorded on a 300 e 75 MHz spectrometer, respectively. The attributions were based on ^{1}H and ^{13}C NMR experiments, chemical shifts are reported in ppm downfield from TMS (δ ppm), multiplicity (s = singlet, bs = broad singlet, d = doublet, t = triplet, q = quadruplet, quint = quintuplet, sext = sextuplet, sept = septuplet, m = multiplet), coupling constant (Hz) and integration.

GC analyses were performed using a HP SERIES 5890 II equipped with a fire ion detector (FID, temperature 350 °C). Analytes were separated using a Restek Rtx-5MS (30 m×0.25 mm×0.25 μm) capillary column with nitrogen as a carrier gas at 1 mL min^{-1}. The injector temperature was 250 °C. The GC oven temperature was held at 80 °C for 2 min, increased to 250 °C by a temperature ramp of 10 °C min^{-1}, and held for 10 min.

GC/MS analyses were carried out on a Thermo Scientific DSQII single quadrupole GC/MS system (TraceDSQII mass spectrometer, Trace GC Ultra gas chromatograph, TriPlus autosampler - ThermoFisher Scientific, Waltham, MA, USA). Chromatography was performed on a Rxi-5Sil MS capillary column (30 m length×0.25 mm ID×0.25 μm film thickness, Restek, Milan, Italy) with Helium (>99.99 %) as carrier gas at a constant flow rate of 1.0 mL min-1. An injection volume of 1 μL was employed. The injector temperature was set at 250 °C and it was operated in split mode, with a split flow of 10 mL min^{-1}. The oven temperature was programmed from 80 °C (isothermal for 2 min) to 220 °C at the rate of 10 °C min^{-1}, then from 220 °C to 300 °C (isothermal for 5 min) at the rate of 4 °C min^{-1}. Mass transfer line temperature was set at 260 °C. Total GC running time was 41 min. All mass spectra were acquired with an electron ionization system (EI, Electron Impact mode) with ionization energy of 70 eV and source temperature of 250°C, with spectral acquisition in Full Scan mode, positive polarity, over a mass range of 35–650 Da with a scan rate of 940 amu s^{-1}. The chromatogram acquisition, detection of mass spectral peaks and their waveform processing were performed using Xcalibur MS Software Version 2.1 (Thermo Scientific Inc.). Assignment of chemical structures to chromatographic peaks was based on the comparison with the databases for GC-

MS NIST Mass Spectral Library (NIST 08) and Wiley Registry of Mass Spectral Data (8th Edition).

HRMS data were acquired using a X500B QTOF System (SCIEX, Framingham, MA 01701 USA) available at the CGS of the University of Pavia, equipped with the Twin Sprayer ESI probe and coupled to an ExionLC™ system (SCIEX). The SCIEX OS software 2.1.6 was used as operating platform. For MS detection the following parameters were applied: Curtain gas 30 psi, Ion source gas 1 45 psi, Ion source gas 2 55 psi, Temperature 450°C, Polarity negative, Ion spray voltage -4500 V, TOF mass range 50-1600 Da, declustering potential -60 V and collision energy -10 V.

Cyclic Voltammetry was carried out by means of a Amel model 4330 module equipped with a 20 mL standard three-electrode cell with a glassy carbon (0.49 cm^2 geometrical area) working electrode, a platinum wire as auxiliary electrode and an Ag/AgCl, 3 M NaCl reference electrode, all obtained from BASi Electrochemistry. Acetonitrile containing 0.1 M lithium perchlorate were used as solvent and supporting electrolyte, scanning the potential in the range from 0 mV to + 2500 mV, with a 5 mM compound concentration and a scan speed of 50 mV s^{-1}.

4.5.1 Chart of starting materials.

The starting materials were commercially available and used as received.

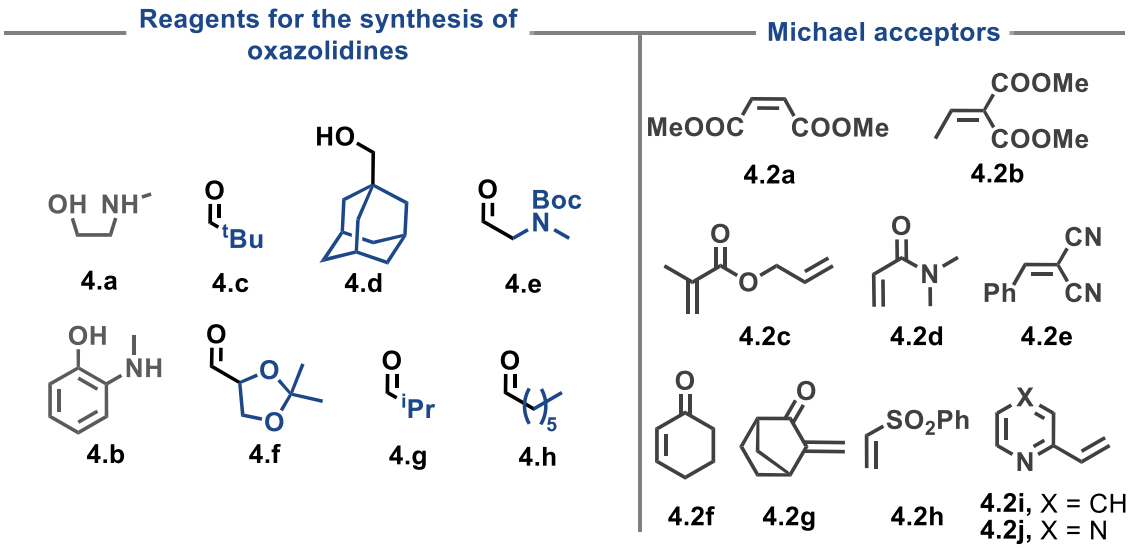

4.5.2 General procedures.

4.5.2.1 General procedure 4.1. Synthesis of 2-substituted *N*-methyl oxazolidines and oxazoles.

Oxazolidines **4.1a-4.1f** and oxazole **4.1g** were synthesized and fully characterized (see Scheme X). 2-(Methylamino)ethanol (**4.a**) or 2-(methylamino)phenol (**4.b**) (1 equiv.) was added to a suspension of $MgSO_4$ (25 mg $mmol^{-1}$) and the corresponding aldehyde (1 equiv.) in Et_2O (1.7 mL $mmol^{-1}$). The mixture was stirred and heated at reflux overnight. The crude mixture was diluted with DCM and filtered. The corresponding solution was concentrated in vacuo affording the desired oxazolidines and oxazole in high purity without further purification was needed.

4.5.2.2 General procedure 4.2. Light-induced photo-redox alkylation process.

In a Pyrex glass vessel (see Table 4.1), a solution of the corresponding oxazolidine **4.1a-4.1g** (0.375 mmol, 1.5 equiv, 0.075 M), olefin **4.2a-4.2j** (0.25 mmol, 1 equiv., 0.05 M) and $[Acr\text{-}Mes]^+(BF_4)^-$ (0.025 mmol, 10 mol%) in DCE (5 mL) was irradiated for 24 h by means of a EvoluChem lamp (emission located at 405 nm, 18W). The photolyzed solution was then concentrated in vacuo and the resulting residue purified by flash column chromatography by means of automated Isolera (Biotage) apparatus and a SiO_2 cartridge.

4.5.3 Characterization data.

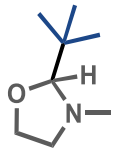

2-*tert*-Butyl-3-methyloxazolidine (4.1a).

From *N*-methylaminoethanol (**4.a**) (11.6 mmol, 1 equiv., 0.93 mL), $MgSO_4$ (314 mg), pivalaldehyde (**4.c**) (11.6 mmol, 1 equiv., 1.3 mL) in Et_2O (20 mL). The crude mixture was diluted with DCM, filtered and the obtained solution was concentrated in vacuo affording **4.1a** (colorless oil, 72% yield) that was used without further purification.

4.1a. ^1H NMR (300 MHz, Acetone-d^6) δ 3.74 (ddt, *J* = 8.8, 6.7, 4.4 Hz, 1H), 3.71–3.60 (m, 2H), 3.01(ddd, *J* = 10.4, 7.6, 6.0 Hz, 1H), 2.64 (ddd, *J* = 10.4, 5.9, 4.5 Hz, 1H), 2.41

(s, 3H), 0.85 (s, 9H). ^{13}C NMR (75 MHz, Acetone-d^6) δ 106.6, 65.3, 56.4, 44.5, 37.1, 25.5. HRMS (EI) m/z: $[M+H]^+$ calculated for $C_8H_{17}NO$ 143.1383, found 143.1379.

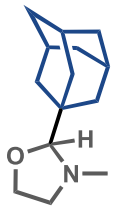

(2-Adamantan-1-yl)-3-methyloxazolidine (4.1b).

From *N*-methylaminoethanol (**4.a**) (6.1 mmol, 1 equiv., 0.49 mL), $MgSO_4$ (153 mg), adamantane-1-carbaldehyde[41] (6.1 mmol, 1 equiv., 1 g) in Et_2O (10 mL). The crude mixture was diluted with DCM, filtered and the obtained solution was concentrated in vacuo affording **4.1b** (colorless oil, 99% yield) that was used without further purification.

4.1b. ^{1}H NMR (300 MHz, Acetone-d^6) δ 3.80–3.57 (m, 2H), 3.50 (s, 1H), 2.95 (dt, J = 10.3, 6.9 Hz, 1H), 2.63 (dt, J = 10.3, 5.1 Hz, 1H), 2.39 (s, 3H), 2.00–1.85 (m, 3H), 1.83–1.42 (m, 13H). ^{13}C NMR (75 MHz, acetone-d^6) δ 106.8, 65.2, 56.4, 44.8, 39.1, 38.4, 38.1, 29.1, 29.0. HRMS (EI) m/z: $[M+H]^+$ calculated for $C_{14}H_{23}NO$ 222.1852, found 222.1841.

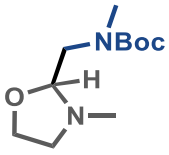

***tert*-Butyl methyl((3-methyloxazolidin-2-yl)methyl)carbamate (4.1c).**

From *N*-methylaminoethanol (**4.a**) (2.9 mmol, 1 equiv., 0.23 mL), $MgSO_4$ (75 mg), *N*-Boc-2-aminoacetaldehyde (**4.e**) (2.9 mmol, 1 equiv. 0.48 mL) in Et_2O (5 mL). The crude mixture was diluted with DCM, filtered and the obtained solution was concentrated in vacuo affording **4.1c** (pale yellow oil, 86% yield) that was used without further purification.

4.1c. ^{1}H NMR (300 MHz, Acetone-d^6) δ 1.42 (s, 9H), 2.37 (s, 3H), 2.49–2.58 (q, 1H, J = 9 Hz), 2.81–2.84 (m, 1H), 2.85 (s, 3H), 3.42–3.48 (dd, 1H, J = 3 and 15 Hz), 3.76–3.80 (m, 2H), 3.95–3.99 (m, 1H). ^{13}C NMR (75 MHz, Acetone- d^6) δ 148.1, 98.0, 79.6, 65.4, 55.2, 52.9, 40.6, 28.9, 30.1. HRMS (EI) m/z: $[M+H]^+$ calculated for $C_{11}H_{22}N_2O_3$ 231.1703, found 231.1699.

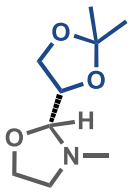

2-(2,2-Dimethyl-1,3-dioxolan-4-yl)-3-methyloxazolidine (4.1d).

From *N*-methylaminoethanol (**4.a**) (7.7 mmol, 1 equiv., 0.62 mL), $MgSO_4$ (193 mg), 2,2-dimethyl-1,3-dioxolane-4-carbaldehyde (**4.f**) (7.7 mmol, 1 equiv. 0.96 mL) in Et_2O (13 mL). The crude mixture was diluted with DCM, filtered and the obtained solution was concentrated in vacuo affording **4.1d** (pale yellow oil, 78% yield), that was used without further purification.

4.1d. ^{1}H NMR (200 MHz, Acetone-d^6) δ 4.10–4.02 (m, 1H), 4.01–3.92 (m, 2H), 3.85–3.73 (m, 3H), 3.21–3.07 (m, 1H), 2.60–2.46 (m, 1H), 2.42 (s, 3H), 1.34 (s, 3H), 1.27 (s, 3H). ^{13}C NMR (75 MHz, Acetone-d^6) δ 110.2, 98.9, 98.4, 79.1, 78.4, 67.1, 66.7, 66.2, 65.4, 56.0, 55.7, 42.8, 40.8, 27.3, 27.1, 26.1, 26.0. HRMS (EI) m/z: $[M+H]^+$ calculated for $C_9H_{17}NO_3$ 188.1281, found 188.1276.

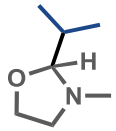

2-*iso*-Propyl-3-methyloxazolidine (4.1e).

From *N*-methylaminoethanol (**4.a**) (13.9 mmol, 1 equiv., 1.1 mL), $MgSO_4$ (348 mg), 2-methylpropanal (**4.g**) (13.9 mmol, 1 equiv. 1.3 mL) in Et_2O (24 mL). The crude mixture was diluted with DCM, filtered and the obtained solution concentrated in vacuo affording **4.1e** (colorless oil, 95% yield,) that was used without further purification. Spectroscopical data are in accordance with the literature.[42]

4.1e. ^{1}H NMR (300 MHz, Acetone-d^6) δ 3.82–3.60 (m, 2H), 3.58 (d, J = 4.0 Hz, 1H), 3.09 (ddd, J = 9.5, 6.2, 4.1 Hz, 1H), 2.51 (ddd, J = 9.4, 7.9, 7.2 Hz, 1H), 1.68 (dd, J = 6.8, 4.0 Hz, 1H), 0.91 (d, J = 6.9 Hz, 3H), 0.85 (d, J = 6.7 Hz, 3H). ^{13}C NMR (75 MHz, Acetone-d^6) δ 102.4, 65.0, 55.7, 40.2, 19.1, 16.2. HRMS (EI) m/z: $[M+H]^+$ calculated for $C_7H_{15}NO$ 130.1226, found 130.1224.

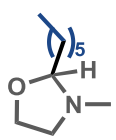

2-Hexyl-3-methyloxazolidine (4.1f).

From *N*-methylaminoethanol (**4.a**) (7 mmol, 1 equiv., 0.56 mL) was added to a suspension of $MgSO_4$ (185 mg), heptanal (**4.h**) (7 mmol, 1 equiv. 0.98 mL) in Et_2O (12 mL). The crude mixture was diluted with DCM, filtered and the obtained solution was concentrated in vacuo affording **4.1f** (colorless oil, 90% yield) that was used without further purification. Spectroscopic data are in accordance with the literature.[43]

4.1f. ^{1}H NMR (300 MHz, Acetone-*d*^{6}) δ 3.79–3.69 (m, 3H), 3.10 (ddd, *J* = 9.8, 5.8, 4.2 Hz, 1H), 2.49 (dt, *J* = 9.5, 8.0 Hz, 1H), 2.26 (s, 3H), 1.59–1.23 (m, 10H), 0.88 (d, *J* = 6.9 Hz, 3H). ^{13}C NMR (75 MHz, Acetone-*d*^{6}) δ 98.0, 64.6, 55.5, 39.1, 34.1, 32.7, 25.5, 23.3, 14.3. HRMS (EI) m/z: $[M+H]^+$ calculated for $C_{10}H_{21}NO$ 172.1696, found 172.1693.

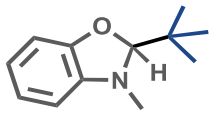

2-(*tert*-Butyl)-3-methyl-2,3-dihydrobenzo[*d*]oxazole (4.1g).

From *N*-methylaminophenol (**4.b**) (2.9 mmol, 1 equiv., 0.31 mL), $MgSO_4$ (75 mg), pivalaldehyde (**4.c**) (2.9 mmol, 1 equiv., 0.33 mL) in Et_2O (5 mL). The crude mixture was diluted with DCM, filtered and the obtained solution was concentrated in vacuo affording **4.1g** (dark blue oil 93%, yield) that was used without further purification.

4.1g. ^{1}H NMR (300 MHz, Acetone-*d*^{6}) δ 6.77–6.54 (m, 4H), 4.97 (s, 1H), 2.85 (s, 3H), 0.96 (s, 10H). ^{13}C NMR (75 MHz, Acetone-*d*^{6}) δ 152.1, 152.0, 143.4, 143.4, 121.4, 120.6, 110.1, 109.7, 107.3, 41.2, 38.1, 24.3. HRMS (EI) m/z: $[M+H]^+$ calculated for $C_{12}H_{17}NO$ 192.1383, found 192.1375.

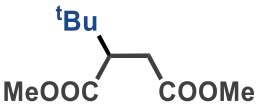

Dimethyl 2-(*tert*-butyl)succinate (4.3).

From **4.1a** (0.375 mmol, 1.5 equiv., 0.075 M, 58 µL), **4.2a** (0.25 mmol, 1 equiv., 0.05 M, 31 µL), $[Acr\text{-}Mes]^+(BF_4)^-$ (0.025 mmol, 10 mol%, 10 mg) in DCE (5 mL). Purification by column chromatography (eluent: Cyclohexane/AcOEt 100/0 to 4/1) afforded **4.3** (colorless oil, 44 mg, 88% yield). Spectroscopic data are in accordance with the literature.[44]

4.3. ^{1}H NMR (300 MHz, Chloroform-*d*) δ 3.69 (s, 3H), 3.66 (s, 3H), 2.87 – 2.39 (m, 3H), 0.96 (s, 9H). ^{13}C NMR (75 MHz, Chloroform-*d*) δ 174.9, 173.3, 51.9, 51.5, 51.4, 32.8, 29.9, 27.9.

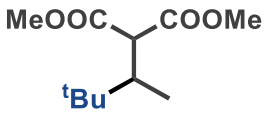

Dimethyl 2-(3,3-dimethylbutan-2-yl)malonate (4.4).

From **4.1a** (0.375 mmol, 1.5 equiv., 0.075 M, 58 µL), **4.2b** (0.25 mmol, 1 equiv., 0.05 M, 35 µL), [Acr-Mes]$^{+}$(BF_4)$^{-}$ (0.025 mmol, 10 mol%, 10 mg) in DCE (5 mL). Purification by column chromatography (eluent: Cyclohexane/AcOEt 100/0 to 4/1) afforded **4.4** (pale yellow oil, 42 mg, 78% yield). Spectroscopic data are in accordance with the literature.

Compound **4.4** was obtained in 72% yield when starting from 1 mmol of **4.2b**.

4.4. ^{1}H NMR (300 MHz, Chloroform-*d*) δ 3.71 (s, 3H), 3.70 (s, 3H), 3.55 (d, *J* = 5.4 Hz, 1H), 2.23 (qui, *J* = 7.1 Hz, 1H), 0.99 (d, *J* = 7.2, 3H), 0.88 (s, 9H). ^{13}C NMR (75 MHz, Chloroform-d) δ 170.5, 169.8, 52.9, 52.4, 51.9, 42.8, 33.4, 27.3, 12.0. HRMS (EI) m/z: [M+H]$^{+}$ calculated for $C_{11}H_{20}O_4$ 217.1434, found 217.1431.

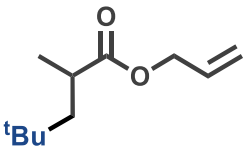

Allyl 2,4,4-trimethylpentanoate (4.5).

From **4.1a** (0.375 mmol, 1.5 equiv., 0.075 M, 58 µL), **4.2c** (0.25 mmol, 1 equiv., 0.05 M, 33 µL), [Acr-Mes]$^{+}$(BF_4)$^{-}$ (0.025 mmol, 10 mol%, 10 mg) in DCE (5 mL). Purification by column chromatography (eluent: Cyclohexane/AcOEt 100/0 to 9/1) afforded **4.5** (colorless oil, 21 mg, 46% yield).

4.5. ^{1}H NMR (300 MHz, Chloroform-*d*) δ 6.05–5.79 (m, 1H), 5.41–5.17 (m, 2H), 4.64–4.44 (m, 2H), 2.63–1.98 (m, 2H), 1.95–1.80 (m, 1H), 1.17 (d, *J* = 6.9 Hz, 3H), 0.89 (s, 9H). ^{13}C NMR (75 MHz, Chloroform-*d*) δ 177.7, 132.5, 118.2, 65.3, 65.1, 47.9, 36.4, 29.6, 20.5. Anal. Calcd. for $C_{11}H_{20}O_2$ C, 71.70, H, 10.94. Found 71.7, 10.8. GC-MS (m/z): 184.3 (20, M^{+}), 127.3 (100), 109.2 (20), 97.3 (10).

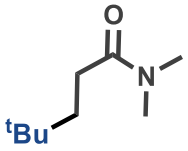

***N,N'*-4,4-tetramethylpentanamide (4.6).**

From **4.1a** (0.375 mmol, 1.5 equiv., 0.075 M, 58 µL), **4.2d** (0.25 mmol, 1 equiv., 0.05 M, 25 µL), $[Acr\text{-}Mes]^+(BF_4)^-$ (0.025 mmol, 10 mol%, 10 mg) in DCE (5 mL). Purification by column chromatography (eluent: DCM/MeOH 100/0 to 95/5) afforded **4.6** (colorless oil, 34.3 mg, 87% yield). Spectroscopic data are in accordance with the literature.[45]

4.6. ^{1}H NMR (300 MHz, Chloroform-*d*) δ 3.01 (s, 6H), 2.43 – 2.32 (m, 2H), 1.63 – 1.47 (m, 2H), 0.92 (s, 9H). ^{13}C NMR (75 MHz, Chloroform-*d*) δ 171.6, 39.11, 30.2, 29.8, 29.3, 29.1.

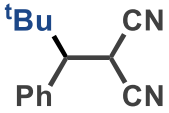

2-(2,2-Dimethyl-1-phenylpropyl)malononitrile (4.7).

From **4.1a** (0.375 mmol, 1.5 equiv., 0.075 M, 58 µL), **4.2e** (0.25 mmol, 1 equiv., 0.05 M, 58 µL), $[Acr\text{-}Mes]^+(BF_4)^-$ (0.025 mmol, 10 mol%, 10 mg) in DCE (5 mL). Purification by column chromatography (eluent: Cyclohexane/AcOEt 100/0 to 9/1) afforded **4.7** (white solid, mp 53.0–54.0 °C, 30.1 mg, 57% yield). Spectroscopic data are in accordance with the literature.[46]

4.7. ^{1}H NMR (300 MHz, acetone-d_6) δ 7.55 – 7.47 (m, 2H), 7.47 – 7.33 (m, 3H), 5.07 (d, *J* = 6.4 Hz, 1H), 3.33 (d, *J* = 6.4 Hz, 1H), 1.11 (s, 9H). ^{13}C NMR (75 MHz, acetone-d_6) δ 138.4, 130.4, 129.2, 129.0, 115.3, 115.1, 56.4, 35.5, 28.7, 25.7.

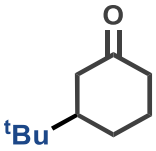

3-(*tert*-Butyl)cyclohexan-1-one (4.8).

From **4.1a** (0.375 mmol, 1.5 equiv., 0.075 M, 58 µL), **4.2f** (0.25 mmol, 1 equiv., 0.05 M, 24 µL), $[Acr\text{-}Mes]^+(BF_4)^-$ (0.025 mmol, 10 mol%, 10 mg) in DCE (5 mL). Purification by column chromatography (eluent: Cyclohexane/AcOEt 100/0 to 9/1)

afforded **4.8** (colorless oil, 19.5 mg, 51% yield). Spectroscopic data are in accordance with the literature.[47]

4.8. ^{1}H NMR (300 MHz, Chloroform-*d*) δ 2.49-2.40 (m, 1H), 2.39–2.30 (m, 1H), 2.29–2.20 (m, 1H), 2.17 (s, 1H), 2.14–1.99 (m, 2H), 1.99–1.89 (m, 1H), 1.38–1.23 (m, 2H), 0.89 (s, 9H). ^{13}C NMR (75 MHz, Chloroform-*d*) 13C NMR (75 MHz, Chloroform-*d*) δ 213.2, 49.5, 43.8, 41.5, 32.9, 27.3, 26.3, 25.8.

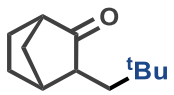

3-Neopentylbicyclo[2.2.1]heptan-2-one (4.9).

From **4.1a** (0.375 mmol, 1.5 equiv., 0.075 M, 58 µL), **4.2g** (0.25 mmol, 1 equiv., 0.05 M, 28 µL), [Acr-Mes]$^{+}$(BF_4)$^{-}$ (0.025 mmol, 10 mol%, 10 mg) in DCE (5 mL). Purification by column chromatography (eluent: Cyclohexane/AcOEt 100/0 to 9/1) gave **4.9** (pale yellow oil, 30.5 mg, 71% yield). Spectroscopic data are in accordance with the literature.[48]

4.9. ^{1}H NMR (300 MHz, Acetone-d_6) δ 2.65 (d, *J* = 5.1 Hz, 1H), 2.46 (d, *J* = 5.0 Hz, 1H), 1.89–1.46 (m, 6H), 1.33–1.10 (m, 3H), 0.92 (s, 9H). ^{13}C NMR (75 MHz, Acetone-d_6) δ 218.9, 51.8, 50.4, 41.3, 40.1, 37.7, 31.1, 30.0, 25.9, 22.0. HRMS (EI) m/z: [M+H]$^{+}$ calculated for $C_{12}H_{20}O$ 181.1587, found 181.1585.

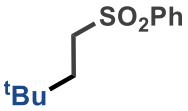

((3,3-Dimethylbutyl)sulfonyl)benzene (4.10).

From **4.1a** (0.375 mmol, 1.5 equiv., 0.075 M, 58 µL), **4.2h** (0.25 mmol, 1 equiv., 0.05 M, 42 mg), [Acr-Mes]$^{+}$(BF_4)$^{-}$ (0.025 mmol, 10 mol%, 10 mg) in DCE (5 mL). Purification by column chromatography (eluent: DCM/MeOH 100/0 to 95/5) afforded **4.10** (pale yellow oil, 46.6 mg, 82% yield). Spectroscopic data are in accordance with the literature.[49]

4.10. ^{1}H NMR (300 MHz, Chloroform-*d*) δ 7.96–7.86 (m, 2H), 7.70–7.51 (m, 3H), 3.12–2.99 (m, 2H), 1.66–1.53 (m, 2H), 0.86 (s, 9H).^{13}C NMR (75 MHz, Chloroform-*d*) δ 139.4, 133.7, 129.4, 128.2, 53.1, 35.8, 30.2, 29.0.

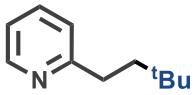

2-(3,3-Dimethylbutyl)pyridine (4.11).

From **4.1a** (0.375 mmol, 1.5 equiv., 0.075 M, 58 µL), **4.2i** (0.25 mmol, 1 equiv., 0.05 M, 26 µL), $[Acr\text{-}Mes]^+(BF_4)^-$ (0.025 mmol, 10 mol%, 10 mg) in DCE (5 mL). Purification by column chromatography (eluent: Cyclohexane/AcOEt 100/0 to 8/1) gave **4.11** (pale yellow oil, 26.7 mg, 65% yield). Spectroscopic data are in accordance with the literature.[50]

4.11. ^{1}H NMR (300 MHz, Chloroform-*d*) δ 8.52 (d, *J* = 5.0 Hz, 1H), 7.60 (td, *J* = 7.7, 1.9 Hz, 1H), 7.17 (d, *J* = 7.9 Hz, 1H), 7.13–7.04 (m, 1H), 2.85–2.72 (m, 2H), 1.70–1.55 (m, 2H), 0.98 (s, 9H). ^{13}C NMR (75 MHz, Chloroform-*d*) δ 163.2, 149.0, 136.8, 122.9, 121., 44.4, 33.9, 30.7, 29.5.

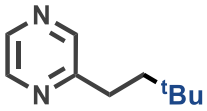

2-(3,3-Dimethylbutyl)pyrazine (4.12).

From **4.1a** (0.375 mmol, 1.5 equiv., 0.075 M, 58 µL), **4.2 j** (0.25 mmol, 1 equiv., 0.05 M, 25 µL), $[Acr\text{-}Mes]^+(BF_4)^-$ (0.025 mmol, 10 mol%, 10 mg) in DCE (5 mL). Purification by column chromatography (eluent: Cyclohexane/AcOEt 100/0 to 4/1) gave **4.12** (pale yellow oil, 28.5 mg, 69% yield). Spectroscopic data are in accordance with the literature.[51]

4.12. ^{1}H NMR (300 MHz, Chloroform-*d*) δ 8.49 (d, *J* = 1.9 Hz, 2H), 8.40 (d, *J* = 2.2 Hz, 1H), 2.87–2.74 (m, 2H), 1.68–1.54 (m, 2H), 0.98 (s, 9H). ^{13}C NMR (75 MHz, Chloroform-*d*) δ 158.8, 144.6, 143.9, 142.0, 44.0, 31.2, 30.7, 29.4. HRMS (EI) m/z: $[M+H]^+$ calculated for $C_{10}H_{16}N_2$ 165.1386, found 165.1380. GC-MS (m/z): 164.3 (40), 149.40, 107.1 (100), 942 (20).

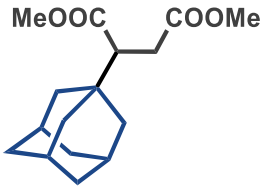

Dimethyl 2-(adamantan-1-yl)succinate (4.13).

From **4.1b** (0.375 mmol, 1.5 equiv., 0.075 M, 82 mg), **4.2a** (0.25 mmol, 1 equiv., 0.05 M, 31 µL), $[Acr\text{-}Mes]^+(BF_4)^-$ (0.025 mmol, 10 mol%, 10 mg) in a DCE /MeOH mixture 5:1 (5 mL). Purification by column chromatography (eluent: Cyclohexane/AcOEt 100/0 to 9/1) afforded **4.13** (white solid, mp 50–51.8 °C, 60.1 mg, 87% yield). Spectroscopic data in accordance with the literature.[44]

4.13. ^{1}H NMR (300 MHz, Chloroform-*d*) δ 3.69 (s, 3H), 3.65 (s, 3H), 2.83–2.70 (m, 1H), 2.53 (t, *J* = 2.8 Hz, 1H), 2.48 (t, *J* = 2.5 Hz, 1H), 1.98 (s, 3H), 1.74–1.58 (m, 10H), 1.46 (d, *J* = 12.5 Hz, 2H). ^{13}C NMR (75 MHz, Chloroform-*d*) δ 173.5, 52.4, 51.9, 51.4, 40.1, 36.9, 34.6, 31.1, 28.7.

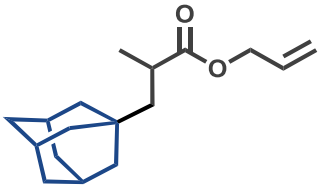

Allyl 3-(adamantan-1-yl)-2-methylpropanoate (4.14).

From **4.1b** (0.375 mmol, 1.5 equiv., 0.075 M, 82 mg), **4.2c** (0.25 mmol, 1 equiv., 0.05 M, 33 µL), $[Acr\text{-}Mes]^+(BF_4)^-$ (0.025 mmol, 10 mol%, 10 mg) in a DCE/MeOH mixture 5:1 (5 mL). Purification by column chromatography (eluent: Cyclohexane/AcOEt 100/0 to 4/1) gave **4.14** (pale yellow oil, 59.7 mg, 91% yield).

4.14. ^{1}H NMR (300 MHz, acetone-d_6) δ 5.95 (ddt, *J* = 17.3, 10.8, 5.6 Hz, 1H), 5.33 (dq, *J* = 17.2, 1.7 Hz, 1H), 5.20 (dq, *J* = 10.4, 1.5 Hz, 1H), 4.55 (dq, *J* = 5.7, 1.4 Hz, 2H), 2.57 (ddp, *J* = 14.1, 7.1, 3.6 Hz, 1H), 1.91 (s, 4H), 1.75–1.63 (m, 9H), 1.48 (dq, *J* = 11.9, 2.6 Hz, 6H), 1.40 (d, *J* = 12.6 Hz, 2H), 1.12 (d, *J* = 7.0 Hz, 3H), 1.04 (dd, *J* = 14.1, 3.2 Hz, 1H). ^{13}C NMR (75 MHz, acetone-d_6) δ 177.4, 133.8, 117.9, 65.2, 49.3, 43.0, 37.7, 36.5, 34.9, 33.3, 20.8. HRMS (EI) m/z: $[M+H]^+$ calculated for $C_{17}H_{26}O_2$ 263.2006, found 263.2002.

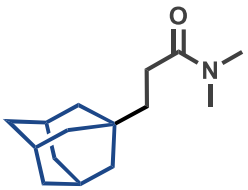

3-(Adamantan-1-yl)-N,N-dimethylpropanamide (4.15).

From **4.1b** (0.375 mmol, 1.5 equiv., 0.075 M, 82 mg), **4.2d** (0.25 mmol, 1 equiv., 0.05 M, 25 µL), $[Acr\text{-}Mes]^+(BF_4)^-$ (0.025 mmol, 10 mol%, 10 mg) in a DCE/MeOH mixture 5:1 (5 mL). Purification by column chromatography (eluent: Cyclohexane/AcOEt 100/0 to 9/1) afforded **4.15** (pale yellow oil, 40.8 mg, 70% yield). Spectroscopic data in accordance with the literature.[52]

4.15. ^{1}H NMR (300 MHz, Chloroform-*d*) δ 3.08-2.89 (m, 6H), 2.32–2.21 (m, 2H), 1.96 (s, 3H), 1.80–1.58 (m, 10H), 1.46–1.37 (m, 2H).^{13}C NMR (75 MHz, Chloroform-*d*) δ ^{13}C NMR (75 MHz, Chloroform-d) δ 174.2, 42.3, 39.4, 37.3, 37.1, 32.1, 28.8, 27.1.

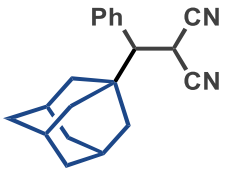

2-((Adamantan-1-yl)(phenyl)methyl)malononitrile (4.16).

From **4.1b** (0.375 mmol, 1.5 equiv., 0.075 M, 82 mg), **4.2e** (0.25 mmol, 1 equiv., 0.05 M, 38 mg), $[Acr\text{-}Mes]^+(BF_4)^-$ (0.025 mmol, 10 mol%, 10 mg) in a DCE/MeOH mixture 5:1 (5 mL). Purification by column chromatography (eluent: Cyclohexane/AcOEt 100/0 to 95/5) gave **4.16** (white solid, mp 167–169 °C, 59.4 mg, 83% yield). Spectroscopic data in accordance with the literature.[53]

4.16. ^{1}H NMR (300 MHz, Chloroform-*d*) δ ^{1}H NMR (300 MHz, DMSO-d6) δ 7.49-7.29 (m, 4H), 4.24 (d, *J* = 5.3 Hz, 1H), 2.80 (d, *J* = 5.4 Hz, 1H), 2.03 (s, 3H), 1.73–1.54 (m, 12H). ^{13}C NMR (75 MHz, Chloroform-*d*) δ 135.4, 129.8 128.8, 128.7, 113.6, 113.43, 58.2, 40.6, 36.7, 36.5, 28.5, 23.9.

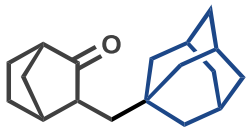

3-((Adamantan-1-yl)methyl)bicyclo[2.2.1]heptan-2-one (4.17).

From **4.1b** (0.375 mmol, 1.5 equiv., 0.075 M, 82 mg), **4.2g** (0.25 mmol, 1 equiv., 0.05 M, 28 µL), [Acr-Mes]$^+$(BF_4)$^-$ (0.025 mmol, 10 mol%, 10 mg) in a DCE/MeOH mixture 5:1 (5 mL). Purification by column chromatography (eluent: Cyclohexane/AcOEt 100/0 to 9/1) afforded **4.17** (white solid, mp 68.8–70.0 °C, 62 mg, 86% yield).

4.17. ^{1}H NMR (300 MHz, Chloroform-*d*) δ 2.63 (s, 1H), 2.59 (d, *J* = 5.1 Hz, 1H), 2.05 (dd, *J* = 8.8, 4.2 Hz, 1H), 1.95 (s, 3H), 1.74–1.56 (m, 10H), 1.49 (s, 6H), 1.42 (s, 3H), 1.04 (dd, *J* = 14.5, 9.1 Hz, 1H). ^{13}C NMR (75 MHz, Chloroform-*d*) δ 221.2, 50.1, 49.8, 42.9, 41.0, 40.1, 37.6, 37.2, 32.6, 28.8, 27.1, 25.5, 21.6. HRMS (EI) m/z: [M+H]$^+$ calculated for $C_{18}H_{26}O$ 259.2056, found 259.2045.

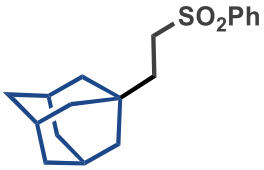

1-(2-(Phenylsulfonyl)ethyl)adamantane (4.18).

From **4.1b** (0.375 mmol, 1.5 equiv., 0.075 M, 82 mg), **4.2h** (0.25 mmol, 1 equiv., 0.05 M, 42 mg), [Acr-Mes]$^+$(BF_4)$^-$ (0.025 mmol, 10 mol%, 10 mg) in a DCE/MeOH mixture 5:1 (5 mL). Purification by column chromatography (eluent: DCM/MeOH 100/0 to 95/5) gave **4.18** (pale yellow oil, 28.3 mg, 37% yield). Spectroscopic data in accordance with the literature.[52]

4.18. ^{1}H NMR (300 MHz, Chloroform-*d*) δ 7.93–7.87 (m, 2H), 7.69–7.60 (m, 1H), 7.60–7.51 (m, 2H), 3.11–2.98 (m, 2H), 1.93 (s, 3H), 1.72–1.51 (m, 6H), 1.51–1.43 (m, 2H), 1.39 (s, 6H). ^{13}C NMR (75 MHz, Chloroform-*d*) δ 139.4, 133.7, 128.1, 51.4, 42.0, 36.9, 36.0, 32.0, 28.5.

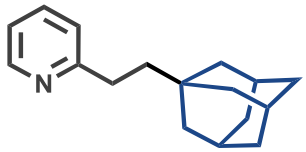

2-(2-Adamantan-1-yl)ethyl)pyridine (4.19).

From **4.1b** (0.375 mmol, 1.5 equiv., 0.075 M, 82 mg), **4.2i** (0.25 mmol, 1 equiv., 0.05 M, 26 µL), $[Acr\text{-}Mes]^+(BF_4)^-$ (0.025 mmol, 10 mol%, 10 mg) in a DCE/MeOH mixture 5:1 (5 mL). Purification by column chromatography (eluent: Cyclohexane/AcOEt 100/0 to 9/1) afforded **4.19** (colorless oil, 25.8 mg, 43% yield). Spectroscopic data in accordance with the literature.[S10]

4.19. ^{1}H NMR (300 MHz, Chloroform-*d*) δ 8.51 (dt, *J* = 5.0, 1.3 Hz, 1H), 7.57 (td, *J* = 7.6, 1.9 Hz, 1H), 7.14 (d, *J* = 7.8 Hz, 1H), 7.07 (ddd, *J* = 7.6, 4.9, 1.2 Hz, 1H), 2.80–2.68 (m, 2H), 1.98 (s, 3H), 1.82–1.58 (m, 10H), 1.56–1.54 (m, 2H), 1.53–1.44 (m, 2H). ^{13}C NMR (75 MHz, Chloroform-*d*) δ 163.6, 149.3, 136.4, 122.8, 120.9, 44.9, 42.6, 37.4, 32.6, 32.0, 28.9.

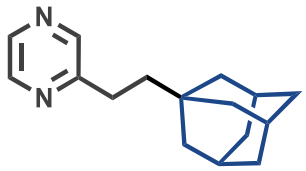

2-(2-Adamantan-1-yl)ethyl)pyrazine (4.20).

From **4.1b** (0.375 mmol, 1.5 equiv., 0.075 M, 82 mg), **4.2j** (0.25 mmol, 1 equiv., 0.05 M, 25 µL), $[Acr\text{-}Mes]^+(BF_4)^-$ (0.025 mmol, 10 mol%, 10 mg) in a DCE/MeOH mixture 5:1 (5 mL). Purification by column chromatography (eluent: Cyclohexane/AcOEt 100/0 to 9/1) afforded **4.20** (pale yellow oil, 26.8 mg, 44% yield).

4.20. ^{1}H NMR (300 MHz, chloroform-*d*) δ 8.48 (s, 2H), 8.40 (s, 1H), 2.86–2.70 (m, 2H), 2.07–1.92 (m, 3H), 1.68 (qd, *J* = 11.8, 5.9 Hz, 6H), 1.58–1.40 (m, 8H). ^{13}C NMR (75 MHz, chloroform-*d*) δ 158.8, 144.5, 143.6, 141.7, 44.1, 42.2, 37.0, 32.4, 28.9, 28.6. HRMS (EI) m/z: $[M+H]^+$ calculated for $C_{16}H_{22}N_2$ 243.1856, found 243.1851.

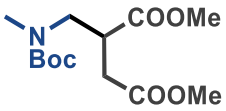

Dimethyl 2-(((*tert*-butoxycarbonyl)(methyl)amino)methyl)succinate (4.21).

From **4.1c** (0.375 mmol, 1.5 equiv., 0.075 M, 85 mg), **4.2a** (0.25 mmol, 1 equiv., 0.05 M, 31 µL), $[Acr\text{-}Mes]^+(BF_4)^-$ (0.025 mmol, 10 mol%, 10 mg) in DCE (5 mL). Purification by column chromatography (eluent: Cyclohexane/AcOEt 100/0 to 9/1) afforded **4.21** (pale yellow oil, 68.1 mg, 86% yield). Spectroscopic data in accordance with the literature.[54]

4.21. ^{1}H NMR (300 MHz, Chloroform-*d*) δ 3.70 (s, 3H), 3.67 (s, 3H), 3.47 (d, *J* = 6.8 Hz, 2H), 3.15 (m, 1H), 2.84 (s, 3H), 2.72 (dd, *J* = 16.9, 8.5 Hz, 1H), 2.48 (dd, *J* = 16.8, 5.3 Hz, 1H), 1.45 (s, 9H). ^{13}C NMR (75 MHz, Chloroform-*d*) δ 173.8, 172.1, 79.9, 52.3, 51.9, 50.5, 40.6, 33.5, 28.5.

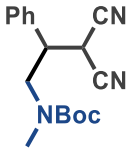

***tert*-Butyl (3,3-dicyano-2-phenylpropyl)(methyl)carbamate (4.22).**

From **4.1c** (0.375 mmol, 1.5 equiv., 0.075 M, 85 mg), **4.2e** (0.25 mmol, 1 equiv., 0.05 M, 38 mg), $[Acr\text{-}Mes]^+(BF_4)^-$ (0.025 mmol, 10 mol%, 10 mg) in DCE (5 mL). Purification by column chromatography (eluent: Cyclohexane/AcOEt 100/0 to 7/3) afforded **4.22** (pale yellow oil, 53.2 mg, 72% yield). Spectroscopic data in accordance with the literature.[55]

4.22. ^{1}H NMR (300 MHz, Chloroform-*d*) δ 7.48–7.39 (m, 3H), 7.38–7.31 (m, 2H), 4.14 (s, 1H), 3.99 (dd, *J* = 13.9, 8.2 Hz, 1H), 3.65–3.55 (m, 1H), 3.50 (dd, *J* = 13.9, 6.0 Hz, 1H), 2.81 (s, 3H), 1.48 (s, 9H). ^{13}C NMR (75 MHz, Chloroform-*d*) δ 135.1, 129.5, 129.4, 128.2, 112.2, 111.7, 81.1, 51.8, 45.6, 35.8, 28.5, 27.3.

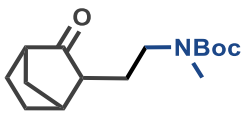

***tert*-Butyl methyl(2-(3-oxobicyclo[2.2.1]heptan-2-yl)ethyl)carbamate (4.23).**

From **4.1c** (0.375 mmol, 1.5 equiv., 0.075 M, 85 mg), **4.2g** (0.25 mmol, 1 equiv., 0.05 M, 28 µL), $[Acr\text{-}Mes]^+(BF_4)^-$ (0.025 mmol, 10 mol%, 10 mg) in DCE (5 mL).

Purification by column chromatography (eluent: Cyclohexane/AcOEt 100/0 to 1/1) afforded **4.23** (pale yellow oil, 39 mg, 54% yield).

4.23. ^{1}H NMR (300 MHz, Chloroform-*d*) 3.39–3.10 (m, 2H), 2.83 (s, 3H), 2.75–2.56 (m, 2H), 2.01–1.75 (m, 3H), 1.71–1.53 (m, 6H), 1.45 (s, 9H). ^{13}C NMR (75 MHz, Chloroform-*d*) δ 219.8, 155.8, 79.5, 51.3, 50.4, 38.5, 37.2, 34.1, 28.6, 27.0, 25.5, 21.3. HRMS (EI) m/z: $[M+Na]^+$ calculated for $C_{15}H_{25}NO_3Na$ 290.1727, found 290.1723.

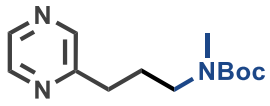

***tert*-Butyl methyl(3-(pyrazin-2-yl)propyl)carbamate (4.24).**

From **4.1c** (0.375 mmol, 1.5 equiv., 0.075 M, 85 mg), **4.2 j** (0.25 mmol, 1 equiv., 0.05 M, 25 µL), $[Acr\text{-}Mes]^+(BF_4)^-$ (0.025 mmol, 10 mol%, 10 mg) in DCE (5 mL). Purification by column chromatography (eluent: Cyclohexane/AcOEt 100/0 to 1/1) afforded **4.24** (pale yellow oil, 26.7 mg, 43% yield).

4.24. ^{1}H NMR (300 MHz, Chloroform-*d*) δ 8.47 (dd, *J* = 5.1, 1.8 Hz, 2H), 8.40 (d, *J* = 2.5 Hz, 1H), 3.30 (s, 3H), 2.95–2.74 (m, 5H), 1.98 (qui, *J* = 7.4 Hz, 2H), 1.43 (s, 9H). ^{13}C NMR (75 MHz, Chloroform-*d*) δ 155.9, 144.7, 144.2, 142.4, 48.3, 34.2, 32.7, 28.6, 27.4, 27.3. HRMS (EI) m/z: $[M+H]^+$ calculated for $C_{13}H_{21}N_3O_2$ 252.1707, found 252.1711.

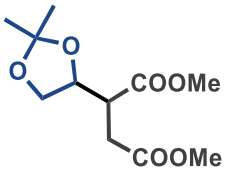

Dimethyl 2-(2,2-dimethyl-1,3-dioxolan-4-yl)succinate (4.25).

From **4.1d** (0.375 mmol, 1.5 equiv., 0.075 M, 69 mg), **4.2a** (0.25 mmol, 1 equiv., 0.05 M, 31 µL), $[Acr\text{-}Mes]^+(BF_4)^-$ (0.025 mmol, 10 mol%, 10 mg) in DCE (5 mL). Purification by column chromatography (eluent: Cyclohexane/AcOEt 100/0 to 7/3) afforded **4.25** (mixture of diastereoisomers d.r. 1:1, pale yellow oil, 51.4 mg, 90% yield). Spectroscopic data in accordance with the literature.[56]

4.25. (Mixture of diastereoisomers). ^{1}H NMR (300 MHz, Chloroform-*d*) δ 4.35 (q, *J* = 6.1 Hz, 1H), 4.29–4.06 (m, 2H), 4.03–3.94 (m, 2H), 3.84–3.75 (m, 1H), 3.71 (s, 4H), 3.68 (s, 4H), 3.25–3.13 (m, 1H), 2.85–2.72 (m, 2H), 2.51 (dd, *J* = 16.8, 4.7 Hz, 1H),

1.47 (s, 1H), 1.43–1.34 (m, 7H), 1.32 (s, 6H). ^{13}C NMR (75 MHz, Chloroform-*d*) δ 172.6, 172.2, 109.7, 75.3, 66.4, 52.3, 52.0, 44.4, 32.0, 26.4, 25.1.

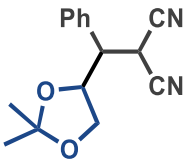

2-((2,2-Dimethyl-1,3-dioxolan-4-yl)(phenyl)methyl)malononitrile (4.26).

From **4.1d** (0.375 mmol, 1.5 equiv., 0.075 M, 69 mg), **4.1e** (0.25 mmol, 1 equiv., 0.05 M, 38 mg), [Acr-Mes]$^+$(BF_4)$^-$ (0.025 mmol, 10 mol%, 10 mg) in DCE (5 mL). Purification by column chromatography (eluent: Cyclohexane/AcOEt 100/0 to 95/5) afforded **4.26** (mixture of diastereoisomers d.r. 1:1, pale yellow solid, 97–99.9 °C, 41 mg, 65% yield).

4.26. ^{1}H NMR (300 MHz, Chloroform-*d*) δ 7.49–7.30 (m, 5H), 4.68–4.58 (m, 1H), 4.48 (d, *J* = 4.1 Hz, 1H), 3.94 (dd, *J* = 8.9, 6.2 Hz, 1H), 3.56 (dd, *J* = 9.0, 5.2 Hz, 1H), 3.16 (dd, *J* = 10.5, 4.1 Hz, 1H), 1.50 (s, 3H), 1.40 (s, 3H). ^{13}C NMR (75 MHz, Chloroform-*d*) δ 133.4, 129.8, 129.7, 128.6, 111.1, 77.6, 77.2, 76.7, 75.0, 67.9, 50.9, 27.3, 27.2, 25.2. HRMS (EI) m/z: [M+Na]$^+$ calculated for $C_{15}H_{16}N_2O_2Na$ 279.1104, found 279.1106.

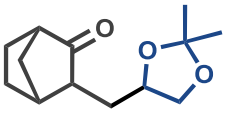

3-((2,2-Dimethyl-1,3-dioxolan-4-yl)methyl)bicyclo[2.2.1]heptan-2-one (4.27).

From **4.1d** (0.5 mmol, 2 equiv., 0.1 M, 92 mg), **4.2g** (0.25 mmol, 1 equiv., 0.05 M, 29 µL), [Acr-Mes]$^+$(BF_4)$^-$ (0.025 mmol, 10 mol%, 10 mg) in DCE (5 mL). Purification by column chromatography (eluent: Cyclohexane/AcOEt 100/0 to 1/1) afforded **4.27** (mixture of diastereoisomers d.r. 1:1, colorless oil, 41 mg, 74% yield).

4.27. (Mixture of diastereoisomers). ^{1}H NMR (300 MHz, Chloroform-*d*) δ 4.29–4.10 (m, 1H), 4.11–3.99 (m, 1H), 3.60–3.48 (m, 1H), 2.72–2.65 (m, 1H), 2.61 (t, *J* = 5.1 Hz, 1H), 2.25-2.15 (m, 1H), 2.02–1.43 (m, 8H), 1.39 (d, *J* = 2.8 Hz, 4H), 1.34 (s, 4H). ^{13}C NMR (75 MHz, Chloroform-*d*) δ 219.5, 109.1, 109.0, 75.6, 74.2, 69.7, 69.5, 51.5, 50.6, 50.4, 39.8, 38.6, 37.3, 31.0, 30.2, 27.1, 25.9, 25.8, 25.6, 25.5, 21.6, 21.5. HRMS (EI) m/z: [M+H]$^+$ calculated for $C_{13}H_{20}O_3$ 247.1305, found 247.1306.

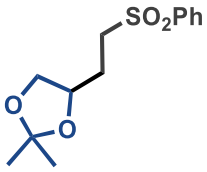

2,2-Dimethyl-4-(2-(phenylsulfonyl)ethyl)-1,3-dioxolane (4.28).

From **4.1d** (0.5 mmol, 2 equiv., 0.1 M, 92 mg), **4.2h** (0.25 mmol, 1 equiv., 0.05 M, 42 mg), $[Acr\text{-}Mes]^+(BF_4)^-$ (0.025 mmol, 10 mol%, 10 mg) in DCE (5 mL). Purification by column chromatography (eluent: Cyclohexane/AcOEt 100/0 to 2/3) afforded **4.28** (pale yellow oil, 55 mg, 82% yield). Spectroscopic data are in accordance with the literature.[57]

4.28. ^{1}H NMR (300 MHz, Chloroform-*d*) δ 7.91 (d, *J* = 7.9, Hz, 2H), 7.74–7.59 (m, 1H), 7.62–7.48 (m, 2H), 4.23–4.08 (m, 1H), 4.03 (dd, *J* = 8.2, 6.0 Hz, 1H), 3.54 (dd, *J* = 8.2, 6.1 Hz, 1H), 3.29 (ddd, *J* = 14.3, 10.7, 5.2 Hz, 1H), 3.15 (ddd, *J* = 14.1, 10.7, 5.4 Hz, 1H), 2.07–1.95 (m, 1H), 1.95–1.83 (m, 1H), 1.32 (s, 3H), 1.28 (s, 3H). ^{13}C NMR (75 MHz, chloroform-*d*) δ 139.2, 133.9, 129.5, 128.1, 109.6, 73.9, 68.9, 52.9, 27.1, 26.9, 25.5.

4.6 References.

1) (a) Albini, A., Fagnoni, M. *Photochemically-Generated Intermediates in Synthesis*, John Wiley & Sons, Inc: Hoboken, NJ, **2013**, p. 380. (b) Ravelli, D., Protti, S., Fagnoni, M. Carbon-Carbon Bond Forming Reactions via Photogenerated Intermediates. *Chem. Rev.* **2016**, *116*, 9850–9913. (c) *Visible Light Photocatalysis in Organic Chemistry*, Stephenson, C. R. J., Yoon, T. P., MacMillan, D. W. C., Eds., Wiley-VCH: Weinheim, Germany, **2018**, p. 456. (d) *Chemical Photocatalysis*, 2nd ed., Konig, B., Ed., De Gruyter, **2020**, Vol. 512. (e) Protti, S., Ravelli, D., Fagnoni, M. Designing Radical Chemistry by Visible-Light Promoted Homolysis. *Trends Chem*. **2022**, *4*, 305–317.
2) (a) Hoffmann, N. Photochemical reactions of aromatic compounds and the concept of the photon as a traceless reagent. *Photochem. Photobiol. Sci.* **2012**, *11*, 1613–1641. (b) Bonfield, H. E., Knauber, T., Levesque, F., Moschetta, E. G., Susanne, F., Edwards, L. J. Photons as a 21st century reagent. *Nat. Commun*. **2020**, *11*, No. 804.
3) For recent reviews on the photogeneration of alkyl radicals see: (a) Goddard, J. P., Ollivier, C., Fensterbank, L. Photoredox Catalysis for the Generation of Carbon

Centered Radicals. *Acc. Chem. Res.* **2016**, *49*, 1924−1936. (b) Matsui, J. K., Lang, S. B., Heitz, D. R., Molander, G. A. Photoredox-Mediated Routes to Radicals: The Value of Catalytic Radical Generation in Synthetic Methods Development. *ACS Catal.* **2017**, *7*, 2563−2575. (c) Roslin, S., Odell, L. R. Visible- Light Photocatalysis as an Enabling Tool for the Functionalization of Unactivated C(sp^3)-Substrates. *Eur. J. Org. Chem.* **2017**, 1993−2007. (d) Pitre, S. P., Weires, N. A., Overman, L. E. Forging C(sp^3)−C(sp^3) Bonds with Carbon-Centered Radicals in the Synthesis of Complex Molecules. *J. Am. Chem. Soc*. **2019**, *141*, 2800−2813. (e) Crespi, S., Fagnoni, M. Generation of Alkyl Radicals: From the Tyranny of Tin to the Photon Democracy. *Chem. Rev.* **2020**, *120*, 9790−9833. (f) Niu, P., Li, J., Zhang, Y., Huo, C. One Electron Reduction of Redox-Active Esters to Generate Carbon-Centered Radicals. *Eur. J. Org. Chem*. **2020**, 5801−5814. (g) Correia, J. T. M., Fernandes, V. A., Matsuo, B. T., Delgado, J. A. C., de Souza, W. C., Paixão, M. W. Photoinduced deaminative strategies: Katritzky salts as alkyl radical precursors. *Chem. Commun*. **2020**, *56*, 503−514. (h) Karmakar, S., Silamkoti, A., Meanwell, N. A., Mathur, A., Kumar Gupta, A. Utilization of C(sp^3)-Carboxylic Acids and Their Redox- Active Esters in Decarboxylative Carbon-Carbon Bond Formation. *Adv. Synth. Catal*. **2021**, *363*, 3693−3736. (i) Parida, S. K., Mandal, T., Das, S., Kumar Hota, S., De Sarkar, S., Murarka, S. Single Electron Transfer-Induced Redox Processes Involving *N*-(Acyloxy)-phthalimides. *ACS Catal*. **2021**, *11*, 1640−1683. (j) Capaldo, L., Ravelli, D., Fagnoni, M. Direct Photocatalyzed Hydrogen Atom Transfer (HAT) for Aliphatic C−H Bonds Elaboration. *Chem. Rev*. **2022**, *122*, 1875−1924. (k) Corce, V., Ollivier, C., Fensterbank, L. Boron, silicon, nitrogen and sulfur-based contemporary precursors for the generation of alkyl radicals by single electron transfer and their synthetic utilization. *Chem. Soc. Rev.* **2022**, *51*, 1470−1510.

4) Yoshida, J.-i., Kataoka, K., Horcajada, R., Nagaki, A. Modern Strategies in Electroorganic Synthesis Modern Strategies in Electroorganic Synthesis. *Chem. Rev.* **2008**, *108*, 2265−2299.

5) (a) Roth, H. G., Romero, N. A., Nicewicz, D. A. Experimental and Calculated Electrochemical Potentials of Common Organic Molecules for Applications to Single-Electron Redox Chemistry. *Synlett*. **2016**, *27*, 714−723. (b) Chu, L., Ohta, C., Zuo, Z., MacMillan, D. W. C. Carboxylic Acids as A Traceless Activation Group

for Conjugate Additions: A Three-Step Synthesis of (±)-Pregabalin. *J. Am. Chem. Soc*. **2014**, *136*, 10886−10889.

6) Knauber, T., Chandrasekaran, R., Tucker, J. W., Chen, J. M., Reese, M., Rankic, D. A., Sach, N., Helal, C. Ru/Ni Dual Catalytic Desulfinative Photoredox Csp^2-Csp^3 Cross-Coupling of Alkyl Sulfinate Salts and Aryl Halides*. Org. Lett.* **2017**, *19*, 6566−6569.
7) Yasu, Y., Koike, T., Akita, M. Visible Light-Induced Selective Generation of Radicals from Organoborates by Photoredox Catalysis. *Adv. Synth. Catal.* **2012**, *354*, 3414−3420.
8) Corce, V., Chamoreau, L. M., Derat, E., Goddard, J. P., Ollivier, C., Fensterbank, L. Silicates as Latent Alkyl Radical Precursors: Visible-Light Photocatalytic Oxidation of Hypervalent Bis-Catecholato Silicon Compounds. *Angew. Chem., Int. Ed.* **2015**, *54*, 11414−11418.
9) Nawrat, C. C., Jamison, C. R., Slutskyy, Y., MacMillan, D. W. C., Overman, L. E. Oxalates as Activating Groups for Alcohols in Visible Light Photoredox Catalysis: Formation of Quaternary Centers by Redox-Neutral Fragment Coupling. J. Am. Chem. Soc. **2015**, *137*, 11270−11273.
10) Klauck, F. J. R., James, M. J., Glorius, F. Deaminative Strategy for the Visible-Light Mediated Generation of Alkyl Radicals. *Angew. Chem., Int. Ed.* **2017**, *56*, 12336−12339.
11) Gutierrez-Bonet, Á., Tellis, J. C., Matsui, J. K., Vara, B. A., Molander, G. A. 1,4-Dihydropyridines as Alkyl Radical Precursors: Introducing the Aldehyde Feedstock to Nickel/Photoredox Dual Catalysis. *ACS Catal.* **2016**, *6*, 8004−8008.
12) Fagnoni, M., Mella, M., Albini, A. Radical addition to alkenes via electron transfer photosensitization. *J. Am. Chem. Soc.* **1995**, *117*, 7877−7881.
13) Yoshida, J.-i., Nishiwaki, K. Redox Selective Reactions of Organo-Silicon and -Tin Compounds. *J. Chem. Soc. Dalton Trans*. **1998**, *16*, 2589−2596.
14) Mella, M., Fasani, E., Albini, A. Electron Transfer Photoinduced Cleavage of Acetals. A Mild Preparation of Alkyl Radicals. *J. Org. Chem.* **1992**, *57*, 3051−3057.
15) Hu, J., Wang, J., Nguyen, T. H., Zheng, N. The chemistry of amine radical cations produced by visible light photoredox catalysis. *Beilstein J. Org. Chem*. **2013**, *9*, 1977−2001.

16) Jonsson, M., Wayner, D. D. M., Lusztyk, J. Redox and Acidity Properties of Alkyl- and Arylamine Radical Cations and the Corresponding Aminyl Radicals. *J. Phys. Chem. A.* **1996**, *100*, 17539−17543.

17) (a) Beatty, J. W., Stephenson, C. R. J. Amine Functionalization via Oxidative Photoredox Catalysis: Methodology Development and Complex Molecule Synthesis. *Acc. Chem. Res.* **2015**, *48*, 1474−1484. (b) Morris, S. A., Wang, J., Zheng, N. The Prowess of Photogenerated Amine Radical Cations in Cascade Reactions: From Carbocycles to Heterocycles. *Acc. Chem. Res.* **2016**, *49*, 1957−1968.

18) Fagnoni, M., Dondi, D., Ravelli, D., Albini, A. Photocatalysis for the formation of the C-C Bond. *Chem. Rev.* **2007**, *107*, 2725−2756.

19) Murugesan, K., Donabauer, K., Narobe, R., Derdau, V., Bauer, A., Konig, B. Photoredox-Catalyzed Site-Selective Generation of Carbanions from C(sp^3)−H Bonds in Amines. *ACS Catal.* **2022**, *12*, 3974−3984.

20) Zhu, M., Zheng, N. Photoinduced cleavage of N-N bonds of aromatic hydrazines and hydrazides by visible light. *Synthesis.* **2011**, 2223−2236.

21) Capaldo, L., Lafayette Quadri, L., Ravelli, D. Photocatalytic hydrogen atom transfer: the philosopher's stone for late-stage functionalization? *Green Chem.* **2020**, *22*, 3376−3396.

22) The generation of alkyl radicals from an amine radical cation has been investigated by computational analyses, see: Hammerum, S., Norrman, K., Solling, T. I., Andersen, P. E., Bo Jensen, L., Vulpius, T. Competing Simple Cleavage Reactions: The Elimination of Alkyl Radicals from Amine Radical Cations. *J. Am. Chem. Soc.* **2005**, *127*, 6466−6475.

23) (a) Sundberg, R. J., Desos, P., Gadamasetti, K. G., Sabat, M. Photoactive C16-C21 Fragmentation of Catharanthine. *Tetrahedron Lett.* **1991**, *32*, 3035−3038. (b) Cocquet, G., Rool, P., Ferroud, C. A Catalytic Versus Stoichiometric Electron Transfer Promoted Selective C16-C21 Bond Cleavage of Catharanthine. *Tetrahedron Lett.* **2001**, *42*, 839−841. (c) Beatty, J. W., Stephenson, C. R. J. Synthesis of (−)-Pseudota-bersonine, (−)-pseudovincadifformine, and (+)-Coronaridine Enabled by Photoredox Catalysis in Flow. *J. Am. Chem. Soc.* **2014**, *136*, 10270−10273.

24) Maity, S., Zhu, M., Shinabery, R. S., Zheng, N. Intermolecular [3 + 2] Cycloaddition of Cyclopropylamines with Olefins by Visible-Light Photocatalysis. *Angew. Chem., Int. Ed.* **2012**, *51*, 222–226.

25) Cai, S., Zhao, X., Wang, X., Liu, Q., Li, Z., Wang, D. Z., Visible-Light-Promoted, C–C. Bond Cleavage: Photocatalytic Generation of Iminium Ions and Amino Radicals. Angew. Chem., Int. Ed. **2012**, *51*, 8050–8053.

26) (a) Lv, X.-Y., Abrams, R., Martin, R. Dihydroquinazolinones as adaptative C(sp^3) handles in arylations and alkylations via dual catalytic C–C bond-functionalization. *Nat. Commun.* **2022**, *13*, No. 2394. (b) Li, L., Fang, L., Wu, W., Zhu, J. Visible-Light-Mediated Intermolecular Radical Conjugate Addition for the Construction of Vicinal Quaternary Carbon Centers*. Org. Lett.* **2020**, *22*, 5401–5406.

27) Fagnoni, M., Protti, S., Ravelli, D., Albini, A. Spectroscopic characterization of photo-accumulated radical anions. A Litmus test to evaluate the efficiency of Photoinduced Electron Transfer (PET) processes. *Beilstein J. Org. Chem*. **2013**, *9*, 800–808.

28) Wu, Y., Kim, D., Teets, T. S. Photophysical Properties and Redox Potentials of Photosensitizers for Organic Photoredox Transformations. *Synlett*. **2022**, *33*, 1154–1179.

29) (a) Quasdorf, K. W., Overman, L. E. Catalytic enantioselective synthesis of quaternary carbon stereocentres. *Nature*. **2014**, *516*, 181–191. (b) Liu, Y., Han, S.-J., Liu, W.-B., Stoltz, B. M. Catalytic Enantioselective Construction of Quaternary Stereocenters: Assembly of Key Building Blocks for the Synthesis of Biologically Active Molecules. *Acc. Chem. Res.* **2015**, *48*, 740–751. (c) Jamison, C. R., Overman, L. E. Fragment Coupling with Tertiary Radicals Generated by Visible-Light Photocatalysis. *Acc. Chem. Res*. **2016**, *49*, 1578–1586. (d) Ling, T., Rivas, F. All-carbon quaternary centers in natura products and medicinal chemistry: recent advances. *Tetrahedron.* **2016**, *72*, 6729–6777. (e) Xue, W., Jia, X., Wang, X., Tao, X., Yin, Z., Gong, H. Nickel-catalyzed formation of quaternary carbon centers using tertiary alkyl electrophiles. *Chem. Soc. Rev.* **2021**, *50*, 4162–4184.

30) (a) De Clercq, E. Antiviral agents active against influenza A viruses. *Nat. Rev. Drug Discov.* **2006**, *5*, 1015–1025. (b) Lamoureux, G., Graciela, A. Use of the

adamantane structure in medicinal chemistry. *Curr. Med. Chem.* **2010**, *17*, 2967–2978. (c) Wanka, L., Iqbal, K., Schreiner, P. R. The lipophilic bullet hits the targets: medicinal chemistry of adamantane derivatives. *Chem. Rev.* **2013**, *113*, 3516–3604. (d) Stockdale, T. P., Williams, C. M. Pharmaceuticals that contain polycyclic hydrocarbon scaffolds. *Chem. Soc. Rev.* **2015**, *44*, 7737–7763. (e) Štimac, A., Sekutor, M., Mlinaric-Majerski, K., Frkanec, L., Frkanec, R. Adamantane in Drug Delivery Systems and Surface Recognition. *Molecules*, **2017**, *22*, 297.

31) Agnew-Francis, K. A., Williams, C. M. Catalysts Containing the Adamantane Scaffold. *Adv. Synth. Catal.* **2016**, *358*, 675–700.

32) Barton, D. H. R., Sas, W. The invention of radical reactions. Part XIX. The synthesis of very hindered quinones. *Tetrahedron.* **1990**, *46*, 3419–3430.

33) (a) Pratsch, G., Lackner, G. L., Overman, L. E. Constructing Quaternary Carbons from *N*-(Acyloxy)phthalimide Precursors of Tertiary Radicals Using Visible-Light Photocatalysis. *J. Org. Chem.* **2015**, *80*, 6025–6036. (b) Okada, K., Okamoto, K., Morita, N., Okubo, K., Oda, M. Photosensitized decarboxylative Michael addition through *N*-(acyloxy)phthalimides via an electron-transfer mechanism. *J. Am. Chem. Soc.* **1991**, *113*, 9401–9402.

34) (a) Lackner, G. L., Quasdorf, K. W., Overman, L. E. Direct Construction of Quaternary Carbons from Tertiary Alcohols via Photoredox-Catalyzed Fragmentation of *tert*-Alkyl *N*-Phthalimidoyl Oxalates. *J. Am. Chem. Soc.* **2013**, *135*, 15342–15345. (b) Wang, Q., Yue, L., Bao, Y., Wang, Y., Kang, D., Gao, Y., Yuan, Z. Oxalates as Activating Groups for Tertiary Alcohols in Photoredox-Catalyzed gem-Difluoroallylation To Construct All-Carbon Quaternary Centers. *J. Org. Chem.* **2022**, *87*, 8237–8247.

35) (a) Furst, L., Narayanam, J. M. R., Stephenson, C. R. J. Total Synthesis of (+)-Gliocladin C Enabled by Visible-Light Photoredox Catalysis. *Angew. Chem., Int. Ed.* **2011**, *50*, 9655–9659. (b) Zhu, Y., Zhang, L., Luo, S. Asymmetric α-Photoalkylation of β-Ketocarbonyls by Primary Amine Catalysis: Facile Access to Acyclic All-Carbon Quaternary Stereocenters. *J. Am. Chem. Soc.* **2014**, *136*, 14642–14645.

36) Nambo, M., Tahara, Y., Yim, J. C.-H., Yokogawa, D., Crudden, C. M. Synthesis of quaternary centres by single electron reduction and alkylation of alkylsulfones. *Chem. Sci.* **2021**, *12*, 4866–4871.

37) Qin, T., Cornella, J., Li, C., Malins, L. R., Edwards, J. T., Kawamura, S., Maxwell, B. D., Eastgate, M. D., Baran, P. S. A general alkyl-alkyl cross-coupling enabled by redox-active esters and alkylzinc reagents. *Science,* **2016**, *352*, 801–805.

38) (a) Hand, R., Nelson, R. F. The Electrochemical Oxidation of *N,N*-Dimethylaniline. *J. Electrochem. Soc.* **1970**, *117*, 1353–1357. (b) Dombrowski, G. W., Dinnocenzo, J. P., Zielinski, P. A., Farid, S., Wosinska, Z. M., Gould, I. R. Efficient Unimolecular Deprotonation of Aniline Radical Cations. *J. Org. Chem*. **2005**, *70*, 3791–3800. (c) Brown, T. A., Chen, H., Zare, R. N. Detection of the Short-Lived Radical Cation Intermediate in the Electrooxidation of *N,N*-Dimethylaniline by Mass Spectrometry. *Angew. Chem., Int. Ed.* **2015**, *54*, 11183–11185.

39) Zhao, H., Leonori, D. Minimization of Back-Electron Transfer Enables the Elusive sp3 CH Functionalization of Secondary Anilines. *Angew. Chem., Int. Ed.* **2021**, *60*, 7669–7674.

40) Capaldo, L., Riccardi, R., Ravelli, D., Fagnoni, M. Acyl Radicals from Acylsilanes: Photoredox Catalyzed Synthesis of Unsymmetrical Ketones. *ACS Catal.* **2018**, *8*, 304–309.

41) Takeuchi, K., Kitagawa, I., Akiyama, F., Shibata, T., Kato, M., Okamoto, K. Rin Expansion of Bridgehead Aldehydes with 1-Adamantanecarbonyl Cation or Benzoyl Trifluoromethanesulfonate: A New Route to Bicyclic and Tricyclic 1,2-Diols. *Synthesis,* **1987**, 612–615.

42) Bureau, R., Mortier, J., Joucla, M. Formation of azomethine ylids by thermolysis of oxazolidines. Study of the reaction in solution and in the gaseous phase. *Bull. Soc. Chim. Fr*. **1993**, *130*, 584–596.

43) Waller, R. W., Diorazio, L. J., Taylor, B. A., Motherwell, W. B., Sheppard, T. D., Isocyanide based multicomponent reactions of oxazolidines and related systems. *Tetrahedron*, **2010**, *66,* 6496–6507.

44) Rohe, S., Morris, A. O., McCallum, T., Barriault, L. Hydrogen Atom Transfer Reactions via Photoredox Catalyzed Chlorine Atom Generation. *Angew. Chem. Int. Ed.* **2018**, *57*, 15664–15669.

45) Zhou, X., Zhang, G., Gao, B., Huang**,** H. Palladium-Catalyzed Hydrocarbonylative C–N Coupling of Alkenes with Amides. *Org. Lett.* **2018**, *20,* 2208–2212.

46) Uchikura, T., Moriyama, K., Toda, M., Mouri, T., Ibáñez, I., Akiyama, T. Benzothiazolines as radical transfer reagents: hydroalkylation and hydroacylation of alkenes by radical generation under photoirradiation conditions. *Chem. Commun*. **2019**, *55*, 11171–11174.

47) Pitre, S. P., Allred, T. K., Overman, L. E. Lewis Acid Activation of Fragment-Coupling Reactions of Tertiary Carbon Radicals Promoted by Visible-Light Irradiation of EDA Complexes. *Org. Lett.* **2021**, *23*, 1103–1106.

48) Petrier, C., De Souza Barbosa, J., Dupuy, C., Luche, J. L. Ultrasound in organic synthesis. Preparation of organozinc reagents and their nickel-catalyzed reactions with α,β-unsaturated carbonyl compounds, *J. Org. Chem.* **1985**, *50*, 5761–5765.

49) Xue, F., Wang, F., Liu, J., Di, J., Liao, Q., Lu, H., Zhu, M., He, L., He, H., Zhang, D., Song, H., Liu, X.Y., Qin. Y. A Desulfurative Strategy for the Generation of Alkyl Radicals Enabled by Visible-Light Photoredox Catalysis. *Angew. Chem. Int. Ed.* **2019**, *57*, 6667–6671.

50) Pang, H., Wang, Y., Gallou, F., Lipshutz, B. H. Fe-catalyzed reductive couplings of terminal (hetero) aryl alkenes and alkyl halides under aqueous micellar conditions. *J. Am. Chem. Soc.* **2019**, *141*, 17117–17124.

51) Braquet P., Pirotzky E., Godfroid J.-J., Heymans F. 2-substituted *N,N*'-ditrimethoxybenzoyl piperazines and therapeutic compositions containing them. *US Pat.* **1991**, US5019576 A S22.

52) Sato, R., Okamoto, R., Ishizuka, T., Nakayama, A., Karanjit, S., Namba, K. Microwave-assisted Tertiary Carbon Radical Reaction for Construction of Quaternary Carbon Center. Chem. Lett. **2019**, *48*, 414–417.

53) Xu, Q. H., Wei, L. P., Xiao, B. Alkyl-GeMe3: Neutral Metalloid Radical Precursors upon Visible-Light Photocatalysis. Angew. Chem. Int. Ed. **2022**, *61*, e202115592.

54) Schweitzer-Chaput, B., Horwitz, M. A., Beato, E. P., Melchiorre, P. Photochemical generation of radicals from alkyl electrophiles using a nucleophilic organic catalyst. Nat. Chem. **2019**, *11*, 129–135.

55) Ohmatsu, K., Suzuki, R., Suzuki, R., Furukawa, Y., Sato, M., Ooi, T. Zwitterionic 1, 2, 3-triazolium amidate as a catalyst for photoinduced hydrogen-atom transfer radical alkylation. ACS Catal. **2020**, *10*, 2627–2632.
56) Hayakawaa, M., Shimizua, R., Omoria, H., Shirotaa, H., Uchidaa, K., Mashimoa, H., Ryuusei, H. X., Seiya, Y., Yoshiki, N., Chuanxiang, W., Tadashi, L., Ouchia A. Photochemical addition of cyclic ethers/acetals to olefins using tBuOOtBu: Synthesis of masked ketones/aldehydes and diols. *Tetrahedron* **2020**, *76*, 131557.
57) Raviola, C., Ravelli, D. Efficiency and Selectivity Aspects in the C–H Functionalization of Aliphatic Oxygen Heterocycles by Photocatalytic Hydrogen Atom Transfer. *Synlett.* **2019**, *30*, 803–808.

Chapter 5

Photoredox Catalyzed Release of Carbon-based Radicals from 2-substituted-1,3-imidazolidines

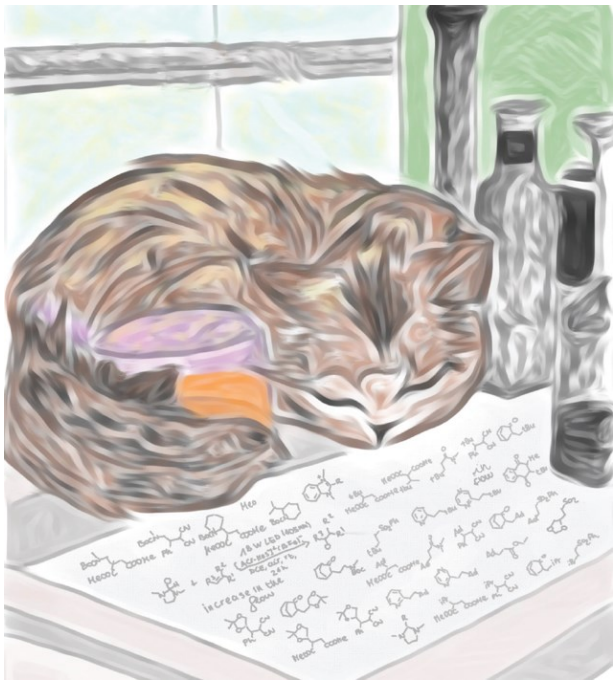

This chapter is based on:

Luguera Ruiz, A.; Mariani, E; Protti, S.; Fagnoni, M. Photoredox catalyzed release of carbon-based radicals from 2-substituted-1,3-imidazolidines. *Org. Chem. Front.* **2024**, *11*, 661-667. Highlighted as graphical abstract: *Org. Chem. Front.* **2024**, *11*, 1015-1016.

5.1 Introduction.

Carbon based radicals were probably the most used intermediates in synthesis in the past decades.[1] In this context, photoredox catalysis has become the elective method for their generation in a more sustainable and fancy manner than classical synthetic methodologies.[2,3] During the last few years, photoredox generation of alkyl radicals has allowed for the development of protocols for the formation of C(sp^3)–C(sp^3) bonds which is currently a hot topic in organic synthetic chemistry.[2,4] Such a strategy made use of radical precursors bearing redox active moieties that allow their easy oxidation/reduction by a suitable photoexcited catalyst (PC).[2d] Several PCs exhibiting variable oxidation/reduction capability have been designed and investigated for this purpose, but in the case of substrates difficult to oxidize/reduce, the number of suitable PCs strongly decreased.

For these reasons, the redox active moiety is often charged, to shift the radical precursors to a "comfort zone" that allows testing several visible light absorbing PCs. The preparation of these precursors may be in some cases troublesome or impose restrictions to the reaction conditions (the choice of solvent, the compatibility of additives and so on).

The obvious, but not trivial strategy to overcome such limitations is having recourse to easily oxidizable/reducible uncharged derivatives, and recently, we reported that substituted oxazolidines (E_{ox} ca. 1.3 V vs. SCE) perfectly fulfill this requirement.[5] However, we were intrigued to search for further uncharged super electron donors (SEDs)[6] able to release a set of radical intermediates upon oxidation, including tertiary, α-oxy and α-amino carbon-based radicals. In this context, we focused our attention on aminals. The most famous compounds belonging to this class are *N,N*-dimethyldihydrobenzoimidazoles (**5.I**, Scheme 5.1). 1,3-Dimethyl-2-phenylbenzimidazoline (DMBI) was extensively used to promote a single electron transfer reaction (SET) acting as a reducing agent on compounds R'–X with no need of any additives (Scheme 5.1, path a).[7,8] When R'–X is a haloketone, a reductive dehalogenation occurred via the fragmentation of the resulting radical anion and hydrogen incorporation from radical **5.V** (paths a′ and a″).[7d,8b] The radical cation (**5.II**) formed from the aminal may lose a proton to give radical **5.III** (path *b*) again

prone to reduce R'–X leading to the corresponding benzimidazolium salt **5.IV** (path *c*).[9] To strengthen the reducing power of compounds **5.I** the process was later promoted by light via a photoinduced electron transfer reaction (Scheme 5.1).[10] Interestingly, aminals **5.I** may also act as efficient hydrogen atom donors to radicals (e.g. **5.V**, path *d*)[9] More recently, even radical **5.III** has found application as a surrogate of an acyl radical **5.VI** in the reaction with styrenes.[11]

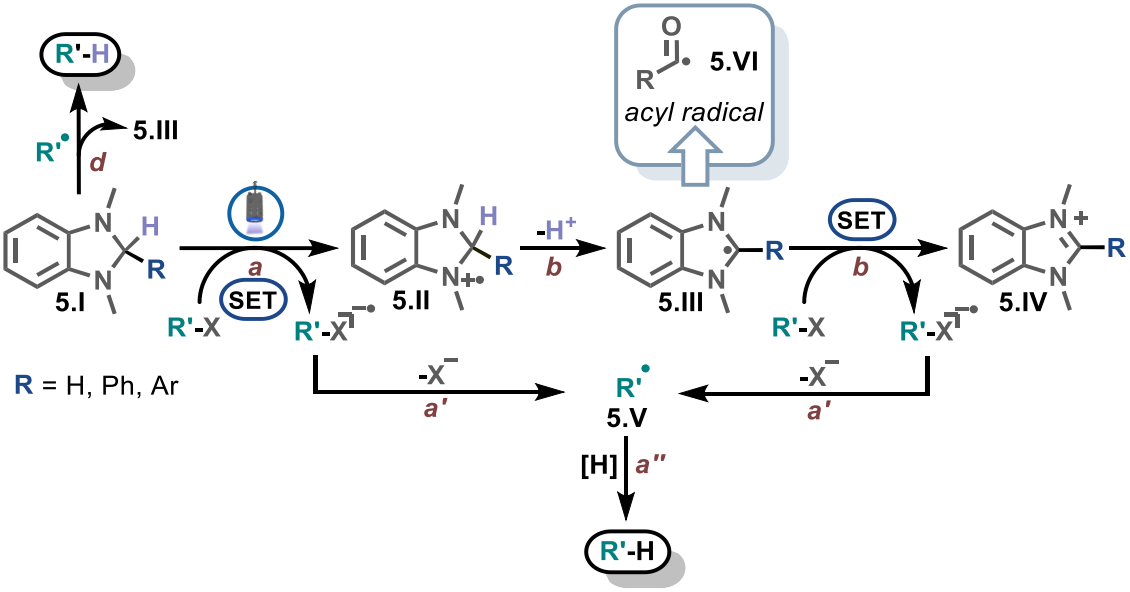

Scheme 5.1. Various pathways in the (photo)chemistry of *N,N*-dimethyldihydrobenzo imidazoles **5.I.**

In this context, a modified DMBI structure (dihydroquinazolinones, **5.VII**) has emerged as a radical precursor (Scheme 5.2a).[12] The strategy relies on the aromatic stabilization energy (ASE) of the redox moiety **5.VIII** when released from the fragmentation of the radical cation.[13]

In such a way, the efficiency in the fragmentation of the radical cation pushed the liberation of a plethora of different radicals by C–C bond cleavage. However, the strategy suffers from some drawbacks such as the poor atom economy of the process (due to the weight of the aromatized fragment **5.VIII**) and the fact that pre-aromatic derivatives **5.VII** must be obtained only from methyl or phenyl ketones. This is probably since the C–C bond cleavage of the other substituents present in position 2 in compound **5.VII** must be suppressed thanks to the instability of the methyl/phenyl radicals with respect to the desired radical released (mostly tertiary or, however, stabilized). The radical may, however, be liberated even under

photosensitized conditions.[14] Related imidazolidinones have likewise an increased role in dual photocatalytic reactions as chiral bases while remaining, however, photochemically inactive.[15]

Inspired by these studies and by our achievement in the light induced visible light generation of radical intermediates[5] we envisioned that simple aminals such as 2-substituted 1,3-dimethylimidazolidines **5.IX** (Scheme 5.2b) could be valid candidates to test the release of carbon radicals via C–C bond cleavage by a photoredox SET process. We thus reasoned that the presence of two nitrogen atoms may induce good oxidizability, and noteworthily, the stability of the resulting cation **5.X** may drive the fragmentation even if this does not evolve into an aromatic derivative. In this work, we report that readily prepared imidazolidines act as more atom-economical, with respect to quinazolidinones, uncharged alkyl radical precursors as detailed below.

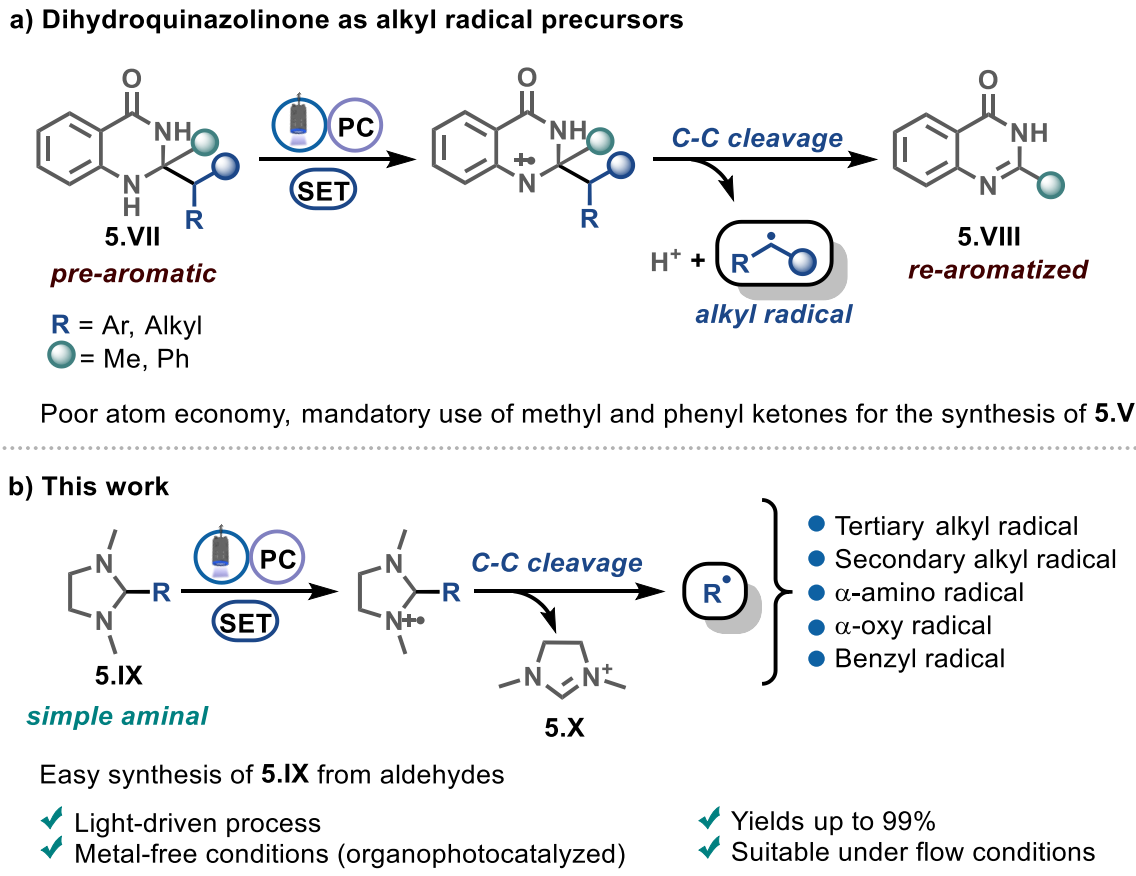

Scheme 5.2. Photocatalyzed generation of carbon-based radicals from the single electron transfer oxidation of (a) dihydroquinazolinones **5.VII** and (b) 2-substituted imidazolidines **5.IX** (this work).

5.2 Results and discussion.

Different imidazolidines **5.1a–j** (Figure 5.1a) were smoothly prepared by condensation of the corresponding aldehyde with *N,N′*-dimethylethylenediamine. These heterocycles exhibit an oxidation potential of ca. 1.0 V vs. SCE as shown in Figure 5.1b for compound **5.1c** (E_{ox} = 1.16 V vs. SCE). The more accessible E_{ox} allowed us to investigate the use of several colored PCs for the radical addition onto electron deficient C=C double bonds.

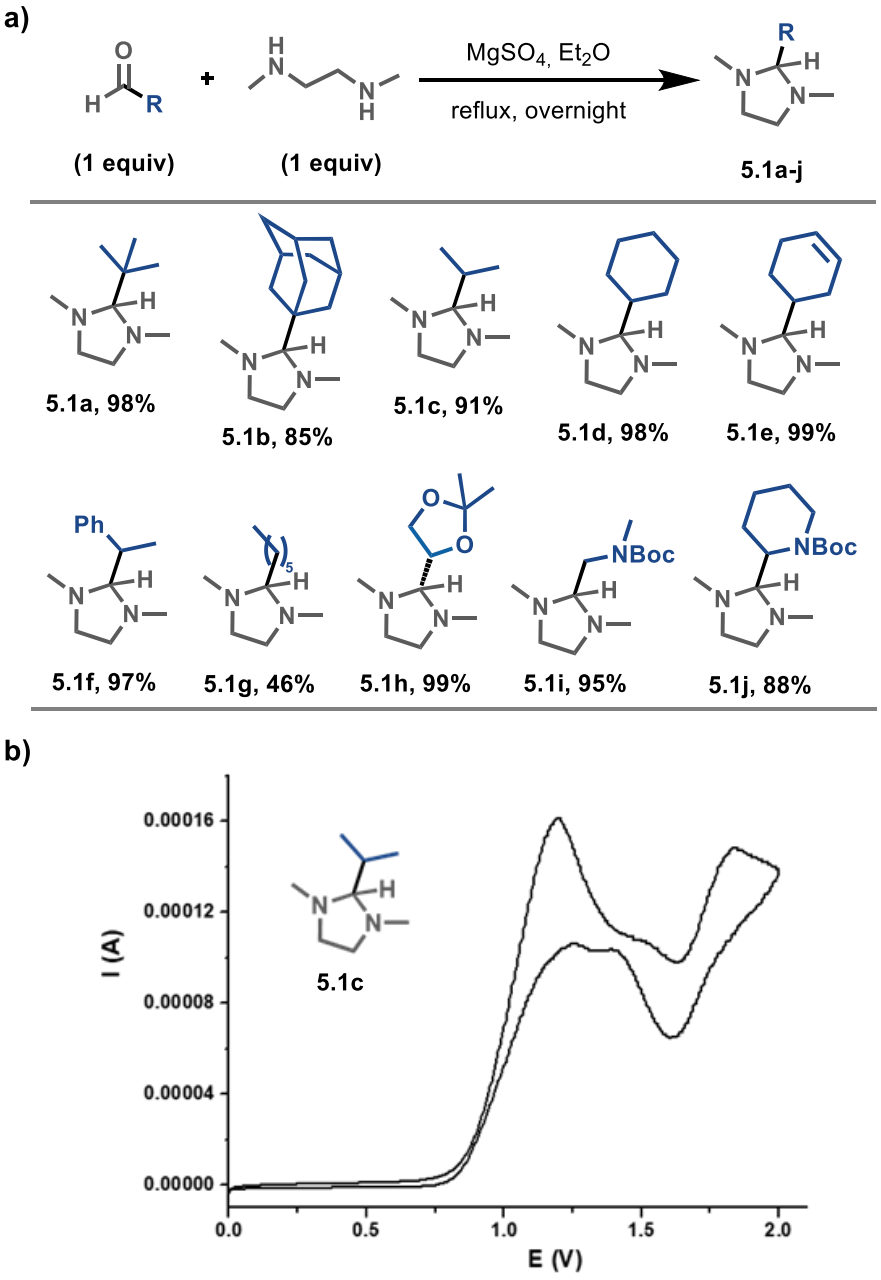

Figure 5.1. a) Synthesis of imidazolidines **5.1a-j**. b) Cyclic voltammetry of imidazolidines **5.1c**.

With the aim of investigating the feasibility of our proposal, we initially focused on the *tert*-butylation of dimethylmaleate **5.2a** by using imidazolidine **5.1a** as the model reactant. Different reaction parameters were investigated, and these included the nature of the photocatalyst, the reaction media, the stoichiometric ratio, and the influence of oxygen on the reaction outcome (Table 5.1).

Table 5.1. Optimization of the reaction model for the photoinduced *tert*-butylation of **5.2a**. Picture of irradiation set-up: A) Before irradiation. B) During irradiation.

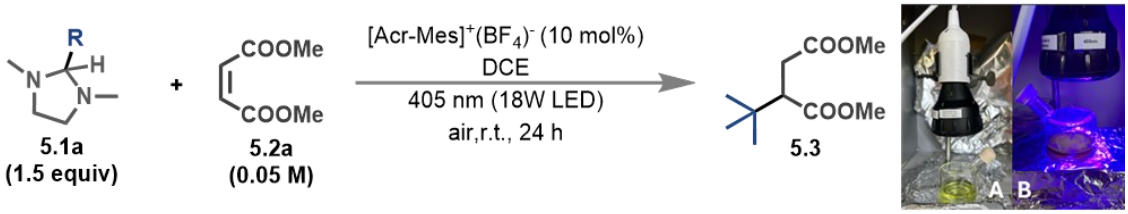

Entry	Deviations from the standard conditions	5.3 (% Yield)
1	$Ph_3Pyrylium^+$ BF_4^- (10 mol%)	-
2	$Ir(ppy)_3$ (5 mol%), N_2	-
3	4CzIPN (10 mol%), N_2	98
4	**None**	**99**
5	Acr-Mes^+ BF_4^- (10 mol%), N_2	90
6	3CzClIPN (10 mol%), N_2, CPME	51
7	3CzClIPN (10 mol%), N_2, DMC	22
8	MeOH as solvent	-
9	MeCN as solvent	-
10	DCM as solvent	84
11	**5.1a** (1.25 equiv.)	53
12	Acr-Mes^+ BF_4^- (5 mol%)	71
13	No light	-
14	**Natural sunlight**, 2 days, 6 hours/day	32
15	TEMPO (1.0 equiv.)	50

CPME: Cyclopentyl methyl ether.
DMC: Dimethylcarbonate.

Gratifyingly, the desired product **5.3** was isolated in almost quantitative amount, 99% yield (Table 5.1, entry 4), when $[Acr\text{-}Mes]^+(BF_4)^-$ (E^*_{RED} > 2.19 V vs. SCE [16]) was used as a PC. Similar results were found by employing 4CzIPN (E^*_{RED} > 1.38 V vs.

SCE[16]) under N_2 atmosphere (entry 3). The 3CzClIPN photocatalyst (E^*_{RED} > 1.56 V vs. SCE [16]) showed a poor performance (entry 6-7) whereas the use of both pyrylium salts (entry 1) and $Ir(ppy)_3$ (entry 2) did not lead to the desired product. A slight decrease in the reaction yield was observed when performing the reaction under a N_2 atmosphere (entry 5). No product formation occurred when the reaction was carried out in polar solvents (entry 8-9). Alternative halogenated media (e.g. DCM) gave a lower *tert*-butylation yield (entry 10). On off experiments (Figure 5.2) and the absence of light (entry 13) confirmed the photochemical nature of the process. In addition, a decrease of the overall yield to 50% occurred when one equivalent of TEMPO was present in the reaction media (entry 15).

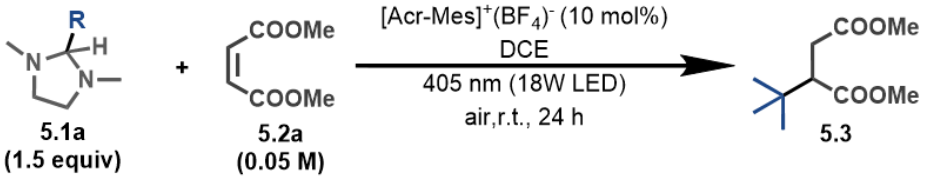

Entry	t (h)	Irradiation	5.3 (% Yield)
1	0.0	OFF	-
2	0.5	ON	38
3	1.0	OFF	49
4	1.5	ON	**68**
5	2.0	OFF	68
6	2.5	ON	73
7	3.0	OFF	73
8	4.0	ON	99
9	5.0	OFF	99

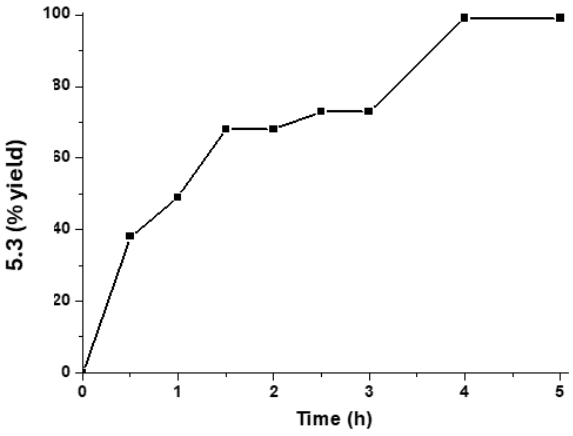

Figure 5.2. On-Off experiment for the photoredox catalysed synthesis of **5.3**.

In view of these results, we adopted the followed conditions: an air-equilibrated DCE solution of **5.1a** (1.5 equiv.), **5.2a** (0.05 M), and $[Acr\text{-}Mes]^+(BF_4)^-$ (10 mol%), under irradiation at 405 nm (EvoluChem 18 W LED) for 24 h. In some cases, the use of 4CzIPN was considered as a convenient alternative to $[Acr\text{-}Mes]^+(BF_4)^-$ as the PC. We thus explored the scope of the reaction by adding the generated alkyl radicals to electron-poor alkenes and vinyl heteroarenes as sketched in Scheme 5.3-5.4. Notably, all *tert*-butylated derivatives **5.3–5.11** were obtained in satisfactory yields,

as well as adamantyl derivatives **5.12–5.19** that were isolated in up to 99% yield. Interestingly, the easy and smooth *tert*-butylation of 1,4-naphthoquinone (Menadione, or commonly named Vitamin K3) is an example of Late-Stage Functionalization (LTF) of bioactive compounds by using this methodology. To the best of our knowledge, the *tert*-butylation of **5.2i** (Menadione) was previously reported only by using rather toxic organomercury derivatives.[17]

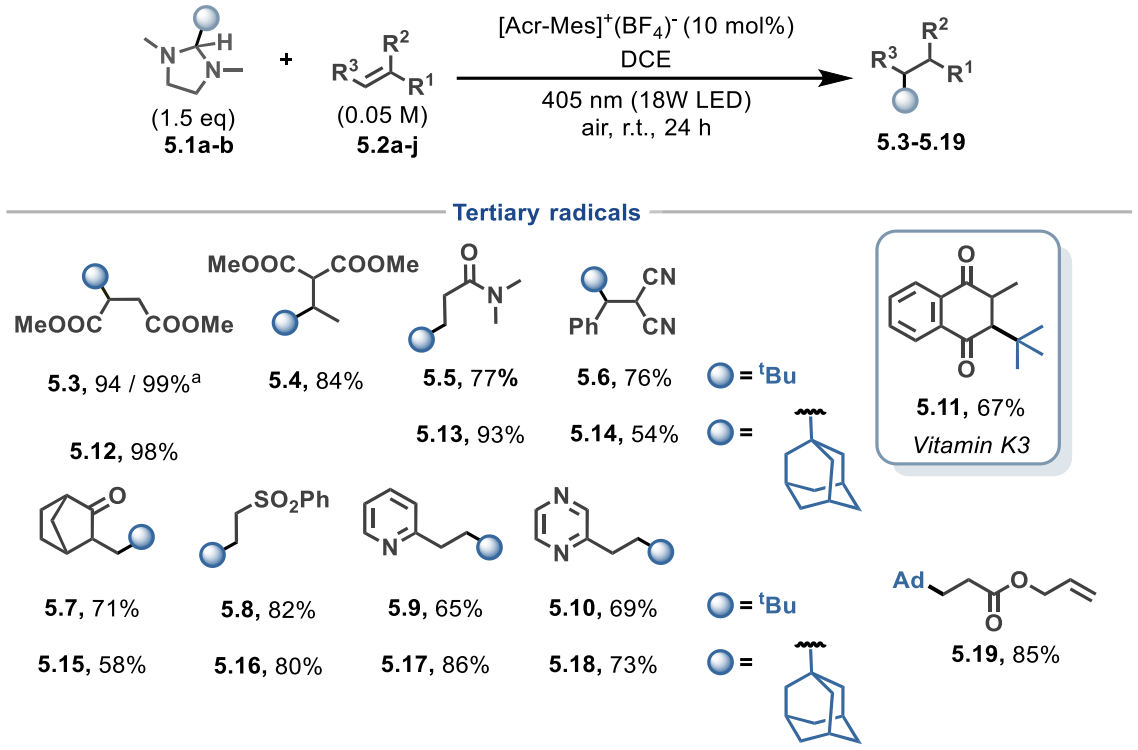

Scheme 5.3. Imidazolidines for the photocatalyzed alkylation of C=C bonds. Conditions: **5.1a–b** (0.075 M, 1.5 equiv., 0.375 mmol), **5.2a-j** (0.25 mmol), $[Acr\text{-}Mes]^+(BF_4)^-$ (10 mol%), DCE (5 mL), air, under 18 W LED irradiation (405 nm) at r.t. for 24 h. Isolated yields. Ad = adamantyl. [a] Reaction performed in flow: **5.2a** (0.4 M), 2 h, fr: 0.8 mL min^{-1}.

A complete regioselectivity was observed when using allyl methacrylate **5.2j** as the electron-poor olefin, where the electrophilic C=C bond was exclusively derivatized to form product **5.19**.

The release of secondary radicals (*iso*-propyl, cyclohexyl and 3-cyclohexenyl) from imidazolidines **5.1c–e** was next tested. Even in this case, the corresponding alkylated compounds **5.20–5.29** were obtained in a satisfactory yield with the only exception of dicyano derivatives **5.21** and **5.25**. When releasing secondary radicals, the adoption of 4CzIPN as the photoredox catalyst was beneficial for the successful

outcome of the reaction (see the results obtained for compounds **5.24**, **5.28**, and **5.29**).

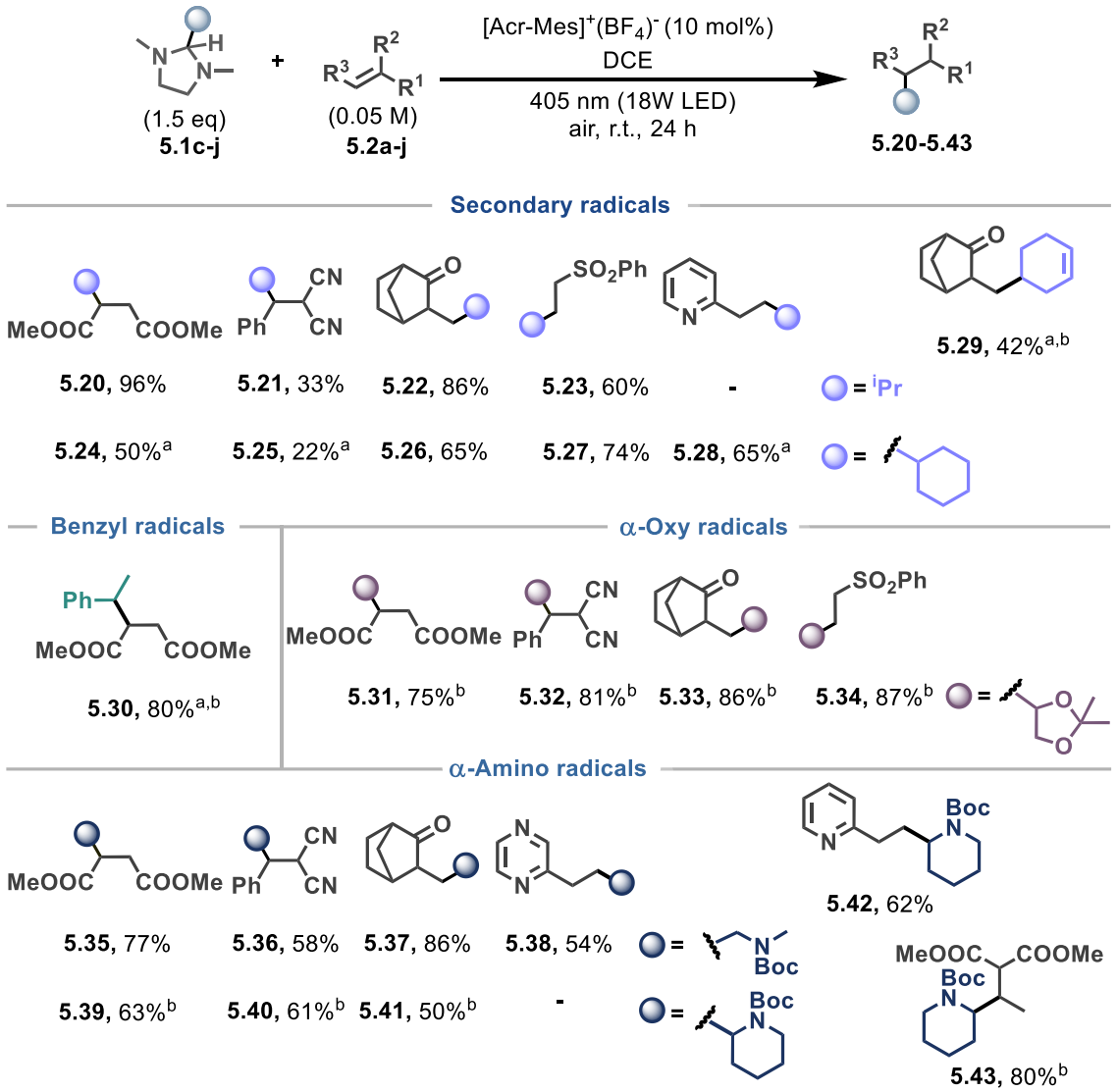

Scheme 5.4. Imidazolidines for the photocatalyzed alkylation of C=C bonds. Conditions: **5.1c–j** (0.075 M, 1.5 equiv., 0.375 mmol), **5.2a-j** (0.25 mmol), [Acr-Mes]$^{+}$(BF$_4$)$^{-}$ (10 mol%), DCE (5 mL), air, under 18 W LED irradiation (405 nm) at r.t. for 24 h. Isolated yields. [a] 4CzIPN (10 mol%) was used as the PC under nitrogen atmosphere. [b] Mixture of two diastereoisomers (dr 1 :1).

The 4CzIPN photocatalyzed benzylation of dimethyl maleate by using **5.1f** afforded the corresponding derivative **5.30** as a mixture of diastereoisomers, a methylated derivative of *L*-benzylsuccinic acid (potent inhibitor of carboxypeptidase A).[18] Unfortunately, any attempts to perform alkylation of olefins with primary alkyl radicals starting from imidazolidine **5.1g** were ineffective. We then turned our attention to electron-rich carbon-centered radicals bearing heteroatom-based substituents (N, O) starting from suitably functionalized imidazolidines **5.1h–j**.

Thus, when using the dioxolane derivative **5.1h**, the desired products **5.31–5.34** were isolated in up to 97% yield (mostly as a 1:1 mixture of diasteroisomers). Analogously, α-amido radicals (photogenerated from **5.1i** and **5.1j**) were exploited to incorporate cyclic and acyclic *N*-Boc protected amines **5.35–5.43** in a different range of electron-poor olefins with yields ranging from 50 to 86%.

The synthesis of **5.3** was also optimized under flow conditions by using a hand-made flow photoreactor (see Figure ES5.1 and ES5.2). In this case, we were able to use less toxic dichloromethane (DCM) in place of DCE as the solvent. To this aim, different parameters were considered, including the light source and its intensity, the residence time and the concentration of the substrates. A complete list of the experiments is included in Table 5.2 (accompanied by the corresponding Space Time Yield (STY) values).

Table 5.2. Optimization of the photoredox catalyzed synthesis of **5.3** under flow conditions.

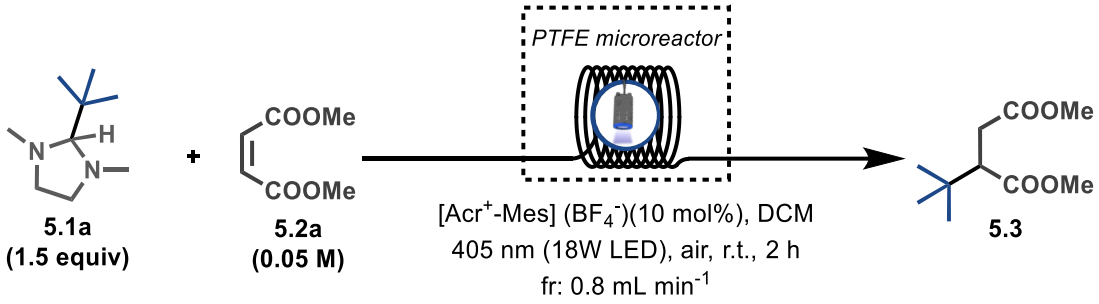

Entry	Deviations from the standard conditions	5.3 (% Yield) (STY, mmol L-1 min-1)
1	390 nm (Kessil lamp 50% Power) fr: 1.2 mL/min, 1.5 h	65 (0.72)
2	fr: 1.6 mL/min, 1 h	43 (0.72)
3	**None, fr: 0.8 mL/min, 2 h**	**99 (0.83)**
4	390 nm (Kessil lamp ,100% Power), fr: 0.8 mL/min, 2 h	96 (0.80)
5	fr:1.6 mL/min, 1 h	44 (0.72)
6	**5.2a** (0.16 M), fr: 0.8 mL/min, 2 h	93 (1.24)
7	**5.2a** (0.4 M), fr:0.8 mL/min, 2 h	88 (2.93)
8	**5.2a (0.4 M), fr:0.8 mL/min, 2 h**	**92 (3.07)**

Gratifyingly, as depicted in entry 3, when the reaction was carried out in DCM, compound **5.3** was isolated in quantitative yield with a residence time of only 2 h. Interestingly, the light source could be replaced with a 390 nm Kessil lamp without a significant decrease of the yield (entry, 4). It is also possible to scale up the reaction from 0.1 M to 0.4 M (1 mmol **5.2a**) with no clogging problems and no precipitate formation inside the reactor tubing (entry 8, 92% yield with a STY of 3.07 mmol $L^{-1}min^{-1}$). On the other hand, an increase in the flow rate, when using either a 405 nm or a 390 nm LED lamp, resulted in a significant lowering of the reaction yield (entries 2 and 5).

In the suggested mechanism, reductive quenching of the photoexcited acridinium catalyst [Acr-Mes]$^{+}$* (or 4CzIPN*) with the concomitant oxidation of imidazolidines **5.1a–j** to generate the corresponding radical cations **5.1a–j**$^{\bullet+}$ occurred (Scheme 5.5, path a). The radical species **R**$^{\bullet}$ was formed upon fragmentation of the C–C bond in **5.1a–f**$^{\bullet+}$, **5.1h–j**$^{\bullet+}$ releasing a stable iminium ion **5.44**$^{+}$ (path *b*). The nucleophilic **R**$^{\bullet}$ was trapped by electron-poor olefins **5.2a–j** (path *c*) and the resulting radical adduct **5.45**$^{\bullet}$ underwent monoelectronic reduction by Acr-Mes$^{\bullet}$ (or 4CzIPN$^{-\bullet}$) to generate the corresponding anion **5.45**$^{-}$ while restoring the starting photocatalyst. Protonation of **5.45**$^{-}$ (path *e*) by adventitious water afforded the desired products **5.3–5.43**. The key role of the carbon centered intermediate **R**$^{\bullet}$ has been further evidenced by the detrimental effect of TEMPO when present in the reaction mixture (Table 5.1, entry 15).

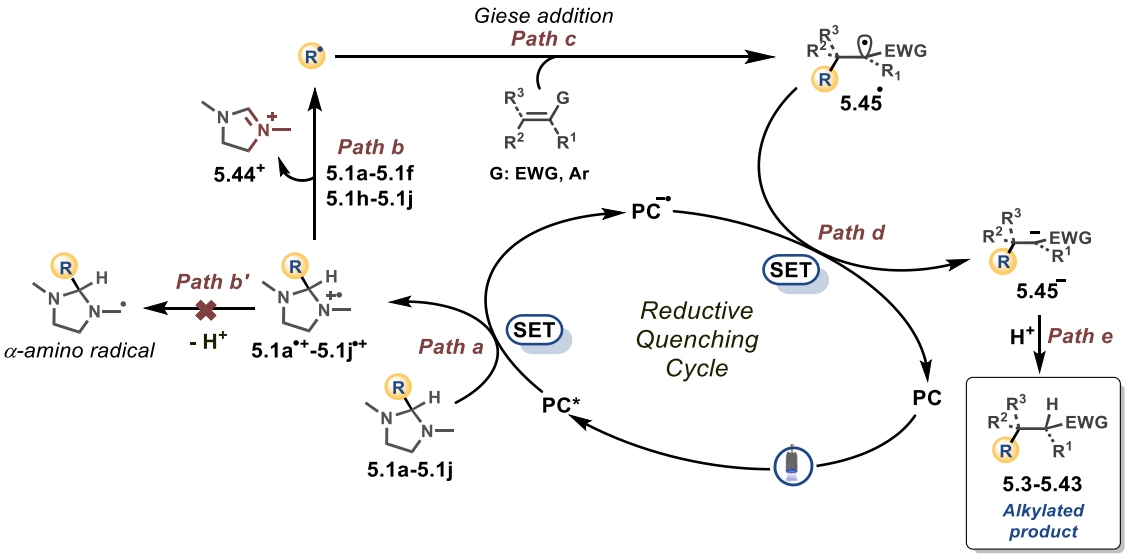

Scheme 5.5. Proposed mechanism for the synthesis of compounds **5.3-5.43**.

As hinted above, the forging of C(sp^3)–C(sp^3) bonds is a current hot topic in organic synthesis. In the present work, we highlighted the potential of imidazolidines **5.1a-j** (smoothly prepared from commercially available aldehydes and 1,2-diamines) as appealing alternatives to both uncharged (including among others, 1,3-dioxolanes,[19] 1,3-oxazolidines,[5] Barton esters,[20] *N*-(acyloxy)phthalimides,[4f,21]) and charged (alkyl tetrafluoro borates,[2d] alkyl carboxylates,[2d] alkyl *N*-phthalimidoyl oxalates[2d]) known radical precursors.

The protocol presented here offers the chance to generate a wide range of carbon-based radicals, including tertiary, secondary, benzyl, α-oxy and α-amido, by exploiting the easy oxidazability of the radical precursors. The latter point has the consequence of both allowing the use of metal-free PCs having poor oxidizing power in the excited state (e.g. 4CzIPN) and liberating a stable iminium ion in the fragmentation of the thus formed radical cation, which is the driving force of the reaction. Contrary to dihydroquinazolinones, there is no possible competitive release of other radicals upon fragmentation, overcoming the requirement to have an aromatic leaving group that strongly affected the atom economy of the process. Furthermore, such a methodology exhibited excellent functional group tolerance, allowing for the alkylation of differently decorated olefins bearing carbonyl and carboxylic groups, sulfones and even of heteroarenes.

5.3 Conclusions.

Summing up, we developed the application of 2-substituted-*N,N*-dimethylimidazolidines as uncharged carbon centered precursors under photoredox catalyzed conditions, for the versatile functionalization of a large variety of C=C bonds. The adoption of super-donors for the liberation of radicals is of urgent importance since it may allow the use of mild oxidative conditions limiting the interference of other reagents/additives that may be oxidized as well in the process when using powerful oxidizing PCs. Furthermore, the data presented herein also evidenced the chance of applying imidazolidines in alkylation strategies on late-stage functionalization and the synthesis of drug-like molecules in batch and under continuous flow conditions.

5.4 Experimental section.

^{1}H and ^{13}C NMR spectra were recorded on 400 and 300 (for ^{1}H) or 100 and 75 (for ^{13}C) MHz spectrometers, respectively. The attributions were based on ^{1}H and ^{13}C NMR experiments; chemical shifts are reported in ppm downfield from TMS (δ ppm), multiplicity (s = singlet, bs = broad singlet, d = doublet, t = triplet, q = quadruplet, quint = quintuplet, sext = sextuplet, sept = septuplet, m = multiplet), coupling constant (Hz) and integration.

GC analyses were performed using a HP SERIES 5890 II equipped with a fire ion detector (FID, temperature 350 °C). Analytes were separated using a Restek Rtx-5MS (30 m×0.25 mm×0.25 μm) capillary column with nitrogen as a carrier gas at 1 mL min^{-1}. The injector temperature was 250 °C. The GC oven temperature was held at 80 °C for 2 min, increased to 250 °C by a temperature ramp of 10 °C min^{-1}, and held for 10 min.

GC/MS analyses were carried out on a Thermo Scientific DSQII single quadrupole GC/MS system (TraceDSQII mass spectrometer, Trace GC Ultra gas chromatograph, TriPlus autosampler - ThermoFisher Scientific, Waltham, MA, USA). Chromatography was performed on a Rxi-5Sil MS capillary column (30 m length×0.25 mm ID×0.25 μm film thickness, Restek, Milan, Italy) with Helium (>99.99 %) as carrier gas at a constant flow rate of 1.0 mL min-1. An injection volume of 1 μL was employed. The injector temperature was set at 250 °C and it was operated in split mode, with a split flow of 10 mL min^{-1}. The oven temperature was programmed from 80 °C (isothermal for 2 min) to 220 °C at the rate of 10 °C min^{-1}, then from 220 °C to 300 °C (isothermal for 5 min) at the rate of 4 °C min^{-1}. Mass transfer line temperature was set at 260 °C. Total GC running time was 41 min. All mass spectra were acquired with an electron ionization system (EI, Electron Impact mode) with ionization energy of 70 eV and source temperature of 250°C, with spectral acquisition in Full Scan mode, positive polarity, over a mass range of 35–650 Da with a scan rate of 940 amu s^{-1}. The chromatogram acquisition, detection of mass spectral peaks and their waveform processing were performed using Xcalibur MS Software Version 2.1 (Thermo Scientific Inc.). Assignment of chemical structures to chromatographic peaks was based on the comparison with the databases for GC-

MS NIST Mass Spectral Library (NIST 08) and Wiley Registry of Mass Spectral Data (8th Edition).

HRMS data were acquired using a X500B QTOF System (SCIEX, Framingham, MA 01701 USA) available at the CGS of the University of Pavia, equipped with the Twin Sprayer ESI probe and coupled to an ExionLC™ system (SCIEX). The SCIEX OS software 2.1.6 was used as operating platform. For MS detection the following parameters were applied: Curtain gas 30 psi, Ion source gas 1 45 psi, Ion source gas 2 55 psi, Temperature 450°C, Polarity negative, Ion spray voltage -4500 V, TOF mass range 50-1600 Da, declustering potential -60 V and collision energy -10 V.

Cyclic Voltammetry for compound **5.1c** was carried out by means of a Amel model 4330 module equipped with a 20 mL standard three-electrode cell with a glassy carbon (0.49 cm^2 geometrical area) working electrode, a platinum wire as auxiliary electrode and an Ag/AgCl, 3 M NaCl reference electrode, all obtained from BASi Electrochemistry. Acetonitrile containing 0.1 M lithium perchlorate were used as solvent and supporting electrolyte, scanning the potential in the range from 0 mV to + 2500 mV, with a 5 mM compound concentration and a scan speed of 50 mV s^{-1}.

5.4.1 Chart of starting material

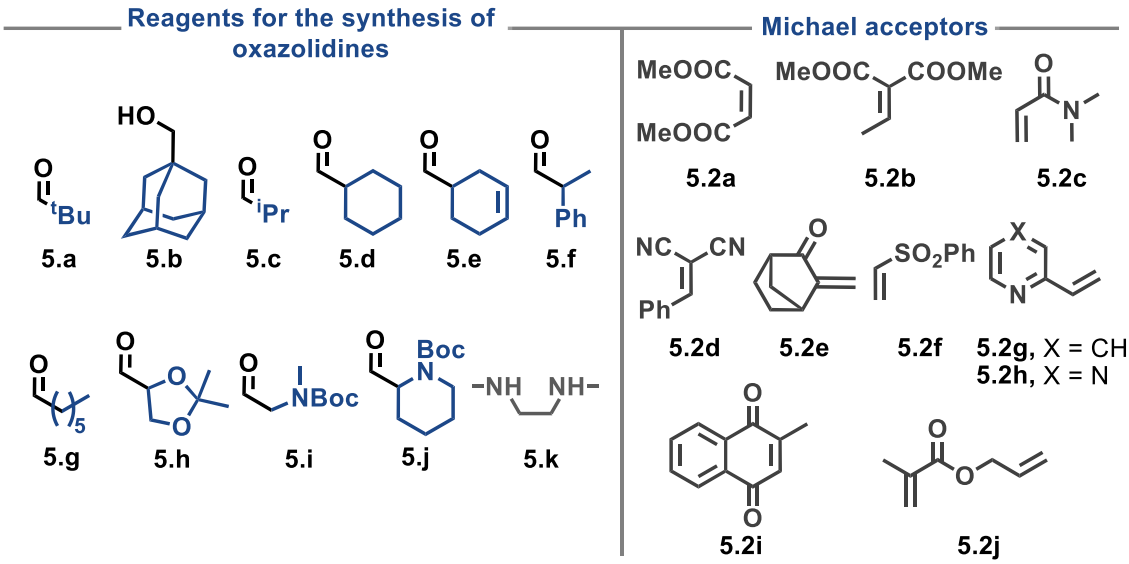

The aldehydes employed for the synthesis of imidazolines **5.1a-j** were commercially available and used as received, with the only exception of adamantane-1-carbaldehyde

that was prepared according to a procedure previously reported.[22] Olefins **5.2a-j** were commercially available and used as received.

5.4.2 General procedures.

5.4.2.1 General procedure for the synthesis of 2-substituted *N,N'*-dimethylimidazolidines.

The desired imidazolidines **5.1a-j** were synthesized by adapting a procedure previously described for the synthesis of 1,3-oxazolidines.[23] *N,N'*-dimethylethylendiamine (1 equiv.) was added to a suspension of $MgSO_4$ (25 mg $mmol^{-1}$) and the corresponding aldehyde (1 equiv.) in Et_2O (1.7 mL $mmol^{-1}$). The reaction mixture was refluxed and stirred overnight, and the resulting residue was diluted with DCM, filtered, and concentrated in vacuo to yield the desired imidazolidine that was employed for the photocatalytic step without any further purification.

5.4.2.2 General procedure for the light-induced photo-redox alkylation process.

A solution of the chosen imidazolidine **5.1a-j** (1.5 equiv.), olefin 2a-j (1 equiv.) and $[Acr\text{-}Mes]^+(BF_4)^-$ or 4CzIPN (10 mol%) in DCE (5 mL) was prepared in a Pyrex glass vessel. The solution was irradiated for 24 h at 405 nm by means of a 18W EvoluChem lamp. The resulting solution was then concentrated in vacuo and the residue was purified by flash column chromatography using an Isolera apparatus (Biotage) and a SiO_2 cartridge (eluant: cyclohexane/ethyl acetate mixture except where indicated).

5.4.2.3 General procedure for the synthesis of compound 3 under flow conditions.

A solution of the imidazolidine **5.1a** (1.5 equiv.), olefin **5.2a** (1 equiv.) and $[Acr\text{-}Mes]^+(BF_4)^-$ (10 mol %) in DCM (2.5 mL) was prepared and charged into a coiled tubing reservoir (PTFE, 1 mm internal diameter, see Figures ES1 and ES2). The reaction mixture was then flown through the coiled reactor (PTFE, 1 mm internal diameter) by a syringe pump set at the corresponding flow rate upon irradiation with a 405 nm (EvoluChem, 18W) or 390 nm (Kessil PR-160L, 40W) LED lamp. Fan cooling was applied to maintain room temperature. The resulting solution was

collected and concentrated in vacuo. The residue was purified by flash column chromatography using an Isolera apparatus (Biotage) and a SiO_2 cartridge (eluant: cyclohexane/ethyl acetate mixture).

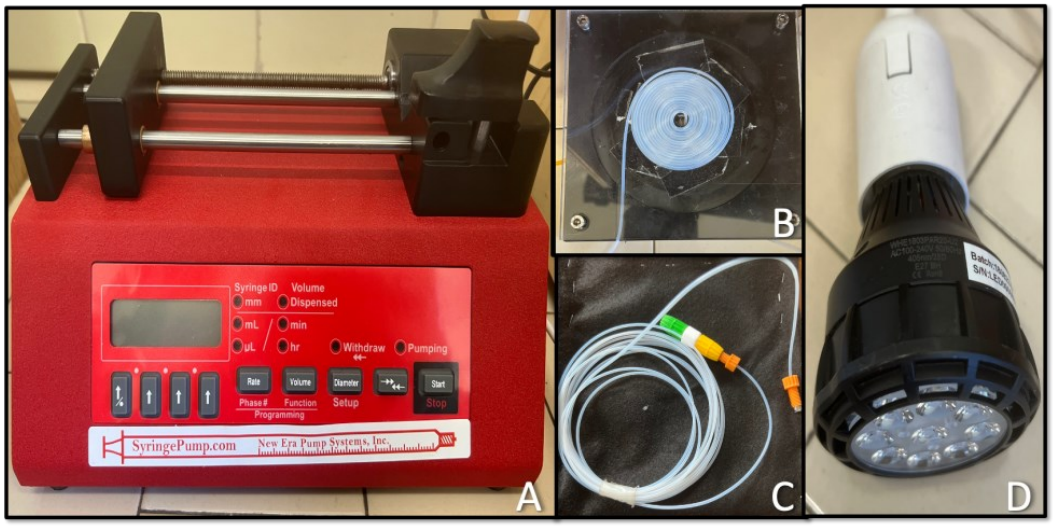

Figure ES5.1. Description of the hand-made flow system. A) Syringe pump. B) Coiled reactor. C) Coiled solution reservoir. D) 405 nm Evoluchem lamp (18W).

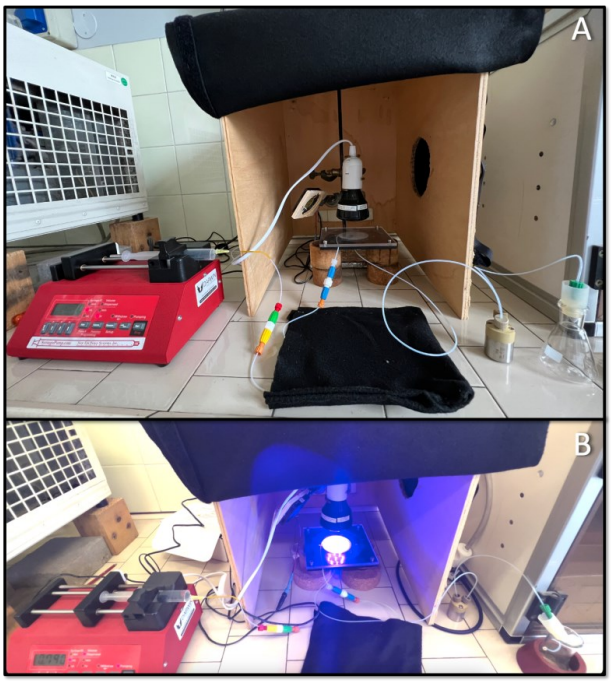

Figure ES5.2. Hand-made flow photoreactor set up. A) Before irradiation. B) During irradiation.

5.4.3 Characterization data.

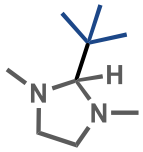

2-tert-Butyl-1,3-dimethylimidazolidine (5.1a).

From *N,N'*-dimethylethylendiamine (1.26 mL, 11.6 mmol, 1 equiv.), MgSO4 (290 mg, 25 mg mmol-1), pivalaldehyde (1.25 mL, 11.6 mmol, 1 equiv.) in Et2O (20 mL). The crude mixture was diluted in DCM, filtered and concentrated in vacuo affording **5.1a** (colorless oil, 98% yield).

5.1a. ^{1}H NMR (300 MHz, acetone-d6) δ 2.99–2.86 (m, 2H), 2.74–2.57 (m, 3H), 2.48 (s, 6H), 0.86 (s, 9H). ^{13}C NMR (75 MHz, acetone-d6) δ 99.0, 55.4, 51.6, 46.8, 38.3, 35.9, 26.6. HRMS (EI) m/z: [M+H]+ calculated for C9H20N2 157.1660, found 157.1699.

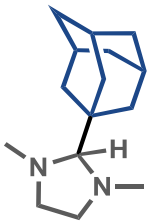

(2-Adamantan-1-yl)-1,3-dimethylimidazolidine (5.1b).

From *N,N'*-dimethylethylendiamine (0.65 mL, 6.0 mmol, 1 equiv.), $MgSO_4$ (150 mg, 25 mg mmol^{-1}) adamantane-1-carbaldehyde[S1] (0.99 g, 6.0 mmol, 1 equiv.) in Et_2O (10 mL). The crude mixture was diluted in DCM, filtered and concentrated in vacuo affording **5.1b** (pale yellow oil, 85% yield).

5.1b. ^{1}H NMR (300 MHz, acetone-d_6) δ 3.04–2.78 (m, 3H), 2.69–2.57 (m, 2H), 2.46 (s, 6H), 1.98–1.86 (m, 3H), 1.74–1.49 (m, 12H).). ^{13}C NMR (75 MHz, acetone-d_6) δ 99.5, 55.5, 47.1, 40.3, 39.4, 38.3, 29.5. HRMS (EI) m/z: $[M+H]^+$ calculated for $C_{15}H_{26}N_2$ 235.2130, found 235.2169.

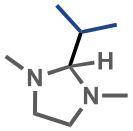

2-*iso*-Propyl-1,3-dimethylimidazolidine (5.1c).

From *N,N'*-dimethylethylendiamine (0.25 mL, 2.8 mmol, 1 equiv.), $MgSO_4$ (70 mg, 25 mg $mmol^{-1}$), isopropylaldehyde (0.3 mL, 2.8 mmol, 1 equiv.) in Et_2O (5 mL). The crude mixture was diluted in DCM, filtered and concentrated in vacuo affording **5.1c** (colourless oil, 91% yield).

5.1c. ^1H NMR (300 MHz, acetone-d_6) δ 2.95–2.84 (m, 2H), 2.56–2.43 (m, 3H), 2.36 (s, 6H), 1.71 (ddp, *J* = 10.0, 6.8, 3.1 Hz, 1H), 0.89 (d, *J* = 6.8 Hz, 6H). ^{13}C NMR (75 MHz, acetone-d_6) δ 95.4, 54.9, 44.0, 32.2, 18.5. HRMS (EI) m/z: $[M+H]^+$ calculated for $C_8H_{18}N_2$ 143.1504, found 143.1543.

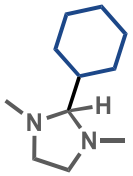

2-Cyclohexyl-1,3-dimethylimidazolidine (5.1d).

From *N,N'*-dimethylethylendiamine (0.19 mL, 1.78 mmol, 1 equiv.), $MgSO_4$ (45 mg, 25 mg $mmol^{-1}$), cyclohexylcarbaldehyde (0.22 mL, 1.8 mmol, 1 equiv.) in Et_2O (3 mL). The crude mixture was diluted in DCM, filtered and concentrated in vacuo affording **5.1d** (colourless oil, 98% yield).

5.1d. ^1H NMR (300 MHz, acetone-d_6) δ 2.93–2.83 (m, 2H), 2.55–2.51 (m, 1H), 2.51–2.44 (m, 2H), 2.36 (s, 6H), 1.77–1.69 (m, 4H), 1.68–1.60 (m, 1H), 1.38 (tt, *J* = 11.6, 2.8 Hz, 1H), 1.27–1.07 (m, 5H). ^{13}C NMR (75 MHz, acetone-d_6) δ 95.2, 54.8, 44.3, 43.2, 28.0, 27.7. HRMS (EI) m/z: $[M+H]^+$ calculated for $C_{11}H_{22}N_2$ 183.1817, found 183.1856.

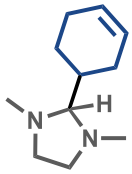

2-Cyclohexenyl-1,3-dimethylimidazolidine (5.1e).

From *N,N'*-dimethylethylendiamine (0.2 mL, 1.8 mmol, 1 equiv.), $MgSO_4$ (45 mg, 25 mg $mmol^{-1}$), 3-cyclohexene-1-carboxaldehyde (0.21 mL, 1.8 mmol, 1 equiv.) in Et_2O (3 mL). The crude mixture was diluted in DCM, filtered and concentrated in vacuo affording **5.1e** (colourless oil, 99% yield).

5.1e. ^1H NMR (300 MHz, acetone-d_6) δ 5.73–5.53 (m, 2H), 3.01–2.81 (m, 2H), 2.65 (d, *J* = 3.3 Hz, 1H), 2.61–2.44 (m, 2H), 2.39 (s, 3H), 2.37 (s, 3H), 2.05–1.93 (m, 4H), 1.82–1.71 (m, 1H), 1.71–1.60 (m, 1H), 1.49–1.25 (m, 1H). ^{13}C NMR (75 MHz, acetone-d_6) δ 128.2, 127.3, 94.4, 54.8, 54.4, 44.6, 43.3, 38.7, 27.6, 26.6, 26.2. HRMS (EI) m/z: $[M+H]^+$ calculated for $C_{11}H_{20}N_2$ 181.1660, found 183.1699.

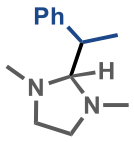

2-(1-Phenylethyl)-1,3-dimethylimidazolidine (5.1f).

From *N,N'*-dimethylethylendiamine (0.16 mL, 1.5 mmol, 1 equiv.), $MgSO_4$ (38 mg, 25 mg $mmol^{-1}$), 2-phenylpropanal (0.2 mL, 1.5 mmol, 1 equiv.) in Et_2O (3 mL). The crude mixture was diluted in DCM, filtered off, and the obtained solution was concentrated in vacuo affording **5.1f** (pale yellow oil, 97% yield).

5.1f. ^1H NMR (300 MHz, acetone-d_6) 7.42–7.19 (m, 4H), 7.19–7.08 (m, 1H), 2.99–2.84 (m, 3H), 2.84–2.72 (m, 1H), 2.55–2.39 (m, 2H), 2.36 (s, 3H), 2.06 (s, 3H), 1.29 (d, *J* = 6.8 Hz, 3H). δ ^{13}C NMR (75 MHz, acetone- d_6) 145.7, 129.3, 128.5, 126.6, 95.6, 54.7, 54.1, 44.5, 43.4, 42.7, 15.1. HRMS (EI) m/z: $[M+H]^+$ calculated for $C_{13}H_{20}N_2$ 205.1699, found 205.1699.

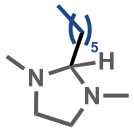

2-Hexyl-1,3-dimethylimidazolidine (5.1g).

From *N,N'*-dimethylethylendiamine (0.24 mL, 2.2 mmol, 1 equiv.), was added to a suspension of $MgSO_4$ (55 mg, 25 mg $mmol^{-1}$), heptanal (0.31 mL, 2.2 mmol, 1 equiv.) in Et_2O (4 mL). The crude mixture was diluted in DCM, filtered off, and the obtained solution was concentrated in vacuo affording **5.1g** (colourless oil, 46% yield).

5.1g. ^1H NMR (300 MHz, acetone-d_6) 2.99 (dd, J = 6.4, 2.1 Hz, 2H), 2.49 (t, J = 3.4 Hz, 1H), 2.36 (dd, J = 6.4, 2.1 Hz, 2H), 2.25 (s, 6H), 1.72–1.30 (m, 3H). ^{13}C NMR (75 MHz, acetone-d_6) 89.2, 53.8, 40.8, 32.8, 31.7, 24.1, 23.3, 14.4, 14.4. HRMS (EI) m/z: $[M+H]^+$ calculated for $C_{11}H_{24}N_2$ 185.2012, found 185.2007.

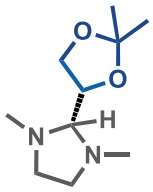

2-(2,2-Dimethyl-1,3-dioxolan-4-yl)-1,3-dimethylimidazolidine (5.1h).

From *N,N'*-dimethylethylendiamine (0.11 mL, 1.15 mmol, 1 equiv.), $MgSO_4$ (30 mg, 25 mg $mmol^{-1}$), 2,2-dimethyl-1,3-dioxolane-4-carbaldehyde (0.14 mL, 1.15 mmol, 1 equiv.) in Et_2O (3 mL). The crude mixture was diluted in DCM, filtered off, and the obtained solution was concentrated in vacuo affording **5.1h** (yellowish oil, 99% yield).

5.1h. ^1H NMR (400 MHz, chloroform- *d*) δ 4.12–4.06 (m, 1H), 4.06–3.99 (m, 1H), 3.90 (dd, J = 7.9, 6.4 Hz, 1H), 3.12–2.98 (m, 2H), 2.97 (d, J = 5.4 Hz, 1H), 2.64–2.56 (m, 2H), 2.52 (s, 3H), 2.49 (s, 3H), 1.43 (s, 3H), 1.34 (s, 3H). δ ^{13}C NMR (100 MHz, chloroform-*d*) δ 109.1, 89.6, 78.5, 66.3, 54.3, 53.8, 44.5, 43.0, 26.6, 25.1 HRMS (EI) m/z: $[M+H]^+$ calculated for $C_{10}H_{20}N_2O_2$ 201.1598, found 201.1589.

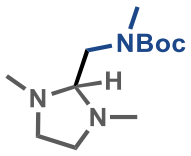

***tert*-Butyl methyl((1,3-dimethylimidazolidin-2-yl)methyl)carbamate (5.1i).**
From *N,N'*-dimethylethylendiamine (0.16 mL, 1.4 mmol, 1 equiv.), $MgSO_4$ (36 mg, 25 mg $mmol^{-1}$), *N*-Boc-2-aminoacetaldehyde (0.24 mL, 1.4 mmol, 1 equiv.) in Et_2O (3 mL). The crude mixture was diluted in DCM, filtered off, and the obtained solution was concentrated in vacuo affording **5.1i** (pale yellow oil, 95% yield).
5.1i. ^1H NMR (400 MHz, chloroform- *d*) δ 3.23 (d, *J* = 11.3 Hz, 2H), 3.10–3.04 (m, 2H), 2.96 (s, 3H), 2.92–2.87 (m, 1H), 2.53–2.47 (m, 2H), 2.41 (s, 6H), 1.47–1.43 (m, 9H).^{13}C NMR (100 MHz, chloroform- *d*) δ 155.9, 88.0, 79.5, 77.4, 53.5, 52.8, 42.4, 36.3, 28.6. HRMS (EI) m/z: $[M+H]^+$ calculated for $C_{12}H_{25}N_3O_2$ 244.2020, found 244.2012.

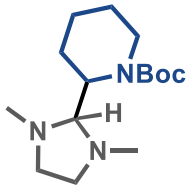

***tert*-Butyl 2-(1,3-dimethylimidazolidin-2-yl)piperidine-1-carboxylate (5.1j).**
From *N,N'*-dimethylethylendiamine (0.25 mL, 2.3 mmol, 1 equiv.), $MgSO_4$ (58 mg, 25 mg $mmol^{-1}$), *tert*-butyl 2-formylpiperidine-1-carboxylate (0.5 g, 2.3 mmol, 1 equiv.) in Et_2O (4 mL). The crude mixture was diluted in DCM, filtered off, and the obtained solution was concentrated in vacuo affording **5.1j** (pale yellow oil, 88% yield).
5.1j. ^1H NMR (300 MHz, acetone-d_6) 3.95 (dd, *J* = 13.2, 4.9 Hz, 1H), 3.88–3.77 (m, 1H), 3.26 (d, *J* = 6.7 Hz, 1H), 3.04–2.86 (m, 3H), 2.71–2.57 (m, 2H), 2.45 (s, 3H), 2.44 (s, 3H), 1.83–1.51 (m, 3H), 1.48–1.36 (m, 12H). ^{13}C NMR (75 MHz, acetone- d_6) δ 206.1, 156.0, 89.6, 78.7, 54.5, 54.0, 45.5, 43.5, 28.7, 26.0, 24.9, 20.4. HRMS (EI) m/z: $[M+H]^+$ calculated for $C_{15}H_{29}N_3O_2$ 284.2333, found 284.2325.

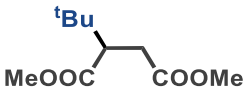

Dimethyl 2-(*tert*-butyl)succinate (5.3).

From **5.1a** (58 mg, 0.375 mmol, 1.5 equiv.), **5.2a** (31 µL, 0.25 mmol, 1 equiv.), [Acr-Mes]$^{+}$(BF$_4$)$^{-}$ (10 mg, 0.025 mmol, 10 mol%) in DCE (5 mL). Purification by column chromatography (eluent: Cyclohexane/AcOEt 100/0 to 8/2) afforded **5.3** (colourless oil, 50.0 mg, 99% yield). Spectroscopic data are in accordance with the literature.[24]

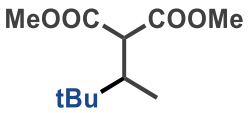

Dimethyl 2-(3,3-dimethylbutan-2-yl)malonate (5.4).

From **6.1a** (58 mg, 0.375 mmol, 1.5 equiv.), **6.2b** (28 µL, 0.25 mmol, 1 equiv.), [Acr-Mes]$^{+}$(BF$_4$)$^{-}$ (10 mg, 0.025 mmol, 10 mol%), in DCE (5 mL). Purification by column chromatography (eluent: Cyclohexane/AcOEt 100/0 to 80/20) afforded **5.4** (yellow oil, 36.6 mg, 84% yield). Spectroscopic data are in accordance with the literature.[25]

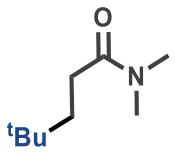

***N,N*,4,4-Tetramethylpentanamide (5.5).**

From **5.1a** (58 mg, 0.075 mmol, 1.5 equiv), **5.2c** (25 µL, 0.25 mmol, 1 equiv.), [Acr-Mes]$^{+}$(BF$_4$)$^{-}$ (10 mg, 0.025 mmol, 10 mol%) in DCE (5 mL). Purification by column chromatography (eluent: DCM/MeOH 100/0 to 95/5) afforded **5.5** (colourless oil, 38.9 mg, 77% yield). Spectroscopic data are in accordance with the literature.[26]

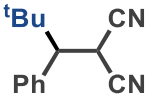

2-(2,2-Dimethyl-1-phenylpropyl)malononitrile (5.6).

From **5.1a** (58 mg, 0.375 mmol, 1.5 equiv.), **5.2d** (38.5 mg, 0.25 mmol, 1 equiv.), [Acr-Mes]$^{+}$(BF$_4$)$^{-}$ (10 mg, 0.025 mmol, 10 mol%) in DCE (5 mL). Purification by column chromatography (eluent: Cyclohexane/AcOEt 100/0 to 90/10) afforded **5.6**

(white powder, 40.2 mg, 76% yield). Spectroscopic data are in accordance with the literature.[27]

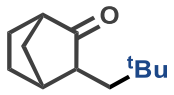

3-Neopentylbicyclo[2.2.1]heptan-2-one (5.7).

From **5.1a** (58 mg, 0.375 mmol, 1.5 equiv.), **5.2e** (28 µL, 0.25 mmol, 1 equiv.), [Acr-Mes]$^{+}$(BF_4)$^{-}$ (10 mg, 0.025 mmol, 10 mol%) in DCE (5 mL). Purification by column chromatography (eluent: Cyclohexane/AcOEt 100/0 to 9/1) afforded **5.7** (yellowish oil, 30.5 mg, 71% yield). Spectroscopic data are in accordance with the literature.[28]

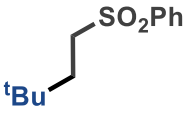

((3,3-Dimethylbutyl)sulfonyl)benzene (5.8).

From **5.1a** (58 mg, 0.375 mmol, 1.5 equiv.), **5.2f** (42 mg, 0.25 mmol, 1 equiv.), [Acr-Mes]$^{+}$(BF_4)$^{-}$ (10 mg, 0.025 mmol, 10 mol%) in DCE (5 mL). Purification by column chromatography (eluent: DCM/MeOH 100/0 to 95/5) gave **5.8** (yellowish oil, 46.6 mg, 82% yield). Spectroscopic data are in accordance with the literature.[29]

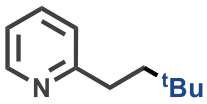

2-(3,3-Dimethylbutyl)pyridine (5.9).

From **5.1a** (58 mg, 0.375 mmol, 1.5 equiv.), **5.2g** (26 µL, 0.25 mmol, 1 equiv.), [Acr-Mes]$^{+}$(BF_4)$^{-}$ (10 mg, 0.025 mmol, 10 mol%) in DCE (5 mL). Purification by column chromatography (eluent: Cyclohexane/AcOEt 100/0 to 80/20) gave **5.9** (yellowish oil, 26.7 mg, 65% yield). Spectroscopic data are in accordance with the literature.[30]

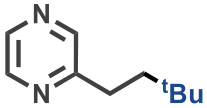

2-(3,3-Dimethylbutyl)pyrazine (5.10).

From **5.1a** (58 mg, 0.375 mmol, 1.5 equiv.), **5.2h** (25 µL, 0.25 mmol, 1 equiv.), [Acr-Mes]$^{+}$(BF_4)$^{-}$ (10 mg, 0.025 mmol, 10 mol%) in DCE (5 mL). Purification by column

chromatography (eluent: Cyclohexane/AcOEt 100/0 to 80/20) afforded **5.10** (yellowish oil, 28.5 mg, 69% yield). Spectroscopic data are in accordance with the literature.[31]

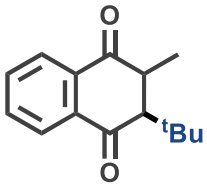

2-(*tert*-Butyl)-3-methyl-2,3-dihydronaphthalene-1,4-dione (5.11).

From **5.1a** (58 mg, 0.375 mmol, 1.5 equiv.), **5.2j** (43 mg, 0.25 mmol, 1 equiv.), 4CzIPN (20 mg, 0.025 mmol, 10 mol%) in DCE (5 mL) under N_2. Purification by column chromatography (eluent: Cyclohexane/AcOEt 100/0 to 80/20) afforded **5.11** (pale orange powder, 38.4 mg, 67% yield).

5.11. ^{1}H NMR (300 MHz, Chloroform-*d*) δ 8.08–7.90 (m, 2H), 7.72 (td, *J* = 6.5, 3.1 Hz, 3H), 3.40 (qd, *J* = 7.1, 4.3 Hz, 1H), 3.03 (d, *J* = 4.4 Hz, 1H), 1.39 (d, *J* = 7.1 Hz, 3H), 1.07 (s, 9H). ^{13}C NMR (75 MHz, Chloroform- *d*) δ 200.0, 185.1, 143.6, 134.2, 133.9, 133.5, 126.6, 126.4, 47.0, 29.9, 27.1, 15.6, 13.1. The compound was not stable under HRMS (EI) analysis.

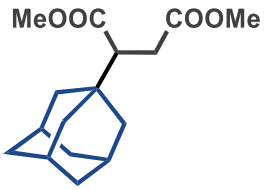

Dimethyl 2-(adamantan-1-yl)succinate (5.12).

From **5.1b** (88 mg, 0.375 mmol, 1.5 equiv.), **5.2a** (31 µL, 0.25 mmol, 1 equiv.), [Acr-Mes]$^+$(BF_4)$^-$ (10 mg, 0.025 mmol, 10 mol%) in DCE (5 mL). Purification by column chromatography (eluent: Cyclohexane/AcOEt 100/0 to 90/10) afforded **5.12** (white powder, mp 50.1–52.3°C, 67.8 mg, 98% yield). Spectroscopic data in accordance with the literature.[24]

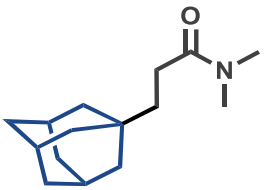

3-(Adamantan-1-yl)-*N,N*-dimethylpropanamide (5.13).

From **5.1b** (88 mg, 0.375 mmol, 1.5 equiv.), **5.2c** (26 µL, 0.25 mmol, 1 equiv.), [Acr-Mes]$^{+}$(BF$_4$)$^{-}$ (10 mg 0.025 mmol, 10 mol%) in DCE (5 mL). Purification by column chromatography (eluent: Cyclohexane/AcOEt 100/0 to 90/10) afforded **5.13** (yellowish oil, 54.6 mg, 93% yield). Spectroscopic data in accordance with the literature.[32]

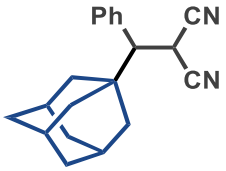

2-((Adamantan-1-yl)(phenyl)methyl)malononitrile (5.14).

From **5.1b** (88 mg, 0.375 mmol, 1.5 equiv.), **5.2d** (38 mg, 0.25 mmol, 1 equiv.), [Acr-Mes]$^{+}$(BF$_4$)$^{-}$ (10 mg 0.025 mmol, 10 mol%) in a DCE (5 mL). Purification by column chromatography (eluent: Cyclohexane/AcOEt 100/0 to 95/5) afforded **5.14** (white powder, mp 166.7–170.8 °C, 39.2 mg, 54% yield). Spectroscopic data in accordance with the literature.[33]

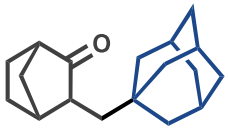

3-((Adamantan-1-yl)methyl)bicyclo[2.2.1]heptan-2-one (5.15).

From **5.1b** (88 mg, 0.375 mmol, 1.5 equiv.), **5.2e** (26 µL, 0.25 mmol, 1 equiv.), [Acr-Mes]$^{+}$(BF$_4$)$^{-}$ (10 mg, 0.025 mmol, 10 mol%) in DCE (5 mL). Purification by column chromatography (eluent: Cyclohexane/AcOEt 100/0 to 90/10) afforded **5.15** (yellowish powder, mp 68.4–70.5 °C 37.4 mg, 58% yield). Spectroscopic data in accordance with the literature.[23]

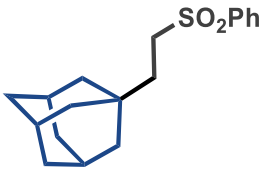

1-(2-(Phenylsulfonyl)ethyl)adamantane (5.16).

From **5.1b** (88 mg, 0.375 mmol, 1.5 equiv.), **5.2f** (42 mg, 0.25 mmol, 1 equiv.), [Acr-Mes]$^{+}$(BF_4)$^{-}$ (10 mg, 0.025 mmol, 10 mol%) in DCE (5 mL). Purification by column chromatography (eluent: DCM/MeOH 100/0 to 95/5) afforded **5.16** (yellowish oil, 60.7 mg, 80% yield). Spectroscopic data in accordance with the literature.[32]

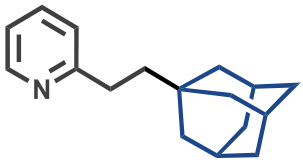

2-(2-Adamantan-1-yl)ethyl)pyridine (5.17).

From **5.1b** (88 mg, 0.375 mmol, 1.5 equiv.), **5.2g** (26 µL, 0.25 mmol, 1 equiv.), [Acr-Mes]$^{+}$(BF_4)$^{-}$ (10 mg, 0.025 mmol, 10 mol%) in DCE (5 mL). Purification by column chromatography (eluent: Cyclohexane/AcOEt 100/0 to 90/10) afforded **5.17** (colourless oil, 52.1 mg, 86% yield). Spectroscopic data in accordance with described in literature.[30]

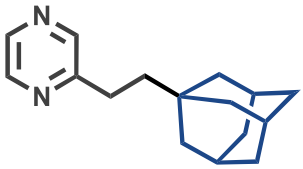

2-(2-Adamantan-1-yl)ethyl)pyrazine (5.18).

From **5.1b** (88 mg, 0.375 mmol, 1.5 equiv.), **5.2h** (25 µL, 0.25 mmol, 1 equiv.), [Acr-Mes]$^{+}$(BF_4)$^{-}$ (10 mg, 0.025 mmol, 10 mol %,) in DCE (5 mL). Purification by column chromatography (eluent: Cyclohexane/AcOEt 100/0 to 9/1) afforded **5.18** (yellowish oil, 44.3 mg, 73% yield). Spectroscopic data in accordance with described in literature.[23]

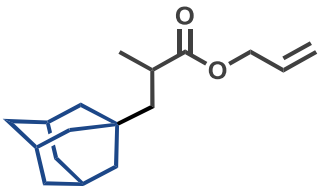

Allyl 3-(adamantan-1-yl)-2-methylpropanoate (5.19).

From **5.1b** (88 mg, 0.375 mmol, 1.5 equiv.), **5.2j** (34 µL, 0.25 mmol, 1 equiv.), [Acr-Mes]$^{+}$(BF$_4$)$^{-}$ (10 mg, 0.025 mmol, 10 mol%) in DCE (5 mL). Purification by column chromatography (eluent: Cyclohexane/AcOEt 100/0 to 80/20) afforded **5.19** (pale yellow oil, 55.7 mg, 85% yield). Spectroscopic data in accordance with described in literature.[23]

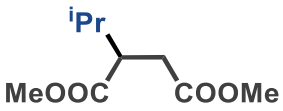

Dimethyl 2-(*iso*-propyl)succinate (5.20).

From **5.1c** (53 mg, 0.375 mmol, 1.5 equiv.), **5.2a** (31 µL, 0.25 mmol, 1 equiv.), [Acr-Mes]$^{+}$(BF$_4$)$^{-}$ (10 mg, 0.025 mmol, 10 mol%) in DCE (5 mL). Purification by column chromatography (eluent: Cyclohexane/AcOEt 100/0 to 80/20) afforded **5.20** (colourless oil, 43.3 mg, 96% yield). Spectroscopic data are in accordance with the literature.[34]

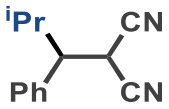

2-(2,2-Dimethyl-1-phenylpropyl)malononitrile (5.21).

From **5.1c** (53 mg, 0.375 mmol, 1.5 equiv.), **5.2d** (38.5 mg, 0.25 mmol, 1 equiv.), [Acr-Mes]$^{+}$(BF$_4$)$^{-}$ (10 mg, 0.025 mmol, 10 mol%) in DCE (5 mL). Purification by column chromatography (eluent: Cyclohexane/AcOEt 100/0 to 90/10) afforded **5.21** (white powder, 16.5 mg, 33% yield). Spectroscopic data are in accordance with the literature.[34]

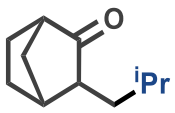

3-*iso*-Butylbicyclo[2.2.1]heptan-2-one (5.22).

From **5.1c** (53 mg, 0.375 mmol, 1.5 equiv.), **5.2e** (28 µL, 0.25 mmol, 1 equiv.), [Acr-Mes]$^{+}$(BF_4)$^{-}$ (10 mg, 0.025 mmol, 10 mol%) in DCE (5 mL). Purification by column chromatography (eluent: Cyclohexane/AcOEt 100/0 to 9/1) afforded **5.22** (yellowish oil, 35.8 mg, 86% yield). Spectroscopic data are in accordance with the literature.[35]

5.22. ^{1}H NMR (400 MHz, Chloroform-*d*) δ 2.62 (d, *J* = 4.9 Hz, 2H), 2.27–2.12 (m, 1H), 2.12–2.03 (m, 1H), 1.83 (d, *J* = 8.8 Hz, 1H), 1.72–1.28 (m, 8H), 1.34–1.11 (m, 1H), 0.92 (dd, *J* = 14.2, 6.6 Hz, 6H). ^{13}C NMR (75 MHz, $CDCl_3$) δ 221.9, 78.6, 78.3, 78.0, 53.1, 51.8, 50.4, 43.7, 39.7, 38.4, 38.1, 36.5, 29.3, 27.6, 26.6, 24.7, 22.7, 22.5.

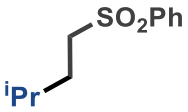

(*Iso*-Pentylsulfonyl)benzene (5.23).

From **5.1c** (53 mg, 0.375 mmol, 1.5 equiv.), **5.2f** (42 mg, 0.25 mmol, 1 equiv.), [Acr-Mes]$^{+}$(BF_4)$^{-}$ (10 mg, 0.025 mmol, 10 mol%)in DCE (5 mL). Purification by column chromatography (eluent: DCM/MeOH 100/0 to 95/5) afforded **5.23** (yellowish oil, 32.1 mg, 60% yield). Spectroscopic data are in accordance with the literature.[36]

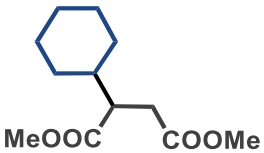

Dimethyl 2-cyclohexylsuccinate (5.24).

From **5.1d** (68 mg, 0.375 mmol, 1.5 equiv.), **5.2a** (31 µL, 0.25 mmol, 1 equiv.), 4CzIPN (20 mg, 0,025 mmol, 10 mol%) in DCE (5 mL) under N_2. Purification by column chromatography (eluent: Cyclohexane/AcOEt 100/0 to 80/20) afforded **5.24** (colourless oil, 28.7 mg, 50% yield). Spectroscopic data are in accordance with the literature.[37]

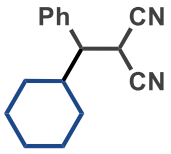

2-(2-Cyclohexyl-1-phenylpropyl)malononitrile (5.25).

From **5.1d** (68 mg, 0.375 mmol, 1.5 equiv.), **5.2d** (38.5 mg, 0.25 mmol, 1 equiv.), 4CzIPN (20 mg, 0,025 mmol, 10 mol%) in DCE (5 mL) under N_2. Purification by column chromatography (eluent: Cyclohexane/AcOEt 100/0 to 90/10) afforded **5.25** (white powder, 13.4 mg, 22% yield). Spectroscopic data are in accordance with the literature.[38]

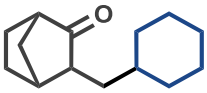

3-(Cyclohexylmethyl)bicyclo[2.2.1]heptan-2-one (5.26).

From **5.1d** (58 µL, 0.375 mmol, 1.5 equiv.), **5.2e** (28 µL, 0.25 mmol, 1 equiv.), [Acr-Mes]$^+$(BF_4)$^-$ (10 mg, 0.025 mmol, 10 mol%) in DCE (5 mL). Purification by column chromatography (eluent: Cyclohexane/AcOEt 100/0 to 90/10) afforded **5.26** (yellowish oil, 33.6 mg, 65% yield). Spectroscopic data are in accordance with the literature.[37]

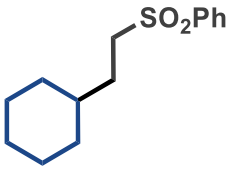

((2-Cyclohexylethyl)sulfonyl)benzene (5.27).

From **5.1d** (68 mg, 0.375 mmol, 1.5 equiv.), **5.2f** (42 mg, 0.25 mmol, 1 equiv.), 4CzIPN (20 mg, 0,025 mmol, 10 mol%) in DCE (5 mL) under N_2. Purification by column chromatography (eluent: DCM/MeOH 100/0 to 95/5) afforded **5.27** (yellowish oil, 46.5 mg, 74% yield). Spectroscopic data are in accordance with the literature.[39]

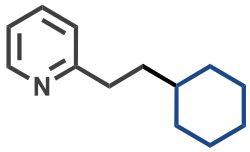

2-(2-Cyclohexylethyl)pyridine (5.28).

From **5.1d** (88 mg, 0.375 mmol, 1.5 equiv.), **5.2g** (26 µL, 0.25 mmol, 1 equiv.), 4CzIPN (20 mg, 0,025 mmol, 10 mol %) in DCE (5 mL) under N_2. Purification by column chromatography (eluent: Cyclohexane/AcOEt 100/0 to 90/10) afforded **5.28** (colourless oil, 30.6 mg, 64% yield). Spectroscopic data in accordance with described in literature.[30]

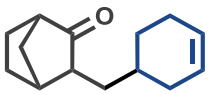

3-(Cyclohex-3-en-1-ylmethyl)bicyclo[2.2.1]heptan-2-one (5.29).

From **5.1e** (90 mg, 0.375 mmol, 2 equiv.), **5.2e** (28 µL, 0.25 mmol, 1 equiv.), 4CzIPN (20 mg, 0,025 mmol, 10 mol%) in DCE (5 mL) under N_2. Purification by column chromatography (eluent: Cyclohexane/AcOEt 100/0 to 90/10) afforded **5.29** (mixture of diastereoisomers d.r. 1:1, yellowish oil, 21.3 mg, 42% yield,).

5.29. ^{1}H NMR (300 MHz, Chloroform- *d*, mixture of diastereoisomers) δ 5.66 (s, 2H), 2.66–2.56 (m, 2H), 2.28–1.99 (m, 5H), 1.89–1.76 (m, 2H), 1.72 – 1.58 (m, 7H), 1.40 (dt, *J* = 13.1, 6.2 Hz, 2H).^{13}C NMR (75 MHz, Chloroform-*d*, mixture of diastereoisomers) δ 201.4, 127.2, 127.2, 126.5, 126.3, 77.6, 76.7, 51.5, 51.4, 50.7, 38.8, 38.6, 37.3, 33.3, 32.8, 32.8, 32.0, 31.9, 31.1, 29.9, 27.9, 25.5, 25.4, 25.2, 21.5, 21.4. HRMS (EI) m/z: $[M+H]^+$ calculated for $C_{16}H_{27}NO_6$ 330.1911, found 330.1909.

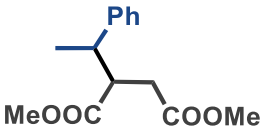

Dimethyl 2-(1-phenylethyl)succinate (5.30).

From **5.1g** (76 mg, 0.375 mmol, 1.5 equiv.) **5.2a** (31 µL, 0.25 mmol, 1 equiv.), 4CzIPN (20 mg, 0,025 mmol, 10 mol %) in DCE (5 mL) under N_2 Purification by column chromatography (eluent: Cyclohexane/AcOEt 100/0 to 8/2) afforded **5.30** (mixture of diastereoisomers d.r. 1:1, yellow oil, 50.0 mg, 80% yield). Spectroscopic data in accordance with described in literature.[40]

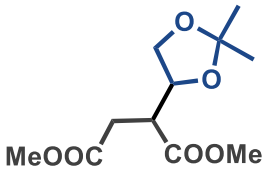

Dimethyl 2-(2,2-dimethyl-1,3-dioxolan-4-yl)succinate (5.31).

From **5.1h** (75 mg 0.375 mmol, 1.5 equiv.), **5.2a** (31 µL, 0.25 mmol, 1 equiv.), [Acr-Mes]$^{+}$(BF_4)$^{-}$ (10 mg, 0.025 mmol, 10 mol%) in DCE (5 mL). Purification by column chromatography (eluent: Cyclohexane/AcOEt 100/0 to 70/30) afforded **5.31** (mixture of diastereoisomers, d.r. 1:1, orange oil, 45.9 mg, 75% yield). Spectroscopic data in accordance with described in literature.[41]

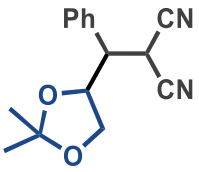

2-((2,2-Dimethyl-1,3-dioxolan-4-yl)(phenyl)methyl)malononitrile (5.32).

From **5.1h** (75 mg 0.375 mmol, 1.5 equiv.), **5.2d** (38 mg, 0.25 mmol, 1 equiv.), [Acr-Mes]$^{+}$(BF_4)$^{-}$ (10 mg, 0.025 mmol, 10 mol%) in DCE (5 mL). Purification by column chromatography (eluent: Cyclohexane/AcOEt 100/0 to 95/5) afforded **5.32** (mixture of diastereoisomers d.r. 1:1, pale yellowish powder, 50.9 mg, 81% yield). Spectroscopic data in accordance with described in literature.[41]

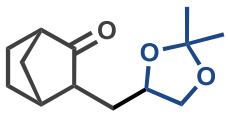

3-((2,2-Dimethyl-1,3-dioxolan-4-yl)methyl)bicyclo[2.2.1]heptan-2-one (5.33).

From **5.1h** (75 mg 0.375 mmol, 1.5 equiv.), **5.2e** (29 µL, 0.25 mmol, 1 equiv.), [Acr-Mes]$^{+}$(BF_4)$^{-}$ (10 mg, 0.025 mmol, 10 mol %,), in DCE (5 mL). Purification by column chromatography (eluent: Cyclohexane/AcOEt 100/0 to 1/1) afforded **5.33** (mixture of diastereoisomers d.r. 1:1, colourless oil, 47.6 mg, 86% yield). Spectroscopic data in accordance with described in literature.[41]

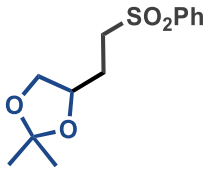

2,2-Dimethyl-4-(2-(phenylsulfonyl)ethyl)-1,3-dioxolane (5.34).

From **5.1h** (75 mg 0.375 mmol, 1.5 equiv.), **5.2f** (42 mg, 0.25 mmol, 1 equiv.), [Acr-Mes]$^{+}$(BF$_4$)$^{-}$ (10 mg, 0.025 mmol, 10 mol%) in DCE (5 mL). Purification by column chromatography (eluent: Cyclohexane/AcOEt 100/0 to 40/60) afforded **5.34** (yellowish oil, 58.7 mg, 87% yield). Spectroscopic data are in accordance with the literature.[42]

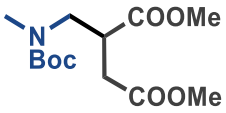

Dimethyl 2-(((*tert*-butoxycarbonyl)(methyl)amino)methyl)succinate (5.35).

From **5.1i** (91 mg, 0.375 mmol, 1.5 equiv.), **5.2a** (31 µL, 0.25 mmol, 1 equiv.), [Acr-Mes]$^{+}$(BF$_4$)$^{-}$ (10 mg, 0.025 mmol, 10 mol%) in DCE (5 mL). Purification by column chromatography (eluent: Cyclohexane/AcOEt 100/0 to 9/1) afforded **5.35** (yellow oil, 55.2 mg, 77% yield). Spectroscopic data in accordance with the literature.[43]

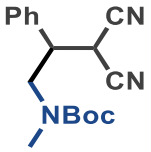

***tert*-Butyl (3,3-dicyano-2-phenylpropyl)(methyl)carbamate (5.36).**

From **5.1i** (91 mg, 0.375 mmol, 1.5 equiv.), **5.2d** (38 mg 0.25 mmol, 1 equiv.), [Acr-Mes]$^{+}$(BF$_4$)$^{-}$ (10 mg, 0.025 mmol, 10 mol%) in DCE (5 mL). Purification by column chromatography (eluent: Cyclohexane/AcOEt 100/0 to 70/30) afforded **5.36** (yellow oil, 43.4 mg, 58% yield). Spectroscopic data in accordance with the literature.[44]

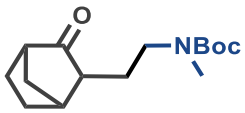

***tert*-Butyl methyl(2-(3-oxobicyclo[2.2.1]heptan-2-yl)ethyl)carbamate (5.37).**
From **5.1i** (91 mg, 0.375 mmol, 1.5 equiv.), **5.2e** (28 µL, 0.25 mmol, 1 equiv.), [Acr-Mes]$^{+}$(BF$_4$)$^{-}$ (10 mg, 0.025 mmol, 10 mol%) in DCE (5 mL). Purification by column chromatography (eluent: Cyclohexane/AcOEt 100/0 to 1/1) afforded **5.37** (yellow oil, 64,9 mg, 86% yield). Spectroscopic data in accordance with the literature.[23]

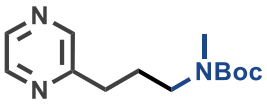

***tert*-Butyl methyl(3-(pyrazin-2-yl)propyl)carbamate (5.38).**
From **5.1i** (91 mg, 0.375 mmol, 1.5 equiv.), **5.2h** (25 µL, 0.25 mmol, 1 equiv.), [Acr-Mes]$^{+}$(BF$_4$)$^{-}$ (10 mg, 0.025 mmol, 10 mol%) in DCE (5 mL). Purification by column chromatography (eluent: Cyclohexane/AcOEt 100/0 to 20/80) afforded **5.38** (yellow oil, 33.2 mg, 54% yield). Spectroscopic data in accordance with the literature.[23]

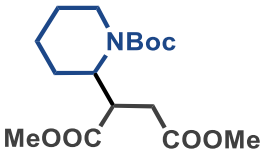

Dimethyl 2-(1-(tert-butoxycarbonyl)piperidin-2-yl)succinate (5.39).
From **5.1j** (106 mg, 0.5 mmol, 1.5 equiv.), **5.2a** (31 µL, 0.25 mmol, 1 equiv.), [Acr-Mes]$^{+}$(BF$_4$)$^{-}$ (10 mg, 0.025 mmol, 10 mol%) in DCE (5 mL). Purification by column chromatography (eluent: Cyclohexane/AcOEt 100/0 to 80/20) afforded **5.39** (mixture of diastereoisomers d.r. 1:1, yellow oil, 54.0 mg, 63% yield).
5.39. ^{1}H NMR (300 MHz, Chloroform-*d* mixture of diastereoisomers) δ 4.36 (s, 1H), 3.99 (s, 1H), 3.71 (s, 3H), 3.65 (s, 3H), 3.36 (td, *J* = 10.8, 4.4 Hz, 1H), 2.69 (td, *J* = 18.0, 11.6 Hz, 2H), 2.42 (dd, *J* = 16.6, 4.4 Hz, 1H), 1.66–1.60 (m, 2H), 1.60–1.50 (m, 4H), 1.47 (s, 9H). ^{13}C NMR (75 MHz, Chloroform-*d* mixture of diastereoisomers) δ 174.3, 172.5, 154.9, 80.2, 52.2, 52.0, 41.7, 38.6, 34.3, 29.8, 28.6, 27.1, 25.3, 19.2. HRMS (EI) m/z: [M+H]$^{+}$ calculated for $C_{16}H_{27}NO_6$ 330.1911, found 330.1909.

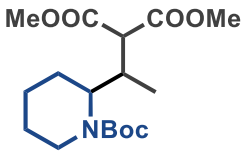

Dimethyl 2-(1-(1-(*tert*-butoxycarbonyl)piperidin-2-yl)ethyl)malonate (5.40). From **5.1j** (106 mg, 0.5 mmol, 1.5 equiv.), **5.2b** (28 µL, 0.25 mmol, 1 equiv.), [Acr-Mes]$^{+}$(BF_4)$^{-}$ (10 mg, 0.025 mmol, 10 mol%), in DCE (5 mL). Purification by column chromatography (eluent: Cyclohexane/AcOEt 100/0 to 1/1) afforded **5.40** (mixture of diastereoisomers d.r. 1:1, pale yellow oil, 68.6 mg, 80% yield).

5.40. ^{1}H NMR (400 MHz, Chloroform-*d*, mixture of diastereoisomers) δ 4.16 (s, 1H), 4.05 (s, 1H), 3.77–3.74 (m, 6H), 3.74–3.71 (m, 6H), 3.66–3.61 (m, 1H), 3.56 (t, *J* = 7.4 Hz, 2H), 3.48 (d, *J* = 4.2 Hz, 1H), 3.25 (d, *J* = 8.1 Hz, 1H), 2.72 (tdd, *J* = 11.1, 9.0, 5.5 Hz, 2H), 2.34 (t, *J* = 7.5 Hz, 1H), 2.31–2.18 (m, 2H), 1.83 (p, *J* = 6.1 Hz, 1H), 1.72–1.55 (m, 12H), 1.48–1.41 (m, 18H), 1.00–0.94 (m, 6H). ^{13}C NMR (100 MHz, Chloroform-*d*, mixture of diastereoisomers) δ 169.3, 169.2, 168.6, 163.0, 155.1, 83.9, 77.3, 77.0, 76.7, 57.5, 52.5, 52.3, 52.2, 40.4, 33.9, 33.4, 31.9, 31.8, 29.4, 29.4, 29.3, 29.1, 28.4, 28.3, 28.1, 26.1, 25.3, 24.8, 24.1, 19.0, 16.9, 14.1, 12.8. HRMS (EI) m/z: [M+H]$^{+}$ calculated for $C_{17}H_{29}NO_6$ 344.2068, found 344.2075.

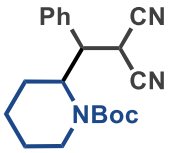

***tert*-Butyl 2-(2,2-dicyano-1-phenylethyl)piperidine-1-carboxylate (5.41).** From **5.1j** (106 mg, 0.5 mmol, 1.5 equiv.), **5.2d** (38 mg 0.25 mmol, 1 equiv.), [Acr-Mes]$^{+}$(BF_4)$^{-}$ (10 mg, 0.025 mmol, 10 mol%) in DCE (5 mL). Purification by column chromatography (eluent: Cyclohexane/AcOEt 100/0 to 1/1) afforded **5.41** (mixture of diastereoisomers d.r. 1:1, yellow powder, 55.6 mg, 61% yield). Spectroscopic data in accordance with the literature.[45]

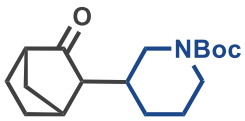

***tert*-Butyl(2-(3-oxobicyclo[2.2.1]heptan-2-yl)methyl)piperidine-1-carboxylate (5.42).**

From **5.1j** (106 mg, 0.5 mmol, 1.5 equiv.), **5.2e** (28 µL, 0.25 mmol, 1 equiv.), [Acr-Mes]$^{+}$(BF_4)$^{-}$ (10 mg, 0.025 mmol, 10 mol%) in DCE (5 mL). Purification by column chromatography (eluent: Cyclohexane/AcOEt 100/0 to 1/1) afforded **5.42** (mixture of diastereoisomers d.r. 1:1, pale yellow oil, 38.7 mg, 50% yield)

5.42. ^{1}H NMR (300 MHz, Chloroform-*d* mixture of diastereoisomers) δ 4.25 (s, 1H), 3.95 (s, 1H), 2.86–2.73 (m, 2H), 2.61 (d, *J* = 5.0 Hz, 1H), 2.33 (ddd, *J* = 15.1, 12.1, 3.3 Hz, 1H), 1.90–1.75 (m, 2H), 1.70–1.63 (m, 4H), 1.63–1.59 (m, 3H), 1.56–1.51 (m, 2H), 1.48–1.43 (m, 12H), 1.40–1.30 (m, 2H), 1.07 (ddd, *J* = 15.0, 11.5, 3.8 Hz, 1H). ^{13}C NMR (75 MHz, Chloroform-*d* mixture of diastereoisomers) δ 155.2, 155.0, 79.4, 79.4, 77.6, 76.7, 51.9, 51.2, 50.7, 50.4, 38.6, 38.3, 37.4, 37.2, 29.8, 28.7, 28.6, 28.5, 27.7, 26.2, 25.8, 25.7, 25.7, 25.6, 21.5, 21.4, 19.2, 19.0. HRMS (EI) m/z: [M+H]$^{+}$ calculated for $C_{18}H_{29}NO_3$ 308.2220, found 308.2221.

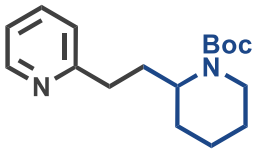

***tert*-Butyl 2-(2-(pyridin-2-yl)ethyl)piperidine-1-carboxylate (5.43).**

From **5.1j** (106 mg, 0.5 mmol, 1.5 equiv.), **5.2g** (25 µL, 0.25 mmol, 1 equiv.), [Acr-Mes]$^{+}$(BF_4)$^{-}$ (10 mg, 0.025 mmol, 10 mol %) in DCE (5 mL). Purification by column chromatography (eluent: Cyclohexane/AcOEt 100/0 to 80/20) afforded **5.43** (mixture of diastereoisomers d.r. 1:1, pale yellow oil, 45.8 mg, 62% yield).

5.43. ^{1}H NMR (400 MHz, Chloroform-*d* mixture of diastereoisomers) δ 8.52 (d, *J* = 3.0 Hz, 1H), 7.58 (td, *J* = 7.7, 1.9 Hz, 1H), 7.16 (d, *J* = 7.8 Hz, 1H), 7.10 (ddd, *J* = 7.5, 5.0, 1.2 Hz, 1H), 4.32 (s, 1H), 3.98 (s, 1H), 2.88–2.63 (m, 3H), 2.16 (dtd, *J* = 13.8, 10.2, 5.8 Hz, 1H), 1.85 (ddt, *J* = 13.7, 10.5, 5.9 Hz, 1H), 1.66–1.55 (m, 6H), 1.44 (s, 9H).^{13}C NMR (100 MHz, Chloroform-*d* mixture of diastereoisomers) δ 162.0, 155.3, 149.3, 136.6, 123.1, 121.2, 79.3, 77.5, 77.2, 76.8, 35.4, 30.1, 28.9, 28.6, 28.2, 25.8, 19.2. HRMS (EI) m/z: [M+H]$^{+}$ calculated for $C_{17}H_{26}N_2O_2$ 291.2067, found 291.2065.

5.5 References.

1) (a) Yan, M., Lo, J. C., Edwards J. T. and Baran, P. S. Radicals: Reactive Intermediates with Translational Potential. *J. Am. Chem. Soc.* **2016**, *138*, 12692–12714; (b) Studer, A. and Curran, D. P. Catalysis of Radical Reactions: A Radical Chemistry Perspective. *Angew. Chem., Int. Ed.* **2016**, *55*, 58–102; (c) Romero, K. J., Galliher, M. S., Pratt, D. A. and Stephenson, C. R. J. Radicals in natural product synthesis. *Chem. Soc. Rev.* **2018**, *47*, 7851–7866; (d) *Free Radicals: Fundamentals and Applications in Organic Synthesis,* Fensterbank, L. and Ollivier, C. G., Eds.; Thieme Verlag KG, Stuttgart, Germany, **2021**.
2) (a) Ravelli, D., Protti, S. and Fagnoni, M. Carbon–Carbon Bond Forming Reactions via Photogenerated Intermediates, *Chem. Rev.* **2016**, *116*, 9850–9913; (b) Goddard, J.-P., Ollivier, C. and Fensterbank, L. Photoredox Catalysis for the Generation of Carbon Centered Radicals, *Acc. Chem. Res.* **2016**, *49*, 1924–1936; (c) Pitre, S. P., Weires, N. A. and Overman, L. E. Forging $C(sp^3)–C(sp^3)$ Bonds with Carbon-Centered Radicals in the Synthesis of Complex Molecules. *J. Am. Chem. Soc.* **2019**, *141*, 2800–2813; (d) Crespi, S. and Fagnoni, M. Generation of Alkyl Radicals: From the Tyranny of Tin to the Photon Democracy, *Chem. Rev.* **2020**, *120*, 9790–9833; (e) Fagnoni, M., Ravelli, D., and Protti, S. in Science of Synthesis: *Free Radicals: Fundamentals and Applications in Organic Synthesis*, Fensterbank, L. and Ollivier, C., Eds.; Thieme, Stuttgart, **2021**, Vol. 2, pp 339–357; (f) Juliá, F., Constantin, T. and Leonori, D. Applications of Halogen-Atom Transfer (XAT) for the Generation of Carbon Radicals in Synthetic Photochemistry and Photocatalysis, *Chem. Rev.* **2022**, *122*, 2292–2352; (g) Capaldo, L. Ravelli, D. and Fagnoni, M. Direct Photocatalyzed Hydrogen Atom Transfer (HAT) for Aliphatic C–H Bonds Elaboration, *Chem. Rev.* **2022**, *121*, 1875–1924.
3) (a) Ravelli, D., Protti, S., Fagnoni, M. and Albini, A. Visible Light Photocatalysis. A Green Choice?, *Curr. Org. Chem*. **2013**, *17*, 2366–2373; (b) *Visible Light Photocatalysis in Organic Chemistry*, Eds.; Stephenson, C. R. J., Yoon, T. P. and MacMillan, D. W. C. Wiley-VCH, Weinheim, Germany **2018**; (c) *Photoorganocatalysis in organic synthesis*, Fagnoni, M., Protti, S. and Ravelli, D.

Eds.; World Scientific Publishing Europe Ltd., Singapore, **2019**; (d) *Chemical Photocatalysis*. 2nd ed.; B. König, Ed.; De Gruyter, **2020.**

4) For recent reviews on the photogeneration of alkyl radicals see: (a) J. Matsui, K., Lang, S. B., Heitz, D. R. and Molander, G. A. Photoredox-Mediated Routes to Radicals: The Value of Catalytic Radical Generation in Synthetic Methods Development, *ACS Catal.* **2017**, *7*, 2563–2575; (b) Roslin, S. and Odell, L. R. Visible-Light Photocatalysis as an Enabling Tool for the Functionalization of Unactivated C(sp^3)-Substrates, *Eur. J. Org. Chem.* **2017**, 1993–2007; (c) Niu, P., Li, J., Zhang, Y. and Huo, C. One-Electron Reduction of Redox-Active Esters to Generate Carbon-Centered Radicals, *Eur. J. Org. Chem*. **2020**, 5801–5814; (d) Correia, J. T. M., Fernandes, V. A., Matsuo, B. T., Delgado, J. A. C., De Souza W. C. and. Paixão, M. W. Photoinduced deaminative strategies: Katritzky salts as alkyl radical precursors, *Chem. Commun*. **2020**, *56*, 503–514; (e) Karmakar, S., Silamkoti, A., Meanwell, N. A., Mathur, A. and Kumar Gupta A. Utilization of C(sp^3)-Carboxylic Acids and Their Redox-Active Esters in Decarboxylative Carbon-Carbon Bond Formation, *Adv. Synth. Catal.* **2021**, *363*, 3693–3736; (f) Kumar Parida, S., Mandal, T., Das, S., Kumar Hota, S., De Sarkar, S. and Murarka, S. Single Electron Transfer-Induced Redox Processes Involving N-(Acyloxy)phthalimides, *ACS Catal.* **2021**, *11*, 1640−1683; (g) Protti, S., Ravelli, D. and Fagnoni, M. Designing Radical Chemistry by Visible-Light Promoted Homolysis, *Trends Chem.* **2022**, *4*, 305−317.

5) Luguera Ruiz, A., La Mantia, M., Merli, D., Protti, S. and Fagnoni, M. Alkyl Radical Generation via C–C Bond Cleavage in 2-Substituted Oxazolidines, *ACS Catal*. **2022**, *12*, 12469–12476.

6) Murphy, J. A. Discovery and Development of Organic Super-Electron-Donors, *J. Org. Chem.* **2014**, *79*, 3731−3746.

7) (a) Chikashita, H., Nishida, S., Miyazaki, M. and Itoh, K. 2-Phenylbenzimidazoline as a reducing agent in the preparation of malononitriles from α,β-unsaturated dinitriles, *Synth. Commun.* **1983**, *13*, 1033–1039; (b) Chikashita, H., Morita, Y. and Itoh, K. An efficient method for the selective reduction of 2-aryl-1-nitroalkenes to 2-aryl-1-nitroalkanes by 2-phenylbenzimidazoline, *Synth. Commun.* **1985**, *15*, 527–533; (c) Chikashita H. and Itoh, K. Reduction of α,β-unsaturated carbonyls, *Bull. Chem. Soc. Jpn.* **1986**, *59*, 1747–1752; (d)

Chikashita, H., Ide, H. and Itoh, K. 1,3-Dimethyl-2-phenylbenzimidazoline as a Novel and Efficient Reagent for Mild Reductive Dehalogenation of -Halo Carbonyl Compounds and Acid Chlorides, *J. Org. Chem.* **1986**, *51*, 5400–5405.

8) (a) Chen, J. and Tanner, D. D. New Method for the Facile Reduction of -Nitro Sulfones to Nitroalkanes via an Electron-Transfer-Hydrogen Atom Abstraction Mechanism, *J. Org. Chem.* **1988**, *53*, 3897–3900; (b) Tanner, D. D. and Chen, J. J. On the Mechanism of the Reduction of α-Halo Ketones by l,3-Dimethyl-2-phenylbenzimidazoline. Reduction by a SET-Hydrogen Atom Abstraction Chain Mechanism, *J. Org. Chem.* **1989**, *54*, 3842–3846; (c) Tanner, D. D., Chen, J. J., Luelo, C. and Peters, P. M. Reversible Cyclopropyl Ring Opening of 1 -Aroyl-2-phenylcyclopropane Radical Anions. Determination of the Ring Opening and Closure Rates of the Intermediate Ketyls, *J. Am. Chem. Soc.* **1992**, *114*, 713–717; (d) Tanner, D. D. and Chen, J. J. Thiophenol-Promoted Radical Chain Reduction of alpha-Substituted Isobutyrophenones by l,3-Dimethyl-2-phenylbenzimidazoline, *J. Org. Chem.* **1992**, *57*, 662–666.

9) Rohrbach, S., Shah, S. R., Tuttle, T. and Murphy, J. A. Neutral Organic Super Electron Donors Made Catalytic, *Angew. Chem. Int. Ed.* **2019**, *58*, 11454–11458.

10) (a) Hasegawa, E., Kato, T., Kitazume, T., Yanagi, K., Hasegawa, K. and Horaguchi, T. Photoinduced Electron Transfer Reactions of α,β-Epoxy Ketones with 2-Phenyl-N,N-dimethylbenzimidazoline (PDMBI): Significant Water Effect on the Reaction Pathway, *Tetrahedron Lett.* **1996**, *37*, 7079–7082; (b) Hasegawa, E., Yoneoka, A., Suzuki, K., Kato, T., Kitazume, T., Yanagi, K. Reductive Transformation of α,β-Epoxy Ketones and Other Compounds Promoted through Photoinduced Electron Transfer Processes with 1,3-Dimethyl-2-phenylbenzimidazoline (DMPBI). *Tetrahedron*. **1999**, *55*, 12957–12968; (c) Feng, Y.-S., Yang, C.-Y., Huang, Q. and Xu, H.-J. Study on comparison of reducing ability of three organic hydride compounds, *Tetrahedron* **2012**, *68*, 5053–5059; (d) Hasegawa, E., Ohta, T., Tsuji, S., Mori, K., Uchida, K., Miura, T., Ikoma, T., Tayama, E., Iwamoto, H., Takizawa, S. and Murata, S. Aryl-substituted dimethylbenzimidazolines as effective reductants of photoinduced electron transfer reactions, *Tetrahedron*. **2015**, *71*, 5494–5505; (e) Hasegawa, E., Nagakura, Y., Izumiya, N., Matsumoto, K., Tanaka, T., Miura, T., Ikoma, T., Iwamoto, H., Wakamatsu, K. Visible Light and Hydroxynaphthylbenzimidazoline

Promoted Transition-Metal-Catalyst-Free Desulfonylation of *N*-Sulfonylamides and *N*-Sulfonylamines, *J. Org. Chem.* **2018**, *83*, 10813−10825; (f) Hasegawa, E., Yoshioka, N., Tanaka, T., Nakaminato, T., Oomori, K., Ikoma, T., Iwamoto, H. and Wakamatsu, K. Sterically Regulated α-Oxygenation of α-Bromocarbonyl Compounds Promoted Using 2-Aryl-1,3-dimethylbenzimidazolines and Air, *ACS Omega*. **2020**, *5*, 7651−7665; (g) Miyajima, R., Ooe, Y., Miura, T., Ikoma, T., Iwamoto, H., Takizawa, S.A. and Hasegawa, E. Triarylamine-Substituted Benzimidazoliums as Electron Donor−Acceptor Dyad-Type Photocatalysts for Reductive Organic Transformations, *J. Am. Chem. Soc.* **2023**, *145*, 10236−10248; (h) Okumura, S., Takahashi, T., Torii, K. and Uozumi, Y. Photocatalytic Cross-Pinacol Coupling Promoted by Carbon Dioxide, *Chem. Eur. J.* **2023**, *29*, e202300840.

11) Saga, Y., Nakayama, Y., Watanabe, T., Kondo, M. and Masaoka, S. Visible-Light-Driven Hydroacylation of Unactivated Alkenes Using Readily Available Acyl Donors, *Org. Lett.* **2023**, *25*, 1136−1141.

12) (a) Li, L., Fang, L., Wu, W. and Zhu, J. Visible-Light-Mediated Intermolecular Radical Conjugate Addition for the Construction of Vicinal Quaternary Carbon Centers, *Org. Lett*. **2020**, *22*, 5401−5406; (b) Lee, S.-C., Li, L.-Y., Tsai, Z.-N., Lee, Y.-H., Tsao, Y.-T., Huang, P.-G., Cheng, C.-K., Lin, H.-B., Chen, T.-W., Yang, C.-H., Chiu, C.-C. and Liao, H.-H. Aromatization as an Impetus to Harness Ketones for Metallaphotoredox-Catalyzed Benzoylation/Benzylation of (Hetero)arenes, *Org. Lett.* **2022**, *24*, 85−89; (c) Mondal, P. P., Das, S., Venugopalan, S., Krishnan, M. and Sahoo, B. Visible-Light-Photocatalyzed Dicarbofunctionalization of Conjugated Alkenes with Ketone-Based Dihydroquinazolinones. *Org. Lett.* **2023**, *25*, 1441−1446; (d) Mondal, P.P., Pal, A., Das, S., Vijayan, S. M., Nair, A. V., Ojha, S. and Sahoo, B. Organophotoredox-Catalyzed Oxidative C(sp2)–H Alkylation of N-Heteroarenes with Dihydroquinazolinones by C–C Cleavage, *Synlett*, **2023**, *34*, 1241–1246; (e) Yang, X., Abrams, R. and Martin, R. Dihydroquinazolinones as adaptative C(sp^3) handles in arylations and alkylations via dual catalytic C–C bond-functionalization, *Nat Commun.* **2022**, *13*, 2394–2402; (f). Rubanov, Z. M, Supranovich, V. I., Levin, V. V. and Dilman, A. D. BF_2-Chelates of *N*-Acylhydrazones as Versatile Coupling Partners in Photoredox Promoted Reactions, *Eur. J. Org. Chem.* **2023**, *26*, e202300247.

13) (a) Von Ragué Schleyer, P. and Puhlhofer, F. Recommendations for the Evaluation of Aromatic Stabilization Energies, *Org. Lett.* **2002**, *4*, 2873–2876; (b) Bhunia, A. and Studer, A. Recent Advances in Radical Chemistry Proceeding through Pro-aromatic Radicals, *Chem.* **2021**, *7*, 2060–2100.

14) Uchikura, T., Nakamura, H., Sakai, H. and Akiyama, T. 2-Silylated Dihydroquinazolinone as a Photocatalytic Energy Transfer Enabled Radical Hydrosilylation Reagent, *Chem. Eur. J.* **2023**, *29*, e202301090.

15) (a) Nicewicz, D. A. and MacMillan, D. W. C. Merging photoredox catalysis with organocatalysis: the direct asymmetric alkylation of aldehydes, *Science*, **2008**, *322*, 77–80; (b) Skubi, K. L., Blum, T. R. and Yoon, T. P. Dual Catalysis Strategies in Photochemical Synthesis, *Chem. Rev.* **2016**, *116*, 10035−10074; (c) Yao, W., Bazan-Bergamino, E. A. and Ngai, M.-Y. Asymmetric Photocatalysis Enabled by Chiral Organocatalysts, *ChemCatChem* **2022**, *14*, e202101292; (d) Malakar, C. C., Dell'Amico, L. and Zhang, W. Dual Catalysis in Organic Synthesis: Current Challenges and *New Trends, Eur. J. Org. Chem.* **2023**, *26*, e202201114.

16) Wu, Y., Kim, D. and Teets, T. S. Photophysical Properties and Redox Potentials of Photosensitizers for Organic Photoredox Transformations, *Synlett,* **2022**, *33*, 1154–1179.

17) Russell, G. A., Kim, B. H. and Kulkarni, S. V. Electron transfer processes. 48. Free-radical alkylations of enones involving proton transfers, *J. Org. Chem*. **1989**, *54*, 3768–3770.

18) (a) Cushman, D.W. and Ondetti. M. A. History of the Design of Captopril and Related Inhibitors of Angiotensin Converting Enzyme. *Hypertension*, **1991**, *4*, 589-592. (b) Cushman, D.W.and Ondetti. M. A. Design of angiotensin converting enzyme inhibitors. *Nat. Med*. **1999**, *10*, 1110–1113.

19) Mella, M., Fasani, E. and Albini, A. Electron Transfer Photoinduced Cleavage of Acetals. A Mild Preparation of Alkyl Radicals, *J. Org. Chem.* **1992**, *57*, 3051−3057.

20) Saraiva, M. F., Couri, M. R. C., Le Hyaric, M., De Almeida, M. V. The Barton ester free-radical reaction: a brief review of applications, *Tetrahedron,* **2009**, *65*, 3563–3572.

21) Zhu, X. and Fu, H. Photocatalytic cross-couplings via the cleavage of N–O bonds, *Chem. Commun.* **2021**, *57*, 9656–9671.

22) Takeuchi, K., Kitagawa, I., Akiyama, Shibata, F. T., Kato, M. and Okamoto, K. Ring-Expansion of Bridgehead Aldehydes with 1-Adamantanecarbonyl Cation or Benzoyl Trifluoromethanesulfonate: A New Route to Bicyclic and Tricyclic 1,2-Diols, *Synthesis,* **1987**, *1987*, 612–615.

23) Luguera Ruiz, A., La Mantia, M., Merli, D., Protti, S. and Fagnoni, M. Alkyl Radical Generation via C–C Bond Cleavage in 2-Substituted Oxazolidines, *ACS Catal.* **2022**, *12*, 12469–12476.

24) Rohe, S., Morris, A. O., McCallum, T. and Barriault, L. Hydrogen Atom Transfer Reactions via Photoredox Catalyzed Chlorine Atom Generation, *Angew. Chem. Int. Ed.* **2018**, *57*, 15664–15669.

25) Provencher, L., Wynn, H., Jones, J. B. and Krawczyk, A. R. Enzymes in organic synthesis 51. Probing the dimensions of the large hydrophobic pocket of the active site of pig liver esterase, *Tetrahedron: Asymm*. **1993**, *4*, 2025–2040.

26) Zhou, X., Zhang, G., Gao, B. and Huang**,** H. Palladium-Catalyzed Hydrocarbonylative C–N Coupling of Alkenes with Amides *Org. Lett.* **2018**, *20,* 2208–2212.

27) Uchikura, T., Moriyama, K., Toda, M., Mouri, T., Ibáñez, I. and Akiyama, T. Benzothiazolines as radical transfer reagents: hydroalkylation and hydroacylation of alkenes by radical generation under photoirradiation conditions, *Chem. Commun*. **2019**, *55*, 11171–11174.

28) Petrier, C., De Souza Barbosa, J., Dupuy, C. and Luche, J. L. Ultrasound in organic synthesis. 7. Preparation of organozinc reagents and their nickel-catalyzed reactions with α,β-unsaturated carbonyl compounds, *J. Org. Chem.* **1985**, *50*, 5761–5765.

29) Xue, F., Wang, F., Liu, J., Di, J., Liao, Q., Lu, H., Zhu, M., He, L., He, H., Zhang, D., Song, H., Liu, X. Y. and Qin, Y. *Angew. Chem. Int. Ed.* **2019**, *57*, 6667–6671.

30) Pang, H., Wang, Y., Gallou, F. and Lipshutz, B. H. Fe-catalyzed reductive couplings of terminal (hetero) aryl alkenes and alkyl halides under aqueous micellar conditions, *J. Am. Chem. Soc.* **2019**, *141*, 17117–17124.

31) Braquet, P., Pirotzky, E., Godfroid, J.-J. and Heymans, F. *US Pat.* **1991**, US5019576 A.

32) Sato, R., Okamoto. R., Ishizuka, T., Nakayama, A., Karanjit, S. and Namba, K. Microwave-assisted Tertiary Carbon Radical Reaction for Construction of Quaternary Carbon Center, *Chem. Lett*. **2019**, *48*, 414–417.

33) Xu, Q. H., Wei, L. P. and Xiao, B. Alkyl-$GeMe_3$: Neutral Metalloid Radical Precursors upon Visible-Light Photocatalysis, *Angew. Chem. Int. Ed.* **2022**, *61*, e202115592.

34) Van Leeuwen, T., Buzzetti, L., Perego, L. A. and Melchiorre, P. A Redox-Active Nickel Complex that Acts as an Electron Mediator in Photochemical Giese Reactions, *Angew. Chem. Int. Ed.* **2019**, *58*, 4953–4957.

35) Kuchin, A. V., Nurushev, R. A., Khalilov, L. M. and Tolstikov, G. A. Comparative Investigation of the Stereo- and Regioselectivity of the Hydroalumination of Olefins of Norbornane Structure with Various Reagents, *J. Gen. Chem*. *USSR*, **1987**, 1574-1579.

36) Xu, F., Wang, F., Liu, J., Di, J., Liao, Q., Lu, H., Zhu, M., He, L., He, H., Zhang, D., Song, H., Liu, X.-Y. and Qin, Y. A Desulfurative Strategy for the Generation of Alkyl Radicals Enabled by Visible-Light Photoredox Catalysis, *Angew. Chem. Int. Ed.* **2018**, *57*, 6667–6671.

37) Wan, T., Capaldo, L., Ravelli, D., Vitullo, W., De Zwart, F. J., De Bruin, B. and Noël, T. Photoinduced Halogen-Atom Transfer by N-Heterocyclic Carbene Ligated Boryl Radicals for $C(sp^3)$–$C(sp^3)$ Bond Formation, *J. Am. Chem. Soc.* **2023**, *145*, 991–999.

38) Fanini, F., Luridiana, A., Mazzarella, D., Alfano, A. I., Van der Heide, P., Rincón, J. A., García-Losada, P., Mateos, C., Frederick, M. O., Nuño, M. and Noël, T. Flow photochemical Giese reaction via silane-mediated activation of alkyl bromides, *Tetrahedron Lett.* **2023**, *117*, 154380.

39) Yu, H., Fu, K., Yang, G., Liu, M., Yang P. and Liu, T. Divergent upgrading pathways of sulfones with primary alcohols: nickel-catalyzed α-alkylation under N_2 and metal-free promoted β-olefination in open air, *Chem. Commun*. **2023**, *59*, 615–618.

40) Capaldo, L., Fagnoni, M. and Ravelli, D. Vinylpyridines as Building Blocks for the Photocatalyzed Synthesis of Alkylpyridines, *Chem. Eur. J.* **2017**, *23*, 6527–6530.

41) He, P., Watts, P., Marken, F. and Haswell, S. J. Self-Supported and Clean One-Step Cathodic Coupling of Activated Olefins with Benzyl Bromide Derivatives in a Micro Flow Reactor, *Angew. Chem. Int. Ed.* **2006**, *45*, 4146–4149.
42) Hayakawaa, M., Shimizua, R., Omoria, H., Shirotaa, H., Uchidaa, K., Mashimoa, H., Ryuusei, H. X., Seiya, Y., Yoshiki, N., Chuanxiang, W., Tadashi, L. and Ouchia, A. A. Photochemical addition of cyclic ethers/acetals to olefins using tBuOOtBu: Synthesis of masked ketones/aldehydes and diols, *Tetrahedron,* **2020**, *76*, 131557.
43) Raviola, C. and Ravelli, D. Efficiency and Selectivity Aspects in the C–H Functionalization of Aliphatic Oxygen Heterocycles by Photocatalytic Hydrogen Atom Transfer, *Synlett,* **2019**, *30*, 803–808.
44) Schweitzer-Chaput, B., Horwitz, M. A., Beato, E. P. and Melchiorre, P. Photochemical generation of radicals from alkyl electrophiles using a nucleophilic organic catalyst, *Nat. Chem.* **2019**, *11*, 129–135.
45) Ohmatsu, K., Suzuki, R., Suzuki, R., Furukawa, Y., Sato, M. and Ooi, T. Zwitterionic 1, 2, 3-triazolium amidate as a catalyst for photoinduced hydrogen-atom transfer radical alkylation, *ACS Catal.* **2020**, *10*, 2627–2632.

Chapter 6

Automated One-pot Library Synthesis with Aldehydes as Radical Precursors

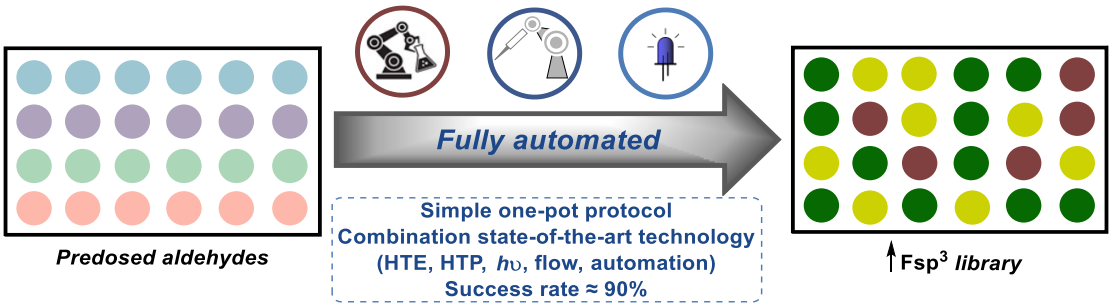

This chapter is based on:

Luguera Ruiz, A.; Pijper, B.; Linares, M.L.; Cañellas, S.; Protti, S.; Fagnoni, M.; Alcázar, J. Automated One-pot Library Synthesis with Aldehydes as Radical Precursors. *ChemRxiv,* **2024**, 10.26434/chemrxiv-2024-xcjgq.

6.1 Introduction.

Active pharmaceutical ingredients (APIs) typically interact with specific biological targets, necessitating a three-dimensional character in bioactive molecules.[1] In the last decades, various 3D descriptors have been extensively studied and correlated with the likelihood of a drug candidate becoming a marketed drug.[2] Among these, the fraction sp^3 character (Fsp^3) has gained prominence for describing the "flatness" or "3D character" of compounds. Fsp^3 is determined by the ratio of hybridized Csp^3 atoms to the total number of carbon atoms in a molecule; hence, a higher Fsp^3 value indicates a greater 3D character. This factor is directly proportional to improved drug-like properties, such as solubility in aqueous media and CYP450 inhibition.[3-7]

Enhancing the "drug-likeness" of candidates by introducing enriched Csp^3 moieties is crucial. The urgent need to discover new therapeutic agents and explore new chemical spaces has driven chemists to develop innovative methodologies and to expand the chemical toolbox for the forging of Csp^3-Csp^3 bonds.[8,9] High-throughput experimentation and the automation of laboratory processes enable medicinal chemists to accelerate drug discovery projects, significantly increasing the efficacy, productivity and chemical space.[10,13]

Photochemistry has opened up new reactivity to form Csp^3-Csp^3 bonds than classical synthetic methodologies.[14-16] Photoredox catalysis involves the interaction of a photocatalyst (PC) with a radical precursor, which is either reduced or oxidized by the excited PC to generate an alkyl radical. This process has expanded the chemical space that can be explored, due to the wide range of available starting materials that can serve as radical sources (e.g. alcohols, carboxylic acids, aldehydes, etc.).[20-24] Transforming functional groups into redox-active species, including Katritzky salts,[17] redox-active esters,[18,19] alkyl tetrafluoroborates,[20] alkyl carboxylates,[20] oxazolidines[21] and Barton esters[22] has further enhanced the range of accessible chemical space.

Recently, we developed new uncharged carbon-centered radical precursors (e.g. imidazolidines)[23] for the generation of alkyl radicals under both batch and flow conditions. Such conditions were effectively used to generate (un)stabilized α-amino, α-oxy, benzyl, silyl, tertiary and secondary radicals for the functionalization

of building blocks like electron-poor olefins and vinyl (hetero)arenes, as well as bioactive compounds. For example, Vitamin K3 (Menadione) a nutraceutical, was successfully *tert*-butylated, showcasing the potential of imidazolidines in late-stage functionalization (Scheme 6.1a). Additionally, a methylated derivative of L-benzylsuccinic acid (3-methylbenzylsuccinic ester, a potent inhibitor of carboxypeptidase A)[24,25] was synthesized using this method (Scheme 6.1b).[23] The alkylated derivatives, prepared with high purity even under flow conditions (Scheme 6.1c), can be used directly as obtained, making the protocol attractive for automated processes.

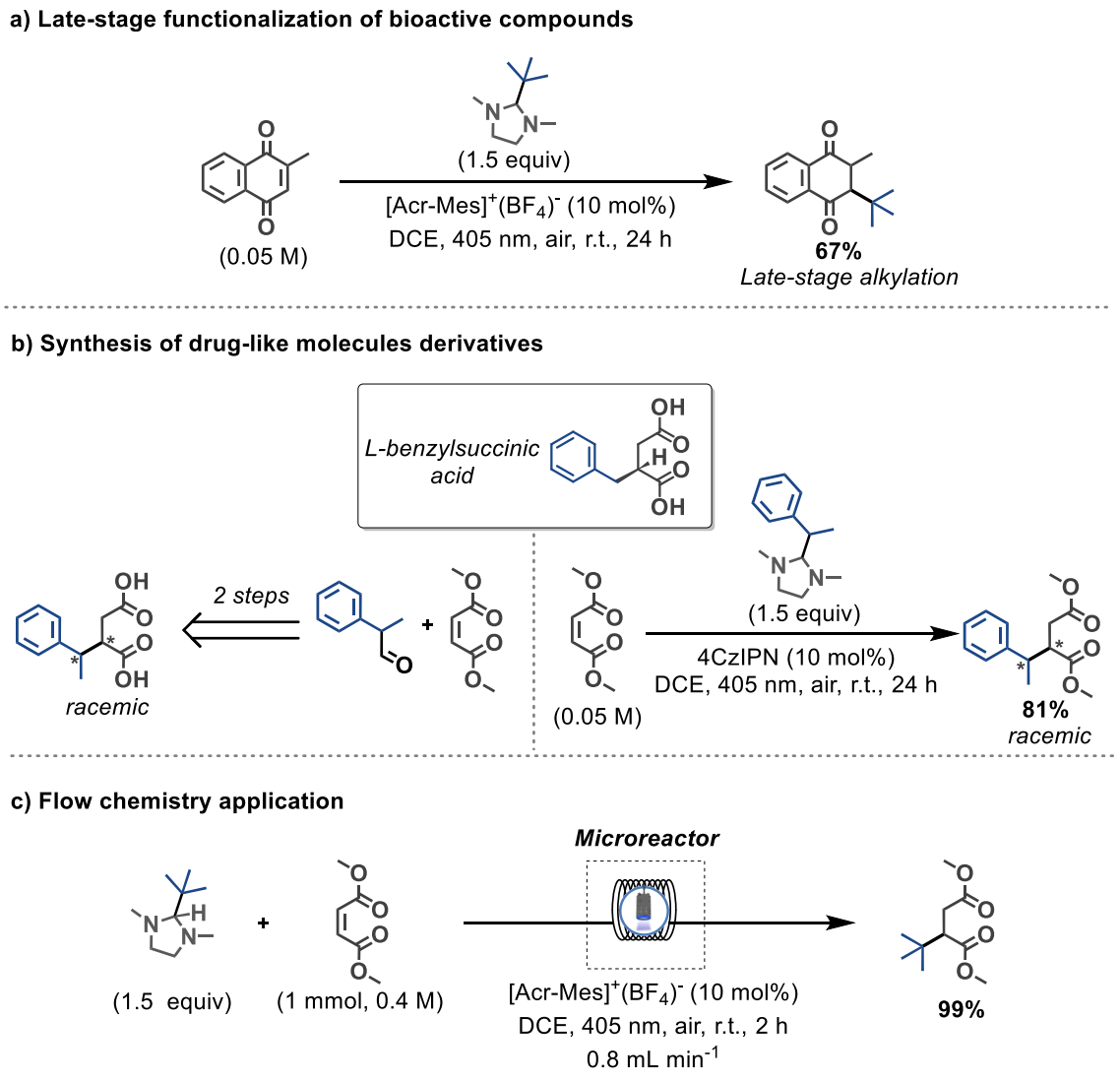

Scheme 6.1. a) Application of imidazolidines in late-stage functionalization of Vitamin K3 (Menadione). b) Synthesis of a methylated drug-like derivative of *L*-benzylsuccinic acid. c) Application of imidazolidines in flow chemistry.

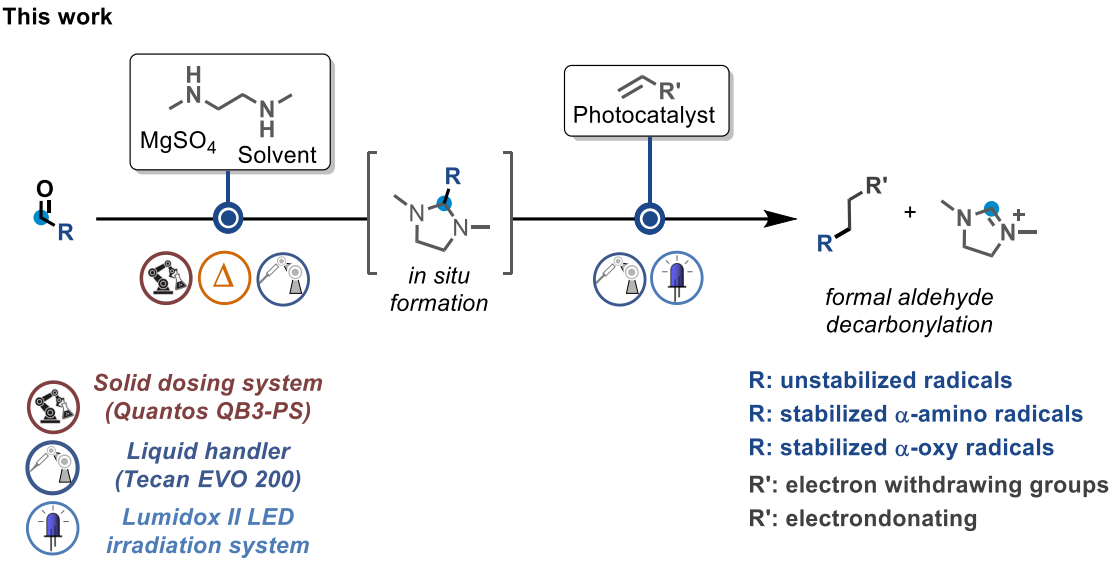

Scheme 6.2. Automated photoinduced one-pot Giese addition.

Building on the previous results obtained by PhotoGreen Lab[21,23] and leveraging Janssen's expertise in developing new chemical transformations and efficient processes through cutting-edge chemical technologies (flow chemistry, High-Throughput Experimentation (HTE) and Purification (HTP), automation, etc.),[8-13] we have implemented a fully automated one-pot photoredox process for synthesizing libraries of synthetically interesting building blocks and drug-like molecules. The transformation involves a one-pot photoinduced "formal decarbonylative addition" of aldehydes, which are transformed *in situ* into redox-active imidazolidines. These imidazolidines are oxidized by the excited photocatalyst, and after further fragmentation of the corresponding radical cations, generate the desired carbon-centered radicals. These radicals then undergo Giese addition onto suitable olefins, leading to the formation of alkylated products (Scheme 6.2).

6.2 Results and discussion.

Building on our previous achievements and on our background on synthetic photochemistry, we applied the alkylation method to modify various common building blocks present on bioactive drug-like compounds and in late-stage modification of drug-like molecules, aiming for a more efficient and streamlined process. We envisioned a fully automated approach by combining the automated preparation of imidazolidines in batch and the synthesis of libraries by using the

R2–R4 automated Vapourtec system, equipped with a liquid handler injector/collector (Figures ES6.1).

Initially, we optimized the batch preparation of imidazolidine **6.I** as a model. We screened different solvents and reaction temperatures using 2-phenylpropanal with *N,N'*-dimethylethylenediamine and $MgSO_4$ (see more information in Table 6.1). Et_2O and DCM were discarded due to their low boiling points, which could cause overpressure at high temperatures. THF and dioxane were also discarded to avoid clogging during the photochemical reaction in the flow system. Instead, we compared the performance of the reaction in DCE and DMF in the automated approach.

Table 6.1. Preliminary study of the solvent influence on the formation of imidazolidine **6.I**.

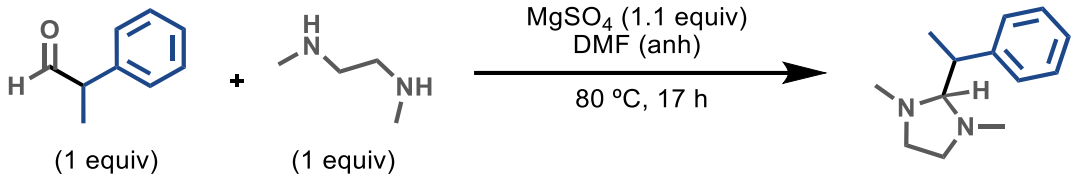

6.I

Entry	Deviations from standard conditions	**6.I** (¹H-NMR % Yield)
1	Et_2O as solvent, 40°C	99
2	THF as solvent, 65°C	98
3	DCM as solvent, 40°C	98
4	DCE as solvent, 80°C	41
5	Dioxane as solvent, 105°C	88
6	**None**	**99**
7	60°C	75
8	40°C	56

Further optimization was performed using a more elaborated aldehyde, viz. benzyl 2-formyl-1-piperidinecarboxylate. We discovered that after 3 h at 80 °C, the corresponding imidazolidine **6.II** was obtained in high purity with a yield over 90% when DMF was used as the solvent (Figure 6.1). To ensure reproducibility, we conducted 24 parallel reactions in the same plate. We used a QB3-PS Quantos solid dosing system to add $MgSO_4$ to the vials containing pre-dosed aldehyde. The

automated liquid handler platform, Tecan EVO200, prepared the reaction mixtures by dispensing a stock solution of *N,N*-dimethylethylendiamine in DMF into the vials.

The results for the automated synthesis of **6.II** are depicted in the heat map in Figure 6.1. The plate was successfully obtained with an average yield exceeding 80%. We tested the formation of **6.II** at different concentrations, from 0.15 M to 0.4 M solutions. As indicated in Figure 6.1, increasing the concentration is not detrimental for the reaction outcome.

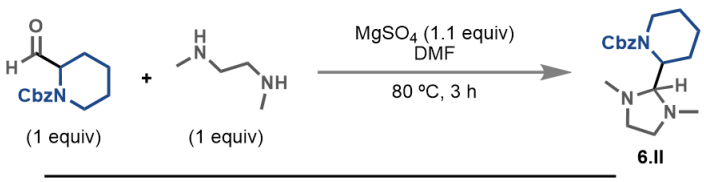

Entry	Deviation from standard condition	6.II (¹H-NMR % Yield)
1	DCE, 1 h	53
2	DCE, 3 h	33
3	DCE, 17 h	10
4	DCE, 17 h	12
5	DMF, 1 h	64
6	**None**	91
7	DMF, 17 h	70
8	DMF, 17 h	71

Experiments performed in 0.15 M

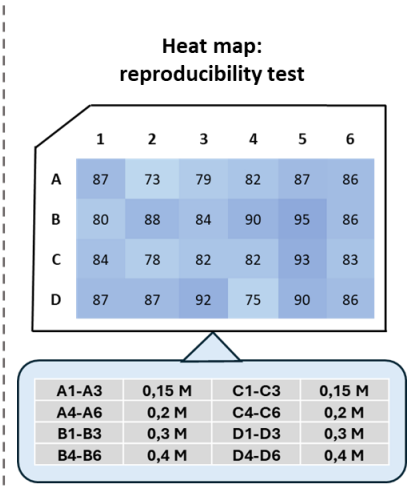

Figure 6.1. Solvent selection and reproducibility tests for the automated synthesis of imidazolidine **6.II** under batch conditions. ¹H-NMR yield was determined by using 1,3-dinitrobenzene as standard.

In parallel, we investigated the photochemical alkylation under flow conditions (see Scheme ES6.1 and Figures ES6.1-ES6.3). We then screened the photochemical alkylation of phenyl vinyl sulfone by **6.II** as the reaction model (Table 6.2), analyzing a large combination of parameters (solvent and solvent mixtures, reaction time and temperature) using rapid automated HTE protocols to obtain a comprehensive data set of reaction conditions in few experiments; therefore, speeding up the optimization of the model reaction. Results of the HTE process are depicted in Table 6.2. [26]

The best conditions found in the HTE protocol in flow were: imidazolidine (4 equiv.), (Ir[dF(CF_3)ppy]$_2$(dtbpy))PF_6 (5 mol%), olefin (1 equiv., 0.05 M) in DMF, 450 nm blue LED irradiation, 60 °C, for 20 min (Table 6.2, entry 76). DMF was the selected

solvent during the formation of imidazolidines and, additionally, it enhances the solubility of drug-like molecules that can be used in the library synthesis.

Table 6.2. HTE results for the reaction optimization of the synthesis of **6.A2**. Calibration curve in Table ES6.1.

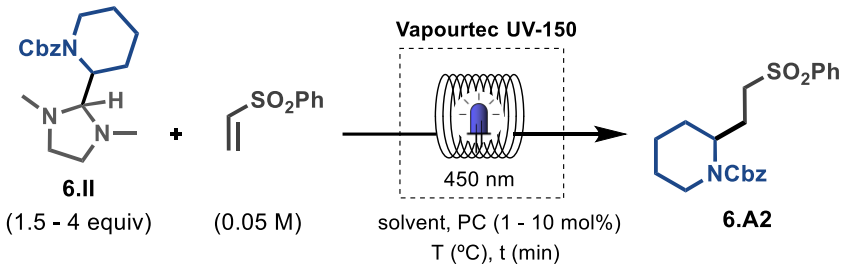

Entry	6.II (equiv.)	Solvent	PC (mol %)	T (°C)	t (min)	6.A2 (% LC-MS yield)
1	1.5	DCM	$[Acr\text{-}Mes]^+BF_4^-$ (10)	40	20	11
2	1.5	DMF-DCM (1:1)	$[Acr\text{-}Mes]^+BF_4^-$ (10)	40	20	10
3	1.5	DCE-DMF (1:1)	$[Acr\text{-}Mes]^+BF_4^-$ (10)	40	20	0
4	1.5	DMF	$[Acr\text{-}Mes]^+BF_4^-$ (10)	40	20	0
5	1.5	DCM-DCE (1:1)	$[Acr\text{-}Mes]^+BF_4^-$ (10)	40	20	27
6	1.5	DCE	$[Acr\text{-}Mes]^+BF_4^-$ (10)	40	20	25
7	1.5	DMF-DCE (1:1)	$[Acr\text{-}Mes]^+BF_4^-$ (10)	40	20	71
8	1.5	DCM	4CzIPN (10)	40	20	15
9	1.5	DMF-DCM (1:1)	4CzIPN (10)	40	20	29
10	1.5	DCM-DCE (1:1)	4CzIPN (10)	40	20	60
11	1.5	DCE	4CzIPN (10)	40	20	36
12	1.5	DMF-DCE (1:1)	4CzIPN (10)	40	20	50
13	1.5	DCM	$(Ir[dF(CF_3)ppy]_2(dtbpy))PF_6$ (10)	40	20	9
14	1.5	DCE	$(Ir[dF(CF_3)ppy]_2(dtbpy))PF_6$ (10)	40	20	44
15	1.5	DMF-DCE (1:1)	$(Ir[dF(CF_3)ppy]_2(dtbpy))PF_6$ (10)	40	20	51
16	1.5	DCM-DMF (1:1)	$(Ir[dF(CF_3)ppy]_2(dtbpy))PF_6$ (10)	40	20	72
17	1.5	DMF	$(Ir[dF(CF_3)ppy]_2(dtbpy))PF_6$ (10)	40	20	70

18	1.5	DCE-DCM (1:1)	(Ir[dF(CF_3)ppy]$_2$(dtbpy))PF_6 (10)	40	5	41
19	1.5	DCE-DCM (1:1)	(Ir[dF(CF_3)ppy]$_2$(dtbpy))PF_6 (10)	40	10	57
20	1.5	DCE-DCM (1:1)	(Ir[dF(CF_3)ppy]$_2$(dtbpy))PF_6 (10)	40	20	61
21	1.5	DCE-DCM (1:1)	(Ir[dF(CF_3)ppy]$_2$(dtbpy))PF_6 (10)	40	40	70
22	1.5	DCE-DCM (1:1)	(Ir[dF(CF_3)ppy]$_2$(dtbpy))PF_6 (10)	60	5	67
23	1.5	DCE-DCM (1:1)	(Ir[dF(CF_3)ppy]$_2$(dtbpy))PF_6 (10)	60	10	79
24	1.5	DCE-DCM (1:1)	(Ir[dF(CF_3)ppy]$_2$(dtbpy))PF_6 (10)	60	20	93
25	1.5	DCE-DCM (1:1)	(Ir[dF(CF_3)ppy]$_2$(dtbpy))PF_6 (10)	60	40	84
26	1.5	DCE-DCM (1:1)	(Ir[dF(CF_3)ppy]$_2$(dtbpy))PF_6 (10)	80	5	74
27	1.5	DCE-DCM (1:1)	(Ir[dF(CF_3)ppy]$_2$(dtbpy))PF_6 (10)	80	10	86
28	1.5	DCE-DCM (1:1)	(Ir[dF(CF_3)ppy]$_2$(dtbpy))PF_6 (10)	80	20	81
29	1.5	DCE-DCM (1:1)	(Ir[dF(CF_3)ppy]$_2$(dtbpy))PF_6 (10)	80	40	86
30	1.5	DCE	(Ir[dF(CF_3)ppy]$_2$(dtbpy))PF_6 (10)	60	5	46
31	1.5	DCE	(Ir[dF(CF_3)ppy]$_2$(dtbpy))PF_6 (10)	60	10	65
32	1.5	DCE	(Ir[dF(CF_3)ppy]$_2$(dtbpy))PF_6 (10)	60	20	72
33	1.5	DCE	(Ir[dF(CF_3)ppy]$_2$(dtbpy))PF_6 (10)	80	5	54
34	1.5	DCE	(Ir[dF(CF_3)ppy]$_2$(dtbpy))PF_6 (10)	80	10	70
35	1.5	DCE	(Ir[dF(CF_3)ppy]$_2$(dtbpy))PF_6 (10)	80	20	69
36	1.5	DMF	(Ir[dF(CF_3)ppy]$_2$(dtbpy))PF_6 (10)	60	5	63
37	1.5	DMF	(Ir[dF(CF_3)ppy]$_2$(dtbpy))PF_6 (10)	60	10	71
38	1.5	DMF	(Ir[dF(CF_3)ppy]$_2$(dtbpy))PF_6 (10)	60	20	66
39	1.5	DMF	(Ir[dF(CF_3)ppy]$_2$(dtbpy))PF_6 (10)	80	5	58

40	1.5	DMF	($Ir[dF(CF_3)ppy]_2(dtbpy)$)PF_6 (10)	80	10	51
41	1.5	DMF	($Ir[dF(CF_3)ppy]_2(dtbpy)$)PF_6 (10)	80	20	57
42	1.5	Et_2O-DCE (1:1)	($Ir[dF(CF_3)ppy]_2(dtbpy)$)PF_6 (10)	40	5	0
43	1.5	Et_2O-DCE (1:1)	($Ir[dF(CF_3)ppy]_2(dtbpy)$)PF_6 (10)	40	10	0
44	1.5	Et_2O-DCE (1:1)	($Ir[dF(CF_3)ppy]_2(dtbpy)$)PF_6 (10)	40	20	0
45	1.5	Et_2O-DCE (1:1)	($Ir[dF(CF_3)ppy]_2(dtbpy)$)PF_6 (10)	40	40	0
46	1.5	Et_2O-DCE (1:1)	($Ir[dF(CF_3)ppy]_2(dtbpy)$)PF_6 (10)	60	5	3
47	1.5	Et_2O-DCE (1:1)	($Ir[dF(CF_3)ppy]_2(dtbpy)$)PF_6 (10)	60	10	0
48	1.5	Et_2O-DCE (1:1)	($Ir[dF(CF_3)ppy]_2(dtbpy)$)PF_6 (10)	60	20	0
49	1.5	Et_2O-DCE (1:1)	($Ir[dF(CF_3)ppy]_2(dtbpy)$)PF_6 (10)	60	40	0
50	1.5	Et_2O-DCE (1:1)	($Ir[dF(CF_3)ppy]_2(dtbpy)$)PF_6 (10)	80	5	5
51	1.5	Et_2O-DCE (1:1)	($Ir[dF(CF_3)ppy]_2(dtbpy)$)PF_6 (10)	80	10	2
52	1.5	Et_2O-DCE (1:1)	($Ir[dF(CF_3)ppy]_2(dtbpy)$)PF_6 (10)	80	20	0
53	1.5	Et_2O-DCE (1:1)	($Ir[dF(CF_3)ppy]_2(dtbpy)$)PF_6 (10)	80	40	2
54	1.5	Et_2O-DMF (1:1)	($Ir[dF(CF_3)ppy]_2(dtbpy)$)PF_6 (10)	40	5	9
55	1.5	Et_2O-DMF (1:1)	($Ir[dF(CF_3)ppy]_2(dtbpy)$)PF_6 (10)	40	10	4
56	1.5	Et_2O-DMF (1:1)	($Ir[dF(CF_3)ppy]_2(dtbpy)$)PF_6 (10)	40	20	2
57	1.5	Et_2O-DMF (1:1)	($Ir[dF(CF_3)ppy]_2(dtbpy)$)PF_6 (10)	40	40	1
58	1.5	Et_2O-DMF (1:1)	($Ir[dF(CF_3)ppy]_2(dtbpy)$)PF_6 (10)	60	5	3
59	1.5	Et_2O-DMF (1:1)	($Ir[dF(CF_3)ppy]_2(dtbpy)$)PF_6 (10)	60	10	6
60	1.5	Et_2O-DMF (1:1)	($Ir[dF(CF_3)ppy]_2(dtbpy)$)PF_6 (10)	60	20	9
61	1.5	Et_2O-DMF (1:1)	($Ir[dF(CF_3)ppy]_2(dtbpy)$)PF_6 (10)	60	40	16

62	1.5	Et_2O-DMF (1:1)	(Ir[dF(CF_3)ppy]$_2$(dtbpy)) PF_6 (10)	80	5	13
63	1.5	Et_2O-DMF (1:1)	(Ir[dF(CF_3)ppy]$_2$(dtbpy)) PF_6 (10)	80	10	10
64	1.5	Et_2O-DMF (1:1)	(Ir[dF(CF_3)ppy]$_2$(dtbpy)) PF_6 (10)	80	20	15
65	1.5	DMF	(Ir[dF(CF_3)ppy]$_2$(dtbpy)) PF_6 (1)	60	20	12
66	1.5	DMF	(Ir[dF(CF_3)ppy]$_2$(dtbpy)) PF_6 (2.5)	60	20	21
67	1.5	DMF	(Ir[dF(CF_3)ppy]$_2$(dtbpy)) PF_6 (5)	60	20	38
68	2	DMF	(Ir[dF(CF_3)ppy]$_2$(dtbpy)) PF_6 (1)	60	20	25
69	2	DMF	(Ir[dF(CF_3)ppy]$_2$(dtbpy)) PF_6 (2.5)	60	20	23
70	2	DMF	(Ir[dF(CF_3)ppy]$_2$(dtbpy)) PF_6 (5)	60	20	58
71	3	DMF	(Ir[dF(CF_3)ppy]$_2$(dtbpy)) PF_6 (1)	60	20	29
72	3	DMF	(Ir[dF(CF_3)ppy]$_2$(dtbpy)) PF_6 (2.5)	60	20	38
73	3	DMF	(Ir[dF(CF_3)ppy]$_2$(dtbpy)) PF_6 (5)	60	20	49
74	4	DMF	(Ir[dF(CF_3)ppy]$_2$(dtbpy)) PF_6 (1)	60	20	31
75	4	DMF	(Ir[dF(CF_3)ppy]$_2$(dtbpy)) PF_6 (2.5)	60	20	51
76	**4**	**DMF**	**(Ir[dF(CF_3)ppy]$_2$(dtbpy)) PF_6 (5)**	**60**	**20**	**66**

After optimizing both steps separately, we translated the optimized conditions into a one-pot protocol in batch. Adopting a one-pot protocol proved to be more efficient and streamlined compared to the flow approach, as it required fewer operations: one filtration and two injection steps. Additionally, tubing cleaning operations between reactions. are supressed, hence, reducing total solvent use and eliminating idle time during the process. These factors made the automated one-pot photoinduced protocol in batch a more efficient process for the desired transformation. Detailed schemes of flow and batch approaches for libraries synthesis are depicted in Scheme 6.3.

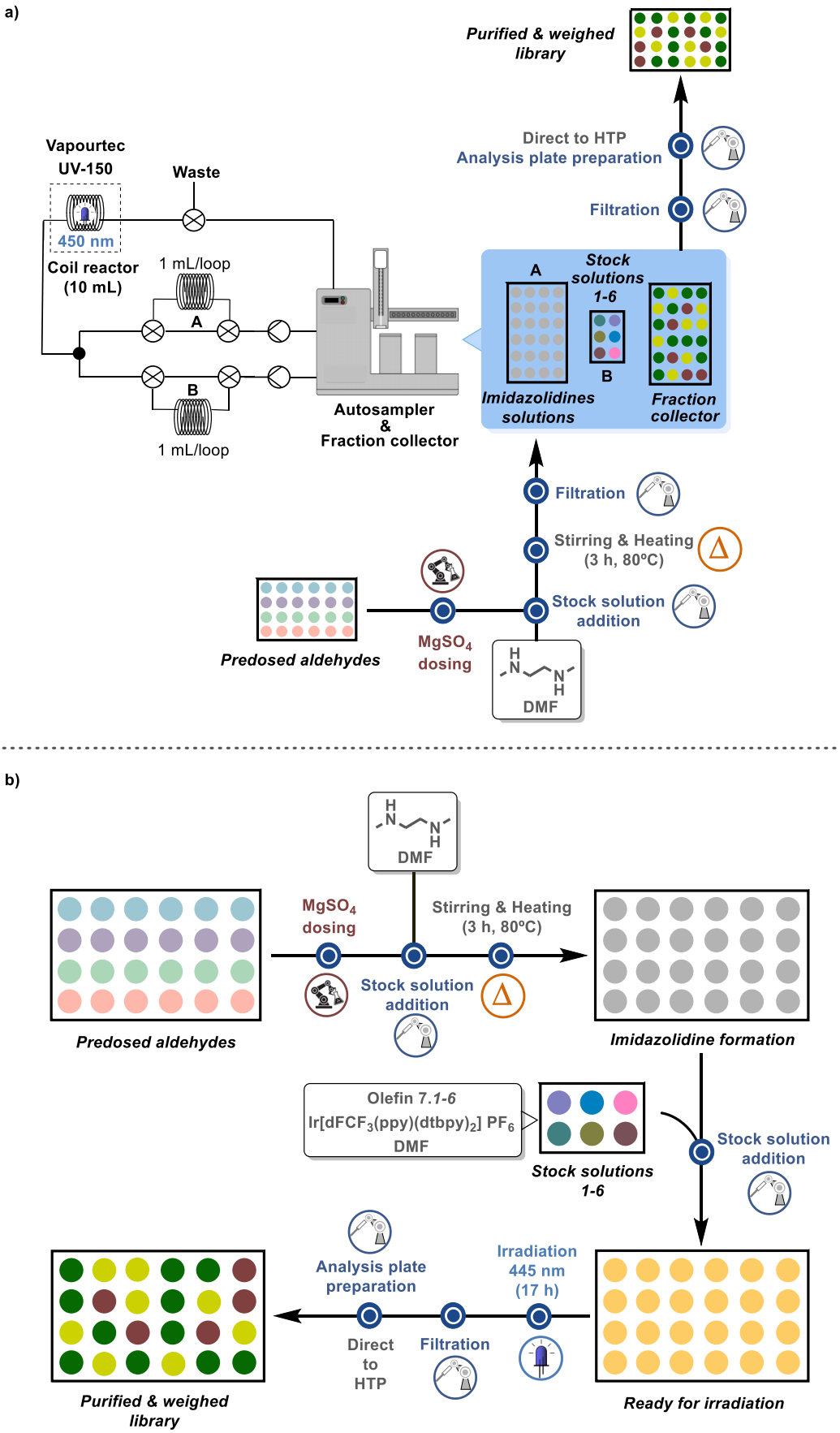

Scheme 6.3: Workflow scheme for the fully automated processes. a) Flow approach. b) One-pot batch approach.

Gratifyingly, the previously optimized conditions for the photoinduced alkylation of phenyl vinyl sulfone (Table 6.2, entry 76) in batch reproduced those found in flow when the *N*-Boc protected piperidine analogue was used as the aldehyde, and the reaction time was prolonged for 17 h at room temperature, yielding the Giese product in 64% yield (more details in Table 6.3). As one-pot protocol, no $MgSO_4$ filtration was needed between the imidazolidine formation and the photoredox reaction.

Table 6.3. Optimization of the photochemical one-pot Giese addition. Modified HTE optimized conditions.

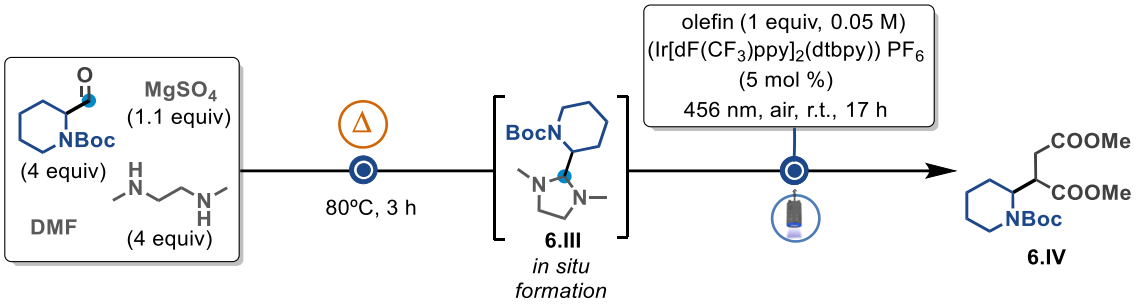

Entry	Deviations from standard conditions	6.VI (%GC-Yield)
1	**None**	**64**
2	$(Ir[dF(CF_3)ppy]_2(dtbpy))\ PF_6$ (3.5 mol %)	50
3	$(Ir[dF(CF_3)ppy]_2(dtbpy))\ PF_6$ (2.5 mol %)	48
4	$(Ir[dF(CF_3)ppy]_2(dtbpy))\ PF_6$ (1 mol %)	35
5	DCE as solvent, $[Acr\text{-}Mes]^+BF_4^-$ (10 mol %)	13

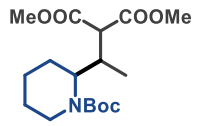

6.VI, 24%

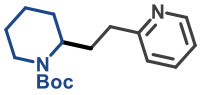

6.V, 50%

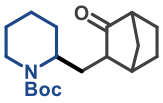

6.VII, 82%

In this one-pot process, the *in situ* prepared imidazolidine **6.III** (DMF, 3 h, 80 °C) was irradiated under blue light (456 nm, Kessil lamp, 50 W, 17 h, r.t.) in the presence of 5 mol% of photocatalyst. This generated the corresponding alkyl radical (via a "formal decarbonylation" of the aldehyde), which, upon addition to the olefin, yielded the alkylated product (for set up information see Figure ES6.4). Furthermore, we tested different Michael acceptors to evaluate the reaction's performance before translating the manual process into an automated one, obtaining compounds **6.IV-6.VII** in moderate to excellent yields (Table 6.3). GC-yields were calculated by using undecane as standard. Additionally, reproducibility

tests on the in-situ formation of imidazolidine **6.III** were performed obtaining an average yield of 92% over 22 reactions (Table 6.4).

Table 6.4. Reproducibility test for the synthesis of imidazolidine **6.III** before being used on the one-pot Giese addition in batch,

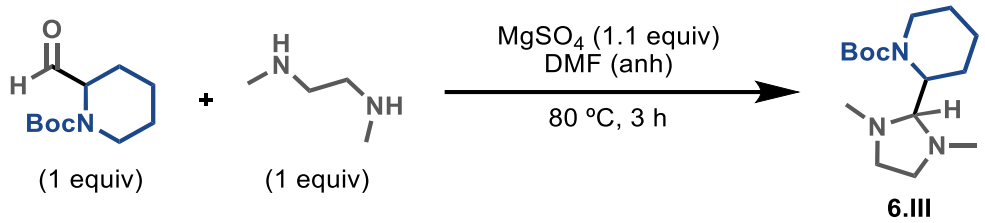

Entry	6.III (% GC-yield)	Entry	6.III (% GC-yield)
1	88	**12**	93
2	95	**13**	91
3	86	**14**	93
4	93	**15**	94
5	89	**16**	94
6	93	**17**	93
7	92	**18**	91
8	94	**19**	93
9	93	**20**	90
10	95	**21**	91
11	94	**22**	94

Finally, we combined a set of automated platforms, including the Q3-PS Quantos for solid dosing, Tecan EVO200 as liquid handler, Lumidox GII LED array irradiation system, 1290 Infinity II Perperative system from Agilent Technologies for purification, and a Tecan weighing station. Inspired by the recent work at Janssen, where various parameters affecting the performance of commercial photoreactors were studied, we chose the Lumidox GII for its ability to provide homogeneous irradiation over the plate.[26] This system can be integrated with the Tecan EVO200 for library synthesis, as shown in Figure ES6.5.

Using this setup, we successfully synthesized a combinatorial library by the combination of four different pre-dosed aldehydes (**6A-D**) with six different olefins and (hetero)arenes (**6.1-6**). This automated protocol significantly enhanced our previously developed methodology,[23] allowing us to isolate and detect compounds from neutral and non-electron poor olefins unexpectedly showing the electronic umpolung of vinyl motifs (**6.A3-6.D3**). For instance, the alkylation of the bioactive

(8*S*-9*R*)-quinine (a natural quinolone alkaloid effective against malaria)[27] yielded compound **6.C6** in 33% yield when an α-oxy radical was added. Additionally, derivatives from vinyl anisole (a vinyl arene) were obtained in low to moderate yields (**6.A3-6.D3**, 9%, 19%), with the main challenge being the formation of the corresponding dialkylated dimer, as detected by LC-MS, which hindered the isolation of those derivatives.

The alkylation of electron-poor olefins was demonstrated by functionalizing phenyl vinyl sulfone and vinyl pyridine (Figure 6.2). Phenyl vinyl sulfone was successfully alkylated by tertiary, secondary, α-oxy, and α-amino radicals achieving yields ranging from moderate to excellent. Surprisingly, the addition of α-amino radicals yielded moderate to excellent results (**6.D2, 6.A2,** 78%, 28%), despite the same reaction failing in batch.[21,23] Additionally, we successfully diversified vinyl pyridine (**6.A1-6.D1)** with yields ranging from 24% to 73%. Both vinyl sulfone and vinyl pyridine functionalities are prevalent in drug-like molecules, such as Axitinib (an anticancer agent)[28] and Rigosertib (an antitumoral agent).[29] These groups are attractive for late-stage functionalization processes and for introducing different functionalities to discover new pyridine-containing and sulfone-based drug-like analogues.[28-30] Moreover, pyridine is present in about 14% of the marketed drugs, making it the second most common *N*-heterocyclic core after piperidine (30%).[31] We demonstrated the successful introduction of an α-amino radical from Cbz protected piperidine into various olefins from moderate (16%) to excellent yields (78%) (**6.A1-6.A5**), thereby incorporating a highly demanded core into different structures.

The synthesis of unnatural amino acids (uaa) has been extensively studied due to the significance of some marketed uaa drugs, such as Levodopa for Alzheimer disease, and for creating new drug candidates like peptidomimetics, cyclic polypeptides, and antimicrobial peptides (AMP).[32] The modification of amino acids (aa) or de novo synthesis of uaa remains challenging due to the limited synthetic methodologies, with biocatalytic or biochemical approaches being the primary routes.[32,33] In this work, we demonstrated the facile functionalization of two different aa via photoredox catalysis, generating seven out of eight possible uaa in a

90% success rate, **6.A4-6.D4** and **6.A5-6.C5**, in moderate to excellent yields (**6.A5**, 16% and **6.B4**, 92%).

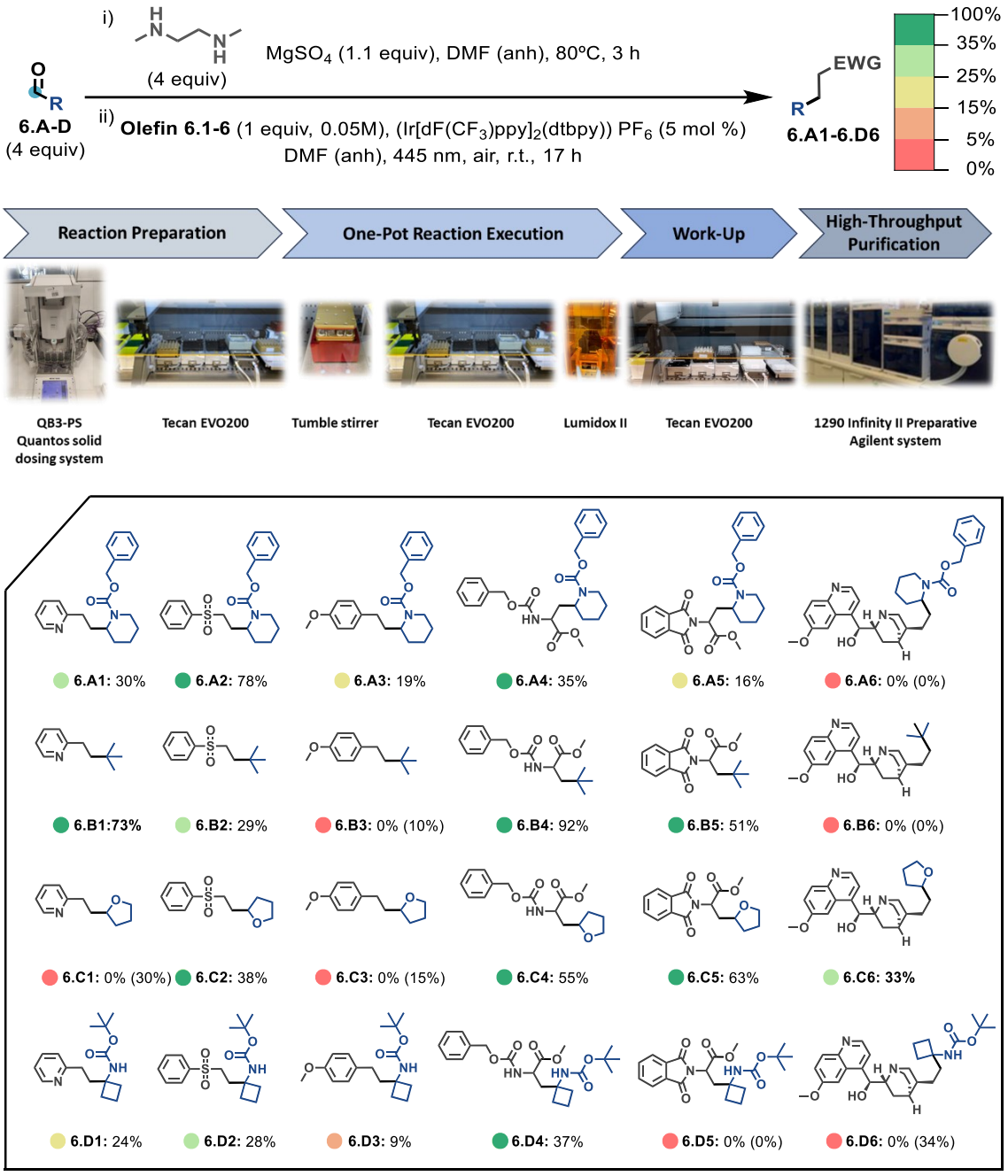

Figure 6.2. Results and workflow for the synthesized library via fully automated photoinduced one-pot Giese addition. Isolated yields (LC-MS conversion of the starting substrate into desired product).

This methodology is an effective protocol for synthesizing and diversifying uaa, obtaining a wide range of uaa with diverse functionalities as building blocks for further synthetically application. During the experiment, we introduced piperidine rings (**6.A4-6.A5**, 35%, 16%), strained cycles such as cyclobutane ring (**6.D4**, 37%),

protected amines (**6.A4-6.A5** and **6.D4**), alkyl moieties like the *tert*-butyl group (**6.B4-6.B5**, 92%, 51%), and ethers (**6.C4-6.C5**, 55%, 63%), paving the way for introducing protected carbonyl groups, as demonstrated in our previous works by introducing dioxolane moieties.[21,23]

6.3 Conclusions.

In this work, we developed a fully automated one-pot photoinduced alkylation process for synthesizing valuable building blocks and drug-like molecules through late-stage functionalization. We demonstrated the potential application of aldehydes as readily available starting material in a one-pot protocol for the photoredox generation of C-centered radicals (tertiary, secondary, α-amino, and α-oxy) for the alkylation of diverse vinyl (hetero)arenes, vinyl amino acids and electron-rich olefins. This protocol effectively synthesizes libraries of unnatural amino acids and facilitates the late-stage functionalization of drug-like molecules.

Moreover, we report this methodology as a tool to enhance the 3D character of the resulting molecules by adding enriched F(sp^3) moieties, exploring diverse chemical space through the formation of C(sp^3)-C(sp^3) bonds, a hot topic in medicinal chemistry. The process is efficient and straightforward, utilizing an automated protocol. It is also worth mentioning that collaborations between academia and industry are becoming increasingly important for innovation in organic chemistry. These partnerships are combining cutting-edge technology with innovative ideas, directly impacting science and society.

6.4 Experimental section.

Unless otherwise specified, reagents were obtained from commercial sources and used without further purification. Para-Dox™ 24-Well Block Assembly with 8 mL (2 DRAM Vials; 8 mL, 17×60 mm) clear glass shell vials and parylene encapsulated stainless steel discs (all purchased from Analytical Sales & Services, Inc.) were employed.

Automated powder dispensing was performed by using a QB3-PS Quantos® solid dosing system. The system consists of a Quantos Dosing Module equipped with up

to 30 container positions and a Mettler-Toledo balance. The required amounts of powder were weighed fully automatically into 8 mL vial.

Liquid handling operations were performed in a Tecan Freedom EVO200 liquid handler equipped with an 8-channel disposable tips Air LiHa (Tecan disposable tips #30057817) and a TeShake (Tecan #10760726). All operations used aluminum blocks as a source or destination plates (Analytical Sales & Services #24017), or plastic microtiter plates for analysis (Waters #186002643).

Reactions were stirred and heated in a VP 710C5-7A- Vertical Tumble Stirrer, equipped with a VP742D - Aluminum Heat Block (V&P Scientific). The photochemical reactions were carried out in a 24-position (18 mm spacing LED arrays) Lumidox® II LED Arrays equipped with 450 nm UV LED directly connected to a chiller.

The Ultra-High Performance Liquid Chromatography (UPLC) measurement was performed using an HClass UPLC® system from Waters® (Milford, MA, USA) equipped with a quaternary solvent delivery pump, an autosampler with flow through needle injector, a column compartment with 2 column positions, a DAD detector, and a sample organizer module for sample introduction into the system. The standard LC methods are: solvent A (HCO_3NH_4 2.5 g/L, 32 mM or H_2O with 0.1% FA), solvent B (CH_3CN or CH_3OH). A gradient was run to 100% B in 2.0 min, kept for 0.5 min, and then equilibrated to initial conditions in 0.5 min. Specific conditions depending on the organic solvent: CH_3CN methods: 1 mL/min flow, temperature: RT, initial conditions: 10% B; MeOH methods: 0.9 mL/min flow, temperature: 45°C, initial conditions: 20% B. Columns: XBridge C18, 2.5 μm, 2.1×50 mm for basic conditions or SunFire C18, 2.5μm, 2.1×50 mm for acidic ones. Flow from the column was brought to the QDa Mass Spectrometer (MS), which was configured with an atmospheric pressure ion source. Data acquisition was performed by means of a Masslynx v4.2 and processed with OpenLynx Browser software.

The High Performance Liquid Chromatography (HPLC) purification was performed using a 1290 Infinity II Preparative system from Agilent Technologies (Waldbronn, Germany) equipped with a 1290 Binary solvent pump and two 1260 isocratic pumps (one for the introduction of the sample into the column and the other one used as

make-up pump), a column compartment with six column positions, one 1290 injector-collector connected with two additional 1290 collectors, a DAD detector and a MSD (Mass Single Detector G6125B) spectrometer (MS). The standard HPLC methods used are Flows: Binary pump: 45 mL/min, ACD pump: 1 mL/min; make-up pump: 0.3 mL/min; Temperature: RT, solvents: A (HCO_3NH_4 2.5 g/L, 32 mM or H_2O with 0.1% FA) and B (CH_3CN or CH_3OH). A gradient was run to 100% B in 12 min, kept for 2.0 min, and then equilibrated to initial conditions in 0.5 min. Columns: XBridge C18, 10 µm, 30×100 mm for basic conditions or SunFire C18, 5µm, 30 x 100mm for acidic ones. Flow from the column was brought to the PDA and the outlet tubbing was brought to the MSD, which was configured with an atmospheric pressure ion source. Analytical StudioTM (Virscidian, Inc, Cary, NC, US) was used to identify on each compound from the library the best analytical method that was scaled up for the preparative run and the purest fractions after purification. Data acquisition was performed with Openlab C.01.10.

Regardless of the analytical technique used, compounds have been characterized by their experimental retention times (Rt) and ions. If not specified differently in the table of data, the reported molecular ion corresponds to the $[M+H]^+$ (protonated molecule) and/or $[M-H]^-$ (deprotonated molecule). In case the compound was not directly ionizable the type of adduct is specified (i.e. $[M+NH_4]^+$, $[M+HCOO]^-$, etc…). For molecules with multiple isotopic patterns (Br, Cl), the reported value is the one obtained for the lowest isotope mass. All results were obtained with experimental uncertainties that are commonly associated with the method used. HRMS data were acquired using a X500B QTOF System (SCIEX, Framingham, MA 01701 USA) available at the CGS of the University of Pavia, equipped with the Twin Sprayer ESI probe and coupled to an ExionLC™ system (SCIEX). The SCIEX OS software 2.1.6 was used as operating platform. For MS detection the following parameters were applied: Curtain gas 30 psi, Ion source gas 1 45 psi, Ion source gas 2 55 psi, Temperature 450°C, Polarity negative, Ion spray voltage -4500 V, TOF mass range 50-1600 Da, declustering potential -60 V and collision energy -10 V.

GC analysis was performed using a HP SERIES 5890 II equipped with a fire ion detector (FID, temperature 350 °C). Analytes were separated by using a Restek Rtx-5MS (30 m × 0.25 mm × 0.25 µm) capillary column with nitrogen as a carrier gas at

1 mL min^{-1}. The injector temperature was 250°C. The GC oven temperature was held at 80°C for 2 min, increased to 250°C by a temperature ramp of 10 °C min^{-1}, and held for 10 min. Undecane was used as internal standard.

^{1}H, ^{13}C, and ^{19}F NMR spectra were recorded on Bruker DPX-400 or Bruker AV-500 spectrometers with standard pulse sequences, operating at 400 MHz and 500M Hz respectively. Chemical shifts (δ) are reported in parts per million (ppm) downfield from tetramethylsilane (TMS), which was used as an internal standard. Multiplicity (s = single, d = doublet, t = triplet, quint = quintet, q = quartet, m = multiplet, dd =double doublet, br d = broad doublet, br s = broad singlet, br t = broad triplet), integration, and coupling constants (*J*) in hertz (Hz).

6.4.1 Chart of starting materials.

The starting materials were commercially available and used as received.

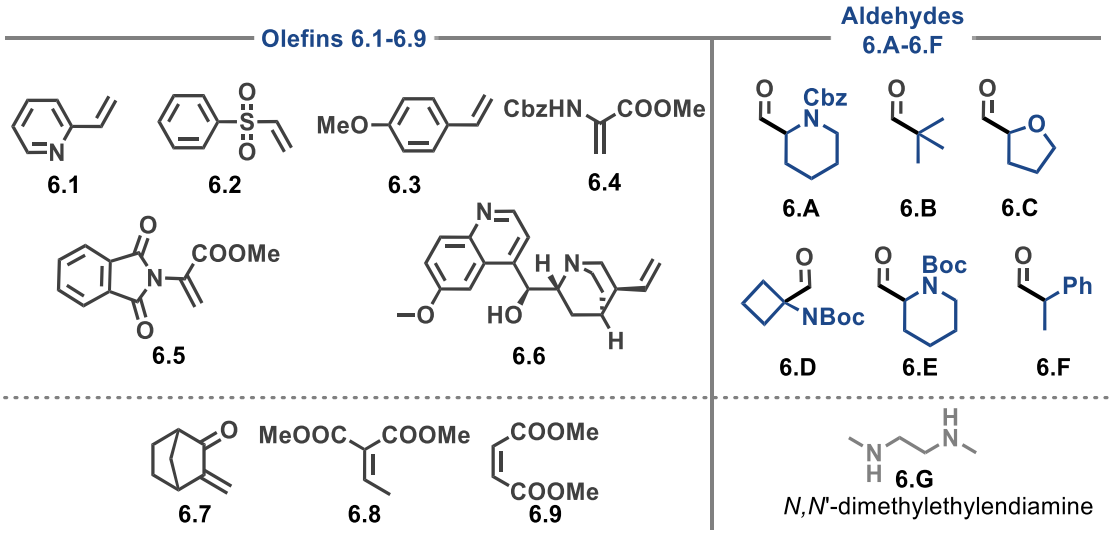

6.4.2 High-Throughput Experimentation for the Giese Addition Flow.

Stock solutions were previously prepared considering the 10% of excess needed for optimal autosampler injections:

Stock solution A: A solution of benzyl 2-(1,3-dimethylimidazolidin-2-yl)piperidine-1-carboxylate (1.5 to 4 equiv., 0.15 to 0.4 M) in the chosen solvent (DMF, DCE, DCM, Et_2O).

Stock solution B: 0.1 M solution of phenyl vinyl sulfone (1 equiv., 0.025 mmol) and the desired photocatalyst (1 to 10 mol %) in the chosen solvent (DMF, DCE, DCM, Et_2O).

The solutions were placed in the Autosampler of the Automatic R2-R4 Vapourtec reactor. Solution A was loaded to loop A and pumped at the corresponding flow rate and mixed through a T-mixer with Solution B flowing at the same flow rate. The final solution is composed by 2-(1,3-dimethylimidazolidin-2-yl)piperidine-1-carboxylate (1.5 to 4 equiv.), phenyl vinyl sulfone (1 equiv., 0.025 mmol, 0.05 M) and the photocatalyst (1 to 10 mol%) in the corresponding solvent or solvent mixture (2 mL). This solution was flown through a 10 mL coil using the same solvent as solvent carrier. During the process the solution was irradiated under blue light (450 nm, UV-150 Photoreactor) at the desired temperature for the corresponding reaction time. The outcoming solution (4.5 mL) was collected into a fraction collector using the Autosampler. The reactions were allowed to cool down to room temperature. The vials were placed in a Para-Dox™ 24-Well Block and 500 µL of triphenylamine (internal standard) in DMF (0.001 M) were dispensed into each vial and properly mixed. Then, 150 µL of MeOH, followed by 50 µL of the reaction mixture were added into a separate 96-well LC block, sealed and analyzed by UPLC-MS.

Table ES6.1. Calibration curve of product **6.A2**.

Product %	Ratio Absorbance P/IS	C (mmol/mL)
100	0,99	0,005
80	0,79	0,004
60	0,59	0,003
40	0,41	0,002
20	0,21	0,001
0	0	0

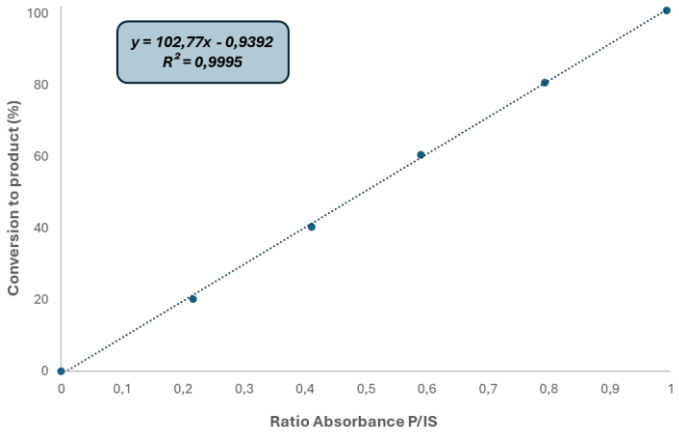

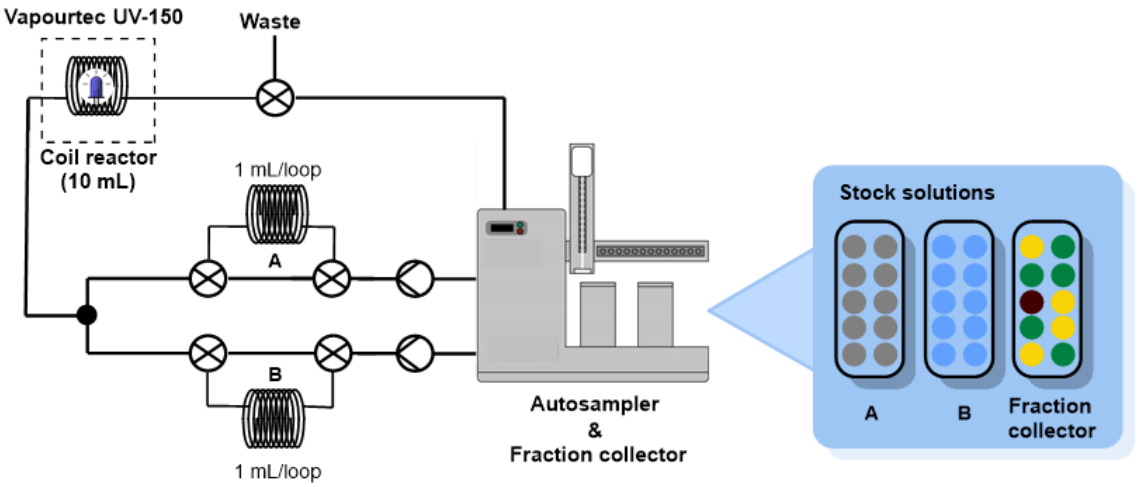

Scheme ES6.1. Illustrative scheme for the system set up.

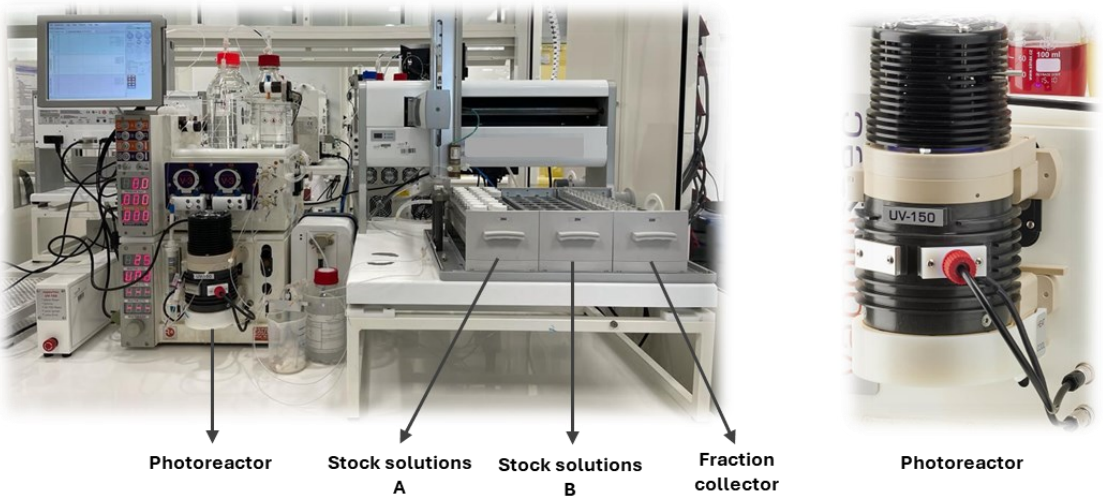

Figure ES6.2. R2–R4 automated Vapourtec system with a liquid handler. Automated platform for High-Throughput Experimentation in flow.

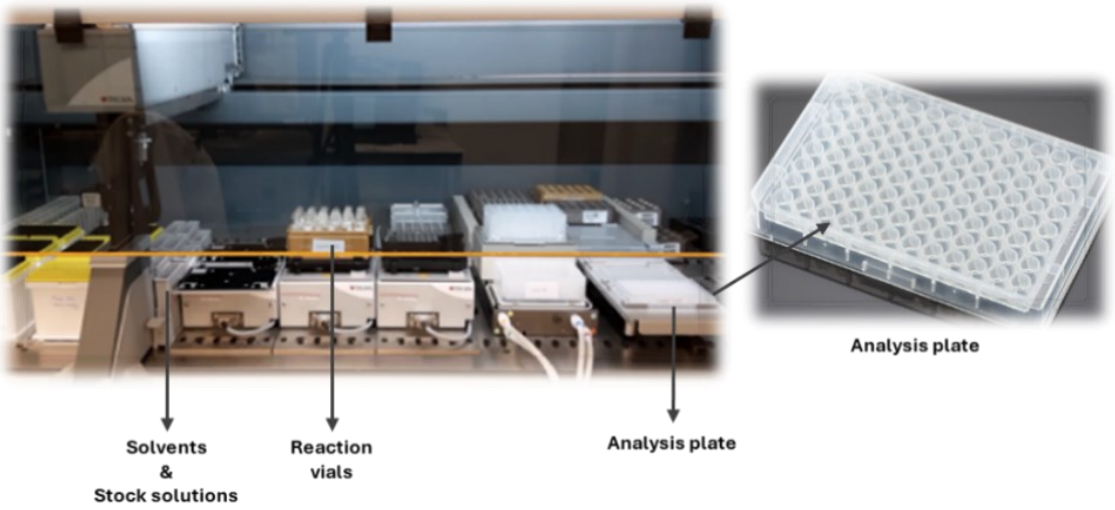

Figure ES6.2. Tecan EVO 200 automated liquid handler. Automated platform for analysis plate preparation and HTE analysis.

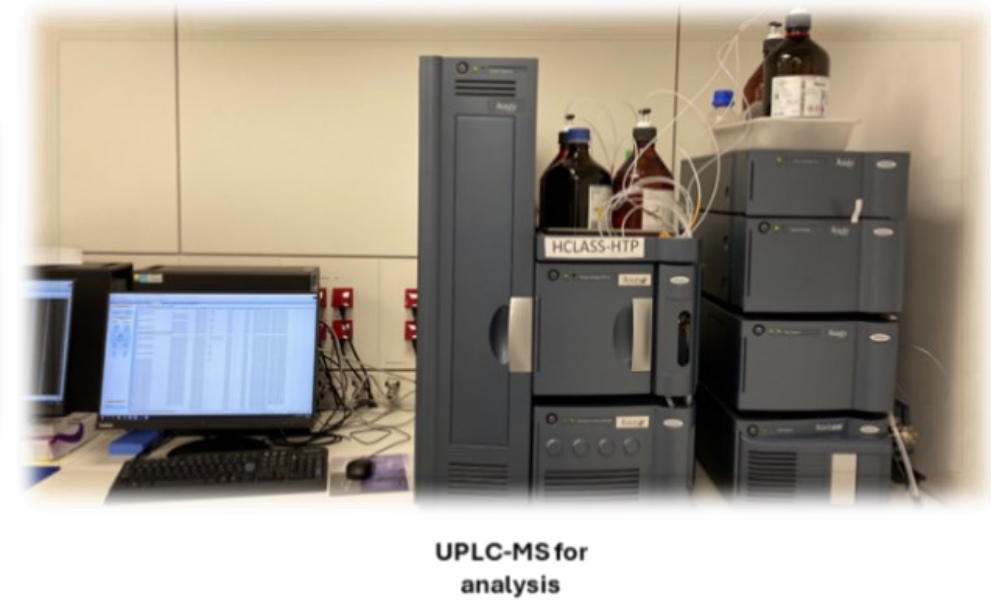

Figure ES6.3. Automated platform for analysis plate preparation and HTE analysis

6.4.3 General procedures.

6.4.3.1 General Procedure 1: synthesis of imidazolidines in batch.

The desired imidazolidines were synthesized by adapting a procedure previously reported in literature.[23] *N,N'*-dimethylethylendiamine (1 equiv.) was added to a suspension of $MgSO_4$ (1.1 equiv.) and the corresponding aldehyde **6.A-F** (1 equiv.) in DMF (0.2 M) in an 8 mL (2 DRAM Vials; 8 mL, 17×60 mm) clear glass shell vials.

The reaction mixture was heated at 80 °C and stirred for 3 h. The resulting mixture was used in the following step without any further filtration or purification.

6.4.3.2 General Procedure 2: one-pot photo-induced Giese reaction in batch.

N,N'-dimethylethylendiamine (0.2 mmol, 4 equiv.) was added to a suspension of $MgSO_4$ (25 mg, 0.22 mmol, 4.4 equiv.) and the corresponding aldehyde **6.A-F** (0.2 mmol, 4 equiv.) in DMF (0.05 M, 1 mL) in an 8 mL (2 DRAM Vials; 8 mL, 17x60 mm) clear glass shell vials. The reaction mixture was heated at 80 °C and stirred for 3 h. To the resulting mixture the corresponding olefin (0.05 mmol, 1 equiv.) and $[Ir[dFCF_3(ppy)]_2(dtbpy)]^+(PF_6)^-$ (5 mol %) were added and blue light irradiation (456 nm, Kessil Lamp, 50 W) was carried out for 17 h at room temperature in a photoreactor (PhotoRedOx Box, Evoluchem™). The mixtures were filtered and analyzed by GC.

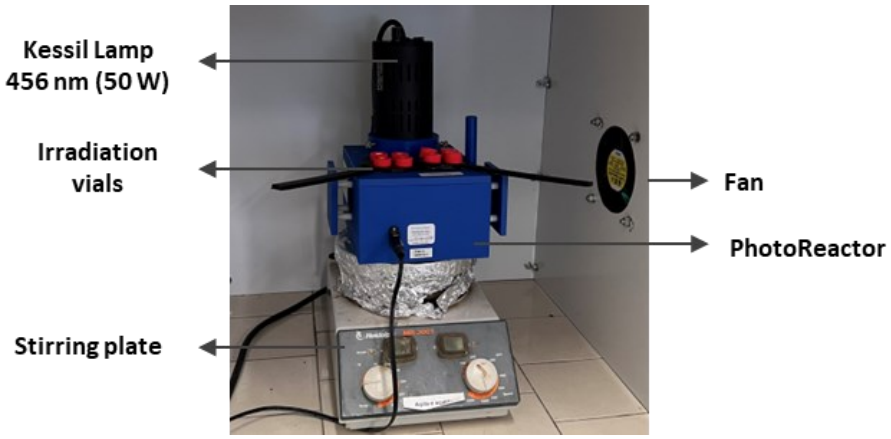

Figure ES6.4. Irradiation set up for the one-pot protocol in batch.

6.4.3.3 General Procedure 3: one-pot photo-induced Giese addition for library synthesis.

The corresponding aldehydes **6.A-F** (0.4 mmol, 4 equiv.) were predosed into 8 mL (17×60 mm) clear glass shell vials containing a parylene encapsulated stainless steel disc. $MgSO_4$ (4.4 equiv.) was automatically dosed by QB3-PS Quantos solid dosing system into the same vials and placed in a 24-well parallel block assembly. Separately, two stock solutions were open-air prepared:

Stock solution A containing the corresponding amount of *N,N*-dimethylaminoetane (4 equiv.) in DMF (0.4 M) was prepared.

<u>Stock solution B1-B6</u>: containing the corresponding olefin (1 equiv.) and ($Ir[dFCF_3(ppy)]_2$ (dtbpy)) PF_6 (5 mol %,) in DMF (0.1 M).

Liquid handling operations were performed in a Tecan Freedom EVO 200. The system dispensed the corresponding amount of stock solution A (1 mL) in each vial. The vials were capped, and the suspensions were heated and stirred in a vertical tumble stirrer, equipped with an aluminum heat block at 80°C for 3 h. The vials were allowed to cool down to room temperature. The system dispensed the corresponding stock solutions B1–B6 into the reaction vials where the corresponding imidizolidines were prepared. The reaction plate was placed in a 24-position Lumidox® II LED Arrays and irradiated under blue light (445 nm UV LED) at room temperature for 17 h. After the full reaction time the reaction plate was filtered over a custom packed 24 wells filter plate with 0.5 g/well SiliaMetS Imidazole (Si-IMI; analytical sales) in the Tecan and washed with 0.5 mL of DMSO. The resulting solutions were purified by RP HPLC (Conditions: Stationary phase: C_{18} XBridge 30×100 mm 10 µm. Mobile phase: NH_4HCO_3 0.25% solution in water and CH_3CN). The desired fractions were collected and concentrated in vacuo to obtain the desired library of compounds. The corresponding products were concentrated under vacuum in a Genevac centrifugal evaporator, placed and weighed in vials by means of a Tecan Weighing Station obtaining the corresponding purified and weighed products.

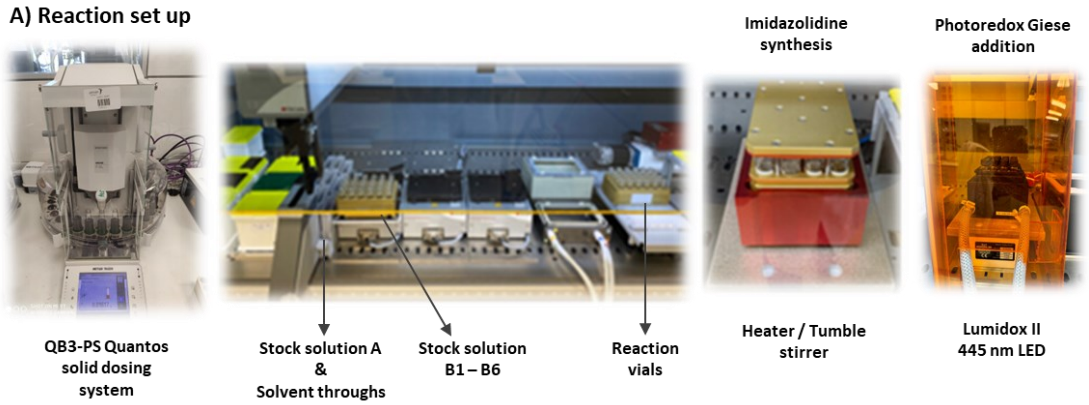

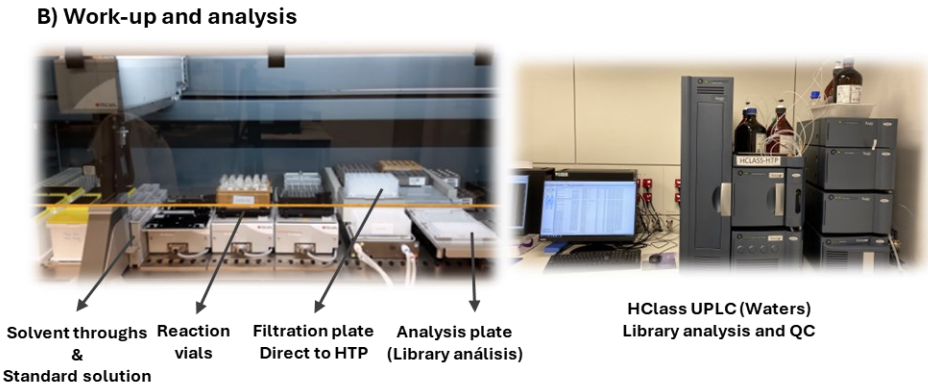

C) Purification and post-purification

1290 Infinity II Preparative Agilent system
(automated RP-HPLC purification)

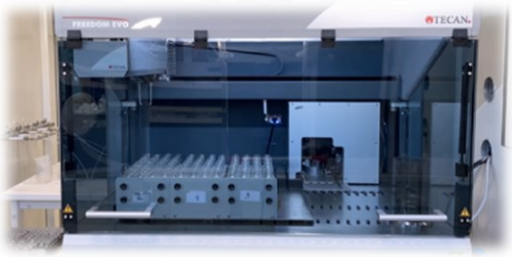

Tecan Weighing Station
(automated net weigh for isolated compounds)

Figure ES6.5. End-to-end fully automated platform for the one-pot photoredox Giese addition.

6.4 Characterization data.

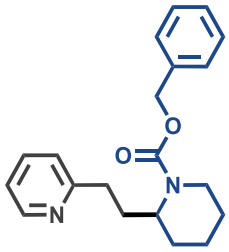

Benzyl 2-(2-(pyridin-2-yl)ethyl)piperidine-1-carboxylate (6.A1).

The product was obtained following General Procedure 6.4.2.3 as a colourless oil (9.7 mg, 30% yield).

6.A1. ^{1}H NMR (400 MHz, chloroform-*d*) δ ppm 8.51 (br d, *J* = 4.2 Hz, 1H), 7.53 (br t, *J* = 7.2 Hz, 1H), 7.29–7.39 (m, 5H), 7.08 (br dd, *J* = 7.2, 5.1 Hz, 2H), 5.12 (s, 2H), 3.95–4.49 (m, 2H), 2.89 (br t, *J* = 12.6 Hz, 1H), 2.63–2.82 (m, 2H), 2.13–2.29 (m, 1H), 1.85–1.96 (m, 1H), 1.56–1.66 (m, 5H), 1.42 (br d, *J* = 9.5 Hz, 1H). ^{13}C NMR (101 MHz, chloroform-*d*) δ ppm 161.6, 155.6, 149.1, 137.0, 136.3, 128.4, 127.8, 127.8, 122.9, 121.0, 50.8, 39.1, 35.1, 29.6, 28.7, 25.5, 19.0. HRMS (ESI-TOF): mass calcd. for $[C_{20}H_{24}N_2O_2 + H]^+$, 325.1916; m/z found, 325.1922.

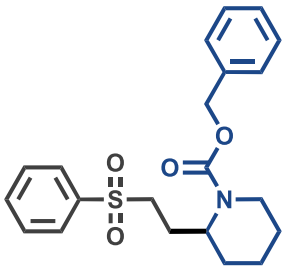

Benzyl 2-(2-(phenylsulfonyl)ethyl)piperidine-1-carboxylate (6.A2).

The product was obtained following General Procedure 3 as a colourless oil (30.4 mg, 78% yield).

6.A2. ^{1}H NMR (400 MHz, chloroform-*d*) δ ppm 7.87 (br d, *J* = 7.5 Hz, 2H), 7.64–7.69 (m, 1H), 7.54–7.59 (m, 2H), 7.31 (br s, 5H), 5.01–5.19 (m, 2H), 4.33 (br s, 1H), 4.04 (br d, *J* = 11.4 Hz, 1H), 3.01–3.20 (m, 1H), 2.86–3.00 (m, 1H), 2.72 (br s, 1H), 2.23–2.38 (m, 1H), 1.72–1.82 (m, 1H), 1.47–1.70 (m, 5H), 1.33–1.44 (m, 1H). ^{13}C NMR (101 MHz, chloroform-*d*) δ ppm 155.3, 139.1, 136.5, 133.7, 129.3, 128.4, 128.0, 127.9, 127.8, 67.1, 53.4, 49.5, 38.9, 28.9, 25.2, 22.6, 18.8. HRMS (ESI-TOF): mass calcd. for $[C_{21}H_{25}NO_4S + H]^+$, 388.1583; m/z found, 388.1574.

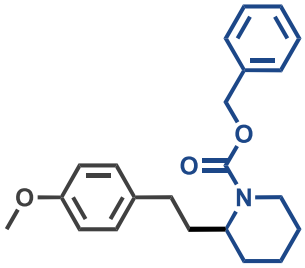

Benzyl 2-(4-methoxyphenethyl)piperidine-1-carboxylate (6.A3).

The product was obtained following General Procedure 3 as a colourless oil (6.8 mg, 19% yield).

6.A3. ^{1}H NMR (400 MHz, chloroform-*d*) δ ppm 7.30–7.40 (m, 5 H), 7.07 (br d, *J* = 7.4 Hz, 2H), 6.80 (br d, *J* = 8.6 Hz, 2H), 5.15 (d, *J* = 2.3 Hz, 2H), 4.02–4.44 (m, 2H), 3.77–3.81 (m, 3H), 2.82–2.93 (m, 1H), 2.41–2.59 (m, 2H), 2.02 (dddd, *J* = 13.8, 10.3, 9.1, 5.9 Hz, 1H), 1.60–1.73 (m, 6H), 1.37–1.49 (m, 1H). ^{13}C NMR (101 MHz, chloroform-*d*) δ ppm 157.7, 155.6, 137.0, 134.0, 129.1, 128.4, 127.8, 127.8, 113.7, 66.9, 55.2, 50.7, 39.2, 31.9, 31.7, 28.5, 25.6, 19.0. HRMS (ESI-TOF): mass calcd. for $[C_{22}H_{27}NO_3 + H]^+$, 354.2069; m/z found, 354.2054.

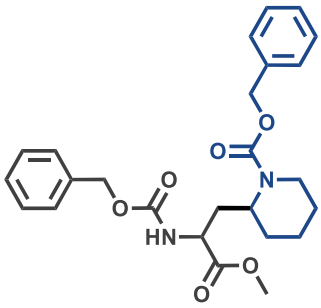

Benzyl 2-(2-(((benzyloxy)carbonyl)amino)-3-methoxy-3-oxopropyl) piperidine-1-carboxylate (6.A4). (Mixture of rotamers).

The product was obtained following General Procedure 3 as a colourless oil (15.7 mg, 35% yield).

6.A4. ^{1}H NMR (400 MHz, chloroform-*d*) δ ppm 7.23–7.47 (m, 10H), 6.36–6.54 (m, 1H), 4.98–5.23 (m, 4H), 3.86–4.64 (m, 3H), 3.55–3.71 (m, 3H), 2.72–2.83 (m, 1H), 1.42–1.88 (m, 8H). ^{13}C NMR (101 MHz, chloroform-*d*) δ ppm 172.2, 156.3, 155.6, 136.5, 135.6, 128.5, 128.4, 128.0, 67.5, 66.8, 51.9, 52.6, 51.4, 46.7, 39.3, 31.8, 28.8, 25.4, 19.2. HRMS (ESI-TOF): mass calcd. for $[C_{25}H_{30}N_2O_6 + H]^+$, 455.2182; m/z found, 455.2140.

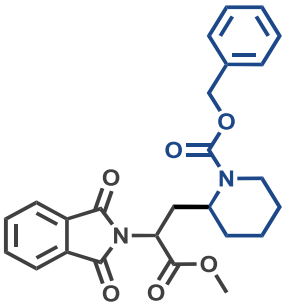

Benzyl 2-(2-(1,3-dioxoisoindolin-2-yl)-3-methoxy-3-oxopropyl)piperidine-1-carboxylate (6.A5). (Mixture of rotamers).

The product was obtained following General Procedure 3 as a colourless oil (7.4 mg, 16% yield).

6.A5. ^{1}H NMR (400 MHz, chloroform-*d*) δ ppm 7.83 (br dd, *J* = 5.0, 3.1 Hz, 1H), 7.59–7.77 (m, 2H), 7.28–7.45 (m, 4H), 6.91–7.24 (m, 2H), 4.76–5.32 (m, 3H), 3.91–4.61 (m, 2H), 3.62–3.76 (m, 3H), 2.67–3.01 (m, 2H), 2.48–2.61 (m, 1H), 1.61–1.74 (m, 5H), 1.28–1.45 (m, 1H). ^{13}C NMR (101 MHz, chloroform-*d*) δ ppm 167.4, 155.2, 133.7, 134.2, 128.3, 127.7, 123.5, 123.3, 66.4, 67.5, 52.8, 49.1, 50.1, 48.8, 47.0, 44.8, 38.7,

39.6, 29.2, 28.0, 24.9, 26.0, 24.3, 21.6, 19.0. HRMS (ESI-TOF): mass calcd. for $[C_{25}H_{26}N_2O_6 + H]^+$, 451.1869; m/z found, 451.1842.

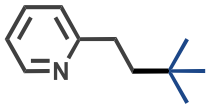

2-(3,3-Dimethylbutyl)pyridine (6.B1).

The product was obtained following General Procedure 3 as a colourless oil (12 mg, 73% yield).

6.B1. ^{1}H NMR (300 MHz, chloroform-*d*) δ ppm 8.53 (d, *J* = 4.6 Hz, 1H), 7.61 (td, *J* = 7.7, 1.8 Hz, 1H), 7.17 (d, *J* = 7.9 Hz, 1H), 7.11 (dd, *J* = 7.3, 5.0 Hz, 1H), 2.75–2.84 (m, 2H), 1.57–1.68 (m, 2H), 0.98 (s, 9H). ^{13}C NMR (75 MHz, chloroform-*d*) δ 162.9, 148.7, 136.5, 122.6, 120.7, 44.1, 33.6, 30.4, 29.2. HRMS (ESI-TOF): mass calcd. for $[C_{11}H_{17}N + H]^+$, 164.1439; m/z found, 164.1435.

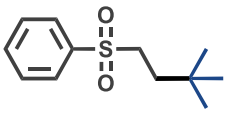

((3,3-Dimethylbutyl)sulfonyl)benzene (6.B2).

The product was obtained following General Procedure 3 as a colourless oil (6.6 mg, 29% yield).

6.B2. ^{1}H NMR (400 MHz, chloroform-*d*) δ ppm 7.90–7.95 (m, 2H), 7.64–7.70 (m, 1H), 7.56–7.62 (m, 2H), 3.03–3.10 (m, 2H), 1.60–1.64 (m, 2H), 0.86–0.90 (m, 9 H). ^{13}C NMR (101 MHz, chloroform-*d*) δ ppm 139.2, 133.6, 129.2, 128.0, 52.9, 35.6, 30.0, 28.9. HRMS (ESI-TOF): mass calcd. for $[C_{12}H_{18}O_2S + H]^+$, 227.1100; m/z found, 227.1119.

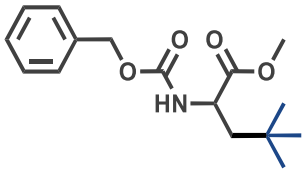

Methyl 2-(((benzyloxy)carbonyl)amino)-4,4-dimethylpentanoate (6.B4).

The product was obtained following General Procedure 3 as a colourless oil (26.9 mg, 92% yield).

6.B4. ^{1}H NMR (400 MHz, chloroform-*d*) δ ppm 7.28–7.41 (m, 5H), 5.11 (s, 2H), 4.42 (td, *J* = 9.0, 3.6 Hz, 1H), 3.73 (s, 3 H), 1.69–1.84 (m, 2H), 1.46 (dd, *J* = 14.3, 9.0 Hz, 1H),

0.97 (s, 9H). ^{13}C NMR (101 MHz, chloroform-*d*) δ ppm 174.0, 155.7, 136.3, 128.4, 128.1, 128.0, 66.9, 52.3, 51.7, 46.1, 30.6, 29.5. HRMS (ESI-TOF): mass calcd. for [$C_{16}H_{23}NO_4$ + H]$^+$, 294.1705; m/z found, 294.1668.

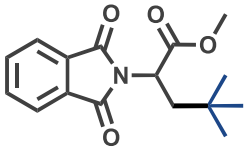

Methyl 2-(1,3-dioxoisoindolin-2-yl)-4,4-dimethylpentanoate (6.B5).

The product was obtained following General Procedure 3 as a colourless oil. (36.5 mg, 51% yield).

6.B5. ^{1}H NMR (400 MHz, chloroform-*d*) δ ppm 7.84–7.90 (m, 2H), 7.71–7.78 (m, 2H), 4.96 (dd, *J* =9.4, 3.3 Hz, 1H), 3.71 (s, 3 H), 2.19–2.34 (m, 2 H), 0.92 (s, 9 H). ^{13}C NMR (101 MHz, chloroform-*d*) δ ppm 170.5, 167.7, 134.1, 131.9, 123.5, 52.8, 49.5, 41.2, 30.3, 29.1. HRMS (ESI-TOF): mass calcd. for [$C_{16}H_{19}NO_4$ + H]$^+$, 290.1381; m/z found, 290.1387.

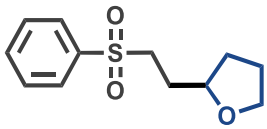

2-(2-(phenylsulfonyl)ethyl)tetrahydrofuran (6.C2).

The product was obtained following General Procedure 3 as a colourless oil (9.1 mg, 38% yield).

6.C2. ^{1}H NMR (400 MHz, chloroform-*d*) δ ppm 7.89–7.96 (m, 2H), 7.63–7.70 (m, 1H), 7.54–7.61 (m, 2H), 3.82–3.90 (m, 1 H), 3.79 (dt, *J* = 8.3, 6.7 Hz, 1H), 3.64–3.73 (m, 1H), 3.25–3.36 (m, 1H), 3.09–3.20 (m, 1H), 1.82–2.03 (m, 6H) 1.41–1.54 (m, 1H). ^{13}C NMR (101 MHz, chloroform-*d*) δ ppm 139.1, 133.6, 129.2, 128.0, 77.0, 67.8, 53.6, 31.2, 28.5, 25.6. HRMS (ESI-TOF): mass calcd. for [$C_{12}H_{16}O_3S$ + H]$^+$, 241.0898; m/z found, 241.0955.

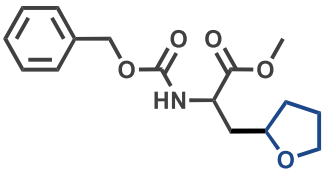

Methyl 2-(((benzyloxy)carbonyl)amino)-3-(tetrahydrofuran-2-yl) propanoate (6.C4).

The product was obtained following General Procedure 3 as a colourless oil (17 mg, 55% yield).

6.C4. ^{1}H NMR (400 MHz, chloroform-*d*) δ ppm 7.28–7.42 (m, 5H), 6.18 (br d, *J* = 8.3 Hz, 1H), 5.07–5.18 (m, 2H), 4.48–4.57 (m, 1H), 3.81–3.90 (m, 2H), 3.64–3.77 (m, 4H), 1.96– 2.14 (m, 2H), 1.78– 1.94 (m, 3H), 1.47 (dq, *J* = 12.1, 8.2 Hz, 1H).^{13}C NMR (101 MHz, chloroform-*d*) δ ppm 172.6, 156.2, 136.5, 128.5, 128.1, 128.1, 76.4, 68.1, 66.8, 53.0, 52.3, 36.7, 32.0, 25.3.HRMS (ESI-TOF): mass calcd. for $[C_{16}H_{21}NO_5 + H]^+$, 308.1498; m/z found, 308.1553.

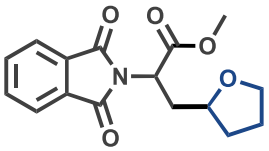

Methyl 2-(1,3-dioxoisoindolin-2-yl)-3-(tetrahydrofuran-2-yl)propanoate (6.C5). (Mixture of rotamers).

The product was obtained following General Procedure 3 as a colourless oil (16.8 mg, 63% yield).

6.C5. ^{1}H NMR (400 MHz, methanol-d_4) δ ppm 7.66–7.84 (m, 4H), 4.91–5.03 (m, 1H), 3.66–3.85 (m, 1H), 3.62 (s, 3H), 3.35–3.58 (m, 1H), 3.21 (dt, *J* =3.3, 1.6 Hz, 1H), 2.12–2.44 (m, 2H), 1.63–1.95 (m, 3H), 1.36–1.49 (m, 1 H). ^{13}C NMR (101 MHz, methanol-d_4) δ ppm 171.3, 171.9, 169.2, 135.6, 136.1, 133.2, 124.6, 76.9, 68.8, 53.4, 51.0, 35.2, 35.6, 31.9, 33.1, 26.1, 26.9. HRMS (ESI-TOF): mass calcd. for $[C_{16}H_{17}NO_5 + H]^+$, 304.1171; m/z found, 304.1179.

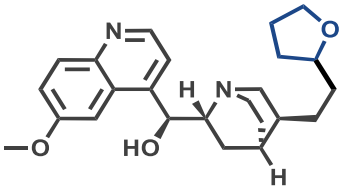

(1*S*)-(6-methoxyquinolin-4-yl)((2*R*,4*R*,5*S*)-5-(2-(tetrahydrofuran-2-yl)ethyl) quinuclidin-2-yl)methanol (6.C6). (Mixture of rotamers).

The product was obtained following General Procedure 3 as a colourless oil (12.9 mg, 33% yield).

6.C6. ^{1}H NMR (400 MHz, chloroform-*d*) δ ppm 8.66 (d, *J* = 4.4 Hz, 1H), 7.98 (d, *J* = 9.2 Hz, 1H), 7.51 (d, *J* = 4.6 Hz, 1H), 7.30–7.40 (m, 1H), 7.24 (d, *J* = 2.5 Hz, 1H), 5.75 (ddd, *J* =17.3, 10.2, 7.6 Hz, 1H), 5.54 (d, *J* = 4.2 Hz, 1H), 4.90–5.01 (m, 2H), 3.94 (s, 1H), 3.90 (s, 3H), 3.33–3.59 (m, 2H), 3.04–3.18 (m, 3H), 2.61–2.75 (m, 3,H) 2.28 (br t, *J* = 8.8 Hz, 2H), 1.99–2.19 (m, 2H), 1.67–1.87 (m, 4H), 1.43–1.62 (m, 3H). ^{13}C NMR (101 MHz, chloroform-*d*) δ ppm 157.7, 147.5, 147.5, 144.2, 141.7, 134.8, 131.6, 130.8, 126.6, 122.3, 121.5, 118.4, 114.4, 105.1, 101.2, 71.9, 59.9, 56.9, 55.7, 43.2, 39.9, 27.8, 27.5, 21.7. HRMS (ESI-TOF): mass calcd. for $[C_{24}H_{32}N_2O_3 + H]^+$, 397.2491; m/z found, 397.2498.

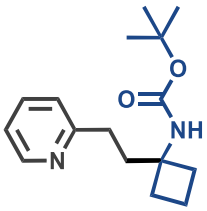

***tert*-Butyl (1-(2-(pyridin-2-yl)ethyl)cyclobutyl)carbamate (6.D1).**

The product was obtained following General Procedure 3 as a colourless oil (6.5 mg, 24% yield).

6.D1. ^{1}H NMR (400 MHz, chloroform-*d*) δ ppm 8.52 (dd, *J* = 4.9, 0.7 Hz, 1H), 7.59 (td, *J* = 7.6, 1.8 Hz, 1H), 7.17 (d, *J* = 7.9 Hz, 1H), 7.11 (ddd, *J* = 7.5, 5.0, 1.2 Hz, 1H), 4.89–5.12 (m, 1H), 2.74–2.84 (m, 2H), 2.17–2.35 (m, 4H), 1.99–2.07 (m, 2H), 1.85–1.97 (m, 1H), 1.75–1.85 (m, 1H) 1.44 (s, 9 H). ^{13}C NMR (101 MHz, chloroform-*d*) δ ppm 162.1, 149.1, 136.4, 122.8, 121.0, 78.4, 56.4, 37.4, 33.0, 32.6, 28.4, 14.5. HRMS (ESI-TOF): mass calcd. for $[C_{16}H_{24}N_2O_2 + H]^+$, 277.1916; m/z found, 277.1969.

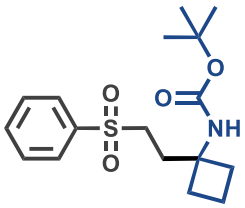

***tert*-Butyl (1-(2-(phenylsulfonyl)ethyl)cyclobutyl)carbamate (6.D2). (Mixture of rotamers).**

The product was obtained following General Procedure 3 as a colourless oil (9.4 mg, 28% yield).

6.D2. ^{1}H NMR (400 MHz, chloroform-*d*) δ ppm 7.89–7.95 (m, 2H), 7.63–7.70 (m, 1H), 7.52–7.61 (m, 2H), 4.41–4.69 (m, 1H), 3.01–3.15 (m, 2H), 2.17–2.25 (m, 2H), 2.08 (br t, *J* = 8.7 Hz, 2H), 1.74–2.02 (m, 4H), 1.35 (s, 9H). ^{13}C NMR (101 MHz, chloroform-*d*) δ ppm 156.9, 139.0, 133.7, 129.3, 128.0, 77.9, 55.2, 52.1, 32.9, 30.5, 28.0, 28.7, 14.4. HRMS (ESI-TOF): mass calcd. for $[C_{17}H_{25}NO_4S + H]^+$, 340.1583; m/z found, 340.1552.

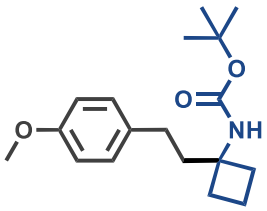

***tert*-Butyl (1-(4-methoxyphenethyl)cyclobutyl)carbamate (6.D3).**

The product was obtained following General Procedure 3 as a colourless oil (2.7 mg, 9% yield).

6.D3. ^{1}H NMR (400 MHz, chloroform-*d*) δ ppm 7.12 (d, *J* = 8.8 Hz, 2H), 6.84 (d, *J* = 8.6 Hz, 2H), 4.63 (br s, 1H), 3.80 (s, 3H), 2.49–2.56 (m, 2H), 1.99–2.28 (m, 6H), 1.87–1.97 (m, 1H), 1.72–1.86 (m, 1H), 1.46 (s, 9H). ^{13}C NMR (101 MHz, chloroform-*d*) δ ppm 157.7, 134.4, 129.2, 113.8, 78.9, 56.4, 55.3, 32.8, 29.5, 28.5, 14.7. HRMS (ESI-TOF): mass calcd. for $[C_{18}H_{27}NO_3 + H]^+$, 306.2069; m/z found, 306.2039.

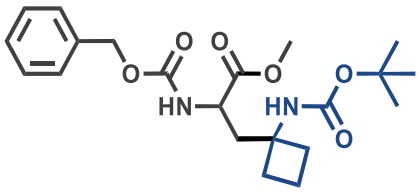

Methyl 2-(((benzyloxy)carbonyl)amino)-3-(1-((tert butoxycarbonyl) amino) cyclobutyl) propanoate (6.D4).

The product was obtained following General Procedure 3 as a colourless oil (14.9 mg, 37% yield).

6.D4. ^{1}H NMR (400 MHz, chloroform-*d*) δ ppm 7.29–7.39 (m, 5H), 5.39 (br d, *J* = 7.2 Hz, 1H), 4.97–5.20 (m, 3H), 4.33–4.43 (m, 1H), 3.74 (s, 3H), 2.34 (dd, *J* = 14.3, 3.7 Hz, 1H), 1.91–2.22 (m, 6H), 1.75–1.87 (m, 1H), 1.42 (s, 9H). ^{13}C NMR (101 MHz, chloroform-*d*) δ ppm 173.2, 155.9, 154.4, 136.1, 128.5, 128.1, 128.0, 79.2, 67.0, 55.5, 52.5, 51.4, 39.2, 33.5, 28.4, 15.1. HRMS (ESI-TOF): mass calcd. for $[C_{21}H_{30}N_2O_6 + H]^+$, 407.2182; m/z found, 407.2220.

6.5 References.

1) Southey, M. W. Y. and Brunavs, M. Introduction to small molecule drug discovery and preclinical development, *Front. Drug Discov*. **2023**, *3*, 10.3389/fddsv.2023.1314077.
2) Kombo, D. C., Tallapragada, K., Jain, R., Chewning, J., Mazurov, A. A., Speake, J. D., Hauser, T. A. and Toler., S. 3D Molecular Descriptors Important for Clinical Success. *J. Chem. Inf. Model*. **2013**, *53*, 327−342.
3) Lovering, F., Bikker, J. and Humblet, C. Escape from Flatland: Increasing Saturation as an Approach to Improving Clinical Success. *J. Med. Chem.* **2009**, *52*, 6752–6756.
4) Walters, W. P., Green, J., Weiss, J. R. and Murcko, M. A. What Do Medicinal Chemists Actually Make? A 50-Year Retrospective. *J. Med. Chem.* **2011**, *54*, 6405–6416.
5) Lovering, F. Escape from Flatland 2: complexity and promiscuity. *Med. Chem. Commun*. **2013**, *3*, 515–519.
6) Meyers, J., Carter, M., Mok, N. Y. and Brown, N. On the origins of three-dimensionality in drug-like molecules. *Future Med. Chem.* **2016**, *8*, 1753–1767.

7) Wei, W., Cherukupalli, S., Jing, L., Liu, X. and Zhan, P. Fsp3: A new parameter for drug-likeness. *Drug Discov. Today.* **2020**, *10*, 1839-1845.
8) Pijper, B., Abdiaj, I., Leonori, D. and Alcázar. J. Development of an Automated Platform for C(sp^3)-C(sp^3) Bond Formation via XAT Chemistry. *ChemCatChem.* **2023**, 15, e202201289.
9) Pijper, B., Martín, R., Huertas-Alonso, A. J., Linares, M. L., López, E., Llaveria, J., Díaz-Ortiz, Á., Dixon, D. J., De la Hoz, A. and Alcázar, J. Fully Automated Flow Protocol for C(sp^3)–C(sp^3) Bond Formation from Tertiary Amides and Alkyl Halides. *Org. Lett.* **2024**, *26*, 2724–2728.
10) Liu, W., Mulhearn, J., Hao, B., Cañellas, S., Last, S., Gómez, J. E., Jones, A., De Vera, A., Kumar, K., Rodríguez, R., Van Eynde, L., Strambeanu, I. I. and Wolkenberg, S. E. Enabling Deoxygenative C(sp^2)-C(sp^3) Cross-Coupling for Parallel Medicinal Chemistry. *ACS Med. Chem. Lett.* **2023**, *14*, 853–859.
11) Abdiaj, I., Cañellas, S., Dieguez, A., Linares, M. L., Pijper, B., Fontana, A., Rodriguez, R., Trabanco, A., Palao, E. and Alcázar, J. End-to-End Automated Synthesis of C(sp^3)-Enriched Drug-like Molecules via Negishi Coupling and Novel, Automated Liquid–Liquid Extraction. *J. Med. Chem.* **2023**, *66*, 716–732.
12) Alonso, M., Cañellas, S., Delgado, F., Serrano, M., Diéguez, A. and Gómez, J. E. Accelerated Synthesis of Bicyclo[1.1.1]pentylamines: A High-Throughput Approach *Org. Lett.* **2023**, *25*, 771–776.
13) Pijper, B., Abdiaj, I., Mazuela, J., Linares, M. L., Gómez, J. E., Rodriguez, R., Arquero, B. C., Palao, E., Cañellas, S. and Alcázar, J. Assembly line library synthesis in flow: A multistep and multivectorial approach. *ChemRxiv*, **2024**, 10.26434/chemrxiv-2024-4st74-v2.
14) *Free Radicals: Fundamentals and Applications in Organic Synthesis*. Eds Fensterbank, L. and Ollivier, C. Georg Thieme Verlag KG, Stuttgart, Germany, **2021**.; (*b*) Studer, A. and Curran, D. P. Catalysis of Radical Reactions: A Radical Chemistry Perspective. *Angew. Chem., Int. Ed.* **2016**, *55*, 58–102; (*c*) Yan, M., Lo, J. C., Edwards, J. T. and Baran, P. S. Radicals: Reactive Intermediates with Translational Potential, *J. Am. Chem. Soc.* **2016**, *138*, 12692–12714.
15) a) Pitre, S. P., Weires, N. A. and Overman, L. E. Forging C(sp^3)-C(sp^3) Bonds with Carbon-Centered Radicals in the Synthesis of Complex Molecules. *J. Am. Chem. Soc.* **2019**, *141*, 2800–2813; b) Ravelli, D., Protti, S. and Fagnoni, M.

Carbon–Carbon Bond Forming Reactions via Photogenerated Intermediates. *Chem. Rev.* **2016**, *116*, 9850–9913; c) Goddard, J.-P., Ollivier, C. and Fensterbank, L. Photoredox Catalysis for the Generation of Carbon Centered Radicals. *Acc. Chem. Res.* **2016**, *9*, 1924–1936.

16) a) *Visible Light Photocatalysis in Organic Chemistry.* Eds Stephenson, C. R. J., Yoon, T. P. and MacMillan, D. W. C. Wiley-VCH, Weinheim, Germany **2018**; b) *Chemical Photocatalysis.* 2nd *ed.*; Ed König, B. De Gruyter, **2020**.
17) Correia, J. T. M., Fernandes, V. A., Matsuo, B. T., Delgado, J. A. C., De Souza, W. C. and Paixão, M. W. Photoinduced deaminative strategies: Katritzky salts as alkyl radical precursors. *Chem. Commun.* **2020**, *56*, 503–514.
18) Niu, P., Li, J., Zhang, Y. and Huo, C. One-Electron Reduction of Redox-Active Esters to Generate Carbon-Centered Radicals. *Eur. J. Org. Chem.* **2020**, *36*, 5801–5814.
19) Parida, S. K., Mandal, T., Das, S., Hota, S. De Sarkar, K, S. and Murarka, S. Single Electron Transfer-Induced Redox Processes Involving N-(Acyloxy)phthalimides. *ACS Catal.* **2021**, *11,* 1640−1683.
20) Crespi, S. and Fagnoni, M. Generation of Alkyl Radicals: From the Tyranny of Tin to the Photon Democracy. *Chem. Rev*. **2020**, *120*, 9790−9833.
21) Luguera Ruiz, A., La Mantia, M., Merli, D., Protti, S. and Fagnoni, M. Alkyl Radical Generation via C–C Bond Cleavage in 2-Substituted Oxazolidines, *ACS Catal.* 2022, 12, 12469–12476.
22) Saraiva, M. F., Couri, M. R. C., Le Hyaric, M., De Almeida, M. V. The Barton ester free-radical reaction: a brief review of applications, *Tetrahedron.* **2009**, *65*, 3563–3572.
23) Luguera Ruiz, A., Mariani, E., Protti, S. and Fagnoni, M. Photoredox catalyzed release of carbon-based radicals from 2-substituted-1,3-imidazolidines. *Org. Chem. Front.* **2024**, *11*, 661–667.
24) Cushman, D. W. and Ondetti, M. A. History of the Design of Captopril and Related Inhibitors of Angiotensin Converting Enzyme. *Hypertension*. **1991**, *4*, 589–592.
25) Cushman, D. W. and Ondetti, M. A. Design of angiotensin converting enzyme inhibitors*. Nat. Med.* **1999**, *10*, 1110–1113.
26) Pijper, B., Saavedra, L. M., Lanzi, M., Alonso, M., Fontana, A., Serrano, M., Gómez, J. E., Kleij, A. W., Alcázar, J. and Cañellas, S. Addressing Reproducibility

Challenges in High-Throughput Photo-chemistry. *ChemRxiv.* **2024**, 10.26434/chemrxiv-2024-n12vr.

27) a) *The Alkaloids: Chemistry and Biology, Volume 82.* Eds Knolker, H. J. Academic Press, Cambridge, United States, **2019**. b) *Evidence-Based Validation of Herbal Medicine.* Eds Mukherjee, P. K. Elsevier, Cambridge, United States, **2015**. c) *Alkaloids.* Eds Aniszewski, T. Elsevier Science, Cambridge, United States, **2015**.
28) Gross-Goupil, M., François, L., Quivy, A. and Ravaud, A. Axitinib: a review of its safety and efficacy in the treatment of adults with advanced renal cell carcinoma. *Clin. Med. Insights Oncol.* **2013,** *29*, 269–277.
29) Zhou, X., Xiao, Q., Fu, D., Zhang, H., Tang, Y., He, J., Hu, Y., Kong, X., Teng, F., Liu, X., Yuan, Y. and Ding, K. Efficacy of rigosertib, a small molecular RAS signaling disrupter for the treatment of KRAS-mutant colorectal cancer. *Cancer Biol. Med.* **2021**, *19*, 213–228.
30) Ahmadi, R. and Emami, S. Recent applications of vinyl sulfone motif in drug design and discovery. *Eur. J. Med. Chem.* **2022**, *234*, 114255–114278.
31) Ling, Y., Hao, Z. Y., Liang, D., Zhang, C. L., Liu, Y. F. and Wang, Y. The Expanding Role of Pyridine and Dihydropyridine Scaffolds in Drug Design. *Drug Des. Dev. Ther.* **2021**, *15*, 4289–4338.
32) Narancic, T., Almahboub, S. A. and O'Connor, K. E. Unnatural amino acids: production and biotechnological potential. *World J. Microbiol. Biotechnol.* **2019**, *35*, 67.
33) Sharma, K., Sharma, K. K., Sharma, A. and Jain, R. Peptide-based drug discovery: Current status and recent advances. *Drug Discov. Today.* **2023**, *2*, 103464–103478.

UNIVERSITÀ
DI PAVIA